UNIVERSIDAD D CÓRDOBA

TESIS DOCTORAL

POR COMPENDIO DE PUBLICACIONES

PROGRAMA DE DOCTORADO EN INGENIERÍA AGRARIA, ALIMENTARIA, FORESTAL Y DEL DESARROLLO RURAL SOSTENIBLE

ANÁLISIS Y MEJORAS EN EL MOVIMIENTO DE SEGUIDORES SOLARES: APLICACIÓN AL RETROSEGUIMIENTO

ANALYSIS AND IMPROVEMENTS FOR SOLAR TRACKERS MOVEMENT: APPLIED TO BACKTRACKING

Autor: Francisco Javier Gómez Uceda

Directores: ***Dr. D. José Cristóbal Ramírez Faz***
Dr. D. Luis Manuel Fernández de Ahumada

Córdoba, mayo 2021

TITULO: *ANÁLISIS Y MEJORAS EN EL MOVIMIENTO DE SEGUIDORES SOLARES: APLICACIÓN AL RETROSEGUIMIENTO*

AUTOR: *Francisco Javier Gómez Uceda*

Campus de Rabanales
Ctra. Nacional IV, Km. 396 A
14071 Córdoba

https://www.uco.es/ucopress/index.php/es/
ucopress@uco.es

Lista de publicaciones originales

Esta tesis se presenta en forma de compendio de publicaciones, de acuerdo con el artículo 53 Reglamento 57/2020 de Consejo de Gobierno, con fecha de publicación el 1 de diciembre de 2020 en BOUCO, y regulado a través del Real Decreto 99/2011, de 28 de enero (modificado por el RD 534/2013; por el RD 43/2015 y por el RD 195/2016), que recogen las enseñanzas oficiales de los estudios de Doctorado.

Dichas publicaciones recogen los resultados que han sido obtenidos en los diferentes trabajos de investigación desarrollados con el fin de alcanzar el objetivo fijado para la realización de la tesis. A continuación, se listan las referidas publicaciones (3) que constituyen los anexos de la presente memoria de tesis.

Artículo 1 (se puede consultar en el Anexo I de este documento)

Gómez-Uceda, FJ; Moreno-García, IM; Jiménez-Martínez, JM; López-Luque, R; Fernández-Ahumada, LM (2020). ***Analysis of the influence of terrain orientation on the design of PV facilities with single-axis trackers***. *Applied Sciences*, *10*(23). https://doi.org/10.3390/app10238531

Applied Sciencies. Factor de impacto (2019): 2,474

Q2 en la categoría "Engineering, Multidisciplinary" (JCR), posición: 32/91

Artículo 2 (se puede consultar en el Anexo II de este documento)

Gómez-Uceda, FJ; Ramírez-Faz, J; Varo-Martínez, M; Fernández-Ahumada, LM. (2021). ***New Omnidirectional Sensor Based on Open - Source Software and Hardware for Tracking and Backtracking of Dual - Axis Solar Trackers in Photovoltaic Plants.*** *Sensors*, 21(3).https://doi.org/10.3390/s21030726

Sensors. Factor de impacto (2019): 3,275

Q1 en la categoría "Instruments and Instrumentation" (JCR), posición: 15/64

Artículo 3 (se puede consultar en el Anexo III de este documento)

Gómez-Uceda, FJ; Moreno-García, IM; Pérez-Castañeda, A; Fernández-Ahumada, LM. (2021). ***Study of the Dependence of Solar Radiation Regarding Design Variables in Photovoltaic Solar Installations with Optimal Dual-Axis Tracking.*** *Applied Sciences, 11(29)*. https://doi.org/10.3390/app11093917

Applied Sciencies. Factor de impacto (2019): 2,474

Q2 en la categoría "Engineering, Multidisciplinary" (JCR), posición: 32/91

TÍTULO DE LA TESIS: ANÁLISIS Y MEJORAS EN EL MOVIMIENTO DE SEGUIDORES SOLARES: APLICACIÓN AL RETROSEGUIMIENTO

DOCTORANDO/A: Francisco Javier Gómez Uceda

INFORME RAZONADO DEL/DE LOS DIRECTOR/ES DE LA TESIS

La presente tesis está centrada en el análisis de seguidores solares de 1 y 2 ejes y en la optimización de la captación radiativa, empleando distintos modelos físicos y empíricos de evaluación de la irradiancia en todas sus componentes. Esto, en primera instancia, permite determinar la orientación óptima de dichas instalaciones y, paralelamente, evaluar la posible interferencia de unos colectores sobre otros mediante el análisis de sombreo, pudiendo así reajustar su orientación mediante técnicas de retroseguimiento, incluyendo variables hasta ahora no evaluadas.

Para ello, se han incluido elementos en la investigación como la influencia de la inclinación del terreno y modificación en la geometría de los colectores, así como el desarrollo de un novedoso sensor, que permite determinar la orientación donde los valores de irradiancia son máximos.

Por consiguiente, el objetivo general ha sido la obtención de mejoras en el rendimiento de los seguidores solares de 1 y 2 ejes.

A lo largo del proceso de elaboración de la tesis, el doctorando ha demostrado una elevada capacidad autónoma de adaptación a las diferentes dificultades que se han ido planteando. Ha quedado patente la adquisición de competencias específicas para el desempeño de una futura carrera en el ámbito científico.

Por todo esto, consideramos que se trata de una Tesis de gran calidad, que aborda un problema en continuo avance tecnológico y con gran aplicabilidad a instalaciones ya en funcionamiento y futuras.

La Tesis se presenta como un compendio de tres publicaciones en algunas de las revistas más prestigiosas en el área de investigación, 1 en el primer cuartil y 2 en el segundo cuartil (JCR).

- APPLIED SCIENCES (2020, Vol. 10, issue 23), Factor de impacto (2019): 2,474.
- SENSORS (2021, Vol. 21, issue 3), Factor de impacto (2019): 3,275.
- APPLIED SCIENCES (2021, Vol. 11, issue 29), Factor de impacto (2019): 2,474.

Por todo ello, se autoriza la presentación de la tesis doctoral.

Córdoba, mayo de 2021

Firma de los directores

RAMIREZ FAZ JOSE CRISTOBAL - 30537627K

Firmado digitalmente por RAMIREZ FAZ JOSE CRISTOBAL - 30537627K
Fecha: 2021.05.09 19:43:36 +02'00'

FERNANDEZ DE AHUMADA LUIS MANUEL - 44362660F

Firmado digitalmente por FERNANDEZ DE AHUMADA LUIS MANUEL - 44362660F
Nombre de reconocimiento (DN): c=ES, serialNumber=IDCES-44362660F, givenName=LUIS MANUEL, sn=FERNANDEZ DE AHUMADA, cn=FERNANDEZ DE AHUMADA LUIS MANUEL - 44362660F
Fecha: 2021.05.10 10:40:00 +02'00'

Fdo.: JOSÉ CRISTÓBAL RAMÍREZ FAZ Fdo.: LUIS MANUEL FERNÁNDEZ DE AHUMADA

A Jimena, Gabriel y mis padres

Agradecimientos

Desde este pequeño apartado, quiero agradecer a mis directores de tesis Pepe y Luisma su dedicación y paciencia durante esta larga travesía, no sin olvidarme de Rafa y Marta. Todos me han hecho partícipe de la gran cantidad de cocimientos que albergan, tanto por su capacidad y prestigio como investigadores, como por su trayectoria profesional.

Quiero expresar mi gratitud al resto de miembros del grupo de investigación "Física para las Energías Renovables", y a mis compañeros de área de conocimiento.

Gracias a todos por vuestra paciencia y comprensión.

Resumen

El Sol es considerado como una fuente de energía inagotable, por lo que su estudio y caracterización constituyen una de las principales líneas de investigación, con el objeto de evaluar su incidencia en instalaciones de captación solar.

En instalaciones PV con seguidores solares, resulta de suma importancia el estudio de aquellas variables susceptibles de proporcionar la orientación óptima para conseguir la máxima eficiencia desde el punto de vista energético.

La irradiancia global se considera un parámetro fundamental para la caracterización solar, por lo que sus componentes (directa, difusa y reflejada) deben ser evaluadas para su óptima utilización. La componente directa está estrechamente ligada con la geometría Sol-Tierra ya que sus rayos asociados provienen directamente de la ubicación del Sol. Por otro lado, la componente difusa está formada por los rayos que llegan desde todas las direcciones de la bóveda celeste exceptuando la dirección Tierra-Sol, mientras que la componente reflejada depende del coeficiente de reflexión de la superficie también denominado *albedo*.

Modelos de irradiancia tales como el de Hay-Davies y el modelo de Pérez, permiten relacionar la función de irradiancia con el vector solar ($\vec{s}$) y el vector normal de los colectores ($\vec{n}$). De esta forma, mediante un proceso de optimización basado en multiplicadores de Lagrange sujeto a una serie de restricciones impuestas, se consigue conocer a priori la orientación óptima de los colectores.

Esta caracterización del óptimo del vector normal al colector ($\vec{n}$) se consigue tanto en seguidores solares de 1 como de 2 ejes, lo que establece un punto de partida para realizar el estudio de la interferencia entre seguidores, y, por consiguiente, determinar la existencia de sombreamiento. El análisis de dicho sombreamiento se realiza mediante elementos vectoriales tanto en el plano (1 eje) como en el espacio (2 ejes), empleando un criterio dicotómico basado en el álgebra de Minkowski.

La determinación de la existencia de sombreo permite paralelamente establecer una alternativa a la orientación inicial mediante una reorientación del seguidor (retroseguimiento), siempre lo más próxima al valor de irradiancia óptima.

En este contexto, la presente tesis doctoral avanza en el estudio del comportamiento de seguidores solares. Los objetivos explicitados en cada artículo son:

- Maximizar la captación de radiación solar en seguidores de 1 y 2 ejes.
- Optimizar trayectorias de seguimiento y su interacción con las variables del terreno.
- Monitorizar el sistema de seguimiento.
- Evaluar todas las componentes de irradiancia global (directa, difusa y reflejada).
- Estudiar los efectos negativos de sombreamiento entre colectores y actuaciones a seguir en caso de que se produzca dicho efecto.
- Proponer técnicas de retroseguimiento.
- Estudiar la influencia de la geometría de colectores PV en la captación radiativa.

Palabras clave: Caracterización solar, seguidores solares, sombreamiento, retroseguimiento.

Abstract

The sun is considered to be an inexhaustible source of energy, so its study and characterisation are two of the main lines of research, to evaluate with the aim of evaluating its impact on solar collection installations.

In PV installations with solar trackers, it is extremely important to study those variables likely to provide the optimum orientation to achieve maximum efficiency from the energy point of view.

Global irradiance is considered a fundamental parameter for solar characterisation, so its components (direct, diffuse and reflected) must be evaluated for its use. The direct component is closely linked to the Sun-Earth geometry as its associated rays come directly from the location of the Sun. On the other hand, the diffuse component is formed by the rays reaching from all directions of the celestial vault except the Earth-Sun direction, while the reflected component depends on the reflection coefficient of the surface, also called *albedo*.

Irradiance models such as Hay-Davies and Perez, allow the irradiance function to be related to the solar vector ($\vec{s}$) and the normal vector of the collectors ($\vec{n}$). In this way, by means of an optimisation process based on Lagrange multipliers subject to a series of imposed restrictions, the optimal orientation of the collectors is known a priori.

This characterisation of the optimum normal vector to the collector ($\vec{n}$) is achieved in both 1-axis and 2-axis solar trackers, which establishes a baseline for performing the study of interference between trackers, and, therefore, determining the existence of shading. The analysis of this shading is performed using vector elements both in the plane (1-axis) and in space (2-axis), using a dichotomous criterion based on Minkowski algebra.

The determination of the existence of shading allows at the same time to establish an alternative to the initial orientation by means of a reorientation of the tracker (backtracking), but always as close as possible to the optimum irradiance value.

In this context, this doctoral thesis advances in the study on the behaviour of solar trackers. The objectives expressed in each article are:

- Maximising solar radiation collection in 1- and 2-axis trackers.
- Optimising tracking trajectories and its interaction with terrain variables.
- Monitoring the tracking system.

- Evaluating all the global irradiance components (direct, diffuse and reflected).
- Studying the negative effects of shading between collectors and actions to be adopted in the event of this effect occurring.
- Proposing back-tracking techniques.
- Studying the influence of the geometry of PV collectors on radiative capture.

Keywords: Solar characterization, solar trackers, shading, backtracking.

Índice de Contenidos

Índice de figuras

Índice de tablas

Lista de símbolos

Magnitudes vectoriales

$\vec{a}$ = vector proyección contenido en panel solar para el análisis de sombreo

$\vec{d}$ = distancia entre centros de dos colectores adyacentes

$\vec{e}$ = vector unitario en la dirección del eje de rotación del colector

$\vec{\imath}, \vec{\jmath}, \vec{k}$ = vectores unitarios asociados a un sistema cartesiano

$\vec{n}$ = vector normal a la superficie del colector

$\overrightarrow{n'}$ = vector normal óptimo a la superficie del colector

$\overrightarrow{n_T}$ = vector normal al terreno

$\vec{q}$ = vector perpendicular al vector $\overrightarrow{n_T}$ y $\vec{e}$

$\vec{s}$ = vector solar

$\overrightarrow{s'}$ = vector solar en un sistema de referencia $\{\vec{q}, \vec{e}, \overrightarrow{n_T}\}$

$\vec{u}$ = vector incluido en el plano del colector

$\vec{v}$ = vector unitario incluido en el plano del colector y perpendicular a $\vec{u}$

$\vec{w}$ = gradiente unitario horizontal de la irradiancia

Magnitudes escalares

a = anchura del colector solar

b = altura del colector solar

d_j = día Juliano

d_i= vector desplazamiento desde el polígono Π_0 a Π'_i

d_{Xi} = componente X del vector d_i

d_{Yi} = componente y del vector d_i

h = anchura del colector

i = índice asignado a cada seguidor solar

j = índice secundario asignado a cada seguidor solar ($i \neq j$)

n'_x, n'_y, n'_z = componentes del vector normal óptimo a la superficie del colector

s_x, s_y, s_z = componentes del vector solar

s'_x, s'_y, s'_z = componentes del vector solar en un sistema de referencia $\{\vec{q}, \vec{e}, \overrightarrow{n_T}\}$

t = hora específica solar

x, y, z = coordenadas cartesianas de la base de cada seguidor solar

x [i], y[i], z[i] = matrices con información de las coordenadas de cada seguidor solar

A_0 = superficie del colector de referencia

A_i = superficie de colector genérico

D_{EW} = distancia entre seguidores en dirección Este-Oeste

D_{NS} = distancia entre seguidores en dirección Norte-Sur

F_1, F_2 = factores de ponderación para la descomposición de la radiación difusa inclinada

H_m = radiación incidente sobre los colectores en cada uno de los días representativos de cada mes acorde a Klein(Klein, 1977)

H_{year} = radiación global anual

H_{year}^{est}= radiación solar anual estimada sobre los colectores según ecuación (5.28)

H_{year}^{adj}= radiación solar anual estimada sobre los colectores según ecuación (5.29)

I = irradiancia solar global en el colector inclinado

I_B = irradiancia solar directa sobre en el plano horizontal

I_D = irradiancia solar difusa

I_{OH} = irradiancia extraterrestre

L_x = longitud horizontal del colector después del corte

L_y = longitud vertical del colector después del corte

N= número de seguidores solares en la instalación

N_D = número de diferentes diseños de interdistancias entre colectores

N_G = número de diferentes geometrías de la forma del colector

N_m = número de días en el mes m

N_S = número de posibles distribuciones espaciales de los seguidores solares en la planta

N_T = número de las diferentes combinaciones de los diseños geométricos resultado del cruce $N_G \cdot N_D \cdot N_S$

P_0 = posición del colector de referencia

P_i = posición de un colector genérico

S_{col}= superficie del colector

T = variable discriminatoria del tipo de configuración

X_{dl}= coordenada-x del vértice correspondiente al corte hecho en la esquina inferior izquierda

X_{dr}= coordenada-x del vértice correspondiente al corte hecho en la esquina inferior derecha

X_{env}= matriz con las coordenadas-x de la forma del colector

X_{ul}= coordenada-x del vértice correspondiente al corte hecho en la esquina superior izquierda

X_{ur}= coordenada-x del vértice correspondiente al corte hecho en la esquina superior derecha

Y_{dl}= coordenada-y del vértice correspondiente al corte hecho en la esquina inferior izquierda

Y_{dr}= = coordenada-y del vértice correspondiente al corte hecho en la esquina inferior derecha

Y_{env}= matriz con las coordenadas-y de la forma del colector

Y_{ul}= coordenada-y del vértice correspondiente al corte hecho en la esquina superior izquierda

Y_{ur}= coordenada-y del vértice correspondiente al corte hecho en la esquina superior derecha

Símbolos griegos

α = ángulo de elevación del colector

β = ángulo de inclinación del terreno

γ = ángulo azimut del eje de rotación del colector

δ = declinación solar

$\varepsilon =$ error de estimación del modelo propuesto

ε_{rel} = error relativo del modelo propuesto

ξ = ángulo de inclinación del colector

θ = ángulo de incidencia de los rayos de sol sobre un plano inclinado

θ_z = ángulo solar cenital

λ, μ, ν = multiplicadores de Lagrange

ρ = albedo

τ = multiplicador escalar del vector solar para la regla del paralelogramo

φ = latitud

Φ = función de Lagrange

χ = azimut del terreno

Ω = velocidad de rotación de la Tierra

Γ = magnitud auxiliar dependiente del día Juliano

Π_0 = polígono del colector de referencia

Π_i = polígono de un colector genérico

Π'_i =proyección del polígono de un colector genérico sobre ψ

ψ = plano que contiene al polígono del colector de referencia Π_0

Acrónimos

GCR = Ground Cover Ratio

FOSH = Free and Open-Source Hardware

HW= Hardware

SPSTC= Semi-passive solar tracking concentrator

Capítulo 1 . Introducción

1.1. Modelos físicos para el seguimiento solar.

1.2. Optimización de la trayectoria de seguimiento.

1.3. Sombreo y retroseguimiento.

1.4. Desarrollo de sensor para la determinación de irradiancia máxima.

1.5. Influencia de la geometría de los captadores e inclinación del terreno.

La población mundial estimada en 9700 millones de personas para el 2050 (United Nations, 2019) implica una relación directa con el consumo energético y por consiguiente el nivel de emisiones a la atmósfera, lo que obliga a definir actuaciones por parte de los gobiernos encaminadas a la reducción de las mismas.

Para ello el avance en la investigación en el sector energético es clave en la lucha contra el cambio climático, pues dos tercios de las emisiones de gases de efecto invernadero mundiales están ligadas a la quema de combustibles fósiles que se usan para la generación de energía (United Nations, 2020).

Si bien la gran mayoría de los países industrializados ha ido dando pequeños pasos, no fue hasta el año 1997, en el Protocolo de Kioto inscrito dentro del Convenio Marco de la ONU sobre Cambio Climático, donde surge el acuerdo más importante, sentando las bases para el compromiso en la reducción de emisiones de efecto invernadero.

El Acuerdo de París en 2015 adoptado en la Conferencia sobre el clima de París (COP21) es el primero donde se produce una vinculación jurídica y establece un marco global para la lucha contra el cambio climático, de aplicación en 2020, y de obligado cumplimiento para los países firmantes (United Nations, 2015).

No obstante, las emisiones de CO_2 a la atmósfera, en contra de lo establecido en dicho Acuerdo, han ido incrementándose anualmente, y desde la ratificación de este, sólo en el pasado año 2020 se han visto reducidas (7% respecto a 2019) por la situación de pandemia mundial a consecuencia de la disminución de la actividad industrial y, fundamentalmente, el transporte (United Nations, 2020).

Dentro de las estrategias de reducción, el fomento del uso de energías renovables frente a las no renovables desempeña un papel clave en este objetivo de sostenibilidad. En 2019, la cuota de energías renovables incluida la energía hidroeléctrica supuso alrededor del 27 % de la oferta eléctrica, cuyo incremento es consecuencia de las nuevas capacidades eólicas y solares (ENERDATA, 2019).

El avance en la investigación y el desarrollo de las energías renovables para mejorar la eficiencia energética y la sostenibilidad global (Sáez-Martínez et al., 2016), han provocado una tendencia al alza iniciada en el año 2000 derivada del avance tecnológico dentro del sector eólico y solar, unido al descenso de los costes de las tecnologías empleadas e implantación de políticas climáticas cada vez más ambiciosas en la UE (Zedalis, 2017).

La Agencia internacional de la Energía (IEA) en su informe anual del año 2019 (IEA, 2019) estimó un aumento en la capacidad energética renovable en el 2019 del 12% de producción frente al año anterior (2018). A pesar de la pandemia COVID-19, en el año 2020 se produjo un incremento en dicha capacidad de casi un 50% (Camera, 2021).

De todas las fuentes que proporcionan energía renovable, destaca la que proporciona el Sol, al ser considerada como la más abundante y limpia (Panwar et al., 2011) y que, si se explota de manera adecuada, podría ser suficiente para satisfacer la demanda energética mundial (Kannan and Vakeesan, 2016).

La producción mundial de energía solar representa el 3% respecto al total del producción de energía eléctrica, mientras que en España alcanza el 6% (ENERDATA, 2019), destacando el papel de la PV (8.623 MW instalados en el año 2019) frente a la solar térmica (2.304 MW instalados en el año 2019) (REE, 2019).

Otro de los aspectos a destacar es la concienciación por parte de las administraciones para el fomento de las energías renovables que en España se traduce en el Plan Nacional Integrado de Energía y Clima (PNIEC 2021-2030) (Ministerio para la Transición Ecológica y el Reto Demográfico, 2020). Uno de sus compromisos es que las energías renovables proporcionen en el 2030 cerca del 42% de la demanda energética y el 74% de la producción eléctrica y, en el caso de la PV, consiga un parque de generación próximo a los 18.921 MW.

La producción de energía en PV se realiza a través de colectores solares dispuestos bien en estructuras fijas, dotando a los paneles de un ángulo de orientación fijo determinado por la latitud del lugar, o bien, mediante seguidores solares que permiten una modificación en la orientación de los colectores para maximizar en cada momento la captación solar.

Las instalaciones con seguimiento presentan una mayor producción energética frente a sistemas fijos convencionales de captación solar (Sumathi et al., 2017). Otros autores (Abdallah, 2004; Gay et al., 1982) estiman un aumento entre el 30%-40% de captación de radiación anual de instalaciones con seguidores frente a instalaciones con paneles fijos.

1.1. Optimización de trayectoria de seguimiento

El seguimiento solar supone una mejora tecnológica en la producción de energía fotovoltaica en la que se ha trabajado durante décadas (Nsengiyumva et al., 2018). Con ella se intenta paliar los efectos negativos de la alta variabilidad del recurso solar, tanto en el tiempo como en

el espacio, reorientando los paneles fotovoltaicos hacia posibles direcciones que incrementen la captación de irradiancia solar.

Para ello, los seguidores solares son muy útiles en grandes plantas fotovoltaicas conectadas a la red, donde es necesario aumentar la energía generada por metro cuadrado de superficie de colectores incrementando así su rendimiento.

Según el tipo de movimiento, los seguidores solares pueden clasificarse (Hafez et al., 2018; Nsengiyumva et al., 2018) en:

- Sistemas de seguimiento de 1 solo eje en los que un elemento móvil adapta su posición girando alrededor de un 1 eje fijo
- Sistemas de seguimiento de 2 ejes en los que el plano del colector gira alrededor de 2 ejes, consiguiendo la orientación hacia cualquier dirección de la bóveda celeste

Algunos autores han analizado el aumento de producción energética en función de la tecnología utilizada de seguimiento y latitud del lugar (Huld et al., 2010; Perpiñan et al., 2009), observando que a mayor latitud, el aumento en la producción puede alcanzar valores cercanos al 57% (Paredes-Parra et al., 2019).

Si bien los seguidores solares de doble eje son de coste más elevado y presentan un mantenimiento e implementación más alto, determinados autores desechan su utilidad en un futuro no muy lejano (Huang et al., 2011; Ismail et al., 2013). Por contrapartida, (Bahrami et al., 2016), presentan comparativas entre la eficiencia de los seguidores solares de 1 solo eje frente al de 2 ejes, llegando estos últimos a incrementar la producción energética entre un 0.42%- 23.4% dispuestos en la misma latitud.

(Eldin et al., 2016) resaltan que cada vez son más las investigaciones que pretenden mejorar la tecnología de los seguidores de doble eje para que la producción supere a los costes de instalación y mantenimiento. Estos autores establecen la conveniencia de los sistemas de monitorización adecuados a las condiciones climáticas del lugar.

No obstante, para un sistema fotovoltaico a escala comercial, la decisión de optar por un sistema simple o dual de seguimiento debe tener en cuenta aspectos tales como el coste del terreno, equipos y mantenimiento. (Martín-Martínez et al., 2019) evaluaron seis plantas

fotovoltaicas en España y, entre sus conclusiones, señalaron que se subestimaba la complejidad del seguimiento de 2 ejes tanto en operación como mantenimiento.

Otra clasificación de los seguidores solares está basada en los sistemas de accionamiento de los mismos y pueden ser clasificados en 5 tipos basándose en la tecnología de seguimiento (Hafez et al., 2018).

Así, podemos distinguir:

- Seguimiento activo, donde es el propio sistema el que determina la ruta solar durante cada día mediante la utilización de sensores. (AL-Rousan et al., 2018) destacan aquellos que buscan la posición del sol por la variación de luz recibida (*sensor driver system*).
- Seguimiento pasivo, en el que el accionamiento no es mecánico, sino que es provocado por el desequilibrio térmico de un gas que se traduce en un movimiento angular para conseguir un grado de iluminación homogéneo en el panel solar (Awasthi et al., 2020).
- Seguimiento semi-pasivo (SPSTC), es un sistema diseñado para el seguimiento solar empleando pequeños esfuerzos mecánicos, como es el caso de estudio empleando un sistema matricial de espejos localizado sobre una lente Fresnel (León et al., 2014).
- Seguimiento manual, en el que el ángulo de inclinación se modifica de manera estacional a través de un sistema de engranajes con el objetivo de facilitar su construcción y mantenimiento. Una de las ventajas de este sistema se observa en seguidores de doble eje al eliminar un motor de accionamiento.
- Seguimiento cronológico, en el que el colector es programado para que realice un movimiento angular fijo cada cierto tiempo establecido (15° por hora), y en el que se consigue un bajo error en el seguimiento (Torres-Roldán et al., 2015). Dentro de esta tipología, encontramos aquellos que incorporan pequeños microprocesadores con estrategias de seguimiento preestablecidas a partir de modelos matemáticos (*microprocessor driver system*).

  En este tipo, el análisis del movimiento en el seguidor puede basarse en algoritmos matemáticos que vienen determinados por el movimiento terrestre y fundamentados en la trigonometría esférica con precisión de milésimas de radianes (Braun and Mitchell, 1983; Riley and Hansen, 2015).

  No obstante, recientemente se ha abierto una nueva línea de determinación de la posición solar mediante herramientas basadas en notación vectorial (Parkin, 2010;

Sproul, 2007), en el que el vector solar ($\vec{s}$), se define como un vector unitario dirigido al centro del disco solar, permitiendo obtener las relaciones astronómicas mediante algebra matricial, productos escalares y vectoriales

Común a todos ellos, encontramos aquellos que disponen de sistemas de seguimiento de lazo abierto (*open loop driver system*), los cuales a partir de ecuaciones matemáticas modifican el movimiento de los actuadores mediante la ubicación de la posición del Sol y, en contraposición, tendremos los de lazo cerrado (*close loop driver system*), que adaptan el movimiento de los actuadores del seguidor a partir de la información suministrada por sensores de movimiento recalculando la posición solar.

Según lo expuesto anteriormente, ambos sistemas (1 eje y 2 ejes) coinciden en la necesidad de un avance en su estudio y comportamiento, buscando la optimización de la trayectoria del seguidor, y evaluar otras variables, tales como el efecto del sombreamiento entre colectores e inclinación del terreno.

1.2. Modelos físicos para el seguimiento solar

Los modelos para realizar el seguimiento solar son múltiples, entre los que destaca el modelo de seguimiento astronómico, cuyo objetivo consiste en optimizar el valor de la componente directa de la irradiancia, minimizando el ángulo entre el vector normal a la superficie del colector ($\vec{n}$) y el solar ($\vec{s}$), Figura (1.1), obviando otras componentes de la irradiancia tales como la componentes difusa y reflejada. Para ello usan los algoritmos que permiten determinar con gran precisión el vector solar (Blanco-Muriel et al., 2001; Grena, 2008; Reda and Andreas, 2004).

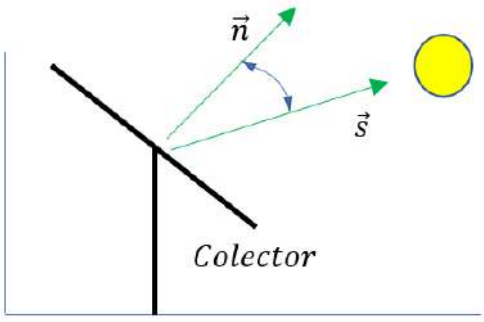

Figure 1.1. Vector normal al colector y vector solar

(Fernández-Ahumada et al., 2017) realizaron el estudio del seguimiento mediante la utilización de modelos racionales incluyendo todas las componentes de la irradiancia debido a que, en días nublados, los colectores en posición horizontal recolectan más energía que aquellos que

han sido posicionados según la estrategia de seguimiento astronómico (Duffie and Beckman, 2013; Mousazadeh et al., 2009).

Esto se fundamenta a que, en dichos períodos, la irradiancia directa es mucho menor que la componente difusa y reflejada y, la mayor parte de los modelos, consideran la componente difusa como una variable obtenida a partir de mediciones de varios años (Duffie and Beckman, 2013). Varios son los modelos empíricos que incluyen las tres componentes (directa, difusa y reflejada) (Fernández-Ahumada et al., 2020a, 2017).

Según lo anterior, la primera aportación de esta tesis y de aplicación a seguidores solares de 1 eje, se centra en la búsqueda del óptimo del vector normal al colector ($\vec{n}$) en establecer su relación con colectores dispuestos en terrenos no horizontales, tomando como base el modelo de Hay-Davies (Hay, 1993) según la ecuación (1.1). Este modelo consta de tres términos que evalúan las componentes directa, difusa y reflejada respectivamente. Los valores de I_B e I_D se determinan mediante el modelo de Collares-Pereira (Collares-Pereira and Rabl, 1979).

$$I = \frac{cos\theta}{cos\theta_z} I_B + \left[\left(\frac{cos\theta}{cos\theta_z}\right)\frac{I_B}{I_{OH}} + \left(1 - \frac{I_B}{I_{OH}}\right)\frac{1+cos\beta}{2}\right] I_D + \rho\frac{1-cos\beta}{2}(I_B + I_D) \quad (1.1)$$

Con la idea de seguir avanzando en la evaluación de la irradiancia en todos sus términos, esta misma metodología se ha seguido en la tercera aportación de la presente tesis, si bien de aplicación a seguidores solares de doble eje, empleando el modelo empírico (Perez et al., 1990) según la ecuación (1.2). De esta forma, se obtienen valores más próximos a mediciones realizadas y que, al igual que en el caso anterior, permiten determinar la orientación óptima del vector normal del colector ($\vec{n}$).

$$I = \frac{cos\,\theta}{cos\,\theta_z} I_B + \left[(1 - F_1)\frac{1 + cos\,\beta}{2} + F_1\frac{a}{b} + F_2\,sin\,\beta\right] I_D + \rho\frac{1 - cos\,\beta}{2}(I_B + I_D) \quad (1.2)$$

Finalmente, obtenida la orientación óptima en cada uno de los modelos utilizados, se procede a la evaluación del análisis de sombreo y técnica de retroseguimiento en cada uno de ellos.

1.3. Sombreo y retroseguimiento

El diseño en la disposición de los colectores fotovoltaicos representa un papel determinante en la producción de energía debido a la interferencia que pueden realizar unos sobre otros por efectos de sombreamiento.

La componente directa se ve comprometida en el caso de sombreamiento de unos colectores sobre otros, lo que disminuye el rendimiento y eleva la temperatura de las células sombreadas, pudiendo provocar una grave alteración en el panel sombreado (*hot spots*) (Belhachat and Larbes, 2015; Satpathy and Sharma, 2019).

(Martínez-Moreno et al., 2010) propusieron un modelo predictivo para la evaluación de pérdidas de potencia causadas por el sombreamiento, el cual fue validado por varios autores (Fartaria and Pereira, 2013; Hu and Yao, 2016), desarrollando modelos más extensos basados en el modelo de Martínez-Moreno. Otros autores tales como (Narvarte and Lorenzo, 2008), estudiaron la productividad de una instalación PV considerando distintos tipos de seguimiento solar y basándose en tres hipótesis simplificadas para estimar las pérdidas por sombreado.

En bibliografía consultada, destacan estudios que han tenido en cuenta la influencia del sombreo en la optimización de instalaciones PV (Díaz-Dorado et al., 2017, 2014). En estos estudios los sombreos son caracterizados considerando una estrategia de seguimiento convencional o astronómico que procura que la superficie colectora conserve la perpendicularidad con los rayos solares la mayor parte del tiempo de seguimiento.

Una posible solución al problema del intersombreo pasaría por una distribución en el terreno con amplias separaciones entre paneles. Sin embargo, el alto precio que este factor representa frente al precio cada vez más bajo de los paneles (Perpiñán, 2012) hace que sea necesario el estudio pormenorizado para la búsqueda de la interdistancia óptima.

No obstante, los efectos de sombreamiento pueden ser reducidos e incluso eliminados utilizando técnicas de retroseguimiento solar que minimicen dicho impacto (Fernández-Ahumada et al., 2020b, 2020a). Esta técnica consiste en desviar de la dirección de máxima irradiancia los captadores para evitar dicho efecto.

Diferentes autores (Lorenzo et al., 2011; Panico et al., 1991; Pedro, 2016) han demostrado que, dentro de las grandes ventajas que se encuentran en la utilización de esta técnica, se

observa la disminución de la interdistancia entre los seguidores. Esto consigue un mejor aprovechamiento del terreno y, por consiguiente, un GCR mayor, una mejora del balance energético frente a las que no disponen de este sistema (Lorenzo et al., 2011) y, por último, una disminución en los costes de mantenimiento al evitar la generación de puntos calientes en los paneles.

En esta tesis, las metodologías de estudio del seguimiento e interdistancia se aplican a seguidores solares de 1 y 2 ejes, lo que amplía el espectro de estudio y resultados. Se ha seguido un enfoque de análisis vectorial para la caracterización astronómica y posicional de los seguidores.

En el caso de seguidores de 1 solo eje, el análisis de intersombreo se ha abordado dentro de un triedro de referencia determinado por el eje del colector ($\vec{e}$), la normal al terreno ($\overrightarrow{n_T}$) y el vector normal a los anteriores ($\vec{q}$), lo que ha permitido relacionarlo con la inclinación del terreno (β) e introducir dicha variable en el estudio y su evaluar su grado de influencia.

En cuanto a seguidores de doble eje, dicho análisis se ha abordado mediante el criterio dicotómico basado en el álgebra de Minkowski (Avnaim and Boissonnat 1989; B. Chazelle 1983).

1.4. Desarrollo de sensor para la determinación de irradiancia máxima

(Eldin et al., 2016) concluyeron la necesidad de monitorizar instalaciones de paneles fotovoltaicos y comprobaron que la potencia de salida de captadores monitorizados se acerca a la óptima, que depende de las condiciones ambientales. Cada vez es más extendido el desarrollo de sistemas de monitorización que basan su estrategia de seguimiento en factores tales como la búsqueda en la esfera celeste de los puntos de máxima irradiancia y que no implican un incremento en el coste de implementación y mantenimiento.

Para ello, el uso de la tecnología basada en HW libre aporta soluciones similares o incluso mejores que las comerciales mediante una inversión de bajo coste (Fuentes et al., 2014) y, paralelamente, permite intercambiar los resultados obtenidos a toda la comunidad científica (Pearce, 2013) además de, por su versatilidad, añadir dispositivos que permitan aumentar la información obtenida (Fuentes et al., 2014).

Paralelamente, el uso de microcontroladores basados en HW libre presenta una ventaja competitiva desde el punto de vista económico frente al control basado en PLC (Singh et al., 2018) y cada vez es más común encontrar en la literatura propuestas basadas en HW libre de aplicación al seguimiento solar. Destacan las basadas en Arduino e IoT por su flexibilidad y bajo coste, sin olvidar su alto nivel de conectividad. Otros autores han desarrollado sistemas basados en IoT y LoRa (Paredes-Parra et al., 2019), mientras que (Pereira et al., 2018) desarrollaron un sistema de captación de datos basándose en tecnología Raspberry Pi e IoT.

Por consiguiente, se observa que cada vez es más frecuente en el ámbito de la energía solar fotovoltaica encontrar propuestas basadas en estrategias de seguimiento mediante HW libre, así como la implementación de sensores de bajo coste y mantenimiento que sigan la trayectoria solar (Kelly and Gibson, 2009; Yao et al., 2014).

La estrategia de seguimiento basada en modelos teóricos y análisis matemáticos nos ha permitido establecer orientaciones óptimas de los colectores y paralelamente evaluar la influencia de intersombreo. En el segundo trabajo de la presente tesis se considera necesario llevar esto a la práctica, lo que se ha traducido en el desarrollo de un sensor dispuesto sobre un seguidor solar omnidireccional basado en HW libre y código abierto (FOSH). Dicho sensor cuenta con un sistema de control sencillo asociado a tecnología IoT y de aplicación en seguidores de doble eje, lo que nos permite determinar en cada instante qué punto de la bóveda de la esfera celeste es el óptimo para obtener la máxima irradiancia global.

Lo anterior, combinado con un estudio previo de análisis de sombreamiento diseñado por los autores (Fernández-Ahumada et al., 2020b, 2020a), permite excluir de las zonas de posible orientación aquellas que producen interferencias entre colectores mediante un escaneo previo.

En esta fase previa se estudia si, a priori, una dirección ha de ser contemplada o no, restringiendo y, por tanto, disminuyendo su proceso de búsqueda de las direcciones espaciales que nos proporcionarán máxima captación solar. Las direcciones pueden aparecer sombreadas y, por tanto, enviar a los seguidores el ángulo de azimut (γ) y elevación (α) idóneos para cada día juliano (d_j) e instante determinado (t).

Esta técnica establece una reorientación de los seguidores considerando mediciones instantáneas de radiación que permiten saber a priori cúal es la orientación óptima del conjunto de seguidores.

El dispositivo, que cuenta con 2 GDL, realiza un barrido bidireccional en azimut [-180°,180°] y elevación [0°,90°]. Toda la estructura soporte ha sido fabricado por impresión aditiva, utilizando como material filamento de acrilonitrilo butadieno estireno (ABS) y encapsulado en cúpula de metacrilato transparente.

En cuanto a la electrónica, cuenta con un conjunto de sensores compuesto por reloj en tiempo real DS1307, con alimentación autónoma mediante batería CR2025. Adicionalmnete se ha dispuesto una célula fotovoltaica calibrada que proporciona valores de intensidad de salida comprendidas entre 36 mA-288 mA para valores de irradiancia entre los 125 W/m^2-1000 W/m^2. Finalmente, se ha completado con dos microinterruptores mecánicos para fijar la posición relativa cero.

El procesamiento se lleva a cabo a través de una placa TTGO ESP32 Lora que integra entradas y salidas analógicas y digitales, así como varias interfaces de comunicación, tanto inalámbricas (Wi-Fi y Bluetooth Low Energy) como cableadas (I2C, SPI, UART). La placa cuenta con módulo de comunicación LoRa, modelo SEMTECH SX1276 que permite la comunicación a una frecuencia de 868 MHz.

El movimiento en los dos ejes se consigue mediante dos motores paso a paso modelo 28BYJ - 48, controlados por dos unidades LM298, con 4096 pasos por revolución lo que proporciona una precisión de 0,001534 radianes por paso. Por último, el módulo de comunicaciones entre el dispositivo y los captadores ha sido diseñado acorde al rango que permita un radio entre 3 km y 15 km.

1.5. Influencia de la geometría de los captadores e inclinación del terreno

La disminución en la potencia de salida provocada por el desajuste I-V de celdas de un módulo PV debido a factores tales como el sombreamiento, ha sido ampliamente analizado por distintos autores (Karatepe et al., 2007; Kawamura et al., 2003; Meyer and Van Dyk, 2004), así como la disminución en el rendimiento energético provocado por el sombreamiento parcial de paneles solares (Kaushika and Gautam, 2003; Meyer and Van Dyk, 2004).

(Perpiñán, 2012), establece que la relación entre la superficie de colectores y del terreno (GCR) depende de las variables de diseño de estas. Actualmente en instalaciones PV que ya están en producción, y en las que no se realiza retroseguimiento se plantean técnicas de eliminación de sombreo mediante la modificación geométrica de los colectores (DEGERiberica, 2020). En la mayoría de los casos, esta actuación se realiza de forma arbitraria, procediendo a la eliminación de aquellos módulos que, mediante la observación diaria, permanecen un alto porcentaje de tiempo interferido por captadores colindantes.

La mayoría de los colectores PV que se encuentran en las plantas conectadas a red son rectangulares, aunque existen ya algunas instalaciones con seguimiento solar a dos ejes donde los colectores presentan otras formas geométricas, como, por ejemplo, las desarrolladas por la empresa Deger Ibérica en Tarragona (España), en Ontario (Canadá) o en Estonia.

Sin embargo, no se han encontrado en la bibliografía trabajos encaminados a la caracterización de la forma geométrica de los colectores o su grado de modularidad en lo que respecta a la optimización del rendimiento de una instalación fotovoltaica ante la posible incidencia de sombras.

En el tercer trabajo académico de esta tesis, se presenta el estudio de la captación radiativa en seguidores de doble eje, con modificación de interdistancias y distribución espacial (cuadrícula y tresbolillo). Como elemento novedoso se han introducido en el estudio colectores PV con geometrías no rectangulares con eliminación de módulos fotovoltaicos, combinándolo con técnica de retroseguimiento para paliar el efecto de intersombreado.

Finalmente, en la mayor parte de los estudios, la búsqueda de la distribución óptima de paneles en PV formula su análisis en cuanto a la disposición de los colectores en terrenos de superficie horizontal.

Dado que, no siempre se disponen de las ubicaciones ideales en cuanto a orientación en inclinación, es necesario incluir en el diseño de las instalaciones la influencia de la orografía tanto en la captación como en el sombreamiento de unos colectores sobre otros, variable incluida en el análisis en nuestro primer trabajo académico.

Capítulo 2 Hipótesis y objetivos

2.1. Hipótesis

2.2. Objetivos

2.1. Hipótesis

- **Hipótesis global (artículos 1, 2 y 3)**

Es necesario avanzar en el estudio del comportamiento de los seguidores solares de 1 y 2 ejes al ser una tecnología cada vez más demandada en captación solar.

- **Hipótesis A (artículos 1 y 3)**

La variable de irradiancia ha de ser analizada en todas sus componentes (directa, difusa y reflejada).

- **Hipótesis B (artículos 1, 2 y 3)**

Los seguidores solares se distribuyen en agrupaciones y, por consiguiente, el efecto de sombreamiento entre ellos ha de ser analizado.

- **Hipótesis C (artículo 1 y 3)**

Orientaciones a priori óptimas pueden verse afectadas por efecto de sombreamiento y, por consiguiente, ser necesaria su reorientación (retroseguimiento).

- **Hipótesis D (artículo 2)**

Se puede mapear la bóveda celeste para la determinación de la orientación óptima de máxima irradiancia excluyendo las zonas de sombreo.

- **Hipótesis E (artículo 1 y 3)**

Variables como inclinación del terreno y geometría de los colectores pueden afectar en estrategias de seguimiento y análisis de sombreos.

2.2. Objetivos

- **Objetivo A (artículos 1 y 3)**

Obtener las trayectorias óptimas de seguimiento en instalaciones fotovoltaicas con seguidores solares de 1 y 2 ejes sin considerar el efecto de intersombreo.

- **Objetivo B (artículo 1)**

Generar conocimiento a partir de las ecuaciones de modelización de la irradiancia incluyendo el análisis de sombreo e inclinación del terreno.

- **Objetivo C (artículo 3)**

Generar conocimiento a partir de las ecuaciones de modelización de la irradiancia incluyendo el análisis de sombreo y geometría de los colectores.

- **Objetivo D (artículo 2)**

Desarrollar un sensor que permita la medición de la irradiancia instantánea e incluya un proceso previo de eliminación de orientaciones que pudieran causar intersombreo entre colectores.

- **Objetivo E (artículo 1 y 3)**

Obtener estrategias de retroseguimiento para seguidores solares de 1 y 2 ejes mediante la evaluación de la irradiancia en todas sus componentes considerando efectos de sombreo y otras variables tales como inclinación del terreno y geometría de los colectores.

Capítulo 3 . Analysis of the influence of terrain orientation on the PV facilities design with single-axis trackers

3.1. Introduction.

3.2. Materials and Methods.

- 3.2.1. Astronomical Bases and Irradiance Model.
- 3.2.2. Optimisation of Collector Orientation.
- 3.2.3. Backtracking.
- 3.2.4. Software Applications for Analysis.

3.3. Results and Discussions.

3.4. Conclusions.

Analysis of the influence of terrain orientation on the PV facilities design with single-axis trackers

Gómez-Uceda, FJ[1]; Moreno-García, IM[2*]; Jiménez-Martínez, JM[3]; López-Luque, R[4]; Fernández-Ahumada, LM[5]

[1] Department of Mechanics, University of Córdoba (Spain).

[2] Department of Electronic and Computer Engineering, University of Córdoba (Spain).

[3] Physics for Renewable Energies Research Group, University of Córdoba (Spain).

[4] Department of Applied Physics, Radiology and Physical Medicine, University of Córdoba (Spain).

[5] Department of Electrical Engineering and Automatics, University of Córdoba (Spain).

***** Correspondence: isabel.moreno@uco.es; Tel.: +34 957212533. Campus of Rabanales, University of Córdoba. 14071. Córdoba (Spain).

Abstract: This paper investigates how to optimally orient the photovoltaic solar trackers of an axis parallel to the terrain applying the sky model of Hay-Davies. This problem has been widely studied. However, there is very limited information on studies that consider the orientation (inclination and azimuth of the terrain). This paper provides a study of incident solar irradiance that can be used for fields with variable orientation and considering different azimuths of the axis of rotation. Also, a case study into the South of Spain is shown, considering different inclination and orientation terrain values. Results obtained of this study indicate as novelty that, for lands that are not South-facing, the rotation axis azimuth of solar trackers should be different from zero and varies in the same direction as the land azimuth in order to maximize energy production. Annual energy production is sensitive to changes in rotation axis azimuth (around 3%).

Keywords: solar energy; single-axis solar tracker; backtracking; optimisation

3.1. Introduction

At present, population growth, the deficiency of natural resources, and global warming mean a challenge around the world. In recent years, various initiatives have been working on the development or replacement of the current power grid to obtain a system that allows greater efficiency in the electrical system, and a reduction in energy waste by reducing losses during distribution (Carballo et al., 2018). Consequently, it contributes to the promotion of renewable sources and minimises the environmental impact in the future. Therefore, there is a requirement to preserve the environment and to improve the penetration of alternative energy resources (United Nations, 2019). Within the framework of renewable energies, solar energy is the one that is emerging for having a more remarkable growth in the last years thanks to the reduction of costs and the legal impulse in many countries (Renewable Energy Agency, 2020; Ribó-Pérez et al., 2019). In the same way, photovoltaic (PV) is one of the technologies with a better future projection due to its simplicity, scalability and continuous manufacture, operation and maintenance reduction costs for solar panels (Kavlak et al., 2018).

However, the lack of the linearity in solar energy received by solar panels mainly caused by Earth-Sun relative displacement is a disadvantage to consider. It is necessary to redefine the solar tracking systems increasing solar irradiance capture by PV collectors and, therefore, improve energy production (Hua et al., 2019).

According to the movement, the following systems can be considered: single-axis tracking systems, where a mobile element adopts its position by rotating around a fixed axis; and two-axis tracking systems, where the collector plane rotates about two fixed axes, allowing the orientation towards any direction of the celestial sphere (Hafez et al., 2018; Nsengiyumva et al., 2018).

Several proposals have analysed the efficiency of energy production using two-axis trackers compared with single-axis tracking and fixed panels (Abdallah and Nijmeh, 2004; Bahrami et al., 2016; Koussa et al., 2011). In this respect, Bahrami et al. (Bahrami et al., 2016) have determined that the increase in solar production of a PV plant with two-axis trackers compared to a system with single-axis trackers at the same latitude is 0.42-23.4%. Similarly, the improvement compared to a fixed-panel system is around 17.22-31.23%. Other authors, such as Hua et al (Hua et al., 2019), have concluded that fluctuations in energy production can be reduced depending on the trackers distribution in the PV plant.

Regarding movement strategy, two types can be distinguished: those based on the information of pyranometers and those based on mathematical statements, determined by terrestrial and solar movement. For this last option two approaches can be considered. On the

one hand, the Sun's position is predicted by spherical trigonometry (Braun and Mitchell, 1983; Duffie and Beckman, 2013; Narvarte and Lorenzo, 2008), and on the other hand, it is calculated by vectorial calculation (Parkin, 2010; Sproul, 2007). This article is based on vectorial calculation.

The most frequently followed strategy in solar tracking is the one based on the astronomical model. This method tries to minimise the angle composed by direct sunrays and the normal vector to the collector plane, thereby increasing the direct part of solar irradiance. However, this strategy is not optimal for the PV energy case since it does not involve the remaining parts (diffuse and reflected) which contribute to energy production. This issue was thoroughly studied by Duffie and Beckman(Duffie and Beckman, 2013), finding that on cloudy days astronomical tracking obtains an irradiance lower than fixed panels because during those days direct radiation fails.

The PV plant yield can be highly affected when panels are shaded among themselves (Fan et al., 2017; Satpathy and Sharma, 2019; Seyedmahmoudian et al., 2016). Two consequences are derived from the shading effect on the panels. The first consequence is the reduction of captured irradiance since the direct component does not reach the cell surface. The second consequence is the increase in temperature of the shaded cell since it works as a resistive load absorbing from the adjacent cells and thus, accelerates its deterioration (Belhachat and Larbes, 2015; Satpathy and Sharma, 2019). In this respect, it would be advisable to arrange the location of the panels in such a way that there is no inter-shadowing. However, given the high price of the terrain and the increasingly low price of the panels, the most common is to find PV plants with distances between panels that produce shade (Saint-Drenan and Barbier, 2019). This important scientific challenge has been widely studied by many authors who have decided to study the reduction in PV production due to shade in the panels (Fan et al., 2017; Perpiñán, 2012; Saint-Drenan and Barbier, 2019; Satpathy and Sharma, 2019).

In addition, solar geometry and PV plant design also affect energy production. So, solutions devoted to simulate all aspects demand significant calculation times (Deline et al., 2013; Martínez-Moreno et al., 2010). However, authors such as Saint-Drenan and Barbier (Saint-Drenan and Barbier, 2019) have started to optimise this issue, featuring a model with a low computational load. The model can maintain the required accuracy levels using a few input parameters. This method has been tested in only two PV plants. The authors recommend extending the validation to other facilities and geometries. Consequently, it is necessary to continue studying the influence of shading on production.

Under this paradigm, the backtracking method is an adequate solution for the inter-shading problem in PV plants (Panico et al., 1992), especially during sunrise and sunset when

the solar beams are very low and there is greater inter-shadowing between PV modules. This method varies the optimum angle of greatest solar incidence to prevent the back panels from being shaded (Figure 3.1). Although the result of using backtracking is a lower angle of incidence of solar collection, it is more favourable than the projection of shadows between adjacent solar panels (Antonanzas et al., 2018).

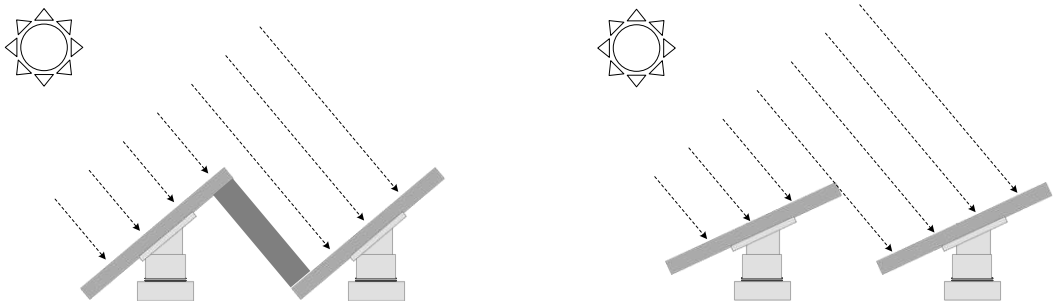

Figure 3.1. Bactracking technique

The use of backtracking has become a technique that increases energy production in photovoltaic plants in cloudy periods. The diffuse component of solar radiation is much more relevant in these cases and, therefore, the "approaches" that ignore this component (such as astronomical ones) are no longer optimal.

This is not the only advantage of employing backtracking. There is also the reduction in hot spots on the trackers, which increases its life span and reduces breakdowns. It also improves the GCR of the installations, which has the effect of reducing the economic impact of the soil required when building plants (Fernández-Ahumada et al., 2020a).

For this reason, there is a niche in scientific work focused on the development of options from backtracking and on the optimisation of solutions responding to the challenge posed by solar panels not exclusively focused on classic tracking (Antonanzas et al., 2018; Kelly and Gibson, 2009; Koussa et al., 2011; Quesada et al., 2015).

From this perspective, a work based on tracking has been proposed with the aim of optimising production throughout the movement including the backtracking sections(Fernández-Ahumada et al., 2020a, 2017). To achieve this, the search for a panel path is underway that generates optimum production under the premise that the panel is isolated and therefore does not receive shade from any adjacent panel. Once this proposal has been considered, a condition is established to verify the possible shading between photovoltaic panels. After these two steps, the shaded orientations are shown against those that are not shaded. Thus, they establish a path that optimises production including the non-shading caused between modules.

Since it is difficult to find a completely horizontal location for photovoltaic plants, further studies and deeper knowledge of photovoltaic trackers are required to offer optimisation guidelines in solar capture. This study has been performed by means of: (**a**) mathematical modelling for solar capture on trackers; (**b**) programming that allows automation of the calculations; (**c**) simulation of the case studies; and (**d**) analysis of optimal conclusions. In this regard, conclusions have been drawn on orientations, land inclinations, distances between modules, etc. in terms of produced energy.

Figure 3.2.a and Figure 3.2.b represent angles χ (azimuth) and β (inclination) for a generic terrain. The angle γ (azimuth of the collector rotation axis) is also represented. This article, based on the Hay-Davies model, characterises solar radiation on trackers using angles χ, β and γ.

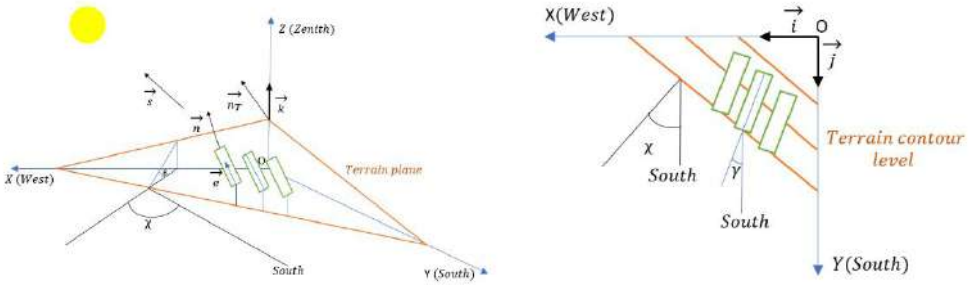

Figure 3.2. Relevant geometry and vectors for the current study and Earth reference system. a) Perspective view; b) Orthogonal view

The remainder of the article is organised as follows. In the next section, Section 2, the model used, mathematical optimisation bases, backtracking and software development are presented. Section 3 outlines how the methodology was tested in Córdoba, Spain, and the results are discussed. In Section 4, conclusions are drawn based on the restrictions shown and further research is indicated.

3.2. Materials and Methods

3.2.1. Astronomical Bases and Irradiance Model

It is fundamental to know the concrete position of the Sun at each moment of the day and on each day of the year, to determine the direction of the solar beams. It is possible to determine the position of the sun accurately by using astronomical geometry. For this purpose, a solar vector is defined, expressed with respect to a terrestrial reference system (Figure 3.2), formed by the axes Ox, towards the West; Oy, towards the South; and Oz in the zenithal direction. The position is determined by equations (3.1) and (3.2):

$$\vec{s} = s_x\vec{\imath} + s_y\vec{\jmath} + s_z\vec{k} \tag{3.1}$$

$$\vec{s} = sin\Omega t \cdot cos\delta\vec{\imath} + (cos\Omega t \cdot cos\delta \cdot sin\varphi - sin\delta \cdot cos\varphi)\vec{\jmath} + (cos\Omega t \cdot cos\delta \cdot cos\varphi + sin\delta \cdot sin\varphi)\vec{k} \tag{3.2}$$

Where δ represents the solar declination, φ the latitude and Ωt the hour angle. This angle is calculated as the Earth's rotation speed, 2π/24 rad/h, for the hours since solar noon (Fernández-Ahumada et al., 2020a).

In PV, all irradiance components (direct, diffuse, and reflected irradiance) are usable. Traditionally the astronomical model has been used. Applying the astronomical model to solar tracking means that the angle formed between the direct solar rays and the normal angle to the collector's surface θ must be as low as possible. With astronomical tracking, the value of the direct irradiance component is maximised, which is appropriate for applications focused on this component (such as concentration technologies). Therefore, this type of tracking is not the most suitable. For instance, on cloudy days, when the solar disk is not visible and direct radiation does not reach the collectors, collectors located on a fixed horizontal position would collect more energy than those with astronomical tracking. So, to study the influence of diffuse and reflected components on solar tracking several sky models are proposed.

The Hay-Davies method (Hay, 1993) is considered for making the calculations in this work since it adequately describes the anisotropy of radiation (Mousazadeh et al., 2009), in addition to being notable for its simplicity as opposed to other more complex models such as those of Muneer (Muneer, 1990) and Perez (Perez et al., 1990), obtaining high quality results (Diez-Mediavilla et al., 2005; Loutzenhiser et al., 2007; Mubarak et al., 2017). This model establishes that a determined fraction of the diffuse irradiance is directed from the direction of the solar disk. Models such as Hay-Davies (Hay, 1993) describe the irradiance affecting a solar panel considering the three components, direct, diffuse and reflected, but considering that the diffuse component has a preferential direction in which the diffuse radiation is greater than in the other. According to Hay-Davies (Hay, 1993), the mathematical expression is the equation (3.3) where the first term appears the direct irradiance I_B, the second term refers to the diffuse irradiance I_D, and the third term corresponds to the reflected component, it considers the visible soil fraction and the albedo, ρ. I_B and I_D have been determined by the Collares-Pereira model (Collares-Pereira and Rabl, 1979).

$$I = \frac{cos\theta}{cos\theta_z} I_B + \left[\left(\frac{cos\theta}{cos\theta_z}\right)\frac{I_B}{I_{OH}} + \left(1 - \frac{I_B}{I_{OH}}\right)\frac{1 + cos\xi}{2}\right] I_D + \rho\frac{1 - cos\xi}{2}(I_B + I_D) \tag{3.3}$$

ξ being the inclination angle of the collector, and θ_Z the solar zenith angle, that is, the angle that forms the solar vector with the zenith axis.

3.2.2.Optimisation of Collector Orientation

The subject of this study is to establish guidelines for designing facilities with solar trackers on a rotation axis $\vec{e}$. This axis is considered as parallel to the terrain; no restrictions are initially imposed on it. The general results are valid for any disposition.

The degrees of freedom of the orientation of a surface are two, azimuth χ and inclination β. In the case of single-axis trackers, it would only be the elevation. The orientation of the panel is characterised by a single vector $\vec{n}$, normal to the surface of the panel. So, the objective will be the calculation of $\vec{n}$ which implies that the solar capture is the maximum.

To continue with the vector treatment, the cosines of the angles θ, θ_Z and ξ that appear in the expressions of the different models of the irradiance are expressed as the scalar products of $\vec{s}, \vec{n}$ and $\vec{k}$, being:

$$cos\theta = \vec{s} \cdot \vec{n} \tag{3.4}$$

$$cos\theta_Z = \vec{s} \cdot \vec{k} \tag{3.5}$$

$$cos\xi = \vec{k} \cdot \vec{n} \tag{3.6}$$

Substituting the previous expressions in the Hay-Davies model (Hay, 1993):

$$I = \frac{\vec{s} \cdot \vec{n}}{\vec{s} \cdot \vec{k}} I_B + \left[\left(\frac{\vec{s} \cdot \vec{n}}{\vec{s} \cdot \vec{k}} \right) \frac{I_B}{I_{OH}} + \left(1 - \frac{I_B}{I_{OH}} \right) \frac{1 + \vec{k} \cdot \vec{n}}{2} \right] I_D + \rho \frac{1 - \vec{k} \cdot \vec{n}}{2} (I_B + I_D) \tag{3.7}$$

To optimise the irradiance $I = I\left(\vec{s} \cdot \vec{n}\,, \vec{k} \cdot \vec{n}\right)$ the Lagrange multiplier method is used, where the following restrictions are defined $\vec{e} \cdot \vec{e} = 1$; $\vec{n} \cdot \vec{n} = 1$; $\vec{e} \cdot \vec{n} = 0$, $\vec{e}$ being the normal ground vector.

$$\Phi(\vec{n}, \lambda, \mu, \nu) = I\left(\vec{s} \cdot \vec{n}\,, \vec{k} \cdot \vec{n}\right) + \lambda(1 - \vec{n} \cdot \vec{n}) + \mu(0 - \vec{e} \cdot \vec{n}) + \nu(1 - \vec{e} \cdot \vec{e}) \tag{3.8}$$

Being the differential:

$$\mathrm{d}\Phi = \left[\frac{\partial I}{\partial(\vec{s} \cdot \vec{n})} \vec{s} + \frac{\partial I}{\partial\left(\vec{k} \cdot \vec{n}\right)} \vec{k} - 2\lambda\vec{n} - \mu\vec{e} \right] \cdot d\vec{n} + [1 - \vec{n} \cdot \vec{n}] d\lambda + d\mu[0 - \vec{e} \cdot \vec{n}] + [1 - \vec{e} \cdot \vec{e}] d\nu \tag{3.9}$$

by matching the brackets to zero.

$$\mathrm{d}\Phi = \left[\frac{\partial I}{\partial(\vec{s}\cdot\vec{n})}\vec{s} + \frac{\partial I}{\partial(\vec{k}\cdot\vec{n})}\vec{k} - 2\lambda\vec{n} - \mu\vec{e}\right]\cdot d\vec{n} + [1-\vec{n}\cdot\vec{n}]d\lambda + d\mu[0-\vec{e}\cdot\vec{n}] + [1-\vec{e}\cdot\vec{e}]dv \tag{3.10}$$

Naming

$$\vec{w} = \frac{\partial I}{\partial(\vec{s}\cdot\vec{n})}\vec{s} + \frac{\partial I}{\partial(\vec{k}\cdot\vec{n})}\vec{k} \tag{3.11}$$

three vectors $\vec{w}$, $\vec{n}$ and $\vec{e}$ appear. These vectors fulfill the relation:

$$\vec{w} - 2\lambda\vec{n} - \mu\vec{e} = 0 \tag{3.12}$$

So, they are linearly dependent and therefore coplanar.

As $\vec{n}$ is perpendicular to $\vec{e}$, it can be expressed more easily.

$$\vec{n} = \frac{\vec{w} - (\vec{w}\cdot\vec{e})\cdot\vec{e}}{|\vec{w} - (\vec{w}\cdot\vec{e})\cdot\vec{e}|} \tag{3.13}$$

Figure 3.3 represents the plane formed by the vectors $\vec{w}$, $\vec{n}$, and $\vec{e}$.

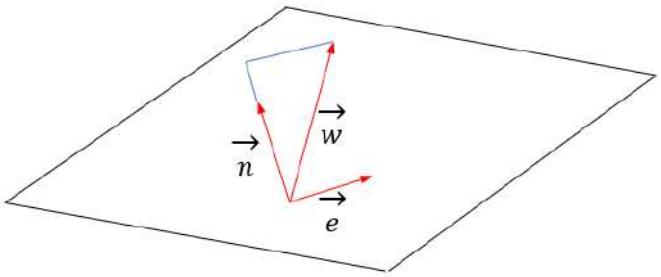

Figure 3.3. Representation of the plane formed by the vectors $\vec{w}$, $\vec{n}$ and $\vec{e}$.

Replacing the vectors $\vec{e}$ and $\vec{w}$ by their expressions results in the equation that defines the vector $\vec{n}$:

$$\vec{n} \tag{3.14}$$

$$= \frac{\frac{\partial I}{\partial(\vec{s}\cdot\vec{n})}}{\sqrt{\left(\frac{\partial I}{\partial(\vec{s}\cdot\vec{n})}\right)^2 + \left(\frac{\partial I}{\partial(\vec{k}\cdot\vec{n})}\right)^2 + 2\left(\frac{\partial I}{\partial(\vec{s}\cdot\vec{n})}\right)\left(\frac{\partial I}{\partial(\vec{k}\cdot\vec{n})}\right)\vec{s}\cdot\vec{k} - \left(\frac{\partial I}{\partial(\vec{s}\cdot\vec{n})}\vec{s}\cdot\vec{e} + \frac{\partial I}{\partial(\vec{k}\cdot\vec{n})}\vec{k}\cdot\vec{e}\right)^2}}\vec{s}$$

$$+ \frac{\frac{\partial I}{\partial(\vec{k}\cdot\vec{n})}}{\sqrt{\left(\frac{\partial I}{\partial(\vec{s}\cdot\vec{n})}\right)^2 + \left(\frac{\partial I}{\partial(\vec{k}\cdot\vec{n})}\right)^2 + 2\left(\frac{\partial I}{\partial(\vec{s}\cdot\vec{n})}\right)\left(\frac{\partial I}{\partial(\vec{k}\cdot\vec{n})}\right)\vec{s}\cdot\vec{k} - \left(\frac{\partial I}{\partial(\vec{s}\cdot\vec{n})}\vec{s}\cdot\vec{e} + \frac{\partial I}{\partial(\vec{k}\cdot\vec{n})}\vec{k}\cdot\vec{e}\right)^2}}\vec{k}$$

$$- \frac{\frac{\partial I}{\partial(\vec{s}\cdot\vec{n})}\vec{s}\cdot\vec{e} + \frac{\partial I}{\partial(\vec{k}\cdot\vec{n})}\vec{k}\cdot\vec{e}}{\sqrt{\left(\frac{\partial I}{\partial(\vec{s}\cdot\vec{n})}\right)^2 + \left(\frac{\partial I}{\partial(\vec{k}\cdot\vec{n})}\right)^2 + 2\left(\frac{\partial I}{\partial(\vec{s}\cdot\vec{n})}\right)\left(\frac{\partial I}{\partial(\vec{k}\cdot\vec{n})}\right)\vec{s}\cdot\vec{k} - \left(\frac{\partial I}{\partial(\vec{s}\cdot\vec{n})}\vec{s}\cdot\vec{e} + \frac{\partial I}{\partial(\vec{k}\cdot\vec{n})}\vec{k}\cdot\vec{e}\right)^2}}\vec{e}$$

This result allows one to calculate the optimal direction of the normal vector for any irradiance model, in any direction of the rotation axis and different positions of the Sun. By replacing the values from the partial derivatives in equation (3.14) obtained from equation (3.7):

$$\frac{\partial I}{\partial(\vec{s}\cdot\vec{n})} = \frac{I_b}{s_z}\left(1 + \frac{I_D}{I_{OH}}\right)$$

$$\frac{\partial I}{\partial(\vec{k}\cdot\vec{n})} = \left(1 - \frac{I_B}{I_{OH}}\right)\frac{I_D}{2} - \frac{\rho}{2}(I_B + I_D) \tag{3.15}$$

Considering equation (3.16), the values of $\vec{n}$ are obtained at any given time for optimum irradiance incidence.

For example, for the simplest case with a direct irradiance model which only considers the first term of equation (3.3), and with the rotation axis of the solar panels horizontal to the ground, a normal vector like the following results:

And the vector $\vec{e}$ is:

$$\vec{e} = \frac{cos\beta\cdot sin\gamma}{\sqrt{sin^2\beta + cos^2\beta cos^2(\gamma-\chi)}}\vec{\imath} + \frac{cos\beta\cdot cos\gamma}{\sqrt{sin^2\beta + cos^2\beta cos^2(\gamma-\chi)}}\vec{\jmath} - \frac{sin\beta\cdot cos(\gamma-\chi)}{\sqrt{sin^2\beta + cos^2\beta cos^2(\gamma-\chi)}}\vec{k} \tag{3.16}$$

β being the inclination of the terrain, χ the azimuth of the terrain, and γ the azimuth of the rotation axis collector.

3.2.3.. Backtracking

In the previous section, the methodology to determine the orientation of the solar tracker to obtain the maximum solar capture has been detailed. This section will describe the method followed to prevent a solar tracker from shading an adjacent tracker. To do so, only two factors must be considered: the position of the sun and the orientation of the panels. To study intershadowing it is convenient to use an auxiliary reference system where the representation plane is perpendicular to the tracker axis. For this purpose, the vector $\vec{q}$, equation (3.17), is defined.

$$\vec{q} = \vec{e} \times \overrightarrow{n_T} \tag{3.17}$$

where $\vec{q}$ is a perpendicular vector to the normal ground vector $\vec{e}$, as well as to the rotation axis vector $\overrightarrow{n_T}$. The solar vector $\vec{s}$and the plane normal vector in the optimal position $\vec{n}$ will be named $\overrightarrow{s'}$ and $\overrightarrow{n'}$ in the reference system composed by $\{\vec{q}, \vec{e}, \overrightarrow{n_T}\}$ (Figure 3.4).

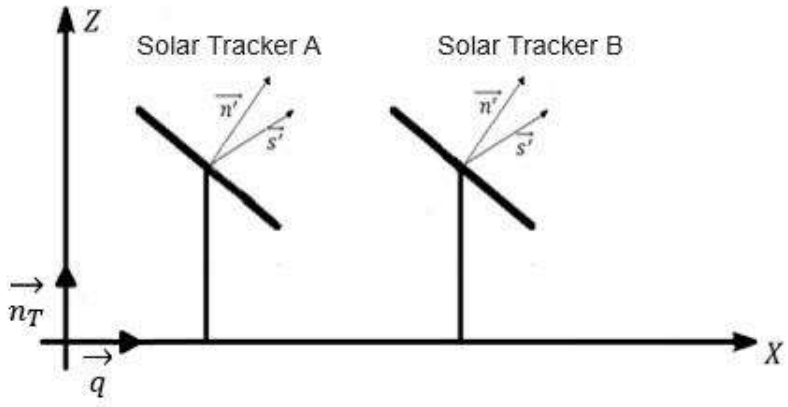

Figure 3.4. Solar trackers, normal vector, and solar vector in the reference system.

The procedure for estimating whether a solar panel B shades the adjacent panel A is to project the shadow of panel B onto the straight line containing the adjacent panel A (Figure 3.5). Since the sun's rays are parallel to each other, the projection of one point is sufficient. First, a vector is defined from the centre of solar panel B with the direction of the solar rays $\tau\overrightarrow{s'}$. Secondly, the central point of the solar panel A is projected to the centre of the panel B, defining $\vec{a}$. The study of this vector will determine whether there is shading.

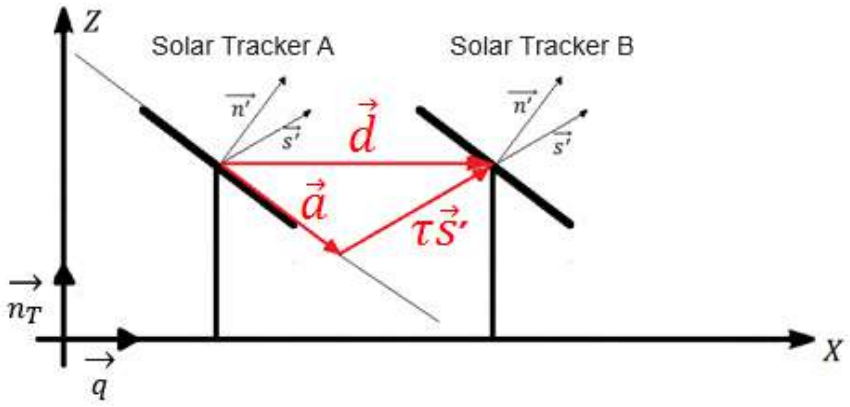

Figure 3.5. Vector in the solar trackers reference system.

To obtain the vector $\vec{a}$, it is multiplied in both terms by the vector $\overrightarrow{n'}$:

$$\vec{d} \cdot \overrightarrow{n'} = 0 + \tau\, \overrightarrow{s'} \cdot \overrightarrow{n'} \;\Rightarrow\; \tau = \frac{n'_x \cdot d}{s'_x \cdot n'_x + s'_z \cdot n'_z} \tag{3.18}$$

Substituting the value of τ from equation (3.18) into equation (3.19) results:

$$\vec{d} = \vec{a} + \frac{n'_x \cdot d}{s'_x \cdot n'_x + s'_z \cdot n'_z}\overrightarrow{s'} \tag{3.19}$$

Vector $\vec{a}$ would be obtained according to the following expression:

$$\vec{a} = \left(d - \frac{n'_x \cdot d}{s'_x \cdot n'_x + s'_z \cdot n'_z} \cdot s'_x\right) \cdot \vec{p} - \frac{n'_x \cdot d}{s'_x \cdot n'_x + s'_z \cdot n'_z} \cdot s'_z \cdot \overrightarrow{n_T} \tag{3.20}$$

As mentioned above, the study of vector $\vec{a}$ will determine whether shading exists. If the module of the vector is less than the width of the panel, shading occurs.

$$|\vec{a}| < h \tag{3.21}$$

To avoid this situation, backtracking is proposed, to look for a new orientation of the panels that prevents shading. The new orientation is intended to undergo a minimum deviation from the optimal capture. The new α inclination angle is that which causes the shadowing of a panel to fall on the edge of the adjacent panel (Figure 3.6).

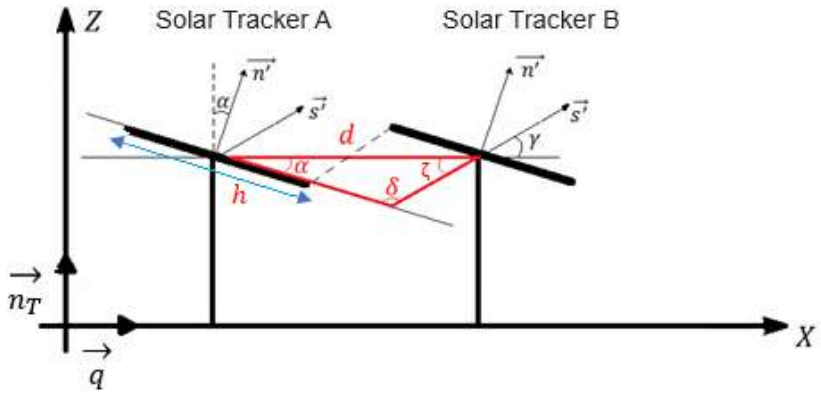

Figure 3.6. Angle α that avoids the shading between solar panels.

This inclination angle α is calculated based on a triangle formed by the line that joins the center of the two panels d, the projection of the centre of the panel on the line of the adjacent $\tau\vec{s'}$ and the distance that corresponds to the module of vector $\vec{a}$ in Figure 3.5, which in Figure 3.6 is equivalent to the width of the panels, h.

The angle ζ is the one that forms the solar vector $\vec{s'}$ with the X axis:

$$\gamma = \arctan\frac{s'_z}{s'_x} \tag{3.22}$$

The value of the angle δ can already be calculated as:

$$sin\delta = \frac{sin\zeta \cdot d}{a} \tag{3.23}$$

And, therefore, the inclination angle of the solar panel is calculated as follows:

$$\alpha = \pi - \delta - \zeta \tag{3.24}$$

The normal vector that leads to the panel to avoid shading is:

$$\vec{n'} = sin\alpha\ \vec{p} + cos\alpha\ \vec{n_T} \tag{3.25}$$

3.2.4. Software Applications for Analysis

To calculate the irradiance received by each solar panel, a function implemented in Visual Basic Application (VBA) for Excel will be used where the calculations described above are developed. As seen in Figure 3.7, the function is based on several input parameters (latitude, Julian day, geometrical values, irradiance model considered) and provides an irradiance value every three minutes. Some restrictions, such as daytime, maximum radiation related to the used model and eventual shading with backtracking response are assumed.

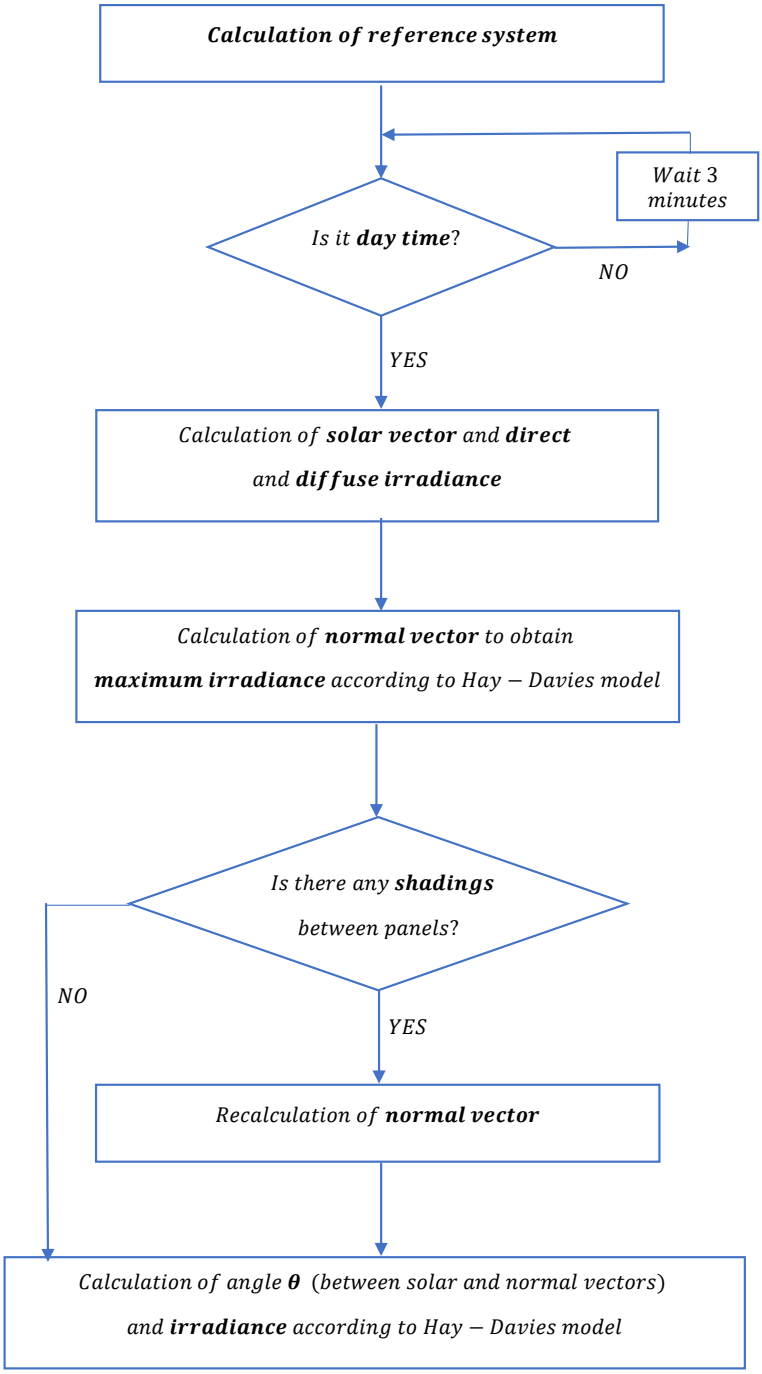

Figure 3.7. Flux diagram for VBA function.

3.3. Results and Discussions

The practical results have obtained the value of the estimated annual radiation using the Hay-Davies model (Hay, 1993) for various land configurations. All the calculations have been made for the province of Córdoba, Spain, considering therefore the same geographical values (latitude =37.75492°N; longitude=5.04548°W), and the same climatic values throughout the year, varying only the values of inclination β and azimuth χ for fixed panel width $h = 3\ m$ and separation between panel lines $d = 6\ m$.

For each inclination β (from 0° to 45°, 1°increment) and terrain azimuth χ (from -60° to 60°, 5° increment), the rotation axis is oriented with a wide range of azimuth γ (from -20° to 20°, 2° increment).

Terrains with negative inclinations have not been considered since PV plants are not commonly installed in shaded areas.

In facilities located in a terrain with null azimuth (South-oriented), independently of its inclination even if it is null, the greater use is arranging the axis of rotation with South orientation (γ= 0°).

For each value of the inclination of the terrain β, it is also observed that the maximum value of irradiance is obtained when the azimuth of the terrain χ is 0°. That is, the optimal situation will be when the terrain is South-oriented and the axis of rotation is directed in that same direction. On the other hand, if the terrain has another orientation, the value of the optimal angle towards which to orient the axis of rotation would move in that same direction. This fact becomes more evident at higher values of the terrain inclination β, although in no case will the azimuth axis γbe as high as that of the terrain χ.

Specifically, results for a case study with a β = 15° inclination are represented in Figure 3.8. Figure 3.8a shows the variation of radiation regarding γ when the azimuth of the terrain $\chi = 0°$. However, when the terrain is not oriented to the South, as shown in Figure 3.8b, where the terrain is turned χ = 30°, the maximum radiation is obtained by orienting the axis with an azimuth γ of 6° towards the South. The losses regarding the maximum radiation obtained in a terrain are shown in Figure 3.8c, where it is again verified that by orienting the axis at 6°, these losses are minimised. Finally, Figure 3.8d shows the optimal orientation to direct the axis for the different values of the terrain azimuth χ. In this way it is possible to estimate the orientation that achieves optimal radiation considering the azimuth of the terrain χ.

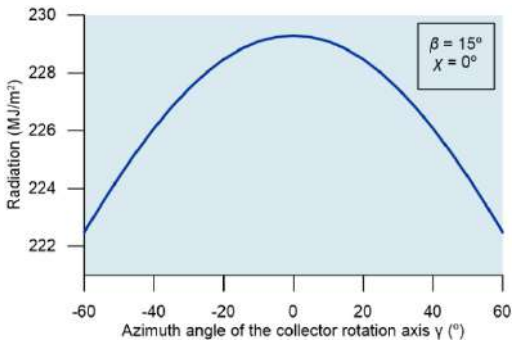

(**a**)

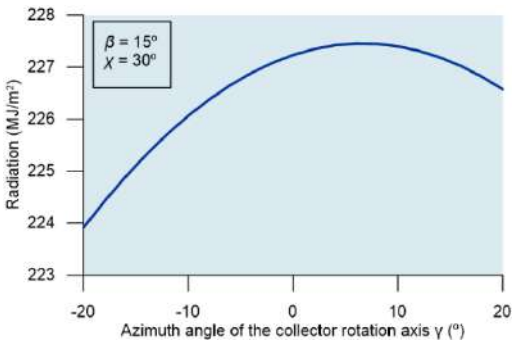

(**b**)

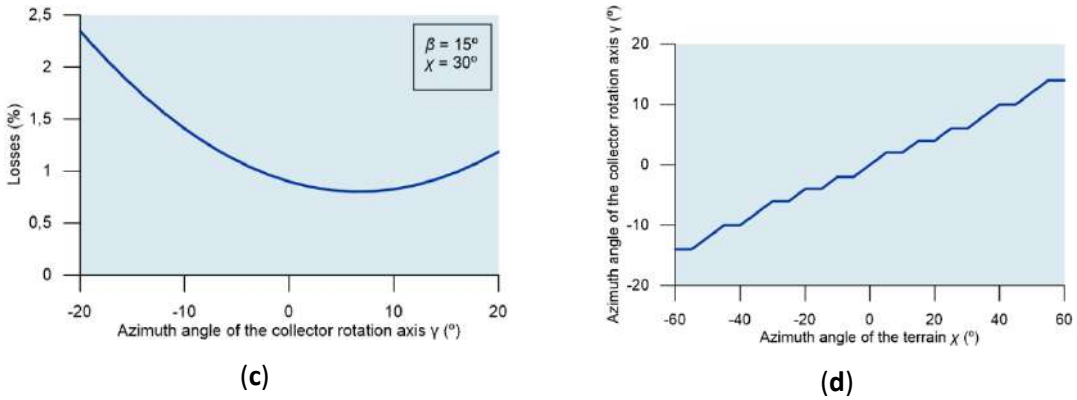

Figure 3.8. Results for a case study for inclination 15°: (a) Maximum radiation; (b) Radiation variation for 30° azimuth; (c) Maximum radiation loss for 30° azimuth; (d) Axis azimuth for optimal terrain radiation.

As already mentioned, for each inclination value the maximum irradiance value is obtained when the terrain is χ = 0°. In addition, as the inclination of the terrain increases, the radiation affecting the panels is greater, as seen in Figure 3.9. The explanation can be found in the latitude where the calculations have been made and since the direction of the Sun is not perpendicular to the horizontal plane. The inclination of the terrain influences the radiation, increasing until a value of β around 21°, where the maximum is reached $\chi = 0°$.

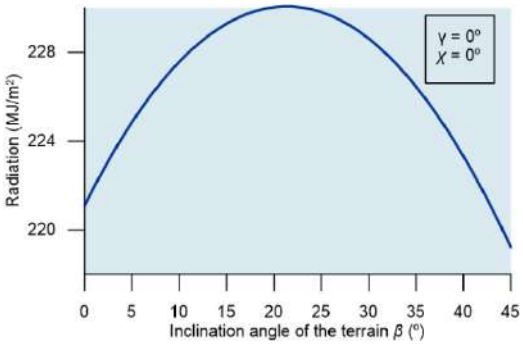

Figure 3.9. Variation of the maximum radiation on the collector with respect to the inclination of the terrain.

The difference observed between the radiation value for a particular axis azimuth and the maximum capture obtained in the optimum direction is greater as the inclination of the terrain increases. Thus, in low-inclination terrains the difference is low and, on the other hand, for steeper inclinations, the losses are considerable. Figure 3.10 shows that, in the specific case of β = 20°, the losses caused by a bad choice of rotation axis direction can reach values above 7%.

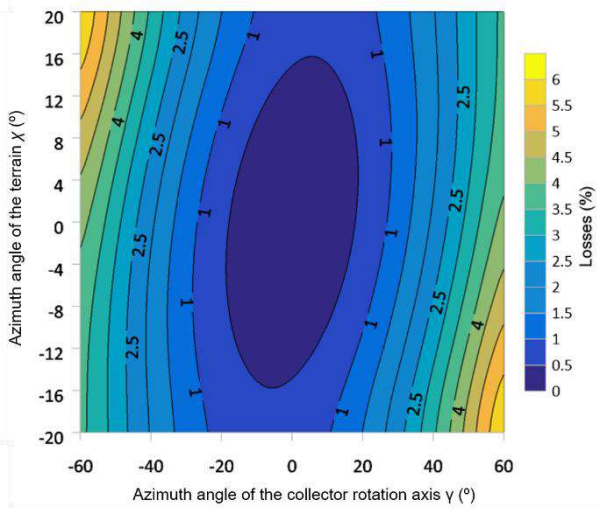

Figure 3.10. Losses for different axis and terrain azimuth values.

Figure 3.11 shows the losses for the conditions $\gamma = 0°$and $\beta = 20°$,considering an azimuth range χ from -60° to 60°. For terrains that are also oriented towards the South or close to it, the losses will be zero or very low. But as the azimuth of the terrain increases, the losses become considerable.

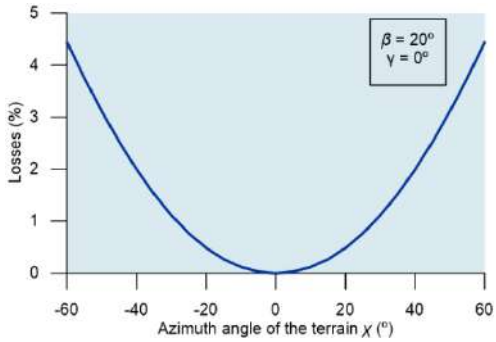

Figure 3.11. Losses with 0° axis azimuth and 20° inclination.

Thus, it is possible to establish a sensitivity of collector axis azimuth γ versus the inclination β and azimuth of the terrain χ. It is worth highlighting the novelty of this result since no references have been found in the literature suggesting this relationship between variables.

Another key factor when configuring the layout of the collectors is the separation between them. This fact has an influence since, the greater the panel separation, the fewer shading effects will be produced and the fewer losses due to a decrease in production. On the other hand, it is not possible to separate the rows of collectors as much as desired, since the costs associated with a higher terrain occupation considerably increase (Saint-Drenan and Barbier, 2019). In Figure 3.12 shows that, depending on this parameter, the irradiance has an asymptotic behaviour. This is since the shadow effects of

one collector on another, when separated by a sufficient distance, are no longer perceived, obtaining an irradiance value like that of an isolated collector without adjacent collectors.

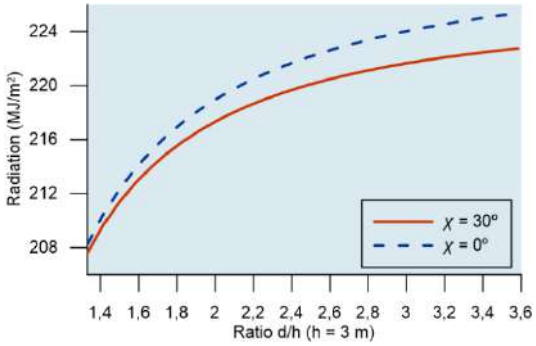

Figure 3.12. Irradiance by varying the ratio d/h (h=3m).

3.4. Conclusions

The solar capture on horizontal one-axis trackers has been mathematically modelled, establishing the rotation axis orientation for any irradiance model. Backtracking has been considered to avoid the shading of some panels on the adjacent ones, modifying its orientation. Considering the results obtained, and those in literature, is achieved an advance in the knowledge of photovoltaic trackers with an axis parallel to the terrain, allowing an optimal design for terrains without the horizontality described in previous works.

A program and a subroutine in VBA have been implemented to automatically calculate the radiation on a solar tracker for different terrain configurations, varying the characteristics of the installation, both the rotation axis orientation and the ratio dimension of the panels h and the separation d between adjacent rows. Simultaneously, it provides the optimal azimuth γ value for the rotation axis to be directed and the loss values for each possible case facing the maximum radiation value for each inclination β of the terrain.

Calculations of radiation on solar panels considering fixed width and distance between lines of panels, varying terrain inclinations β and azimuth χ, were made in Córdoba, Spain.

For any given value regarding the terrain inclination β, it is verified that a higher value of radiation is obtained in those lands that are South-oriented ($\chi = 0°$). The optimum direction for the rotation axis collector γ should also be southwards.

An important contribution of this research is the relationship established between the azimuth γ of the collector axis and the inclination β and azimuth of the terrain. For lands that are not South-facing, the rotation axis azimuth γ of solar trackers should be different from zero and varies in the same direction as the land azimuth χ. If the axis of rotation is positioned in a different direction to the optimum, losses in potential energy production arise. These losses

vary according to the terrain inclination β. The greater the difference between the optimum azimuth γ and the terrain inclination β, the greater the production losses will be.

Another important conclusion concerning the collector layout on the power plant surface has been drawn. As the distance d between rows of collectors increases, a greater amount of radiation is generated. Such growth is asymptotic.

Overall, some progress has been achieved towards the objective of deepening knowledge concerning photovoltaic trackers. Consequently, guidelines are proposed for solar capture optimisation in photovoltaic plants. This work provides a further line of research into the geometric layout optimisation of solar trackers involving more complex models such as Perez (Perez et al., 1990) and Muneer (Muneer, 1990) and real databases.

As a result of the aforementioned aims and conclusions, it is considered that this work is the basis for further work, such as the study of one-axis solar trackers located on terrains with an irregular topography or the study of the collector distribution system, considering potential uses for the land.

Capítulo 4 . New Ominidirectional Sensor based on Open-Source Software and Hardware for tracking and backtracking of dual-axis Solar Trackers in Photovoltaic Plants

4.1. Introduction

4.1.1. Literature Review on Solar Tracking.

4.1.2. Literature Review on Free and Open-Source Hardware and Software applied to PV Energy.

4.2. Proposed Design.

4.2.1. Algorithm for the Detection of Inter-Shading between Collectors.

4.2.2. Design of the Proposed Technological Solution.

4.3. Results and Discussion.

4.4. Conclusions.

New Omnidirectional Sensor based on Open-Source Software and Hardware for tracking and backtracking of dual-axis Solar Trackers in Photovoltaic Plants

Gómez Uceda, FJ[1]; Ramírez-Faz, J[2]; Varo-Martínez, M[3,*]; Fernández-Ahumada, LM[2];

[1] Department of Mechanics. University of Cordoba. Campus of Rabanales, 14071 Cordoba, Spain.

[2] Department of Electrical Engineering and Automatics. University of Cordoba. Campus of Rabanales, 14071 Cordoba, Spain

[3] Department of Applied Physics, Radiology and Physical Medicine. University of Cordoba. Campus of Rabanales, 14071 Cordoba, Spain.

* Correspondence: fa2vamam@uco.es

Abstract: In this work an omnidirectional sensor that enables identification of the direction of the celestial sphere with maximum solar irradiance is presented. The sensor, based on instantaneous measurements, functions as a position server for dual-axis solar trackers in photovoltaic plants. The proposed device has been developed with free software and hardware, which makes it a pioneering solution because it is open and accessible as well as capable of being improved by the scientific community, thereby contributing to the rapid advancement of technology. In addition, the device includes an algorithm developed ex professo that makes it possible to predetermine the regions of the celestial sphere for which, according to the geometric characteristics of the PV plant, there would be shading between the panels. In this way, solar trackers do not have to locate the Sun's position at all times according to astronomical models, while taking into account factors such as shadows or cloudiness that also affect levels of incident irradiance on solar collectors. Therefore, with this device it is possible to provide photovoltaic plants with dual-axis solar tracking with a low-cost device that helps to optimise the trajectory of the trackers and, consequently, their radiative capture and energy production.

Keywords: Free and open-source hardware (FOSH), Sun Position Sensor, Omnidirectional Sensor, Solar Trackers, PV Plants, backtracking)

4.1. Introduction

The industrial and technological development that society has undergone, as well as the increase in the population worldwide, has led to a growing demand for energy (Carballo et al., 2018; Panwar et al., 2011). Satisfying this increase in energy demand only by means of traditional methods of energy production based on fossil and nuclear resources entails serious environmental problems that endanger the sustainability of the Earth, such as pollution and climate change (Caballero et al., 2020; Kannan and Vakeesan, 2016; Obara et al., 2017). In response, the scientific community has highlighted the importance of enhancing the role of renewable energies in the energy models of both developed and developing countries (Carballo et al., 2018; De Castro et al., 2013; Jacobson and Delucchi, 2011). In fact, the number of journals and papers related to renewable energies has experienced a remarkable growth (Novas et al., 2020), which shows the increasing researchers' awareness of the need to contribute to the improvement and the progress of this field of science and its beneficial impact on the challenges of current society.

Among these possible renewable energy sources, solar energy plays a fundamental role (Casares et al., 2014; Nsengiyumva et al., 2018; Sumathi et al., 2017) since, as stated by Kannan and Vakeesan (Kannan and Vakeesan, 2016), it is an abundant source of energy that, being properly exploited, could be enough to satisfy world energy demand. Furthermore, it is available all over the planet, its use has no negative impact on the environment and it is a technology that is easily usable at all levels (industrial, domestic, etc.). The technological improvements achieved in recent years have allowed to reduce the production cost of PV energy to values competitive with those of the energy supplied by the grid (D'Adamo et al., 2020). As a result, the presence of PV technologies in the energy market has experienced a significant growth (IRENA, 2020). However, in order to continue promoting this expansion it is necessary to continue researching into new solutions that will maintain their growing development and technological progress (D'Adamo et al., 2020).

4.1.1. Literature Review on Solar Tracking

Among the solar energy technologies, photovoltaic (PV) is undergoing a remarkable boom due to its simplicity and low cost, as well as the significantly technological enhancements that it has been experiencing. As a consequence, it is becoming a promising source of electricity generation (Eldin et al., 2016). However, despite its rapid technological evolution, there is still plenty of room for optimisation in the efficiency of the management of photovoltaic installations, as well as in the configuration of its design, which would lead to a potential increase in its development.

One possible line of technological improvement of PV that has been worked on for decades is solar tracking (Nsengiyumva et al., 2018). It tries to alleviate the negative effects of the high variability of the solar resource, both in time as well as in space, by reorienting the PV panels towards possible directions that increase solar irradiance collection. In order to do so, solar trackers are very useful both in large PV plants connected to the grid and in small domestic installations in which the space available for the installation of the panels is often reduced and, as a consequence, it is necessary to increase the energy generated per square metre of collecting surface (Gutierrez et al., 2020).

There is a traditional classification of trackers based on the degrees of freedom of the tracking movement according to which they can be categorised into single-axis trackers and dual-axis trackers. The former are characterised by modifying the orientation of the collector plane by turning around a single fixed axis. The latter are characterised by a movement of its plane through the rotation of a system composed of two fixed axes, which allows it to orient itself in any possible direction in the celestial sphere (Lee et al., 2009). Although dual-axis trackers are more expensive and require more work to implement and maintain than single-axis trackers, they offer better performance (Koussa et al., 2011; Maatallah et al., 2011; Seme et al., 2011). In fact, although some authors affirm that dual-axis monitoring systems have no future due to their complexity and high cost (Huang et al., 2011; Ismail et al., 2013), Eldin et al. (Eldin et al., 2016) suggest that at present this type of technology is widespread throughout the world and that multiple research is being developed to improve both the technology and its efficiency/cost ratio, so that its energy production exceeds and compensates for the costs of the installation and maintenance as well as the energy consumption used in the movement of the trackers.

Another possible classification of solar trackers is the one based on the mechanism that enables monitoring. Thus, on the one hand there are passive trackers that do not use mechanical devices for movement. To the contrary, in most cases, they are composed of a pair of actuators, filled with expandable gas, which in the case of imbalance, are levelled with equal lighting by means of thermal expansion (Narendrasinh Parmar et al., 2008). In comparison, active solar trackers use motors commonly governed by control signals for movement in search of the position of the Sun, which are very precise devices except on very cloudy days (Mousazadeh et al., 2009).

Finally, depending on the tracking control strategy, a distinction is made between trackers in which the movement, both in azimuth and elevation, is governed by mathematical models (in open loop) and those in which the system feeds back through irradiance sensors (closed loop).

Various literature review works have systematically collected the data obtained by different solar trackers developed by the scientific community, finding that the energy produced by a PV system with tracking is always greater than that of a system without it (Nsengiyumva et al., 2018; Sumathi et al., 2017), except on spring or summer days with great cloudiness (Koussa et al., 2011; Quesada et al., 2015). More specifically, Eldin et al. (Eldin et al., 2016) carried out a study on the convenience of monitoring systems depending on the climatic conditions of the place and verified that the output power of photovoltaic panels with solar monitoring depends on environmental conditions. Thus, while in cold regions with a high incidence of cloudiness, monitoring strategies are profitable for maximising the power of photovoltaic panels, in places with very hot and sunny climates they are not, due to the negative influence of overheating on performance of photovoltaic panels. Likewise, some authors have analysed the improvements in energy production of PV systems with solar tracking depending on the type of technology used and the latitude of the study site (Huld et al., 2010; Lorenzo et al., 2002; Perpiñan et al., 2009). Thus, it has been shown that, in general, the higher the latitude, the better the monitoring efficiency is achieved, reaching improvements of up to 57% (Mousazadeh et al., 2009).

Similarly, with regard to grid-connected PV installations, a recent study (Rad et al., 2020) has analysed, from a techno-economic-environmental point of view, the use of different solar tracking systems to maximise the photovoltaic power generation in residential solar installations connected to the grid in eight regions of Iran with diverse climates. Based on the study carried out, they found that the dual-axis monitoring system is the most efficient (32% average increase in energy production compared to an installation without monitoring) while the vertical single-axis monitoring system is the most profitable (23% increase in energy production compared to a non-monitored installation with only 1.6% increase in energy cost). In general terms, the study concludes that the use of the solar tracking system in residential installations connected to the grid significantly reduces the number of panels needed, but this reduction in size is not always profitable due to the high cost of the monitoring units. However, the profitability of the installation increases significantly in all cases when the sale of electricity to the grid is allowed.

As far as the monitoring strategy is concerned, the most frequent in the literature is that based on solar astronomical movement, which aims to minimise the angle of incidence θ between the solar rays and the normal to the capture surface. According to this astronomical tracking strategy, various works (Braun and Mitchell, 1983; Duffie and Beckman, 2013; Meinel and Meinel, 1979; Narvarte and Lorenzo, 2008; Neville, 1978; Riley and Hansen, 2015) show prediction models of incident irradiance on the plane of trackers of both single and dual axes,

with a degree of accuracy for solar location in the celestial sphere to the order of mrad (Blanco-Muriel et al., 2001; Grena, 2008; Reda and Andreas, 2004). The models used for astronomical tracking have traditionally been based on spherical trigonometry (Meinel and Meinel, 1979). However, recently, a new paradigm using vector algebra to define the solar movement and that of the trackers can be found in the literature (Chong and Wong, 2009; Fernández-Ahumada et al., 2020a, 2017; Jolly, 1986; Parkin, 2010; Rapp-Arrarás and Domingo-Santos, 2009; Sproul, 2007). For this, these models use the solar vector $\vec{s}$ which is a unit vector that is directed to the centre of the solar disk. Its expression in different coordinate systems and the use of the definition of scalar and vector product enable the deduction of the entire system of astronomical relationships that govern the movement of the solar trackers (Torres-Roldán et al., 2015).

Furthermore, as previously mentioned, the astronomical tracking strategy seeks the optimisation of the direct component of solar irradiance. Consequently, it is adapted to solar concentrators that are based on the use of this component, but not to flat PV collectors in which the remaining components of irradiance (diffuse and reflected) are also used. Thus, on days when the solar disk is not visible and direct irradiance does not reach the collectors, the efficiency of this monitoring strategy is not satisfactory (Duffie and Beckman, 2013; Mousazadeh et al., 2009) and the capture of the collectors is less than that which would be obtained on a horizontal flat surface. Despite this, it is difficult to find references that determine models for solar tracking on these types of days, so it is necessary to continue developing mathematical equations that also take into account the diffuse and reflected components when trying to maximise radiative collection as part of solar tracking strategy.

On the other hand, the energy reduction caused by shading is particularly significant for PV installations. In addition, the shaded cells become overheated which may lead to a fast degradation of the modules. Backtracking is applied to prevent the inter-shading of collectors. This technique consists of shifting the collectors to positions where shadows no longer appear (Lorenzo et al., 2011, 2002; Narvarte and Lorenzo, 2008). Combining these two requirements (optimising global irradiance and performing backtracking) leads to a differentiation within the dedicated and specific tracking strategy for PV plants, studied further in this article

In this line of work, a novel solar tracking strategy with back-tracking has been proposed to optimise the capture of solar irradiance at all times while avoiding inter-shading between collectors in PV plants with dual-axis tracking (Fernández-Ahumada et al., 2020b, 2020a). In this study, based on empirical models for the characterisation of the hemispheric distribution of irradiance, the authors quantify the increases in solar incidence on collectors at a higher

value than 2%. In order to implement this strategy in existing facilities, the device presented in this article is developed and built.

Likewise, other authors (Kelly and Gibson, 2009; Koussa et al., 2011; Salgado-Conrado, 2018; Yao et al., 2014) have implemented tracking systems with sensors that follow the position of the Sun with great precision and that have the advantages of easy implementation, simple design, low cost and a high level of adaptability. However, it is necessary to continue advancing in the search for tracking strategies that enable constant identification of the direction of the celestial sphere in which solar irradiance is maximum in a simple way regarding the hardware and software necessary for its implementation, and that it does not imply an increase in the cost of the technology, either in implementation or maintenance.

4.1.2. Literature Review on Free and Open Source Hardware and Software applied to PV Energy

Despite the great progress that new technologies have experienced in recent decades, the energy supply network based on traditional technologies has not evolved at the same rates (Caballero et al., 2020). However, this is different in the case of renewable energies. In that sense, it is increasingly common to find in the literature proposals based on free hardware in the field of photovoltaic solar energy in general, and in solar tracking, in particular. Thus, for example, the use of microcontrollers (many based on free hardware) in the implementation of various photovoltaic tracking strategies presents an important competitive advantage at an economic level compared to control based on traditional PLCs (Singh et al., 2018). In general terms, with the use of technologies based on free hardware in the field of solar PV energy, not only are lower costs sought, but it is also intended that the results and yields obtained are similar to or better than those achieved by commercial solutions (Fuentes et al., 2014). In this sense, as it is a free hardware system, it can be shared among the scientific community and can be edited and improved by different experts (Pearce, 2014). Another advantage is the fact that the application of the devices shows a wide range of possibilities both at the level of capture (irradiance, temperature, humidity) and control of the complex processes in which it works (García-Valverde et al., 2016). In addition, the possibility of safely, quickly and easily storing the huge amount of data generated by any photovoltaic installation is an important milestone in working with free hardware devices (Gad and Gad, 2015).

Among some of the devices found in the literature is the one by Gutierrez et al. (Gutierrez et al., 2020) that presents a single-axis solar tracker for the integration of buildings controlled with an open-loop control strategy implemented through Arduino and IoT. This makes it a low-cost device with a flexible implementation and applicable anywhere in the world. A new electronic sensor based on free hardware has also been developed, validated and patented to

measure radiation and global radiation on the horizontal surface (Rus-Casas et al., 2019). The device is characterised by high precision and the technologies used in its implementation (Arduino and IoT) make it a low-cost device with a high level of connectivity and ubiquity, which is why it is easily applicable to the monitoring and control of any PV plant and, especially, to "smart-grid" solutions. Paredes-Parra et al. (Paredes-Parra et al., 2019) have also developed a low-cost and open source system, based on IoT and LoRa, which allows remote monitoring and real-time operation of a PV plant and, therefore, facilitating maintenance and supervision tasks. Similarly, Pereira et al. (Pereira et al., 2018) have developed a new multi-user remote data acquisition and transmission system, based on RaspberryPi and IoT technology, to monitor a photovoltaic plant in real time. Therefore, it can be affirmed that the relationship established in the different levels of aggregation of solar energy (generation, Smart grids, integration) is a field in which the use of the aforementioned technologies finds an interesting space due to the versatility shown (Batista et al., 2014; Coelho et al., 2017).

In accordance with all the above and combining the two lines of work presented, this paper describes a sensor that uses an onmidirectional solar tracker, based on Free and open-source hardware (FOSH), which acts as a server of position for dual-axis PV trackers, identifying at each instant in time the optimal orientation of the PV panels from instantaneous irradiance measurements. With this, the solar trackers do not have to search for the position of the sun using algorithms based on solar geometry while taking into account other conditions (cloudiness, shading between panels, etc.) that also influence the irradiance received by the capturing surfaces. In this way it is possible to provide PV plants with dual-axis solar tracking with a low-cost device that helps to optimise the trajectory of its trackers and, consequently, its radiative capture and energy production.

Following this introduction, the remainder of the article is organised as follows: In the next section, Section 2, the proposed design and the algorithms implemented in the device are outlined; Section 3 presents how the system was tested for a PV plant in Peñarroya (Spain), and the results are discussed. In Section 4, conclusions are drawn based on the work developed.

4.2. Proposed Design

The Materials and Methods should be described with sufficient details to allow others to replicate and build on the published results. Please note that the publication of your manuscript implicates that you must make all materials, data, computer code, and protocols associated with the publication available to readers. Please disclose at the submission stage

any restrictions on the availability of materials or information. New methods and protocols should be described in detail while well-established methods can be briefly described and appropriately cited.

To achieve the objective described above, the device presented makes a scan of the celestial sphere, during which the incident irradiance measurement is carried out in order to determine the orientation for which this magnitude is maximum. However, as a novelty, the device incorporates a dichotomous algorithm, designed by the authors (Fernández-Ahumada et al., 2020b, 2020a) that, prior to the scanning of the celestial sphere, identifies those orientations of the solar trackers for which there would be inter-shading between the collectors. With this, the proposed device restricts the search field for the orientation of maximum irradiance to the set of spatial directions in which there is no inter-shading, which in practice implies a backtracking strategy. Once the direction of maximum irradiance has been identified, the azimuth (γ) and elevation (α) angles corresponding to it, stored in the device that acts as a position server, are made available to the solar trackers of the PV installation for their orientation towards the position of maximum capture.

The technological solution presented consists of a pan-tilt type orientation mechanism that allows the positioning of an irradiance sensor in any direction of the celestial sphere, characterised by its azimuth (γ) and its elevation (α), as well as an irradiance measurement and control system in real time. The mechanism is controlled by a microprocessor that is also in charge of carrying out the irradiance readings and their transmission to the solar servers. For its operation the necessary algorithms have been developed and implemented to adjust the movements of the solar trackers so that optimal energy production is achieved. Likewise, the complete architecture of the device has been developed, based on Free and Open-Source hardware (FOSH) and a simple control system with functionalities associated with IoT technologies. All of this makes the device an economically competitive tilt and azimuth server, capable of integrating into dual-axis photovoltaic installations and favouring the optimisation of its energy production. This previous dichotomous algorithm for the detection of inter-shading as well as the electronic and mechanical design of the device is described below.

4.2.1. Algorithm for the Detection of Inter-Shading between Collectors

As mentioned above, the device includes a simple and programmable algorithm in 8-bit AVR RISC microprocessors that, taking into account the characteristics of the PV installation, enables one to know whether a certain orientation (γ, α) of the collectors would imply the partial inter-shading between them for a certain Julian day (d_j) and a specific solar hour (t) prior to the scanning of the celestial sphere. This algorithm is supported by a novel tracking

strategy developed by the authors and which is based on Minkowski algebra (Fernández-Ahumada et al., 2020b, 2020a).

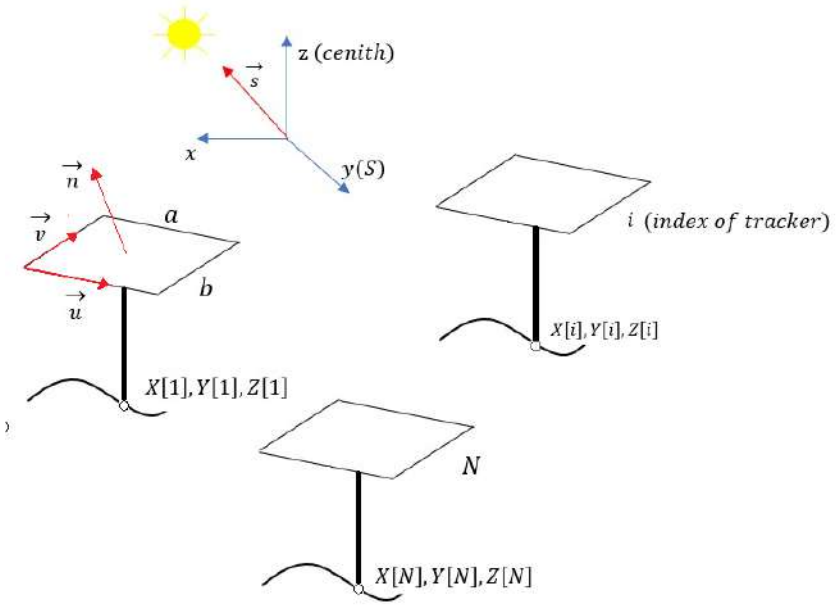

Figure 4.1. Geometric elements necessary to determine the existence of inter-shading according to the algorithm of Fernandez-Ahumada et al. (Fernández-Ahumada et al. 2020b, 2020a).

This procedure can be understood as a Boolean function dependent on (γ, α, d_j, t) in which the result "TRUE" implies the existence of inter-shading and "FALSE" the absence. As auxiliary information this function requires:

1. The width (a) and height (b) of the solar collectors.
2. The set of Cartesian coordinates (x, y, z) of the base of each solar tracker, using as a reference system a local coordinate system in which the Ox axis goes to the West, the Oy to the South and the Oz to the point Zenith. This information is structured by three arrays $x[i], y[i], z[i]$ in which i is the index assigned to each solar tracker (Figure 4.1), so that $1 < i < N$ is verified, where N is the number of trackers in the installation.
3. The solar vector or unit vector that points to the solar disk at each instant of time that, in the reference system considered, is given by the equation (4.1):

$$\vec{s} = s_x\vec{\imath} + s_y\vec{\jmath} + s_z\vec{k} == sin\,\Omega\,t\ \ cos\,\delta\,\vec{\imath} + \\ +(cos\,\Omega\,t\,cos\,\delta\,sin\,\varphi - sin\,\delta\,cos\,\varphi)\vec{\jmath} + \\ +(cos\,\Omega\,t\,cos\,\delta\,cos\,\varphi + sin\,\delta\,sin\,\varphi)\vec{k} \tag{4.1}$$

where: φ is the latitude, Ωt is the hourly angle, defined as the product of the Earth rotation speed ($\Omega = 2\pi/24\,rad/h$) and the time elapsed since solar noon and δ is the

solar declination given by equation (4.2), being Γ and auxiliary angle dependent on the Julian day according to equation (4.3).

$$\delta(rad) = 0.006918 - 0.399912\,cos(\Gamma) + 0.070257 sin(\Gamma) - 0.006758\,cos(2\Gamma) + 0.000907 sin(2\Gamma) - 0.002697\,cos(3\Gamma) + 0.00148 sin(3\Gamma) \quad (4.2)$$

$$\Gamma(rad) = \frac{2\pi(d_n - 1)}{365} \quad (4.3)$$

4. The unit vector $\vec{n}$, which indicates the direction towards which the solar trackers are oriented, being perpendicular to the collectors, and which is given by the equation (4.4).

$$\vec{n} = \cos\alpha \cdot \sin\gamma\vec{\imath} + cos\,\alpha \cdot \cos\gamma\,\vec{\jmath} + \sin\alpha\,\vec{k} \quad (4.4)$$

5. The unit vectors $\vec{u}$ y $\vec{v}$ included in the collector plane, where $\vec{u}$ is horizontal (equation 4.5) and $\vec{v}$ (equation 4.6) perpendicular to $\vec{u}$.

$$\vec{u} = -cos\,\gamma\,\vec{\imath} + \sin\gamma\,\vec{\jmath} \quad (4.5)$$

$$\vec{v} = sin\,\alpha \cdot cos\,\gamma\vec{\imath} - sin\,\alpha \cdot cos\,\gamma\,\vec{\jmath} + cos\,\alpha\,\vec{k} \quad (4.6)$$

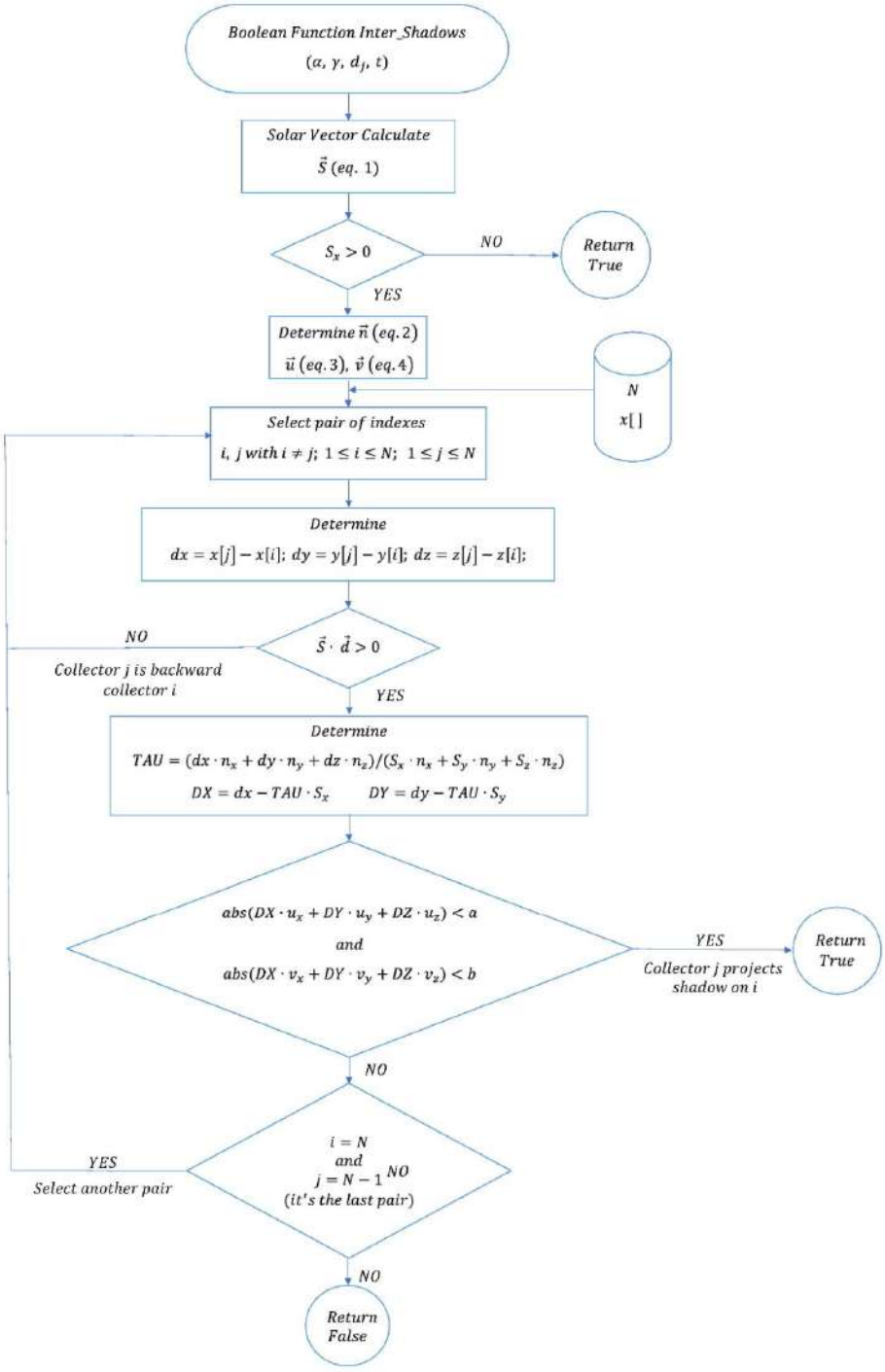

Figure 4.2. Flow chart of the designed and implemented procedure.

4.2.2.Design of the Proposed Technological Solution

The mechanical design of the proposed device has been resolved by means of a flat surface with two degrees of freedom (Figure 4.3). The manufacture has been carried out by means of additive printing on acrylonitrile butadiene styrene (ABS) filament, a thermoplastic

polymer with good properties with regard to distortion and softening temperatures, 96°C and 93°C, respectively. The whole set remains inside a transparent methacrylate dome.

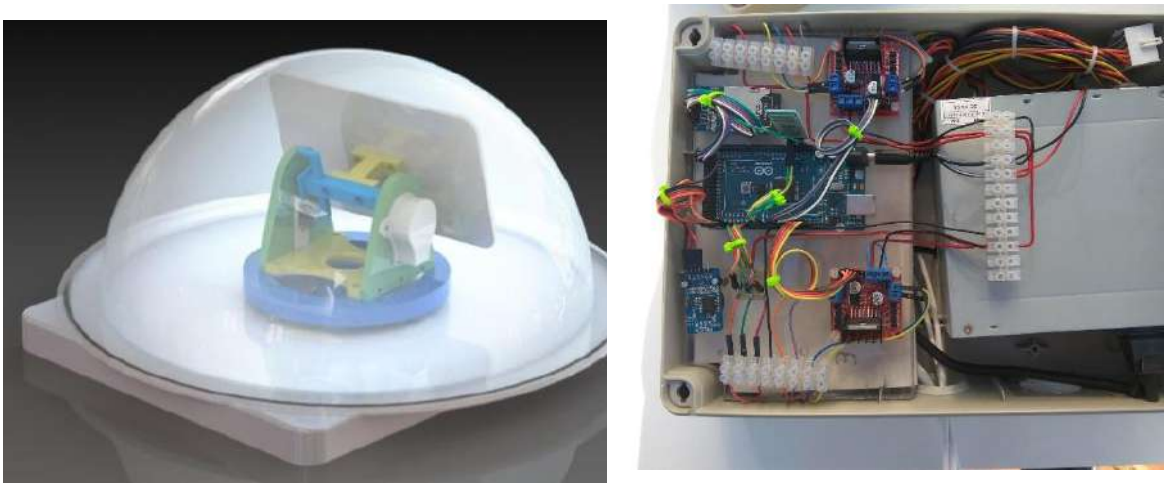

(a) (b)

(c)

Figure 4.3. (a) Design of the system; (b) Electronical components; (c) Photography of the prototype

Figure 4.4 schematically shows the concept of the electronic design of the system in which four blocks are distinguished: sensors, processing, actuators and communications.

- Sensors: On the one hand, the system includes a sensor system whose purpose is to know the solar time corresponding to orientations that are not allowed because they cause inter-shading between the collectors. For this, among the different options to obtain the time (internal clock of the microcontroller, time server or external RTC module), in this

prototype a DS1307 real-time clock has been chosen, with autonomous power supply by means of a CR2025 battery. Likewise, for the irradiance measurement, a calibrated photovoltaic cell of the Fadisol C-0121 type has been used that provides a linear current output with respect to irradiance, comprised between 36 mA for 125 W/ m^2 and 288 mA for 1000 W/m^2. The measurement of the intensity of the electric current provided by these short-circuited photovoltaic cells is measured by means of an INA219 module, consisting of a shunt equipped with a 12-bit analog-digital converter and I2C output. In this way, adjusting the gain in the module configuration, an accuracy of 0.1 mA and a maximum intensity of 400 mA are obtained. Finally, an initialisation of the azimuth and elevation position has been provided, using two mechanical micro-switches that indicate the zero relative position to the microcontroller.

- Processing: In the philosophy of this work, several alternatives for processing have been evaluated, opting for a TTGO ESP32 Lora development board. The ESP32 microcontroller integrates analog and digital inputs and outputs, as well as various communication interfaces, both wireless (WiFi and Bluetooth Low Energy) and wired (I2C, SPI, UART). The selected board also has a LoRa communication module, model SEMTECH SX1276 that enables communication at a frequency of 868 MHz.
- Drive: Two 28BYJ-48 stepper motors, powered at 5 V, with 4096 steps per revolution that provide a maximum precision of 0.001534 radians, have been used to drive the two axes of movement of the omnidirectional server presented. The management of the stepper motors requires a controller, for which two units of the type LM298 have been used.
- Communications: Finally, it has been considered that the communications between the position server and the solar trackers require a range according to the typical dimensions of photovoltaic installations. The receiving devices of the orientation command can be arranged in a radius of up to 15 km around the server (Sinha et al., 2017), which is achieved with direct vision between antennas, in optimal conditions; while in unfavorable conditions, such as suburban areas, 3 km are reached (Augustin et al., 2016).

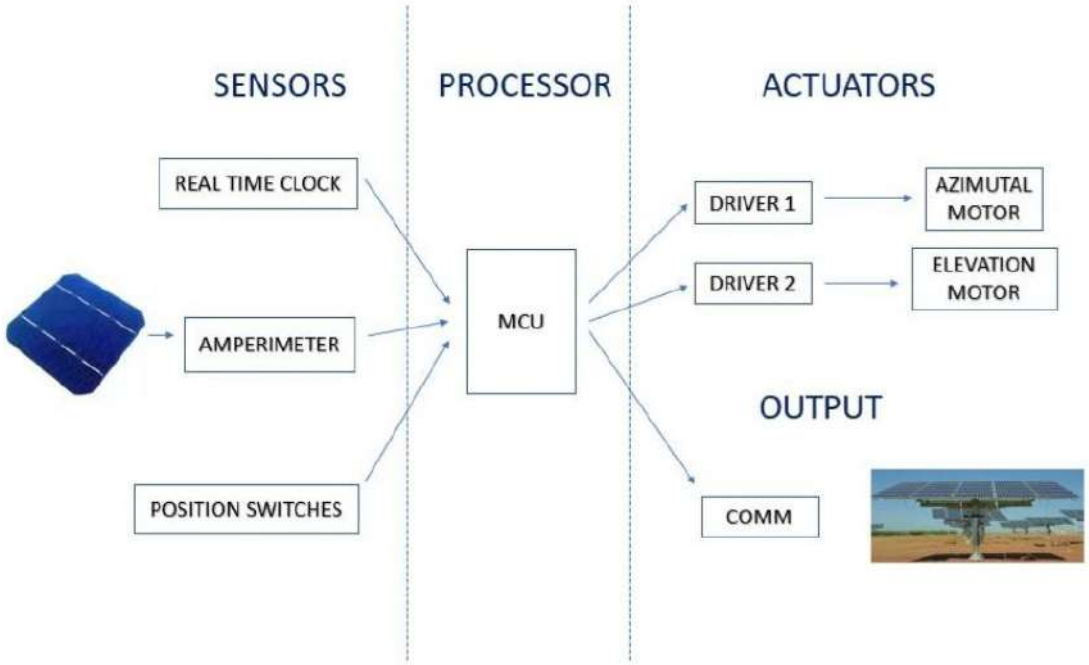

Figure 4.4. Scheme of principle of the proposed system

4.3. Results and Discussion

This section shows the results obtained when applying this device to the "Peñarroya I" PV plant, situated at a location of 38.299224° N latitude and -5.303114° longitude. The plant consists of 29 dual-axis solar trackers whose collectors measure 12m wide (a) by 5m high (b). Figure 4.5 shows its distribution in plan as well as the index assigned to each one and the reference system used to study the system. Table 4.1 shows the coordinates of the base of each collector.

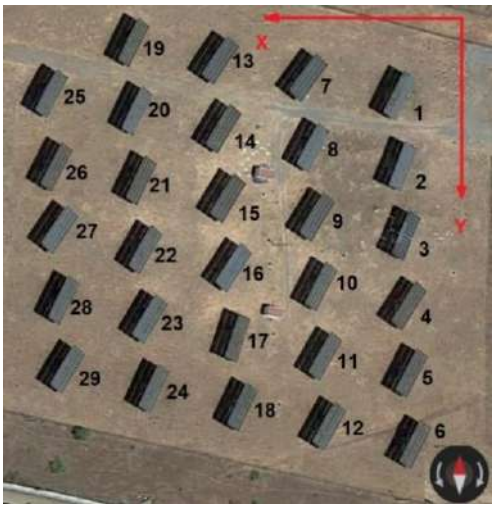

Figure 4.5. Dual-axis trackers plant Peñarroya I

Table 4.1. Coordinates (m) considered for each tracker

Tracker	x(m)	y(m)	z(m)
1	18.50	22.70	0.00
2	22.29	40.70	0.00
3	26.08	58.71	0.00
4	29.88	76.71	0.00
5	33.67	94.72	0.00
6	37.46	112.72	0.00
7	41.50	17.86	0.00
8	45.29	35.86	0.00
9	49.08	53.87	0.00
10	52.87	71.87	0.00
11	56.66	89.88	0.00
12	60.46	107.88	0.00
13	64.49	13.01	0.00
14	68.28	31.02	0.00
15	72.08	49.02	0.00
16	75.87	67.03	0.00
17	79.66	85.03	0.00
18	83.45	103.04	0.00
19	87.49	8.17	0.00
20	91.28	26.17	0.00
21	95.07	44.18	0.00
22	98.86	62.18	0.00
23	102.66	80.19	0.00
24	106.45	98.19	0.00
25	114.27	21.33	0.00
26	118.07	39.34	0.00
27	121.86	57.34	0.00
28	125.65	75.35	0.00
29	129.44	93.35	0.00

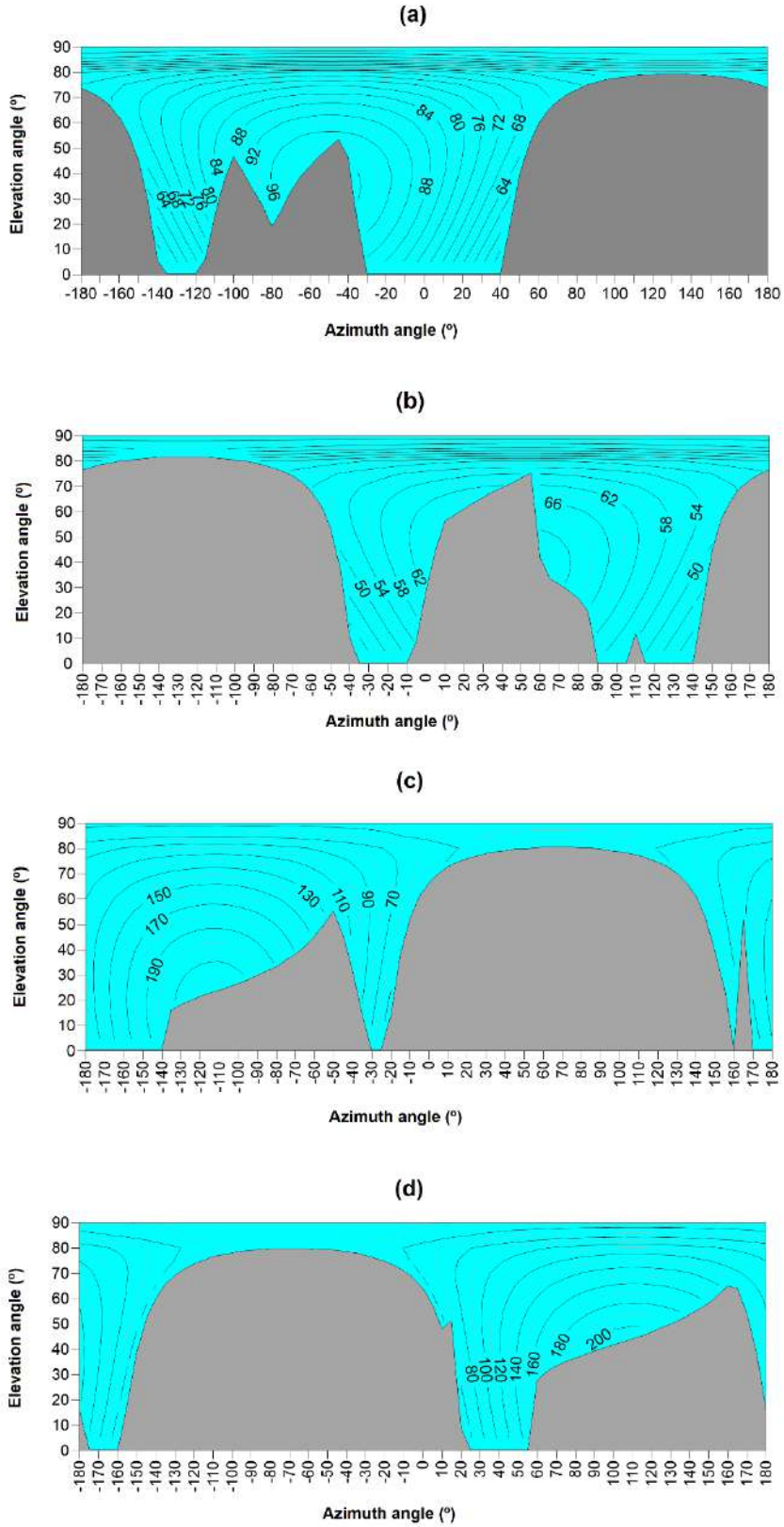

Figure 4.6. Simulation of the irradiance (W/m^2) values registered by the proposed device and the fragmentation of the celestial sphere at different moments of time: (a) December 21st at 8:24 AM in True Solar Time; (b) December 21st at 15:24 PM in True Solar Time; (c) June 21st at 7:30 AM in True Solar Time; (d) June 21st at 15:48 PM in True Solar.

Figure 4.6 shows the graphic representation of the data obtained by the proposed omnidirectional sensor at different times of the year in Lambert projection hemispheric diagram mode (Ramírez-Faz and López-Luque, 2012). These figures show the existence of two regions. Thus, the grey region represents the directions of the celestial sphere in which no measurements are taken since it corresponds to positions for which the algorithm prior to tracking indicates inter-shading of collectors. On the other hand, the blue region corresponds to the orientations of the solar servers for which there is no inter-shading and in which, consequently, irradiance (W/m^2) measurements are made, which are represented by the corresponding iso-level curves (grey lines).

The information shown on each chart is obtained by the sensor during every scanning cycle along the celestial sphere. There is evidence that this is the most complete traceability criterion available in the literature (Lorenzo et al., 2011, 2002; Panico et al., 1991; Schneider, 2012). In general, these methods are limited to the evaluation of installations on flat surfaces, normally horizontal, where only the potential shadows produced by the adjacent collectors are considered. These methods are also limited by the type of tracking they have been developed for. Even for certain types of tracking, such as the tracking of a vertical axis, they have not been computerized due to the lack of a published algorithm (PVsyst SA, 2020). The lack of open-source devices to solve optimal tracking, including backtracking, and of generic algorithms is also evident upon consulting commercial devices to manage backtracking. Although some manufacturers implement algorithms based on artificial intelligence (Array Tecnhologies, 2020; Nextracker TM, 2019) or on customized systems (STI Norland, 2019), authors have not found the theoretical basis of these published.

4.4. Conclusions

The present work shows the construction and design of a device capable of determining the incident solar irradiance on the collector planes of a PV plant with dual-axis trackers depending on their orientation (azimuth and elevation). From this irradiance, obtained by means of instantaneous measurements carried out while tracking the celestial sphere, the device is capable of determining the orientation of the solar trackers for which the incident irradiance on the collectors would be maximum, which allows optimising their energy capture and, consequently, the energy production of the PV plant.

The device described has been developed as Free and open-source hardware (FOSH), which, together with its publication in Open Access, makes it possible for the scientific and/or technological community to access all the details and therefore be able to analyse, modify or improve its design. Thus, it is presented as a pioneering technology in the sector as it is a

solution that is operational but simultaneously open to improvement by the scientific community in the framework of collaborative scientific-technical projects, assuming a revolution in the progress of science and technology.

Furthermore, as a novelty, in this device an ex professo algorithm has been implemented to discriminate at all times those celestial orientations that would imply inter-shading between the collectors of the PV plant. To do this, the device integrates the implementation of tracking and backtracking methodologies characterised and simulated by the authors (Fernández-Ahumada et al., 2020b, 2020a) in different photovoltaic plants under irradiance conditions described by empirical models. In this way, the solar trackers do not have to calculate the solar position using astronomical algorithms while taking into account other factors that also affect the incident solar irradiance, such as cloud cover, inter-shading between collectors, etc.

According to the aforementioned, the authors consider that the implementation of this device in photovoltaic plants will make it possible to improve the production of the PV plants while managers will be able to have real information both in terms of collectors and in other alternatives.

Capítulo 5 . Study of the dependence of solar radiation regarding design variables in photovoltaic solar installations with optimal dual-axis tracking

5.1. Introduction.

5.2. Methodology.

5.2.1. Vector Treatment of the Solar Position and the Estimation of the Solar Irradiance in the Celestial Sphere.

5.2.2. Method to Avoid Inter-Shading of Collectors.

5.2.3. Calculation Scheme of Intercepted Solar Radiation.

5.2.4. Cases Analysed.

5.3. Results.

5.4. Conclusions.

Study of the Dependence of Solar Radiation Regarding Design Variables in Photovoltaic Solar Installations with Optimal Dual-Axis Tracking

Gómez-Uceda, FJ [1]; Moreno-García, IM[2]*; Pérez-Castañeda, A[3]; Fernández-Ahumada, LM[4]

1 Department of Mechanics Engineering, Universidad de Córdoba, 14071 Cordoba, Spain; fjgomez@uco.es

2 Department of Electronic and Computer Engineering, Universidad de Córdoba, 14071 Cordoba, Spain

3 Physics for Renewable Energies Research Group, Universidad de Córdoba, 14071 Cordoba, Spain; perezcastanedaalvaro@gmail.com

4 Department of Electrical Engineering and Automatics, Universidad de Córdoba, 14071 Cordoba, Spain; lmfernandez@uco.es

***** Correspondence: isabel.moreno@uco.es; Tel.: +34-957212533

Abstract: Solar tracking is an efficient strategy to increase the radiative capture of photovoltaic collectors. Within the multiple efforts made in recent decades to improve the production of these facilities, various works have studied solutions to optimize the number of rotation axes (single or dual rotation axes), the degree of collector coverage, the distances between trackers, the geometric arrangement of trackers or the minimization of shading between collectors. However, although in this type of installation it is common to find collectors with geometric shapes other than rectangles, no studies on the influence of the shape of the collectors on the radiative incidence are found in the literature. In this connection, the present work systematically addresses the study of incident solar radiation in photovoltaic installations with dual-axis trackers with collectors of different geometric shapes. By means of the exhaustive study, the conclusion is drawn that, for dual-axis photovoltaic installations with an optimal tracking strategy, the main variables that influence the annual radiative incidence are the spacing between collectors, the coverage ratio (GCR), and the collector surface, while the type of arrangement of collectors and the shape of these do not show predictive values.

Keywords: photovoltaics; dual-axis solar trackers; shading in PV plants; solar tracking; backtracking

5.1. Introduction

There is no doubt about the important role that energy plays in our societies. Its implications go beyond mere technical aspects. Social structuring, economic development, and the environment, among others, are aspects that make up the complex implication of energy in the global agenda (López et al., 2018). In this context, renewable energies have been experiencing sustained growth in recent years. Thus, the International Energy Agency (IEA) foresees a record increase of 218 GW in the year 2021 in the net capacity of renewable electricity installed in the world, in an average scenario, that could reach up to 266 GW, in an accelerated scenario (International Energy Agency -IEA, 2020). In fact, during the first quarter of 2020, renewable energies were the only source of electricity whose demand increased despite the 2.5% decrease in global electricity demand caused by the blockades implemented by different governments to curb the spread of COVID-19 (Renewables 2020 Global Status Report, 2020).

Within the field of renewables, solar energy, in general, and photovoltaic (PV), in particular, are candidates to satisfy a large part of the global energy demand in the coming years due to their abundance and competitiveness (Kannan and Vakeesan, 2016). In fact, in the IEA predictions for the year 2021, solar PV accounts for 54% of the growth in the world's installed net renewable electricity capacity (International Energy Agency -IEA, 2020). The remarkable progress that the technology associated with the implementation of photovoltaic energy has been experiencing has not only driven its boom in recent years (Eldin et al., 2016; Salas and Olias, 2009) but this growth is expected to accelerate during the 2023–25 period (International Energy Agency -IEA, 2020).

One of the fundamental factors in the energy production of PV plants is the incident solar irradiance on the collectors. Among the various strategies that exist to increase this irradiance in solar collectors and, therefore, energy production in PV plants, is solar tracking, which is a technological niche in which there are still possible improvements that can contribute to such an increase (Eldin et al., 2016). This strategy is in contrast with fixed panel structures that have a constant orientation towards the sun depending on the latitude of the place where the PV installation is located. Thus, in the case of solar trackers, the PV modules move while looking for an orientation that generates more energy, either by capturing solar energy for as long as possible (Singh et al., 2018) or by capturing maximum solar irradiance (AL-Rousan et al., 2018; Frydrychowicz-Jastrzębska and Bugała, 2015).

The most common classification of trackers is established based on the number of axes used to move the modules. Thus, we speak of tracking systems on one axis (movement in

azimuth or elevation) or on two axes (movement in azimuth and elevation). Improving the technology of solar tracking systems is an important objective considering the high demand of energy resources, being the research niche for many authors. For example, in (Singh et al., 2018), different tracker motion control systems are studied with regard to their economic evaluation. In (AL-Rousan et al., 2018), the different solar trackers are studied in depth, performing a comparison between them in terms of efficiency, performance, advantages, and disadvantages, while other studies perform an in-depth review of the related literature to define the advantages of the applicability of solar tracking (Hafez et al., 2018; Lee et al., 2009).

In the scientific literature, there are studies that question the use of trackers with one or two axes versus fixed systems or one axis versus two. Specifically, various studies are being developed that question the various possibilities that arise in terms of efficiency, cost, location, production, etc., which is a real scientific challenge. For example, in (Antonanzas et al., 2018; Bahrami and Okoye, 2018; Quesada et al., 2015), authors analyze the effect of different solar trackers strategies considering the location. Other authors provide profits of the tracking photovoltaic systems in comparison with fixed photovoltaic systems (Hammad et al., 2017; Talavera et al., 2019). An interesting result is the one presented in (Hua et al., 2019), where a method for optimal storage capacity was calculated under the power-curtailment and storage/discharge requirements. Hence, although solar tracking systems have a higher cost than fixed systems, their maintenance is more complex and their exposure to environmental conditions is greater (Ali Jallal et al., 2020); the performance of dual-axis trackers are greater than those of fixed systems (Eke and Senturk, 2012; Şenpinar and Cebeci, 2012) and single-axis trackers (Bahrami et al., 2016; Koussa et al., 2011; Seme et al., 2011). Bahrami states in (Bahrami et al., 2016) that a dual-axis tracking system would result in greater irradiance than a single-axis due to its ability to minimize losses associated with cosine effect. Authors in (Koussa et al., 2011) highlight their conclusion that using the two-axis sun tracker system enables the PV panel to collect and produce higher amounts of electrical energy than using single-axis and fixed structures; their study considered five configurations of sun tracking systems and two traditional fixed panels. The results presented in (Seme et al., 2011) show that the optimal trajectories for the tilt and azimuth angle depend on the available solar radiation, solar cell efficiency, tracking system consumption, and the optimization bounds. Therefore, based on these studies, it can be affirmed that the choice of the type of strategy depends on several factors, it being necessary to delve into the technological and economic components to reach useful conclusions (Eldin et al., 2016).

Regarding the tracking mechanism, different driver methods can be distinguished to achieve the objectives of the collector movement (AL-Rousan et al., 2018). Among them, the

sensor driver systems stand out, whose operation is based on the variation of light received by optical sensors that cause the movement of the collectors looking for the position of the sun. Additionally, there are microprocessor driver systems that incorporate small processors with movement strategies programmed through mathematical models to locate the position of the sun. Within these in the bibliography are the open-loop driver systems that modify the movement of the actuators of the modules from mathematical equations that fix the position of the sun from the day and the hour. In contrast, closed-loop driver systems modify the movement of the actuators based on the information provided by position sensors, recalculating the position of the sun. Finally, intelligent driver systems incorporate artificial intelligence techniques to control the movement of collectors (Gómez-Uceda et al., 2021).

Another of the determining factors in the performance of a PV plant is the shading of its modules, since these shadows not only imply a lower incident irradiance (Fernández-Ahumada et al., 2020b) but also give rise to the appearance of hot spots that bring with them overheating and losses in energy production (Lorenzo et al., 2002). In this regard, the behavior of PV modules when they are partially shaded has been widely debated. Several simulation models have been used to find a configuration less susceptible to shadow problems of solar cells (Karatepe et al., 2007; Kaushika and Gautam, 2003; Trzmiel et al., 2020; Woyte et al., 2003). Specifically, Díaz-Dorado et al. (Díaz-Dorado et al., 2011) have analyzed the effect of shading in a PV tracker with partially shaded astronomical tracking based on the exact arrangement of shaded cells and modules. Other authors have analyzed the energy cost in the production of PV plants as a function of the connections between the cells and the modules (Martínez-Moreno et al., 2010) of the ground cover ratio (GCR) of the plant that depends on the variables of their design (Perpiñán, 2012) or of the tracking strategy (Lorenzo et al., 2002; Narvarte and Lorenzo, 2008).

One possible solution to alleviate the effect of shadows in PV plants with solar tracking is back tracking (Panico et al., 1991), which consists of modifying the orientation of the collecting surfaces in shading situations between panels in order to eliminate such shadows. Another possible solution is to modify the geometry of the collecting surfaces. Thus, although most of the PV panels found in PV plants connected to grids are rectangular, there are already some installations with dual-axis solar tracking where the collectors have other geometric shapes, such as those developed by the Deger Ibérica company in Tarragona (Spain), Ontario (Canada), or Estonia, with 15.6 kWp, 24 MWp, and 100 kWp installed, respectively (DEGERiberica, 2020). However, no previous works have been found in the literature aimed at characterizing the geometric shape of the collectors or their degree of modularity in terms of optimizing the performance of a photovoltaic installation in the event of the possible incidence of shading.

In this context, in the present work, the annual radiative uptake has been quantified in a wide set of PV installations with dual-axis monitoring with different geometries in which the shape of the collectors and the design parameters have been systematically varied. For each case, it has been assumed that the collectors follow the optimal solar tracking strategy proposed by Fernández-Ahumada et al. (Fernández-Ahumada et al., 2020a, 2017). Unlike traditional solar tracking methods that search for the position of the sun at each moment using astronomical models (Braun and Mitchell, 1983; Reda and Andreas, 2004; Riley and Hansen, 2015), according to this strategy, the collecting planes are oriented at each instant of time towards the direction of space in which the irradiance is maximum, except during the moments when such orientation implies the shading of one collector over another. When this occurs, normally at the beginning and end of the day, the collectors are oriented in the direction in which, without causing shading, the incident irradiance on the collectors is maximum. In this way, the production of each installation, which is considered proportional to annual solar radiation, is calculated under the hypothesis that each installation will follow an optimal tracking strategy adapted to its own geometry. Therefore, this study aims to advance the characterization of the electrical behavior of shaded solar trackers, which is an issue where the scientific community has made a considerable effort, simulating tracking strategies for an improvement in photovoltaic production (Antonanzas et al., 2018; Kelly and Gibson, 2009; Quesada et al., 2015).

To achieve this objective, after this introduction in which the scientific advances made by the scientific community in the field of solar tracking in PV plants are presented, the following section describes the methodology followed in this study to simulate annual solar radiation incident on collectors with a dual-axis tracking strategy that optimizes radiative uptake while avoiding shading between collectors. Similarly, the methodology established for the study of the influence of the design parameters of a PV plant on this annual solar irradiance is explained. Based on this, Section 3 presents the results when applying the methodology described to an existing PV plant (“El Molino”, Córdoba, Spain) with its design parameters systematically modified. Similarly, an adjustment model is proposed that represents in a simplified manner the dependence of the annual solar irradiance with respect to the design variables studied, and these dependencies are quantified. Finally, in Section 4, the main conclusions of the present study are presented.

5.2.Methodology

5.2.1. Vector Treatment of the Solar Position and the Estimation of the Solar Irradiance in the Celestial Sphere

In accordance with the above, this work presents a study of the influence of design variables on the performance of a PV plant with dual-axis tracking and optimal tracking strategy. This tracking strategy, which is described in the following section, will determine the orientation of the solar collectors at all times, which allows for optimizing radiative capture while avoiding shadows between collectors. In the present work, to determine at each instant of time the orientation of these collectors, as well as the position of the Sun in the celestial sphere, vector notation is used.

Figure 5.1 shows the coordinate system used, with the Ox axis oriented towards the west, the Oy axis towards the south, and the Oz axis towards the zenith. In this equation, $\vec{\imath}$, $\vec{\jmath}$, and $\vec{k}$ are the unit vectors on the axes Ox, Oy, and Oz, respectively; the unit vector that points towards the Sun, called the solar vector, $\vec{s}$, will be expressed by Equation (5.1), in which φ is the latitude of the place, δ the declination, and t the solar hour.

$$\vec{s} = s_x\vec{\imath} + s_y\vec{\jmath} + s_z\vec{k} = \tag{5.1}$$

$$sin\,\Omega\, tcos\delta\vec{\imath} + (cos\,\Omega\, tcos\delta sin\varphi - sin\delta cos\varphi)\vec{\jmath} + (cos\,\Omega\, tcos\delta cos\varphi + sin\delta sin\varphi)\vec{k}$$

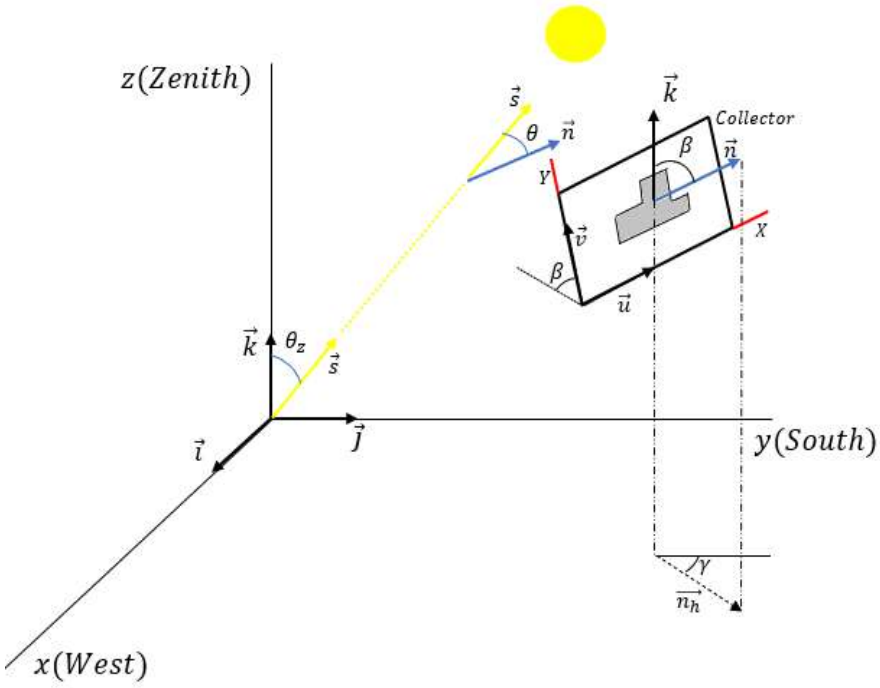

Figure 5.1. Astronomical and geometric magnitudes considered.

Equation (5.2) shows the mathematical expression proposed by Spencer (1971) for calculating the declination, δ, as a function of the daily angle, Γ, which in turn depends on the Julian day, d_n, according to Equation (5.3).

$$\delta(rad) = 0.006918 - 0.399912\,cos(\Gamma) + 0.070257 sin(\Gamma) - 0.006758\,cos(2\Gamma) + 0.000907 sin(2\Gamma) - 0.002697\,cos(3\Gamma) + 0.00148 sin(3\Gamma) \quad (5.2)$$

$$\Gamma(rad) = \frac{2\pi(d_n - 1)}{365} \quad (5.3)$$

The orientation of the collector plane at each instant of time can be represented by the unit vector perpendicular to it, $\vec{n}$, or by the pair of unit vectors, $\vec{u}$ and $\vec{v}$, contained in the collector plane, of which $\vec{u}$ is horizontal and $\vec{v}$ is parallel to the maximum slope direction of the collector plane (Figure 5.1). Thus, *γ* and β being the angles representing the azimuth and inclination of the collectors, respectively, the vectors $\vec{n}$, $\vec{u}$, and $\vec{v}$ will be given by Equations (5.4)–(5.6), respectively.

$$\vec{n} = sin\beta\ sin\gamma\vec{\imath} + sin\beta cos\gamma\vec{\jmath} + cos\beta\vec{k} \quad (5.4)$$

$$\vec{u} = -cos\gamma\ \vec{\imath} + sin\gamma\vec{\jmath} \quad (5.5)$$

$$\vec{v} = -cos\beta\ sin\gamma\vec{\imath} - cos\beta cos\gamma\vec{\jmath} + sin\beta\vec{k} \quad (5.6)$$

For the characterization of the incident solar irradiance on the collector planes, the model of Perez et al. (Perez et al., 1990) has been used. According to this model, the global solar irradiance, *I*, on an inclined plane at an angle β is the sum of the direct, diffuse, and reflected irradiance on an inclined plane, which, in turn, depends on the direct irradiance, I_B, and diffuse, I_D, on a horizontal surface, according to Equation (5.7), where θ is the angle between the normal vector and the collector plane ($\vec{n}$) and the solar vector ($\vec{s}$), θ_z is the zenith angle, *ρ* is the albedo of the surface of incidence of the irradiance before being reflected towards the collector, *a* and *b* are parameters given by Equations (5.8) and (5.9), and F_1 and F_2 are the weighting factors for the decomposition of the inclined diffuse radiation, the second addition, in the three subcomponents considered by the authors: isotropic diffuse, circumsolar diffuse, and diffuse from the horizon (Perez et al., 1990).

$$I = \frac{cos\,\theta}{cos\,\theta_z} I_B + \left[(1 - F_1)\frac{1 + cos\,\beta}{2} + F_1\frac{a}{b} + F_2\,sin\,\beta\right] I_D + \rho\frac{1 - cos\,\beta}{2}(I_B + I_D) \quad (5.7)$$

$$a = \max(\cos\theta, 0) \quad (5.8)$$

$$b = \max(\cos 85°, \cos\theta_z) \quad (5.9)$$

Substituting the vector expressions (5.10), (5.11), and (5.12) in Equation (5.7), we obtain Equation (5.13), in which the dependence of *I* on $\vec{n}$ is made explicit,

$$cos\,\beta = \vec{k} \cdot \vec{n} \quad (5.10)$$

$$cos\,\theta = \vec{s} \cdot \vec{n} \tag{5.11}$$

$$cos\,\theta_z = \vec{s} \cdot \vec{k} \tag{5.12}$$

$$I = \frac{\vec{s} \cdot \vec{n}}{\vec{s} \cdot \vec{k}} I_B + \left[(1 - F_1) \frac{1 + \vec{k} \cdot \vec{n}}{2} + F_1 \frac{\vec{s} \cdot \vec{n}}{b} + F_2 \sqrt{1 - \left(\vec{k} \cdot \vec{n}\right)^2} \right] I_D + \rho \frac{1 - \vec{k} \cdot \vec{n}}{2} (I_B + I_D) \tag{5.13}$$

The production of a PV plant will be greater to the extent that the incident irradiance on its collectors is greater. In this regard, Fernández-Ahumada et al. (Fernández-Ahumada et al., 2017) showed that the incident irradiance on the collectors is maximum when they are oriented in such a way that their normal vector verifies Equation (5.14). In accordance with this result, the authors propose a new tracking strategy for PV plants with dual-axis trackers in which they are oriented according to Equation (5.14), and consequently, radio capture and energy production are optimized.

$$\vec{n} = \frac{\frac{\partial I}{\partial(\vec{s} \cdot \vec{n})} \vec{s} + \frac{\partial I}{\partial(\vec{k} \cdot \vec{n})} \vec{k}}{\sqrt{\left(\frac{\partial I}{\partial(\vec{s} \cdot \vec{n})}\right)^2 + \left(\frac{\partial I}{\partial(\vec{k} \cdot \vec{n})}\right)^2 + 2 \left(\frac{\partial I}{\partial(\vec{s} \cdot \vec{n})}\right)\left(\frac{\partial I}{\partial(\vec{k} \cdot \vec{n})}\right) \vec{s} \cdot \vec{k}}} \tag{5.14}$$

Therefore, when applying this tracking strategy to the model of Perez et al. (1990), the partial derivatives given by expressions (5.15) and (5.16) are obtained. Substituting these results in Equation (5.14), Equation (5.17) is obtained, which represents the direction of the normal vector to the collecting planes corresponding to the optimal tracking strategy proposed by Fernández-Ahumada et al. (Fernández-Ahumada et al., 2017) for PV plants with dual-axis tracking.

$$\vec{n} = \frac{\frac{\partial I}{\partial(\vec{s} \cdot \vec{n})} \vec{s} + \frac{\partial I}{\partial(\vec{k} \cdot \vec{n})} \vec{k}}{\sqrt{\left(\frac{\partial I}{\partial(\vec{s} \cdot \vec{n})}\right)^2 + \left(\frac{\partial I}{\partial(\vec{k} \cdot \vec{n})}\right)^2 + 2 \left(\frac{\partial I}{\partial(\vec{s} \cdot \vec{n})}\right)\left(\frac{\partial I}{\partial(\vec{k} \cdot \vec{n})}\right) \vec{s} \cdot \vec{k}}} \tag{5.15}$$

$$\frac{\partial I}{\partial(\vec{k} \cdot \vec{n})} = \left(\frac{(1 - F_1)}{2} - F_2 \frac{\vec{k} \cdot \vec{n}}{\sqrt{1 - \left(\vec{k} \cdot \vec{n}\right)^2}} \right) I_D - \rho \frac{(I_B + I_D)}{2} \tag{5.16}$$

$$\vec{n} = \frac{\left(\frac{I_B}{\vec{s} \cdot \vec{k}} + F_1 \frac{I_D}{b}\right) \vec{s} + \left(\frac{(1 - F_1)\, I_D}{2} - F_2 \frac{\vec{k} \cdot \vec{n}}{\sqrt{1 - \left(\vec{k} \cdot \vec{n}\right)^2}} I_D - \rho \frac{(I_B + I_D)}{2} \right) \vec{k}}{\sqrt{\left(\frac{I_B}{\vec{s} \cdot \vec{k}} + F_1 \frac{I_D}{b}\right)^2 + \left(\frac{(1 - F_1)\, I_D}{2} - F_2 \frac{\vec{k} \cdot \vec{n}}{\sqrt{1 - \left(\vec{k} \cdot \vec{n}\right)^2}} I_D - \rho \frac{(I_B + I_D)}{2} \right)^2 + 2 \left(\frac{I_B}{\vec{s} \cdot \vec{k}} + F_1 \frac{I_D}{b}\right) \left(\frac{(1 - F_1)\, I_D}{2} - F_2 \frac{\vec{k} \cdot \vec{n}}{\sqrt{1 - \left(\vec{k} \cdot \vec{n}\right)^2}} I_D - \rho \frac{(I_B + I_D)}{2} \right) \vec{s} \cdot \vec{k}}} \tag{5.17}$$

Given the difficulty of solving the variable $\vec{n}$ in Equation (5.17), an iterative method based on the series convergence of vectors $\{\vec{n}_0 (= \vec{s}), \vec{n}_1, \vec{n}_2, \ldots, \vec{n}_j\}$ is proposed, in which each vector $\vec{n}_j$ is obtained as a function of $\vec{n}_{j-1}$ according to Equation (5.18), and consequently, $\vec{n}$

will be given by Equation (5.19). Given the nature of the problem, in this work, it has been considered that *j* = 25 is a sufficiently high value since the correct convergence of this value has been verified for all the practical cases studied.

$$\vec{n}_j = \frac{\left(\frac{I_B}{\vec{s}\cdot\vec{k}} + F_1\frac{I_D}{b}\right)\vec{s} + \left(\frac{(1-F_1)\,I_D}{2} - F_2\frac{\vec{k}\cdot\vec{n}_{j-1}}{\sqrt{1-\left(\vec{k}\cdot\vec{n}_{j-1}\right)^2}}I_D - \rho\frac{(I_B+I_D)}{2}\right)\vec{k}}{\sqrt{\left(\frac{I_B}{\vec{s}\cdot\vec{k}} + F_1\frac{I_D}{b}\right)^2 + \left(\frac{(1-F_1)\,I_D}{2} - F_2\frac{\vec{k}\cdot\vec{n}}{\sqrt{1-\left(\vec{k}\cdot\vec{n}\right)^2}}I_D - \rho\frac{(I_B+I_D)}{2}\right)^2 + 2\left(\frac{I_B}{\vec{s}\cdot\vec{k}} + F_1\frac{I_D}{b}\right)\left(\frac{(1-F_1)\,I_D}{2} - F_2\frac{\vec{k}\cdot\vec{n}}{\sqrt{1-\left(\vec{k}\cdot\vec{n}\right)^2}}I_D - \rho\frac{(I_B+I_D)}{2}\right)\vec{s}\cdot\vec{k}}} \quad (5.18)$$

$$\vec{n} = \lim_{j\to\infty}\vec{n}_j \quad (5.19)$$

5.2.2. Method to Avoid Inter-Shading of Collectors

According to the studies found in the bibliographic review, the shading of solar panels negatively affects their energy production. Therefore, to optimize the performance of a PV plant with dual-axis solar trackers, as those discussed in this study, it is necessary to accompany an adequate tracking strategy with a procedure that prevents the collectors from shading each other.

In this regard, Fernández-Ahumada et al. (Fernández-Ahumada et al., 2020a) presented a dichotomous criterion to quickly determine whether or not there is inter-shading between collectors. The method is based on the fact that, in an installation with collectors of the same geometric shape oriented towards the same direction of the celestial sphere (characterized by its normal vector, $\vec{n}$), the shadow cast by a collector Π_i on the plane ψ that contains the reference collector Π_0 is a polygon Π'_i with the same shape as the contour of the collector (Figure 5.2).

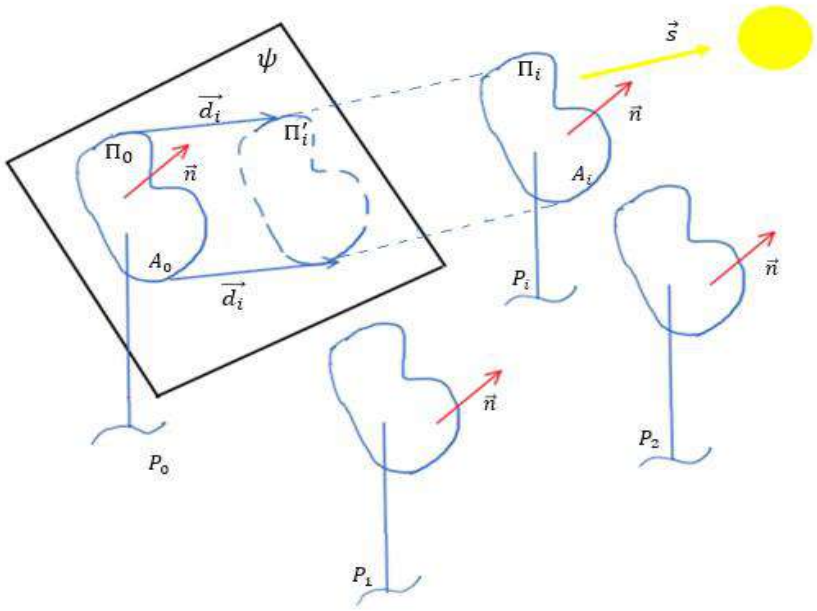

Figure 5.2. Shadow cast by a collector Π_i on the plane ψ that contains the reference collector Π_0

Hence, vector $\vec{d}_i$ is the geometric displacement vector from polygon Π_0 to Π'_i. This vector, as shown by the authors, is obtained through the equation (5.20), although it must be considered that, for the collector Π_i to be able to shade the collector Π_0, the conditions expressed in Equations (5.21)–(5.23) must be fulfilled.

$$\vec{d_i}=\overrightarrow{P_oP_i}-\frac{\overrightarrow{P_oP_i}\cdot\vec{n}}{\vec{s}\cdot\vec{n}}\vec{s} \tag{5.20}$$

$$\vec{s}\cdot\vec{k}>0 \tag{5.21}$$

$$\vec{s}\cdot\vec{n}>0 \tag{5.22}$$

$$\overrightarrow{P_0P_i}\cdot\vec{n}>0 \tag{5.23}$$

From expression (5.20), given that $\vec{d}_i$ is a vector included in the collector plane ψ, Equations (5.24) and (5.25) allow for determination of the components of this vector in the OXY reference system contained in the plane ψ and defined by the vectors $\vec{u}$ y $\vec{v}$.

$$d_{Xi}=\vec{d}_i\cdot\vec{u} \tag{5.24}$$

$$d_{Yi}=\vec{d}_i\cdot\vec{v} \tag{5.25}$$

Knowing $\vec{d}_i$ and its components d_{Xi} and d_{Yi}, the dichotomous criterion proposed by Fernández-Ahumada et al. (Fernández-Ahumada et al., 2020a), based on Minkowski's algebra (Avnaim and Boissonnat, 1989; Chazelle, 1983; Lozano-Pérez, 1983) and whose validity is demonstrated in Appendix A, it is established that there will be an intersection of the polygons Π_0 and Π'_i. Therefore, mutual shading between the panels Π_0 y Π_i, if, when representing

vector $\vec{d}_i$ from the origin of coordinates, the end of the vector is included within the plane curve *Σ,* which is obtained as the envelope of the family of all polygons that can be drawn on the plane ψ by translating the polygon Π_0 with the condition that its perimeter is in contact with the coordinate origin of the reference system contained in ψ (Figure 5.3).

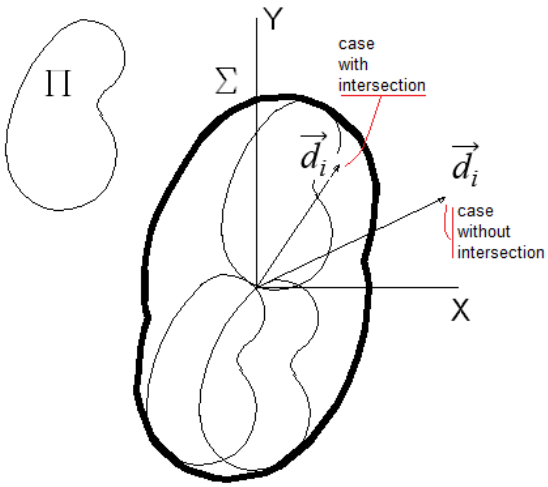

Figure 5.3. Determination of Σ, auxiliary curve of the intersection criterion and existence of shadow between panels.

It is important to note that, since photovoltaic collectors are built by annexing rectangular photovoltaic modules, the resulting geometric shape for the collector is, in general, a closed polygon in which all sides of the perimeter are contained in two directions perpendicular to each other, as shown by the orange line in Figure 5.4. This fact leads to the determination of the envelope Σ being simplified and able to be performed analytically. Furthermore, this envelope (blue trace in Figure 5.4) will also be a closed polygon with the sides parallel and perpendicular to the directions of the perimeter of the collectors (Figure 5.4). Therefore, the envelope is mathematically described by the coordinates $X_{env}(k)$ and $Y_{env}(k)$ of each vertex *k* of the polygon ($1 < k < N_{env}$, N_{env} being the total number of vertices of Σ). In Appendix B, the analytical obtaining of the enclosure for photovoltaic collectors is detailed in a generic way.

According to Figure 5.4, the end of vector $\vec{d}_i$ would be located inside the envelope Σ and, therefore, there would be shading between the panels Π_0 y Π_i if there is some vertex *k* for which the mathematical condition given by Equation (5.26) is fulfilled.

$$\begin{gathered}\left[sign(d_{Xi}) = sign\left(X_{env}(k)\right)\right] and \left[sign(d_{Yi}) = sign\left(Y_{env}(k)\right)\right] and \\ \left[|d_{Xi}| < |X_{env}(k)|\right] and \left[|d_{Yi}| < |Y_{env}(k)|\right]\end{gathered} \tag{5.26}$$

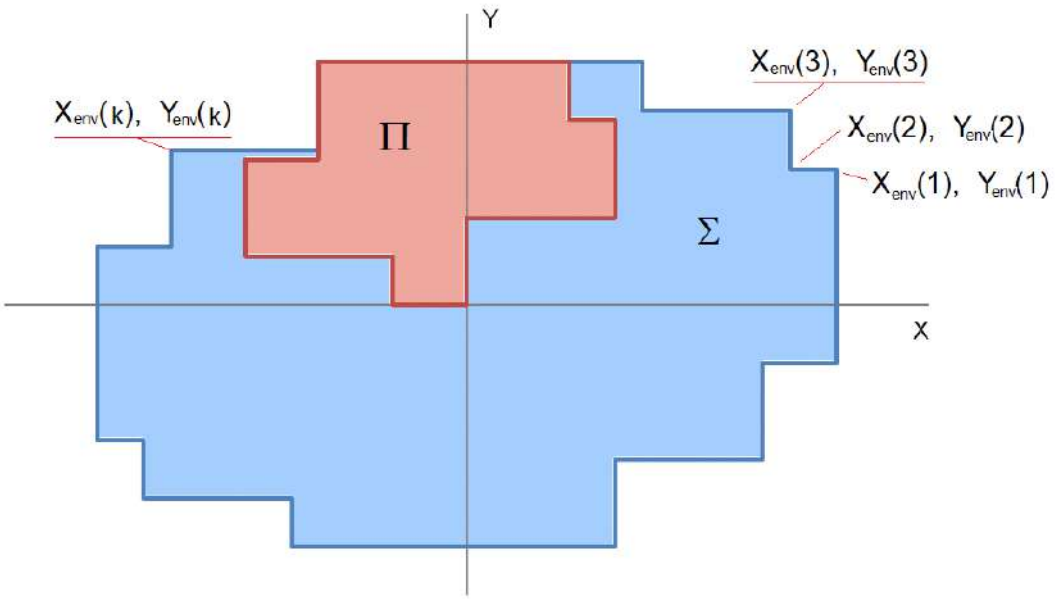

Figure 5.4. Form. Generic shape of a solar collector (orange) and its envelope Σ (blue).

In accordance with the above, Figure 5.5 shows, by means of a flow diagram, the inter-shading $(\vec{n})$ function, especially designed to implement the method described in this section to determine the existence of shadow between modules in PV installations with dual-axis tracking and regular distribution of collectors. This Boolean function depends on the vector $\vec{n}$, Equation (5.19), returning a value "true" if $\vec{n}$ implies inter-shading and "false" otherwise. As can be seen in Figure 5.5, only possible shading is studied in the reference collector, considered representative of the set, which is totally surrounded by N_t trackers.

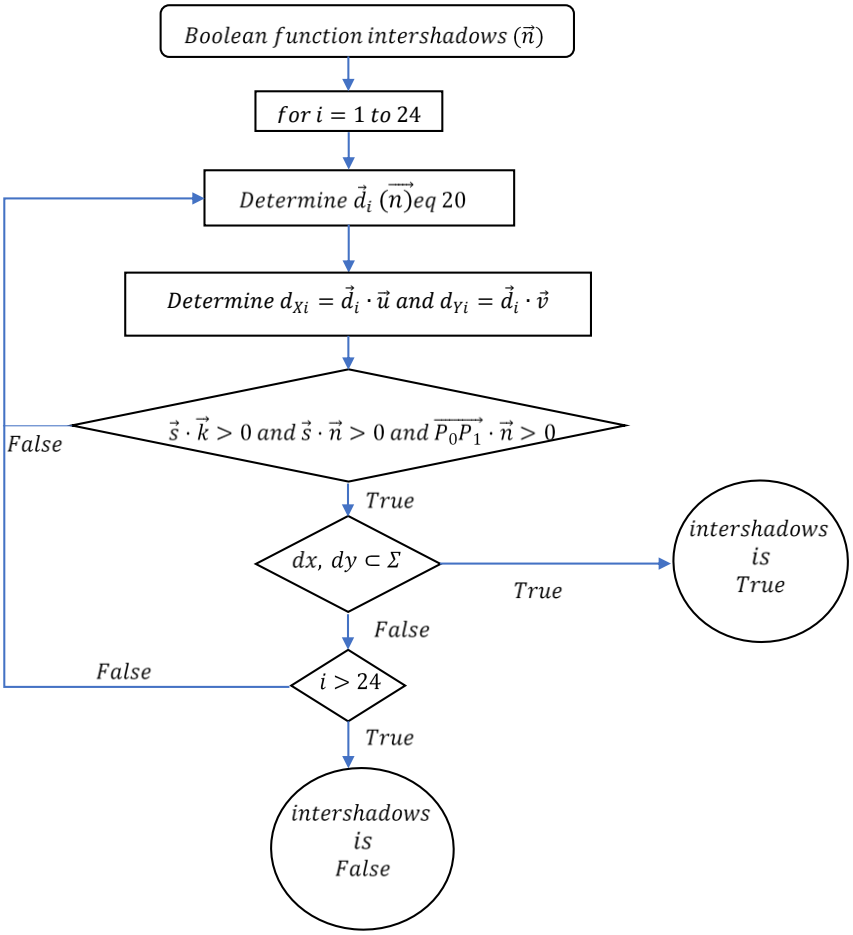

Figure 5.5. Flow diagram of the inter-shading function ($\vec{n}$).

In this way, in the case that the value of $\vec{n}$, obtained from Equation (5.19), does not imply shadows between collectors, $intershadows(\vec{n}) = False$, the optimal tracking strategy will propose the orientation of the collectors according to the address of $\vec{n}$. On the contrary, if the value of $\vec{n}$, obtained from Equation (5.19), implies shadows between collectors, $intershadows(\vec{n}) = True$, the orientation that does not imply shadows and that maximizes the incident irradiance must be sought. In that case, back tracking is used following the process indicated in Figure 5.6.

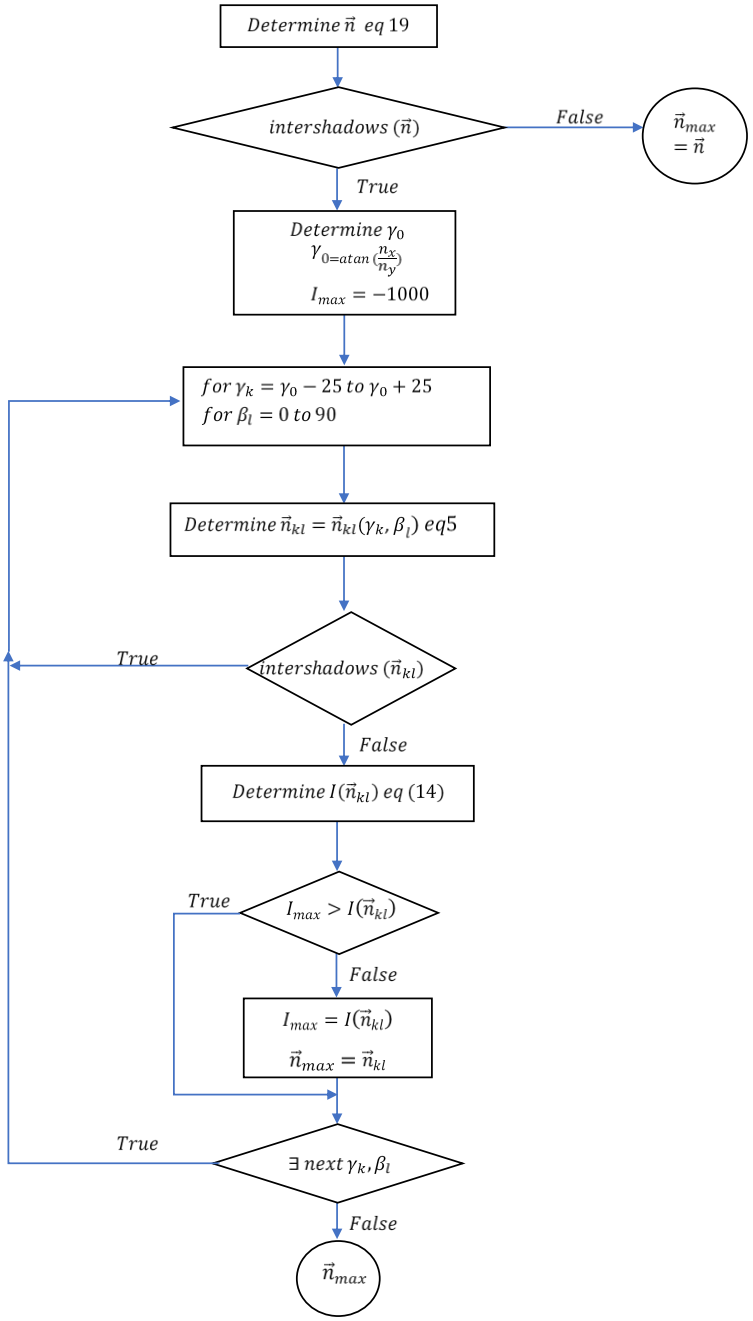

Figure 5.6. Flow diagram to determine the orientation ($\vec{n}$) of maximum irradiance uptake without any inter-shading between collectors.

5.2.3. Calculation Scheme of Intercepted Solar Radiation

With the methodology described for solar tracking, the incident solar irradiance on solar collectors has been simulated for the 12 representative days, according to Klein (Klein, 1977). From this irradiance, the incident radiation on the collectors on each representative day *m* has been calculated using Equation (5.27), where the integral has been approximated by discretizing the sum in time intervals of three minutes.

$$H_m = \int_{t_{sunrise,m}}^{t_{sunset,m}} \left[\frac{\vec{s}\cdot\vec{n}}{\vec{s}\cdot\vec{k}} I_B + \left[(1-F_1)\frac{1+\vec{k}\cdot\vec{n}}{2} + F_1\frac{\vec{s}\cdot\vec{n}}{b} + F_2\sqrt{1-\left(\vec{k}\cdot\vec{n}\right)^2} \right] I_D + \rho\frac{1-\vec{k}\cdot\vec{n}}{2}(I_B+I_D) \right] dt \quad (5.27)$$

Once the daily radiation has been calculated for the representative days proposed by Klein (Klein, 1977) for each of the 12 months of the year (m = 1,2, ..., 12), the annual global radiation (H_{year}) is calculated according to Equation (5.28), where N_m is the number of days in the month m.

$$H_{year} = \sum_{m=1}^{12} N_m \cdot H_m \quad (5.28)$$

5.2.4. Cases Analyzed

In this work, the effect of the shape of the collectors on the capture of annual radiation in a PV plant with dual-axis tracking has been studied. To generate the study scenarios, the design of "El Molino", a photovoltaic installation located in Córdoba (latitude = 37.75492° N; longitude = 5.04548° W) was used as a starting point. It is an installation with dual-axis trackers (with azimuth and elevation movement) and rectangular collectors 8 m wide and 5 m high. Each collector is made up of 25 photovoltaic modules 1m high and 1.6m wide (Figure 5.7a). The trackers are arranged in a regular grid on horizontal ground, initially separated by a distance D_{EW} =20 m in the EW direction and D_{NS} =14 m in the NS direction (Figure 5.7b).

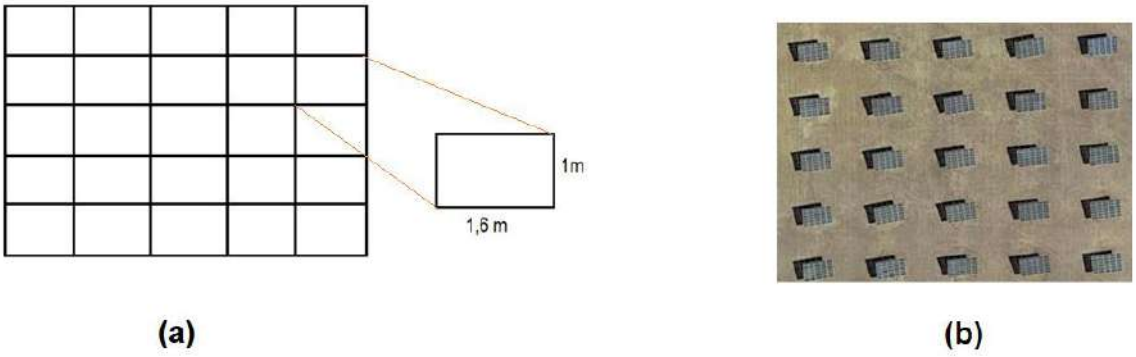

Figure 5.7. Design characteristics of the "El Molino" facility: (a) Constitution of the collectors; (b) Arrangement of collectors.

Case studies arise by introducing different variations in the original design and crossing all possible sources of variation. Specifically, the variations introduced consist of:

- *Modification of the collector shape.* The possibility of introducing cuts at the vertices has been considered to study the collectors with the shape indicated in Figure 5.8. Letting (X_{ul}, Y_{ul}), (X_{ur}, Y_{ur}), (X_{dl}, Y_{dl}), and (X_{dr}, Y_{dr}) be the coordinates of the vertices corresponding to the cuts made in the upper left, upper right, lower left, and lower right corners, the possible values considered (in metres) for each of these pairs were (0,0),

(1,1.6), (1,3.2), (2,1.6), and (2,3.2). The crossing of all the possibilities generated N_G = 5^4 = 625 different forms of collector.

- *Modification of the inter-distances*. Letting D_{NS} be the distance in the NS direction between rows of collectors and D_{EW} the distance in the EW direction between columns of collectors, the possibilities D_{NS} = 10 m, 12.5 m, 15 m, 17.5 m, and 20 m and D_{EW} = 10 m, 15 m, 20 m, and 25 m were studied. The crossing of these possibilities gave rise to N_D = 20 designs of different distances.
- *Modification of the spatial distribution of the solar trackers.* For each pair of distances (D_{NS}, D_{EW}), N_S = 2, possible spatial distributions of the solar trackers in the plant were studied, both the regular grid arrangement oriented to the south (Figure 5.9a) and staggered (Figure 5.9b). In both configurations, it was considered that the reference collector in the study (*i* = 0) was surrounded by 24 collectors.

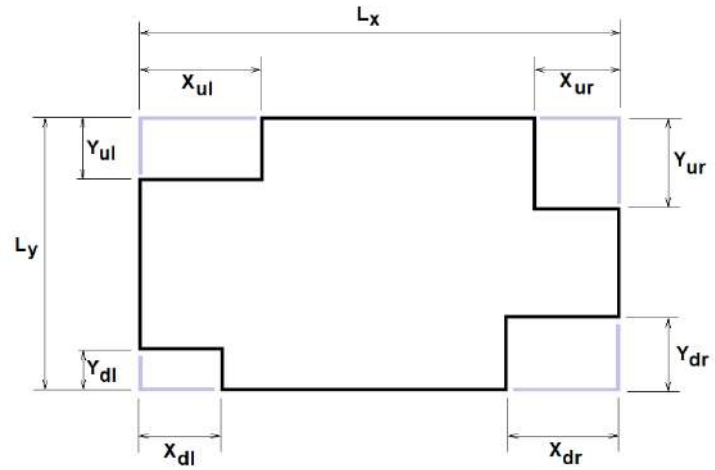

Figure 5.8. Generic way of describing the clipped vertex collector.

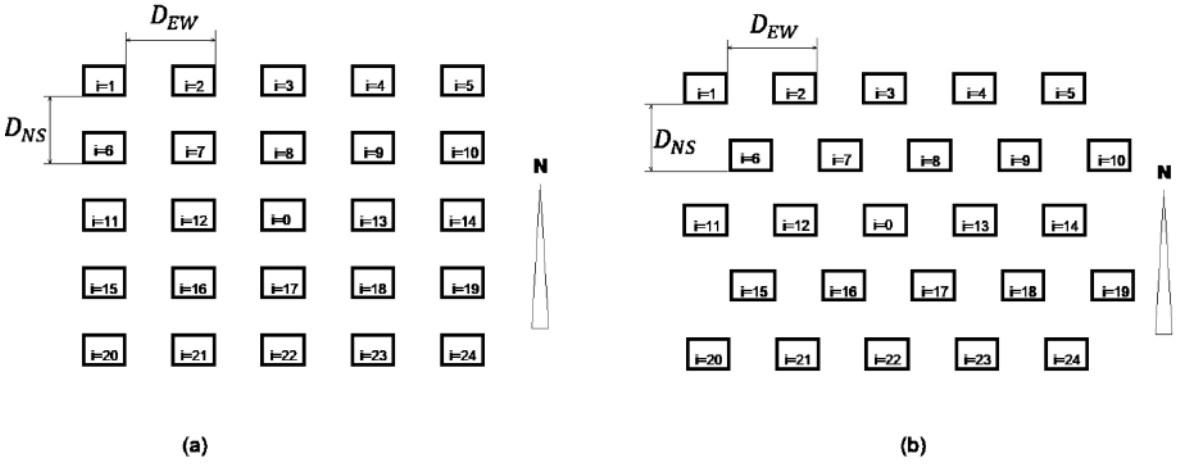

Figure 5.9. Considered spatial arrangements and location of the reference collector in the study (i = 0): (a) regular grid; (b) staggered.

The crossing of all the possibilities generated $N_T = N_G \cdot N_D \cdot N_S = 25000$ different combinations of geometric designs for the PV plant "El Molino" with dual-axis tracking and its collectors. For each of these designs, the annual incident radiation on the collectors was obtained by the method set forth, equation (5.28), considering the 12 characteristic days proposed by Klein (Klein, 1977), and the monthly mean radiation values (Posadillo and López Luque, 2008) set forth in Table 5.1.

Table 5.1. Data considered for the estimation of the annual solar irradiance in "El Molino" PV Plant (Cordoba, Spain): horizontal daily radiation, H (Posadillo and López Luque, 2008) *and representative day proposed by* (Klein, 1977) *each month of the year.*

Month	***H* (J/m^2)**	**Representative Day**
January	7401000	17
February	11097000	47
March	14158000	75
April	17307000	105
May	19017000	135
June	24263000	162
July	25719000	198
August	23411000	228
September	17983000	258
October	11895000	288
November	8228000	318
December	6237000	344

5.3.Results

This section describes the incident radiation values on collectors and the results of the study of the influence of the design variables on the solar incidence on the PV plant designs considered. The synoptic values obtained for the annual incident radiation in collectors are summarized in Table 5.2. Figure 5.10 shows the distribution of values obtained depending on the membership intervals.

Table 5.2. Descriptive parameters of the set of values of Hyear (kWh/m^2).

Number of Cases	**25000**
Average	2172.0
Minimum	2040.2
Maximum	2233.8
Median	2189.6

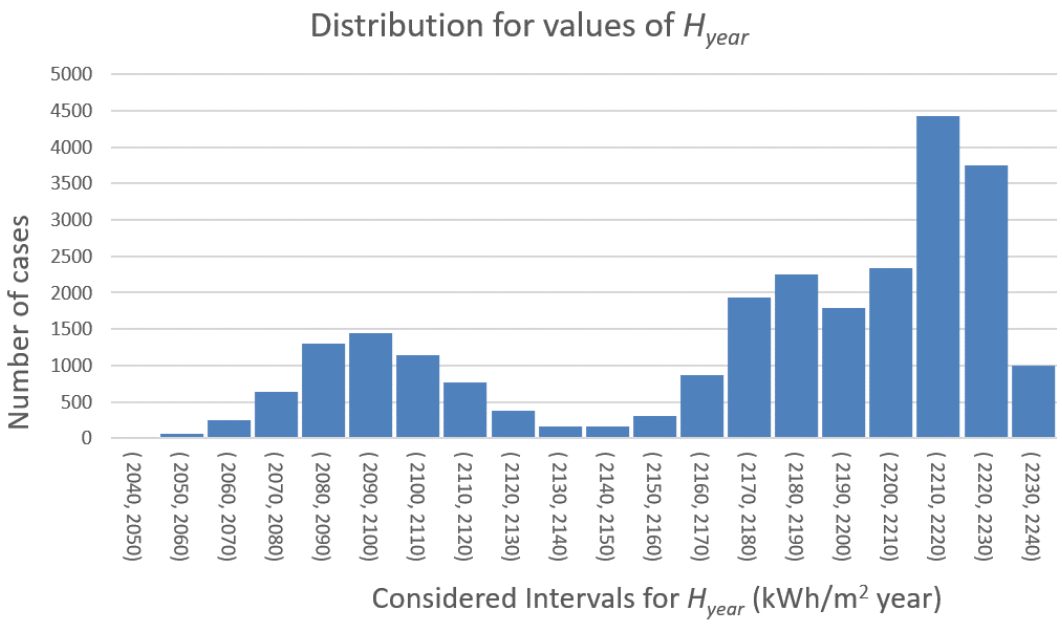

Figure 5.10. Distribution of annual solar radiation values (H) according to membership intervals.

In the set of values obtained, it is observed that certain forms of the collector offer the same value. These are the cases in which the set of cuts A, B, C and D of Figure 5.11a are permuted as shown in Figure 5.11b–d,f–i. A detailed analysis of the procedure followed makes it possible to verify that the shape of the solar collector does not influence directly but rather through its envelope. As a consequence, the collector shapes of the first column (5.11 (a), 5.11 (b), 5.11 (c), 5.11 (d)) give rise to identical annual radiation results since they all give rise to the same envelope Σ (represented in Figure 5.11e). On the other hand, the coincidence of radiation outcomes in the results between the collector shapes of the first (Figure 5.11a–d) and the second column (Figure 5.11f–i) should be understood as a consequence of the symmetry with respect to the NS axis of the studied configurations and of the symmetry with respect to this plane in the positions of the sun between the hours of the morning and afternoon.

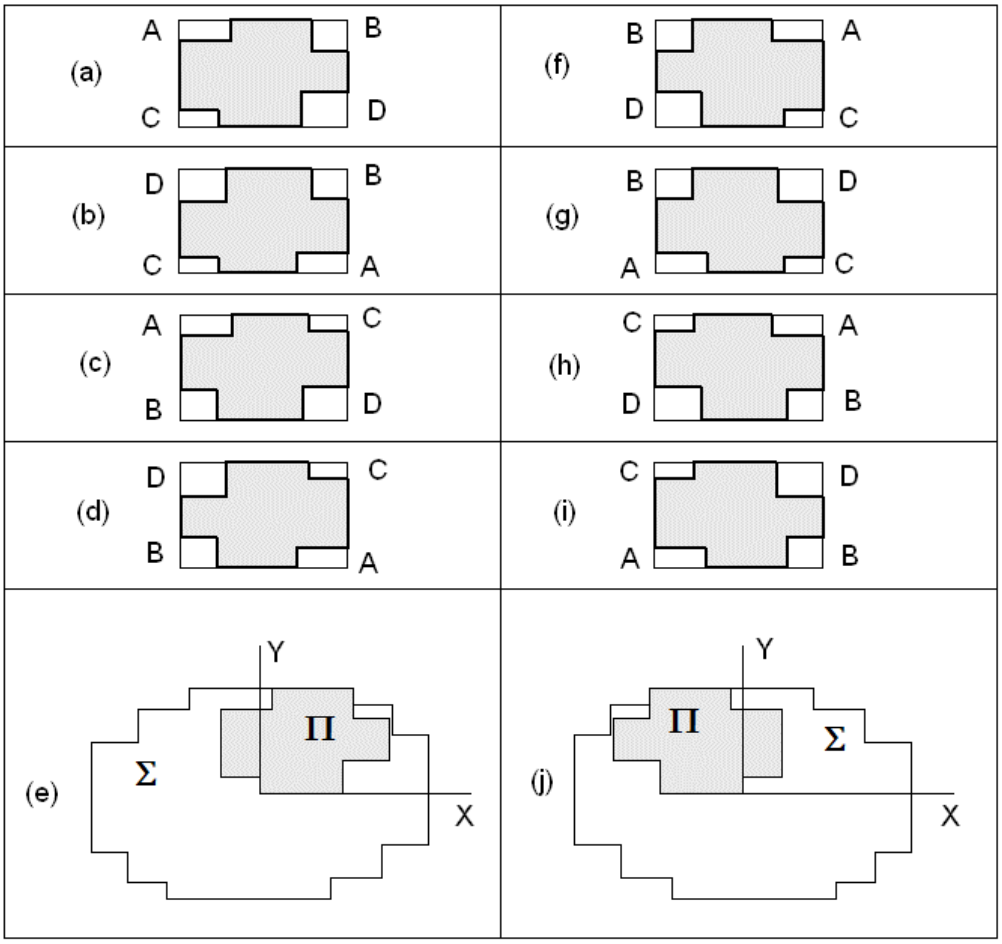

Figure 5.11. Set of collector shapes that generate identical annual incident radiation results. The forms (a–d) generate the same envelope Σ (e) and the set of symmetric figures with respect to a vertical axis (f–i) generate a symmetric envelope Σ' of Σ (j).

The dependence of the values obtained with respect to the considered design variables was studied using an approximation and simplified model, in which the calculated annual radiation was expressed as a function of the following explanatory variables:

- Collector surface $S_{col}(m^2)$.
- Distance between trackers in east–west direction, $D_{EW}\ (m)$
- Distance between trackers in north–south direction, $D_{NS}\ (m)$
- Discriminatory variable of the type of configuration T (T = 1 for staggered configurations and T = 0 for regular grids).

In this sense, it is worth highlighting that the model described and used (for each of the 25,000 cases) can be considered a mathematical function of the variables proposed. However, the complexity of the model and the need to aggregate results on the different representative days made it difficult to know the weight or influence of each variable on the final results. Thus, to overcome this difficulty, this paper proposes to replace this complex function with a mathematical function of simple expression reproducing the result of the complex model with

the least possible error. The reader should assume that this is not a statistical problem but rather a problem of adjustment or approximation of a simple expression function to a complex function, so that statistical methods are not applicable. To address the fit, the set of simple variables was extended with composite variables obtained as products and ratios of simple variables. The proposed function (5.29) was selected from the set of fits to linear functions of composite variables. It lacks a clear physical meaning, but it allows for reproduction of the results of the model with an average relative error equal to 2.561 kWh/m^{2}year; therefore, it is considered suitable for the study of the relative weight of the variables.

Equation (5.29) shows the mathematical expression of this model for which the parameters *a, b, c, d, e, f, g, h, l, r,* and *w* have been obtained by the least squares method (Table 5.3), with an adjustment coefficient R^2 = 0.993. Table 5.4 shows the synoptic values of the estimation errors of the model ε and ε_{rel}, given by Equations (5.30) and (5.31), where H_{year}^{est} is the annual solar irradiance on the solar collectors estimated according to equation (5.28) and H_{year}^{adj} is the one approximated by the model (5.29). The low value obtained for the mean square error means that the equation can be considered valid for the study of dependence of the annual solar irradiance with respect to the variables S_{col}, D_{EW}, D_{NS}, and T.

$$H_{year}^{adj} = a + b\,S_{col} + c\,D_{EW} + \frac{d}{D_{EW}} + eD_{NS} + f\ {D_{NS}}^2 + g\ \frac{D_{EW}}{D_{NS}} + h\left(\frac{D_{EW}}{D_{NS}}\right)^2 + l\ \frac{S_{col}}{D_{NS}\,D_{EW}} + r\ \frac{D_{NS}\,D_{EW}}{S_{col}} + w\,T \tag{5.29}$$

$$\varepsilon = \left|H_{year}^{est} - H_{year}^{adj}\right| \tag{5.30}$$

$$\varepsilon_{rel} = \frac{\left|H_{year}^{est} - H_{year}^{adj}\right|}{H_{year}^{est}} \tag{5.31}$$

Table 5.3. Values obtained for the model of equation (5.29).

Parameter	Units	Value
a	kWh/m^2 year	2656.366
b	kWh/m^4 year	−0.960
c	kWh/m^3 year	6.921
d	kWh/m year	−25.783
e	kWh/m^{3}year	−756.012
f	kWh/m^4 year	0.512
g	kWh/m^2 year	−167.750

h	kWh/m^2 year	19.071
l	kWh/m^2 year	−364.603
r	kWh/m^2 year	−1.365
w	kWh/m^2 year	−1.661

Table 5.4. Synoptics of the errors ε equation (5.30) and εrel equation (5.31) obtained for the model given by equation (5.29).

	$\boldsymbol{\varepsilon}$ **(kWh/m^2 year)**	$\boldsymbol{\varepsilon_{rel}}$ **(Dimensionless)**
Number of cases	25000	25000
Average	3.302	$1.53 \cdot 10^{-3}$
Minimum	$4.67 \cdot 10^{-4}$	$2.099 \cdot 10^{-7}$
Maximum	35.913	$1.66 \cdot 10^{-2}$
Median	2.561	$1.15 \cdot 10^{-3}$

It is important to note that the model adjusted in Equation (5.30) does not consider the geometric shape of the collectors itself since, given that the mean error, $\bar{\varepsilon}$, of the proposed model is 3.3 kWh/m^{2}year (Table 5.4), the geometric shape would not have an explanatory capacity superior to this $\bar{\varepsilon}$. This reasoning allowed us to conclude the little influence of the shape of the collectors in facilities that follow the tracking/ back-tracking policy considered in this work.

For a better interpretation of the adjusted Equation (5.29), we can consider it as the addition of four terms separated by parentheses in Equation (5.32).

$$H_y^{adj} = a + \{b\, S_{col}\} + \left\{c\, D_{EW} + \frac{d}{D_{EW}} + eD_{NS} + f\ {D_{NS}}^2 + g\, \frac{D_{EW}}{D_{NS}} + h\left(\frac{D_{EW}}{D_{NS}}\right)^2\right\} + \left\{l\, \frac{S_{col}}{D_{NS}\, D_{EW}} + r\, \frac{D_{NS}\, D_{EW}}{S_{col}}\right\} + \{wT\} \quad (5.32)$$

The first term only depends on the collector surface S_{col}. Given that $b < 0$, it was found that, as the collectors were larger, the lower the annual incident radiation. This effect was due to the greater possibility of inter-shading as the collectors had more surface area. With the cases studied, the variation interval of the final result due exclusively to this term was 24 kWh/m^{2}year.

The second term marks the importance of the geometric design of the plant given by D_{EW} and D_{NS}, regardless of whether it is a staggered or grid configuration. In the group of cases studied, the variation interval was 116 kWh/m^{2}year.

The third term is interpreted as a function of the ground cover ratio (*GCR*) parameter defined by Equation (5.33).

$$GCR = \frac{S_{col}}{D_{NS}\, D_{EW}} \tag{5.33}$$

According to this definition, the third term considered in the model given by Equation (5.29) can be rewritten obtaining the expression (5.34). Thus, this term showed that the variation in this term was 104 kWh/m^{2}year for the GCR values considered in the set of cases studied.

$$\left\{ l\, \frac{S_{col}}{D_{NS}\, D_{EW}} + m\, \frac{D_{NS}\, D_{EW}}{S_{col}} \right\} = \left\{ l\, GCR + \frac{m}{GCR} \right\} \tag{5.34}$$

Finally, given that the parameter w was negative, the term {*wT*} implied a small difference of 1.6 kWh/m^2 year to the detriment of the installations that were arranged in a staggered pattern compared to those with a regular grid.

5.4.Conclusions

This work presents a novel methodology for the productive study of PV solar collectors mounted on dual-axis trackers. The study, applied to multiple cases, generated as variations with respect to the design adopted in an existing PV Plant ("El Molino", located in Córdoba) allows for identification of the design variables that fundamentally influence the annual incident irradiation on the solar collectors and, therefore, on the energy production of the PV plant. Specifically, by systematically varying the geometry of the collectors, the distance between them, and their spatial distribution, 25,000 case studies were simulated. For all of them, the annual incident solar radiation on the solar collectors was calculated, using for this the irradiance estimation model of Perez (Perez et al., 1990) and assuming that they were governed by a tracking strategy that optimized radiative capture while avoiding inter-shading between collectors (Fernández-Ahumada et al., 2020a, 2017). Although a comprehensive methodology was used to study the case, it was difficult with the data set to understand the influence of each variable on the final result. Therefore, a simple function was fitted, which accurately reproduced the result of the complex model $\varepsilon\_rel = 0.00115$. From the irradiance data obtained for the different PV plant designs, a simple mathematical model has been obtained, Equation (5.29) with a high level of adjustment ($R^2 = 0.993$) that represents the dependence of the annual solar irradiance on the PV plant with respect to design variables

such as collector surface, S_{col}, NS and EW distances between collectors D_{NS} and D_{EW}, and spatial distribution of the collectors: regular or staggered grid. Thus, the proposed model has made it possible to identify that the main variables that influence the annual incidence of irradiance are, in order of greatest influence, the geometric design of the plant as a function of the distances between its collectors, (D_{NS}, D_{EW}), the *GCR* of the installation and the surface of its collectors (S_{col}), which can lead to variations in the electrical production of the PV plant of up to 116 kWh/m^{2}year, 104 kWh/m^{2}year, and 24kWh/m^{2}year. However, for practical purposes, with regard to the spatial distribution of the collectors, it is not appropriate to assume a better behaviour of the regular grid arrangement with respect to the staggered shape since the margin of 1.6 kWh/m^{2}year for this variable falls within the uncertainty margin of the radiation prediction models. Similarly, the geometric shape of the collectors does not exert a significant influence on the irradiance received since it gives rise to variations of 3.3026 kWh/m^{2}year , which, therefore, are lower than the uncertainty margin of the estimation model itself. Future works will study the influence of the shape in confluence with the orientation of the terrain.

Capítulo 6 . Conclusiones

6.1. Conclusiones del primer artículo

6.2. Conclusiones del segundo artículo

6.3. Conclusiones del tercer artículo

Se detallan a continuación las conclusiones de este trabajo distribuidas por cada uno de los artículos académicos que lo conforman.

6.1. Conclusiones del primer artículo

Se ha modelizado la captación solar en seguidores a 1 eje, cuyo movimiento evita el sombreamiento mutuo (técnica de retroseguimiento). Se ha interrelacionado dicha captación con las características de inclinación y acimut del terreno donde se ubica la instalación. Esto se conseguido mediante la implementación de una subrutina en VBA que toma datos de orientación del eje del colector, dimensiones y separación. Esto permite obtener el valor óptimo de azimut del colector (γ), y por consiguiente conseguir una orientación para obtener el valor máximo de radiación según la inclinación del terreno.

El aporte más novedoso de este trabajo consiste en el estudio de la relación existente entre los valores de acimut del terreno χ, el acimut del eje del colector γ y la inclinación del terreno (β). Así se ha obtenido, que para instalaciones orientadas hacia el Sur (χ=0°), la orientación óptima del eje del colector es en la misma dirección (γ=0°), independientemente de la inclinación del terreno. Si el terreno tuviese otra orientación, el acimut óptimo en el que ha de orientarse el seguidor, debe ser en la misma dirección que el acimut terrestre. El estudio indica que, para la latitud y valores climáticos de Córdoba, la relación entre el acimut óptimo de seguidores y el acimut del terreno viene dada por la Figura (3.8.d). Si el eje de rotación se posiciona en una dirección diferente, surgen pérdidas de energía que varían según la inclinación del terreno, las cuales han sido caracterizadas en Figura (3.8.c).

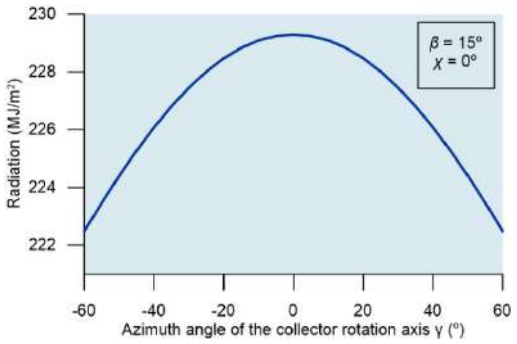

(**a**)

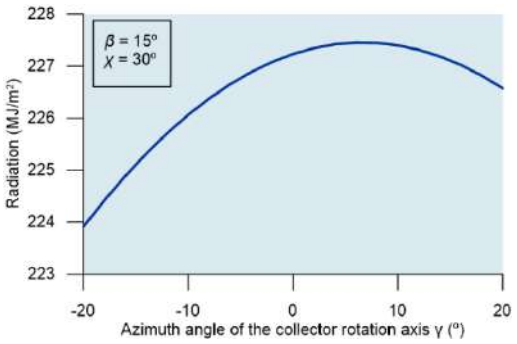

(**b**)

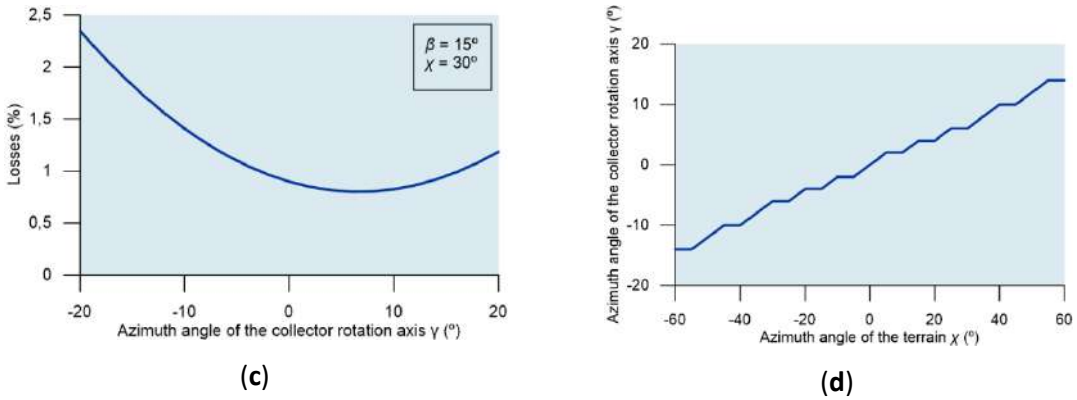

Figure 3.8. Results for a case study for inclination 15°: (a) Maximum radiation; (b) Radiation variation for 30° azimuth; (c) Maximum radiation loss for 30° azimuth; (d) Axis azimuth for optimal terrain radiation.

Por otro lado, se ha observado que, para terrenos y eje del colector con orientación Sur, el valor de radiación máxima se obtiene para inclinaciones β=21° (Figura 3.9).

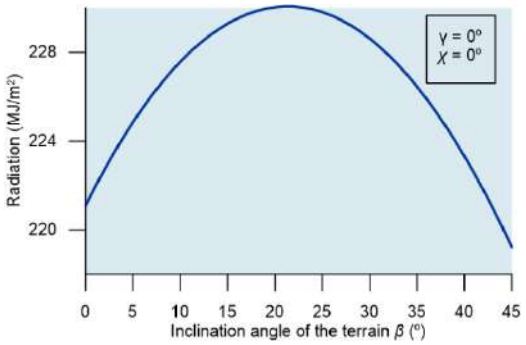

Figure 3.9. Variation of the maximum radiation on the collector with respect to the inclination of the terrain.

Respecto a otra influencia en la inclinación del terreno, se ha demostrado que al alejarse de la orientación óptima del eje de rotación del colector, las pérdidas aumentan considerablemente conforme la inclinación del terreno es mayor, llegando a valores cercanos al 7% en el caso de estudio de un terreno de inclinación β=20°.

En este trabajo se presentan avances significativos en el ámbito de los seguidores fotovoltaicos de 1 eje. Se abren nuevas líneas de investigación en la optimización del comportamiento de seguidores solares que involucren modelos más complejos.

6.2. Conclusiones del segundo artículo

El dispositivo desarrollado evalúa de forma instantánea el valor de la irradiancia global solar incidente, lo que permite establecer la orientación óptima de los captadores en la bóveda celeste, y por tanto optimizar la producción de energía en PV. Consta de un mecanismo hardware y algoritmo de control.

Se ha desarrollado un algoritmo *exprofeso* para el control del sombreamiento y realización del retroseguimiento que ha sido implementado en el microprocesador ATMEL 2560 (incorporado en la placa Arduino Mega). La lógica de control permite discriminar a priori aquellas zonas donde los seguidores solares generan sombreo. Para ello el programa de control requiere, como datos de entrada, las variables geométricas del campo de colectores y su ubicación geográfica.

El dispositivo toma medidas sistemáticas de irradiancia en aquellas direcciones en las que no existe sombreamiento entre colectores y ofrece aquella dirección en la que la irradiancia es máxima. De esta forma el dispositivo es útil para realizar retroseguimiento en cualquier instalación PV.

Lo anterior, unido a que la tecnología usada para la construcción de dicho dispositivo haya sido realizada en hardware libre y código abierto (FOSH) y, por tanto, de acceso libre (Open Access), hace que se presente como una tecnología pionera en estrategias de seguimiento y que, paralelamente, permita a la comunidad científica acceder, modificar o incluso mejorar su diseño.

6.3.Conclusiones del tercer artículo

En el tercer trabajo académico se ha profundizado en la caracterización de los seguidores solares de doble eje y, a diferencia del primer artículo, se ha optado por la evaluación de la irradiancia mediante un modelo más complejo (Perez et al., 1990) para la caracterización del vector normal a los colectores ($\vec{n}$).

Paralelamente, se ha introducido como novedad en el estudio, la modificación de la geometría de los colectores, mediante eliminación de módulos en los vértices, con lo que el análisis de intersombreado mediante el criterio dicotómico basado en el álgebra de Minkowski (Avnaim and Boissonnat 1989; B. Chazelle 1983) presenta una envolvente irregular a diferencia de seguidores de 1 eje.

Se presenta como caso de estudio la instalación PV “El Molino” localizada en Córdoba, mediante la simulación de 25.000 variantes geométricas. Esto ha permitido evaluar la radiación solar incidente anual combinando geometrías diferentes de colectores, modificación de la interdistancia entre ellos y disposición espacial en forma de matriz regular y tresbolillo.

El resultado obtenido muestra que colectores con geometrías diferentes, presentan valores de radiación equivalente cuando tienen la misma envolvente, o bien cuando presentan simetría respecto el eje NS.

La radiación anual estimada se ha ajustado a una función empírica simple por mínimos cuadrados (R^2 = 0.993). El modelo empírico desestima la geometría de los colectores como variable explicativa. En caso de ser explicativa su aporte sería inferioral valor de 3.3 kWh/m^2 año.

Paralelamente, el modelo propuesto ha permitido identificar las variables que influyen notablemente en la incidencia anual de la irradiancia, y que vienen determinadas por la distancia entre colectores (D_{NS}, D_{EW}), superficie de colector (S_{col}) y el GCR de la instalación. Se puede llegar a explicar variaciones en la producción eléctrica de 116 kWh/m^2 año, 24kWh/m^2 año y 104 kWh/m^2 año respectivamente.

En lo que respecta a la distribución espacial de forma regular frente a tresbolillo, no es conveniente asumir un mejor comportamiento de uno frente a otro, debido a que la variación de 1.6 kWh/m^2 año se sitúa dentro del margen de incertidumbre de los modelos de predicción de radiación.

Finalmente, este estudio abre la puerta a futuras investigaciones en el análisis del comportamiento de colectores con geometrías irregulares, introduciendo variables de estudio como la inclinación del terreno, caracterizada en el primer trabajo académico.

Bibliografía

Abdallah, S., 2004. The effect of using sun tracking systems on the voltage–current characteristics and power generation of flat plate photovoltaics. Energy Convers. Manag. 45, 1671–1679.

Abdallah, S., Nijmeh, S., 2004. Two axes sun tracking system with PLC control. Energy Convers. Manag. https://doi.org/10.1016/j.enconman.2003.10.007

AL-Rousan, N., Isa, N.A.M., Desa, M.K.M., 2018. Advances in solar photovoltaic tracking systems: A review. Renew. Sustain. Energy Rev. 82, 2548–2569. https://doi.org/10.1016/j.rser.2017.09.077

Ali Jallal, M., Chabaa, S., Zeroual, A., 2020. A novel deep neural network based on randomly occurring distributed delayed PSO algorithm for monitoring the energy produced by four dual-axis solar trackers. Renew. Energy 149, 1182–1196. https://doi.org/10.1016/j.renene.2019.10.117

Antonanzas, J., Urraca, R., Martinez-de-Pison, F.J., Antonanzas, F., 2018. Optimal solar tracking strategy to increase irradiance in the plane of array under cloudy conditions: A study across Europe. Sol. Energy 163, 122–130. https://doi.org/10.1016/j.solener.2018.01.080

Array Tecnhologies, 2020. Backtracking and Diffuse Light Strategies with SmarTrack from Array Technologies [WWW Document].

Augustin, A., Yi, J., Clausen, T., Townsley, W.M., 2016. A study of Lora: Long range & low power networks for the internet of things. Sensors (Switzerland) 16. https://doi.org/10.3390/s16091466

Avnaim, F., Boissonnat, J.-D., 1989. Polygon placement under translation and rotation. RAIRO-Theor. Informatics Appl. 23, 5–28.

Awasthi, A., Shukla, A.K., Murali Manohar, S.R., Dondariya, C., Shukla, K.N., Porwal, D., Richhariya, G., 2020. Review on sun tracking technology in solar PV system. Energy Reports 6, 392–405. https://doi.org/10.1016/j.egyr.2020.02.004

Bahrami, A., Okoye, C.O., 2018. The performance and ranking pattern of PV systems incorporated with solar trackers in the northern hemisphere. Renew. Sustain. Energy Rev. 97, 138–151. https://doi.org/10.1016/j.rser.2018.08.035

Bahrami, A., Okoye, C.O., Atikol, U., 2016. The effect of latitude on the performance of different solar trackers in Europe and Africa. Appl. Energy 177, 896–906. https://doi.org/10.1016/j.apenergy.2016.05.103

Batista, N.C., Melício, R., Mendes, V.M.F., 2014. Layered Smart Grid architecture approach and field tests by ZigBee technology. Energy Convers. Manag. 88, 49–59. https://doi.org/10.1016/j.enconman.2014.08.020

Belhachat, F., Larbes, C., 2015. Modeling, analysis and comparison of solar photovoltaic array configurations under partial shading conditions. Sol. Energy 120, 399–418. https://doi.org/10.1016/j.solener.2015.07.039

Blanco-Muriel, M., Alarcón-Padilla, D.C., López-Moratalla, T., Lara-Coira, M., 2001. Computing the solar vector. Sol. Energy 70, 431–441. https://doi.org/10.1016/S0038-092X(00)00156-0

Braun, J.E., Mitchell, J.C., 1983. Solar geometry for fixed and tracking surfaces. Sol. Energy 31, 439–444. https://doi.org/10.1016/0038-092X(83)90046-4

Caballero, V., Vernet, D., Zaballos, A., 2020. A Heuristic to Create Prosumer Community Groups in the Social Internet of Energy. Sensors 20, 3704. https://doi.org/10.3390/s20133704

Camera, F. La, 2021. Nuevo récord mundial de capacidad energética renovable en 2020 1–3.

Carballo, J.A., Bonilla, J., Roca, L., Berenguel, M., 2018. New low-cost solar tracking system based on open source hardware for educational purposes. Sol. Energy 174, 826–836. https://doi.org/10.1016/j.solener.2018.09.064

Casares, F.J., Lopez-Luque, R., Posadillo, R., Varo-Martinez, M., 2014. Mathematical approach to the characterization of daily energy balance in autonomous photovoltaic solar systems. Energy. https://doi.org/10.1016/j.energy.2014.05.053

Chazelle, B., 1983. The polygon containment problem. Adv. Comput. Res. 1, 1–33.

Chong, K.K., Wong, C.W., 2009. General formula for on-axis sun-tracking system and its application in improving tracking accuracy of solar collector. Sol. Energy 83, 298–305. https://doi.org/10.1016/j.solener.2008.08.003

Coelho, V.N., Weiss Cohen, M., Coelho, I.M., Liu, N., Guimarães, F.G., 2017. Multi-agent systems applied for energy systems integration: State-of-the-art applications and trends in microgrids. Appl. Energy 187, 820–832. https://doi.org/10.1016/j.apenergy.2016.10.056

Collares-Pereira, M., Rabl, A., 1979. The average distribution of solar radiation-correlations between diffuse and hemispherical and between daily and hourly insolation values. Sol. Energy. https://doi.org/10.1016/0038-092X(79)90100-2

D'Adamo, I., Gastaldi, M., Morone, P., 2020. The post COVID-19 green recovery in practice: Assessing the profitability of a policy proposal on residential photovoltaic plants. Energy Policy 147, 111910. https://doi.org/https://doi.org/10.1016/j.enpol.2020.111910

De Castro, C., Mediavilla, M., Miguel, L.J., Frechoso, F., 2013. Global solar electric potential: A review of their technical and sustainable limits. Renew. Sustain. Energy Rev. https://doi.org/10.1016/j.rser.2013.08.040

DEGERiberica, 2020. referencias [WWW Document].

Deline, C., Dobos, A., Janzou, S., Meydbray, J., Donovan, M., 2013. A simplified model of uniform shading in large photovoltaic arrays. Sol. Energy 96, 274–282. https://doi.org/10.1016/j.solener.2013.07.008

Díaz-Dorado, E., Cidrás, J., Carrillo, C., 2017. Discretized model for partially shaded PV arrays composed of PV panels with overlapping bypass diodes. Sol. Energy 157, 103–115. https://doi.org/https://doi.org/10.1016/j.solener.2017.08.004

Díaz-Dorado, E., Cidrás, J., Carrillo, C., 2014. Discrete I–V model for partially shaded PV-arrays. Sol. Energy 103, 96–107. https://doi.org/10.1016/J.SOLENER.2014.01.037

Díaz-Dorado, E., Suárez-García, A., Carrillo, C.J., Cidrás, J., 2011. Optimal distribution for photovoltaic solar trackers to minimize power losses caused by shadows. Renew. Energy 36, 1826–1835. https://doi.org/10.1016/j.renene.2010.12.002

Diez-Mediavilla, M., De Miguel, A., Bilbao, J., 2005. Measurement and comparison of diffuse solar irradiance models on inclined surfaces in Valladolid (Spain). Energy Convers. Manag. 46, 2075–2092. https://doi.org/10.1016/j.enconman.2004.10.023

Duffie, J.A., Beckman, W.A., 2013. Solar engineering of thermal processes. John Wiley & Sons.

Eke, R., Senturk, A., 2012. Performance comparison of a double-axis sun tracking versus fixed PV system. Sol. Energy 86, 2665–2672. https://doi.org/10.1016/j.solener.2012.06.006

Eldin, S.A.S., Abd-Elhady, M.S., Kandil, H.A., 2016. Feasibility of solar tracking systems for PV panels in hot and cold regions. Renew. Energy 85, 228–233. https://doi.org/10.1016/j.renene.2015.06.051

ENERDATA, 2019. Anuario Estadístico Energético [WWW Document]. URL https://datos.enerdata.net/energias-renovables/eolica-solar-produccion.html

Fan, X., Deng, F., Chen, J., 2017. Voltage band analysis for maximum power point tracking of stand-alone PV systems. Sol. Energy 144, 221–231. https://doi.org/10.1016/J.SOLENER.2017.01.032

Fartaria, T.O., Pereira, M.C., 2013. Simulation and computation of shadow losses of direct normal, diffuse solar radiation and albedo in a photovoltaic field with multiple 2-axis trackers using ray tracing methods. Sol. Energy 91, 93–101. https://doi.org/10.1016/j.solener.2013.02.008

Fernández-Ahumada, L.M., Casares, F.J., Ramírez-Faz, J., López-Luque, R., 2017. Mathematical study of the movement of solar tracking systems based on rational models. Sol. Energy 150, 20–29. https://doi.org/10.1016/j.solener.2017.04.006

Fernández-Ahumada, L.M., Ramírez-Faz, J., López-Luque, R., Varo-Martínez, M., Moreno-García, I.M., Casares de la Torre, F., 2020a. A novel backtracking approach for two-axis solar PV tracking plants. Renew. Energy 145, 1214–1221. https://doi.org/10.1016/j.renene.2019.06.062

Fernández-Ahumada, L.M., Ramírez-Faz, J., López-Luque, R., Varo-Martínez, M., Moreno-García, I.M., Casares de la Torre, F., 2020b. Influence of the design variables of photovoltaic plants with two-axis solar tracking on the optimization of the tracking and backtracking trajectory. Sol. Energy 208, 89–100. https://doi.org/10.1016/j.solener.2020.07.063

Frydrychowicz-Jastrzębska, G., Bugała, A., 2015. Modeling the Distribution of Solar Radiation on a Two-Axis Tracking Plane for Photovoltaic Conversion. Energies 8, 1025–1041. https://doi.org/10.3390/en8021025

Fuentes, M., Vivar, M., Burgos, J.M., Aguilera, J., Vacas, J.A., 2014. Design of an accurate, low-cost autonomous data logger for PV system monitoring using Arduino™ that complies with IEC standards. Sol. Energy Mater. Sol. Cells 130, 529–543. https://doi.org/10.1016/j.solmat.2014.08.008

Gad, H. E., Gad, Hisham E., 2015. Development of a new temperature data acquisition system for solar energy applications. Renew. Energy 74, 337–343.

https://doi.org/10.1016/j.renene.2014.08.006

García-Valverde, R., Chaouki-Almagro, S., Corazza, M., Espinosa, N., Hösel, M., Søndergaard, R.R., Jørgensen, M., Villarejo, J.A., Krebs, F.C., 2016. Portable and wireless IV-curve tracer for >5kV organic photovoltaic modules. Sol. Energy Mater. Sol. Cells 151, 60–65. https://doi.org/10.1016/j.solmat.2016.02.012

Gay, C.F., Yerkes, J.W., Wilson, J.H., 1982. Performance advantages of two-axis tracking for large flat-plate photovoltaic energy systems, in: 16th Photovoltaic Specialists Conference. pp. 1368–1371.

Gómez-Uceda, F.J., Ramirez-Faz, J., Varo-Martinez, M., Fernández-Ahumada, L.M., 2021. New Omnidirectional Sensor Based on Open-Source Software and Hardware for Tracking and Backtracking of Dual-Axis Solar Trackers in Photovoltaic Plants. Sensors 21, 726. https://doi.org/10.3390/s21030726

Grena, R., 2008. An algorithm for the computation of the solar position. Sol. Energy 82, 462–470. https://doi.org/10.1016/j.solener.2007.10.001

Gutierrez, S., Rodrigo, P.M., Alvarez, J., Acero, A., Montoya, A., 2020. Development and Testing of a Single-Axis Photovoltaic Sun Tracker through the Internet of Things. Energies 13, 2547. https://doi.org/10.3390/en13102547

Hafez, A.Z., Yousef, A.M., Harag, N.M., 2018. Solar tracking systems: Technologies and trackers drive types – A review. Renew. Sustain. Energy Rev. 91, 754–782. https://doi.org/10.1016/j.rser.2018.03.094

Hammad, B., Al-Sardeah, A., Al-Abed, M., Nijmeh, S., Al-Ghandoor, A., 2017. Performance and economic comparison of fixed and tracking photovoltaic systems in Jordan. Renew. Sustain. Energy Rev. https://doi.org/10.1016/j.rser.2017.05.241

Hay, J.E., 1993. Calculating solar radiation for inclined surfaces: Practical approaches. Renew. Energy 3, 373–380. https://doi.org/10.1016/0960-1481(93)90104-O

Hu, Y., Yao, Y., 2016. A methodology for calculating photovoltaic field output and effect of solar tracking strategy. Energy Convers. Manag. 126, 278–289. https://doi.org/10.1016/j.enconman.2016.08.007

Hua, Z., Ma, C., Lian, J., Pang, X., Yang, W., 2019. Optimal capacity allocation of multiple solar trackers and storage capacity for utility-scale photovoltaic plants considering output characteristics and complementary demand. Appl. Energy 238, 721–733. https://doi.org/10.1016/j.apenergy.2019.01.099

Huang, B.J., Ding, W.L., Huang, Y.C., 2011. Long-term field test of solar PV power generation using one-axis 3-position sun tracker. Sol. Energy 85, 1935–1944. https://doi.org/10.1016/j.solener.2011.05.001

Huld, T., Cebecauer, T., Šúri, M., Dunlop, E.D., 2010. Analysis of one-axis tracking strategies for PV systems in Europe. Prog. Photovoltaics Res. Appl. 18, 183–194. https://doi.org/10.1002/pip.948

IEA, 2019. World Energy Investment 2019 Message from the Executive Director 176.

International Energy Agency -IEA, 2020. Renewables 2020. Paris.

IRENA, 2020. Renewable Capacity Statistics 2020, International Renewable Energy Agency.

Ismail, M.S., Moghavvemi, M., Mahlia, T.M.I., 2013. Design of an optimized photovoltaic and microturbine hybrid power system for a remote small community: Case study of Palestine. Energy Convers. Manag. 75, 271–281. https://doi.org/10.1016/j.enconman.2013.06.019

Jacobson, M.Z., Delucchi, M.A., 2011. Providing all global energy with wind, water, and solar power, Part I: Technologies, energy resources, quantities and areas of infrastructure, and materials. Energy Policy 39, 1154–1169. https://doi.org/10.1016/j.enpol.2010.11.040

Jolly, P.G., 1986. Derivation of solar angles using vector algebra. Sol. Energy 37, 429–430.

Kannan, N., Vakeesan, D., 2016. Solar energy for future world: - A review. Renew. Sustain. Energy Rev. 62, 1092–1105. https://doi.org/https://doi.org/10.1016/j.rser.2016.05.022

Karatepe, E., Boztepe, M., Çolak, M., 2007. Development of a suitable model for characterizing photovoltaic arrays with shaded solar cells. Sol. Energy 81, 977–992. https://doi.org/10.1016/j.solener.2006.12.001

Kaushika, N.D., Gautam, N.K., 2003. Energy yield simulations of interconnected solar PV arrays. IEEE Trans. Energy Convers. 18, 127–134. https://doi.org/10.1109/TEC.2002.805204

Kavlak, G., McNerney, J., Trancik, J.E., 2018. Evaluating the causes of cost reduction in photovoltaic modules. Energy Policy 123, 700–710. https://doi.org/10.1016/j.enpol.2018.08.015

Kawamura, Hajime, Naka, K., Yonekura, N., Yamanaka, S., Kawamura, Hideaki, Ohno, H., Naito, K., 2003. Simulation of I-V characteristics of a PV module with shaded PV cells. Sol. Energy Mater. Sol. Cells 75, 613–621. https://doi.org/10.1016/S0927-0248(02)00134-4

Kelly, N.A., Gibson, T.L., 2009. Improved photovoltaic energy output for cloudy conditions with a solar tracking system. Sol. Energy 83, 2092–2102. https://doi.org/10.1016/j.solener.2009.08.009

Klein, S.A., 1977. Calculation of monthly average insolation on tilted surfaces. Sol. Energy. https://doi.org/10.1016/0038-092X(77)90001-9

Koussa, M., Cheknane, A., Hadji, S., Haddadi, M., Noureddine, S., 2011. Measured and modelled improvement in solar energy yield from flat plate photovoltaic systems utilizing different tracking systems and under a range of environmental conditions. Appl. Energy 88, 1756–1771. https://doi.org/10.1016/j.apenergy.2010.12.002

Lee, C.-Y., Chou, P.-C., Chiang, C.-M., Lin, C.-F., 2009. Sun Tracking Systems: A Review. Sensors (14248220) 9, 3875–3890. https://doi.org/10.3390/s90503875

León, N., García, H., Ramírez, C., 2014. Semi-passive solar tracking concentrator. Energy Procedia 57, 275–284. https://doi.org/10.1016/j.egypro.2014.10.032

López, I., Arriaga, A., Pardo, M., 2018. La dimensión social del concepto de desarrollo sostenible: ¿La eterna Olvidada? Rev. Española Sociol. 27. https://doi.org/10.22325/fes/res.2018.2

Lorenzo, E., Narvarte, L., Muñoz, J., 2011. Tracking and back-tracking. Prog. Photovoltaics Res. Appl. 19, 747–753. https://doi.org/10.1002/pip.1085

Lorenzo, E., Pérez, M., Ezpeleta, A., Acedo, J., 2002. Design of tracking photovoltaic systems with a single vertical axis. Prog. Photovoltaics Res. Appl. 10, 533–543. https://doi.org/10.1002/pip.442

Loutzenhiser, P.G., Manz, H., Felsmann, C., Strachan, P.A., Frank, T., Maxwell, G.M., 2007. Empirical validation of models to compute solar irradiance on inclined surfaces for building energy simulation. Sol. Energy 81, 254–267. https://doi.org/10.1016/j.solener.2006.03.009

Lozano-Pérez, T., 1983. Spatial Planning: A Configuration Space Approach. IEEE Trans. Comput. https://doi.org/10.1109/TC.1983.1676196

Maatallah, T., El Alimi, S., Nassrallah, S. Ben, 2011. Performance modeling and investigation of fixed, single and dual-axis tracking photovoltaic panel in Monastir city, Tunisia. Renew. Sustain. Energy Rev. 15, 4053–4066. https://doi.org/10.1016/j.rser.2011.07.037

Martín-Martínez, S., Cañas-Carretón, M., Honrubia-Escribano, A., Gómez-Lázaro, E., 2019. Performance evaluation of large solar photovoltaic power plants in Spain. Energy Convers. Manag. 183, 515–528. https://doi.org/https://doi.org/10.1016/j.enconman.2018.12.116

Martínez-Moreno, F., Muñoz, J., Lorenzo, E., 2010. Experimental model to estimate shading losses on PV arrays. Sol. Energy Mater. Sol. Cells 94, 2298–2303. https://doi.org/10.1016/j.solmat.2010.07.029

Meinel, A.B., Meinel, M.P., 1979. Applied solar energy. Applied Energy.

Meyer, E.L., Van Dyk, E.E., 2004. Assessing the reliability and degradation of photovoltaic module performance parameters. IEEE Trans. Reliab. 53, 83–92.

Ministerio para la Transición Ecológica y el Reto Demográfico, 2020. Plan Nacional Integrado de Energía y Clima 2021-2030. Gob. España 25.

Mousazadeh, H., Keyhani, A., Javadi, A., Mobli, H., Abrinia, K., Sharifi, A., 2009. A review of principle and sun-tracking methods for maximizing solar systems output. Renew. Sustain. Energy Rev. 13, 1800–1818. https://doi.org/10.1016/j.rser.2009.01.022

Mubarak, R., Hofmann, M., Riechelmann, S., Seckmeyer, G., 2017. Comparison of Modelled and Measured Tilted Solar Irradiance for Photovoltaic Applications. Energies 10, 1688. https://doi.org/10.3390/en10111688

Muneer, T., 1990. Solar radiation model for Europe. Build. Serv. Eng. Res. Technol. 11, 153–163. https://doi.org/10.1177/014362449001100405

Narendrasinh Parmar, A.J., Parmar, A.N., Gautam, V.S., 2008. International Journal of Emerging Technology and Advanced Engineering Passive Solar Tracking System, Certified Journal.

Narvarte, L., Lorenzo, E., 2008. Tracking and ground cover ratio. Prog. Photovoltaics Res. Appl. 16, 703–714. https://doi.org/10.1002/pip.847

Neville, R.C., 1978. Solar energy collector orientation and tracking mode. Sol. Energy 20, 7–11. https://doi.org/10.1016/0038-092X(78)90134-2

Nextracker TM, 2019. TrueCapture Smart Control System in Action - Nextracker [WWW Document].

Novas, N., Alcayde, A., Robalo, I., Manzano-Agugliaro, F., Montoya, F.G., 2020. Energies and Its Worldwide Research. Energies 13, 6700. https://doi.org/10.3390/en13246700

Nsengiyumva, W., Chen, S.G., Hu, L., Chen, X., 2018. Recent advancements and challenges in Solar Tracking Systems (STS): A review. Renew. Sustain. Energy Rev. https://doi.org/10.1016/j.rser.2017.06.085

Obara, S., Matsumura, K., Aizawa, S., Kobayashi, H., Hamada, Y., Suda, T., 2017. Development of a solar tracking system of a nonelectric power source by using a metal hydride actuator. Sol. Energy 158, 1016–1025. https://doi.org/10.1016/j.solener.2017.08.056

Panico, D., Garvison, P., Wenger, H., Shugar, D., 1992. Backtracking: A novel strategy for tracking PV systems. Conf. Rec. IEEE Photovolt. Spec. Conf. 1, 668–673. https://doi.org/10.1109/pvsc.1991.169294

Panico, D., Garvison, P., Wenger, H., Shugar, D., 1991. Backtracking: a novel strategy for tracking PV systems, in: The Conference Record of the Twenty-Second IEEE Photovoltaic Specialists Conference - 1991. IEEE, pp. 668–673. https://doi.org/10.1109/PVSC.1991.169294

Panwar, N.L., Kaushik, S.C., Kothari, S., 2011. Role of renewable energy sources in environmental protection: A review. Renew. Sustain. Energy Rev. https://doi.org/10.1016/j.rser.2010.11.037

Paredes-Parra, J.M., García-Sánchez, A.J., Mateo-Aroca, A., Molina-García, Á., 2019. An alternative Internet-of-Things solution based on LoRa for PV power plants: data monitoring and management. Energies 12, 881.

Parkin, R.E., 2010. Solar angles revisited using a general vector approach. Sol. Energy 84, 912–916. https://doi.org/10.1016/j.solener.2010.02.005

Pearce, J.M., 2014. Open-Source Lab, Open-Source Lab: How to Build Your Own Hardware and Reduce Research Costs. Elsevier. https://doi.org/10.1016/C2012-0-07249-3

Pearce, J.M., 2013. Open-source lab: how to build your own hardware and reduce research costs. Newnes.

Pedro, M.C.-R.M., 2016. Modelling of shading effects in photovoltaic optimization.

Pereira, R.I.S., Dupont, I.M., Carvalho, P.C.M., Jucá, S.C.S., 2018. IoT embedded linux system based on Raspberry Pi applied to real-time cloud monitoring of a decentralized photovoltaic plant. Meas. J. Int. Meas. Confed. 114, 286–297. https://doi.org/10.1016/j.measurement.2017.09.033

Perez, R., Ineichen, P., Seals, R., Michalsky, J., Stewart, R., 1990. Modeling daylight availability and irradiance components from direct and global irradiance. Sol. Energy 44, 271–289. https://doi.org/10.1016/0038-092X(90)90055-H

Perpiñán, O., 2012. Cost of energy and mutual shadows in a two-axis tracking PV system. Renew. Energy 43, 331–342. https://doi.org/10.1016/J.RENENE.2011.12.001

Perpiñan, O., Lorenzo, E., Castro, M.A., Eyras, R., 2009. Energy payback time of grid connected PV systems: Comparison between tracking and fixed systems. Prog. Photovoltaics Res. Appl. 17, 137–147. https://doi.org/10.1002/pip.871

Posadillo, R., López Luque, R., 2008. A sizing method for stand-alone PV installations with variable demand. Renew. Energy 33, 1049–1055. https://doi.org/10.1016/j.renene.2007.06.003

PVsyst SA, 2020. PVsyst. Photovoltaic Software [WWW Document].

Quesada, G., Guillon, L., Rousse, D.R., Mehrtash, M., Dutil, Y., Paradis, P.-L., 2015. Tracking strategy for photovoltaic solar systems in high latitudes. Energy Convers. Manag. 103, 147–156. https://doi.org/10.1016/j.enconman.2015.06.041

Rad, M.A.V., Toopshekan, A., Rahdan, P., Kasaeian, A., Mahian, O., 2020. A comprehensive study of techno-economic and environmental features of different solar tracking systems for residential photovoltaic installations. Renew. Sustain. Energy Rev. 129, 109923.

Ramírez-Faz, J., López-Luque, R., 2012. Development of a methodology for quantifying insolation variables in windows and building openings. Renew. Energy 37, 426–433. https://doi.org/10.1016/j.renene.2011.05.040

Rapp-Arrarás, Í., Domingo-Santos, J.M., 2009. Algorithm for the calculation of the horizontal coordinates of the Sun via spatial rotation matrices. Renew. Energy 34, 876–882. https://doi.org/10.1016/j.renene.2008.06.005

Reda, I., Andreas, A., 2004. Solar position algorithm for solar radiation applications. Sol. Energy 76, 577–589. https://doi.org/10.1016/j.solener.2003.12.003

REE, 2019. REE [WWW Document]. URL https://www.ree.es/es/sala-de-prensa/actualidad/nota-de-prensa/2020/03/las-renovables-superan-ya-en-potencia-instalada-al-resto-de-fuentes-de-energia-en-la-peninsula (accessed 4.4.21).

Renewable Energy Agency, I., 2020. Renewable power generation costs in 2019.

Renewables 2020 Global Status Report, 2020. Renewables Global Status Report, REN21 Secretariat.

Ribó-Pérez, D., Van der Weijde, A.H., Álvarez-Bel, C., 2019. Effects of self-generation in imperfectly competitive electricity markets: The case of Spain. Energy Policy 133, 110920. https://doi.org/10.1016/j.enpol.2019.110920

Riley, D., Hansen, C., 2015. Sun-relative pointing for dual-axis solar trackers employing azimuth and elevation rotations. J. Sol. Energy Eng. 137.

Rus-Casas, C., Hontoria, L., Fernández-Carrasco, J.I., Jiménez-Castillo, G., Muñoz-Rodríguez, F., 2019. Development of a utility model for the measurement of global radiation in photovoltaic applications in the internet of things (IoT). Electron. 8, 304. https://doi.org/10.3390/electronics8030304

Sáez-Martínez, F.J., Lefebvre, G., Hernández, J.J., Clark, J.H., 2016. Drivers of sustainable cleaner production and sustainable energy options. J. Clean. Prod. 138, 1–7. https://doi.org/10.1016/j.jclepro.2016.08.094

Saint-Drenan, Y.-M.M., Barbier, T., 2019. Data-analysis and modelling of the effect of inter-row shading on the power production of photovoltaic plants. Sol. Energy 184, 127–147.

Salas, V., Olias, E., 2009. Overview of the photovoltaic technology status and perspective in Spain. Renew. Sustain. Energy Rev. 13, 1049–1057.

https://doi.org/10.1016/j.rser.2008.03.011

Salgado-Conrado, L., 2018. A review on sun position sensors used in solar applications. Renew. Sustain. Energy Rev. https://doi.org/10.1016/j.rser.2017.08.040

Satpathy, P.R., Sharma, R., 2019. Diffusion charge compensation strategy for power balancing in capacitor-less photovoltaic modules during partial shading. Appl. Energy 255, 113826. https://doi.org/10.1016/j.apenergy.2019.113826

Schneider, D., 2012. Control Algorithms for Large-scale Single-axis Photovoltaic Trackers. Acta Polytech. 52. https://doi.org/10.14311/1648

Seme, S., Štumberger, G., Voršič, J., 2011. Maximum efficiency trajectories of a two-axis sun tracking system determined considering tracking system consumption. IEEE Trans. Power Electron. 26, 1280–1290. https://doi.org/10.1109/TPEL.2011.2105506

Şenpinar, A., Cebeci, M., 2012. Evaluation of power output for fixed and two-axis tracking PVarrays. Appl. Energy 92, 677–685. https://doi.org/10.1016/j.apenergy.2011.07.043

Seyedmahmoudian, M., Horan, B., Soon, T.K., Rahmani, R., Than Oo, A.M., Mekhilef, S., Stojcevski, A., 2016. State of the art artificial intelligence-based MPPT techniques for mitigating partial shading effects on PV systems – A review. Renew. Sustain. Energy Rev. 64, 435–455. https://doi.org/10.1016/j.rser.2016.06.053

Singh, R., Kumar, S., Gehlot, A., Pachauri, R., 2018. An imperative role of sun trackers in photovoltaic technology: A review. Renew. Sustain. Energy Rev. https://doi.org/10.1016/j.rser.2017.10.018

Sinha, R.S., Wei, Y., Hwang, S.H., 2017. A survey on LPWA technology: LoRa and NB-IoT. ICT Express 3, 14–21. https://doi.org/10.1016/j.icte.2017.03.004

Sproul, A.B., 2007. Derivation of the solar geometric relationships using vector analysis. Renew. Energy 32, 1187–1205. https://doi.org/10.1016/j.renene.2006.05.001

STI Norland, 2019. Dual-row single-axis tracker-STI H250 [WWW Document].

Sumathi, V., Jayapragash, R., Bakshi, A., Kumar Akella, P., 2017. Solar tracking methods to maximize PV system output – A review of the methods adopted in recent decade. Renew. Sustain. Energy Rev. https://doi.org/10.1016/j.rser.2017.02.013

Talavera, D.L., Muñoz-Cerón, E., Ferrer-Rodríguez, J.P., Pérez-Higueras, P.J., 2019. Assessment of cost-competitiveness and profitability of fixed and tracking photovoltaic systems: The case of five specific sites. Renew. Energy 134, 902–913. https://doi.org/10.1016/j.renene.2018.11.091

Torres-Roldán, M., López-Luque, R., Varo-Martínez, M., 2015. Design of an innovative and simplified polar heliostat for integration in buildings and urban environments. Sol. Energy. https://doi.org/10.1016/j.solener.2015.06.041

Trzmiel, G., Głuchy, D., Kurz, D., 2020. The impact of shading on the exploitation of photovoltaic installations. Renew. Energy 153, 480–498. https://doi.org/10.1016/j.renene.2020.02.010

United Nations, 2020. Emissions Gap Emissions Gap Report 2020.

United Nations, 2019. The sustainable development goals report 2019. United Nations Publ. issued by Dep. Econ. Soc. Aff.

United Nations, 2015. Adoption of the Paris Agreement, Proposal by the President, Draft decision. Conf. Parties, Twenty-first Sess. 21930, 32.

Woyte, A., Nijs, J., Belmans, R., 2003. Partial shadowing of photovoltaic arrays with different system configurations: Literature review and field test results. Sol. Energy 74, 217–233. https://doi.org/10.1016/S0038-092X(03)00155-5

Yao, Y., Hu, Y., Gao, S., Yang, G., Du, J., 2014. A multipurpose dual-axis solar tracker with two tracking strategies. Renew. Energy 72, 88–98. https://doi.org/10.1016/j.renene.2014.07.002

Zedalis, R.J., 2017. International energy law: Rules governing future exploration, exploitation and use of renewable resources. Int. Energy Law Rules Gov. Futur. Explor. Exploit. Use Renew. Resour. 1–341. https://doi.org/10.4324/9781315252056

Anexo I

Primer artículo del compendio: “Análisis de la influencia de la orientación del terreno en el diseño de instalaciones fotovoltaicas con seguidores de un solo eje”

Publicado en la revista Applied Sciences.

Enviado el 5 de noviembre de 2020, aceptado el 27 de noviembre de 2020

Factor de impacto en 2019: 2,474.

applied sciences

MDPI

Article

Analysis of the Influence of Terrain Orientation on the Design of PV Facilities with Single-Axis Trackers

Francisco J. Gómez-Uceda [1], Isabel M. Moreno-Garcia [2,*], José M. Jiménez-Martínez [3], Rafael López-Luque [4] and Luis M. Fernández-Ahumada [5]

1 Department of Mechanics, University of Córdoba, 14071 Cordoba, Spain; fjgomez@uco.es
2 Department of Electronic and Computer Engineering, Campus of Rabanales, University of Córdoba, 14071 Cordoba, Spain
3 Physics for Renewable Energies Research Group, University of Córdoba, 14071 Cordoba, Spain; f72jimaj@uco.es
4 Department of Applied Physics, Radiology and Physical Medicine, University of Córdoba, 14071 Cordoba, Spain; fa1lolur@uco.es
5 Department of Electrical Engineering and Automatics, University of Córdoba, 14071 Cordoba, Spain; lmfernandez@uco.es
* Correspondence: isabel.moreno@uco.es; Tel.: +34-957212533

Received: 5 November 2020; Accepted: 27 November 2020; Published: 29 November 2020

check for updates

Abstract: This paper investigates how to optimally orient the photovoltaic solar trackers of an axis parallel to the terrain, applying the sky model of Hay–Davies. This problem has been widely studied. However, the number of studies that consider the orientation (inclination and azimuth of the terrain) is very limited. This paper provides an examination of incident solar irradiance that can be extended to terrain with variable orientation and in consideration of different azimuths of the axis of rotation. Furthermore, a case study of the south of Spain is provided, considering different inclination and orientation terrain values. The results obtained in this study indicate, as a novelty, that for lands that are not south facing, the rotation axis azimuth of solar trackers should be different from zero and adjusted to the same direction as the land azimuth in order to maximize energy production. Annual energy production is sensitive to changes in the rotation axis azimuths of solar trackers (an influence of around 3% of annual energy production).

Keywords: solar energy; single-axis solar tracker; backtracking; optimisation

1. Introduction

At present, population growth, deficiencies in natural resources and global warming are producing challenges around the world. In recent years, various initiatives have been working on the development or replacement of the current power grid to obtain greater efficiency in the electrical system and a reduction in energy waste by reducing losses during distribution [1]. Such a system would contribute to the promotion of renewable resources and the minimisation of the environmental impact in the future. Therefore, there is a global requirement to preserve the environment and to improve the penetration of alternative energy resources [2]. Within the framework of renewable energies, solar energy is the form of energy that has shown the most remarkable growth in recent years thanks to the reduction of costs and to legal requirements in many countries [3,4]. Similarly, photovoltaic (PV) technology is one of the current technologies with a better future projection due to its simplicity and scalability and the continuous manufacture, operation and maintenance reduction costs it enables for solar panels [5].

However, the lack of the linearity in the solar energy received by solar panels, mainly caused by Earth–Sun relative displacement, is a disadvantage to consider. It is necessary to redefine solar

tracking systems by increasing the solar irradiance capture enabled by PV collectors and therefore improve energy production [6].

Classified according to the type of movement, the following systems can be considered: single-axis tracking systems, in which a mobile element adapts its position by rotating around a fixed axis; and two-axis tracking systems, in which the collector plane rotates around two fixed axes, allowing an orientation towards any direction of the celestial sphere [7,8].

Several studies have analysed the efficiency of energy production using two-axis trackers compared with single-axis tracking and fixed panels [9–11]. Bahrami et al. [10] determined that the increase in solar production of a PV plant with two-axis trackers compared to a system with single-axis trackers at the same latitude is 0.42–23.4%. Similarly, the improvement compared to a fixed-panel system is around 17.22–31.23%. Other authors, such as Hua et al. [6], concluded that fluctuations in energy production can be reduced depending on the tracker distribution in the PV plant.

With regard to movement strategies, two types can be distinguished: those based on information from pyranometers and those based on mathematical statements, determined by terrestrial and solar movement. For this latter option two approaches can be considered. For the first, the sun's position is predicted by spherical trigonometry [12–14], and for the second, it is acquired by vectorial calculation [15,16]. This article uses vectorial calculation.

The most frequently followed strategy in solar tracking is that based on the astronomical model. This method aims to minimise the angle composed by direct sunrays and the normal vector to the collector plane, thereby increasing the direct portion of solar irradiance. However, this strategy is not optimal for the PV energy case since it does not involve the remaining portions (diffuse and reflected) which also contribute to energy production. This issue was thoroughly studied by Duffie and Beckman [13], who found that on cloudy days astronomical tracking obtained an irradiance lower than fixed panels because during those days direct radiation fails.

PV plant yields can be highly affected when panels are shaded by each other [17–19]. Two consequences can be derived from the shading effect on the panels. The first consequence is the reduction of captured irradiance since the direct component does not reach the cell surface. The second consequence is the increase in temperature of the shaded cell since it works as a resistive load absorbing heat from the adjacent cells which thus accelerates its deterioration [18,20]. In this respect, it would be advisable to arrange the location of the panels in such a way that there is no intershading. However, given the high price of the terrain and the increasingly low price of the panels, the most common solution is to construct PV plants with suitable distances between the panels that produce shade [21]. This important scientific challenge has been widely studied by many authors who are interested in the reduction in PV production due to shade from the panels [17,18,21,22].

In addition, solar geometry and PV plant design also affect energy production. Solutions which aim at simulating all the relevant aspects of this issue therefore demand significant calculation times [23,24]. However, authors such as Saint-Drenan and Barbier [21] have started to work on the optimisation of this issue using a model with a low computational load. This model can maintain the required accuracy levels using a few input parameters. However, it has only been tested in two PV plants. The authors therefore recommend extending the validation of this model to other facilities and geometries. Consequently, it is necessary to continue studying the influence of shading on energy production.

Under this paradigm, the backtracking method can provide adequate solutions for the intershading problem in PV plants [25], especially during sunrise and sunset when solar beams are very low and there is greater intershading between PV modules. This method varies the optimum angle of greatest solar incidence to prevent the back panels from being shaded (Figure 1). Although the result of using backtracking is a lower angle of incidence of solar collection, it is more favourable than the projection of shadows among adjacent solar panels [26].

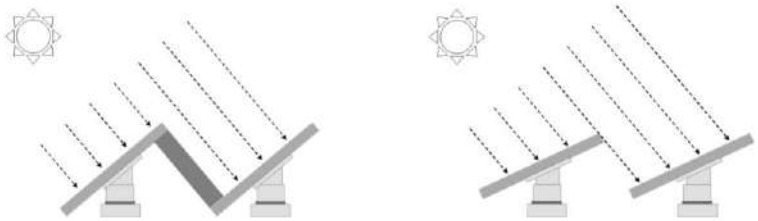

Figure 1. Backtracking method.

Backtracking has become a technique used to increase energy production in photovoltaic plants in cloudy periods. The diffuse component of solar radiation is much more relevant in these cases and "approaches" that ignore this component (such as astronomical ones) are thus no longer optimal.

This is not the only advantage of employing backtracking. There is also the resulting reduction in hot spots on the trackers, which increases their life span and reduces breakdowns. Backtracking also improves the ground cover ratio (GCR) of the installations, which has the effect of reducing the economic impact with regard to the soil required when building plants [27].

For these reasons, there is a niche in scientific work focused on the development of options utilising backtracking and on the optimisation of solutions responding to the challenges posed by solar panels which are not exclusively focused on classical tracking [9,26,28,29].

From this perspective, work based on tracking has been undertaken with the aim of optimising production throughout the movement of a panel path, including the backtracking periods [27]. To achieve this, the search is underway for a panel path that maintains the optimum production under the premise that the panel is isolated and therefore does not receive shade from any adjacent panel. Once this objective has been considered, a condition can be established to verify the possible shading between photovoltaic panels. After these two steps, the shaded orientations can be indicated against those that are not shaded. Thus, a panel path that optimises production, including the non-shading of modules, can be established.

Since it is difficult to find a completely horizontal location for photovoltaic plants, further study and deeper knowledge of photovoltaic trackers are required to offer optimisation guidelines for solar capture. The present study was undertaken to include: (a) mathematical modelling of solar capture on trackers; (b) programming that allows automation of the calculations; (c) simulations of case studies; and (d) analysis of optimal conclusions. In light of this, conclusions were drawn on orientations, land inclinations and distances between modules, etc., in terms of produced energy.

Figure 2a,b represent angles χ (azimuth) and β (inclination) for a generic terrain. The angle γ (azimuth of the collector rotation axis) is also represented. This study, based on the Hay–Davies model, characterises solar radiation on trackers using angles χ, β and γ.

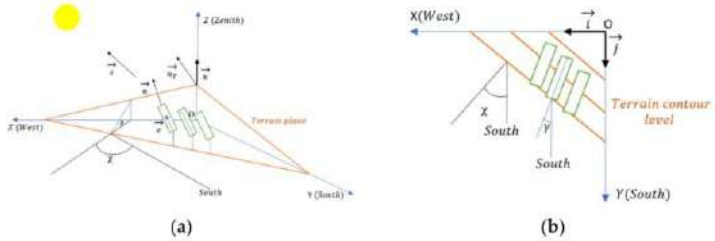

(a) (b)

Figure 2. Relevant geometry and vectors of an Earth reference system for current study. (**a**) Perspective view; (**b**) orthogonal view.

The remainder of this paper is organised as follows. In Section 2 the model used, the mathematical optimisation bases, the backtracking method and the relevant software development are presented. Section 3 outlines how the methodology was tested in Córdoba, Spain, and the results are discussed. In Section 4, conclusions are drawn based on the restrictions shown and potential further research is indicated.

2. Materials and Methods

2.1. Astronomical Bases and Irradiance Model

Knowing the concrete position of the sun at each moment of the day and on each day of the year is fundamental for determining the direction of solar beams. It is possible to determine the position of the sun accurately by using astronomical geometry. For this purpose, a solar vector was defined, expressed with respect to a terrestrial reference system (Figure 2) and formed by the axes Ox, towards the west; Oy, towards the south; and Oz in the zenithal direction. The position was determined by Equations (1) and (2):

$$\vec{s} = s_x \vec{i} + s_y \vec{j} + s_z \vec{k} \tag{1}$$

$$\vec{s} = sin\Omega t \cdot cos\delta \, \vec{i} + (cos\Omega t \cdot cos\delta \cdot sin\varphi - sin\delta \cdot cos\varphi) \, \vec{j} + (cos\Omega t \cdot cos\delta \cdot cos\varphi + sin\delta \cdot sin\varphi) \, \vec{k} \tag{2}$$

where δ represents the solar declination, φ the latitude and Ωt the hour angle. This angle was calculated as the Earth's rotation speed, $2\pi/24$ rad/h, for the hours since solar noon [30].

In PV technology, all irradiance components (direct, diffuse and reflected irradiance) are usable. Traditionally, the astronomical model has been used to determine the position of the sun. Applying the astronomical model to solar tracking means that the angle formed between the direct solar rays and the normal angle to the collector's surface θ must be as low as possible. With astronomical tracking, the value of the direct irradiance component is maximised, which is appropriate for applications focused on this component (such as concentration technologies). Therefore, this type of tracking is not the most suitable for the purposes of this study. For instance, on cloudy days, when the solar disk is not visible and direct radiation does not reach the collectors, those located on a fixed horizontal position collect more energy than those using astronomical tracking. Therefore, to study the influence of diffuse and reflected components on solar tracking, several sky models have been proposed.

The Hay–Davies method [31] was used for the calculations in this work because it adequately describes the anisotropy of radiation [32] in addition to being notable for its simplicity, as opposed to other more complex models such as those of Muneer [33] and Perez [34], and for obtaining high quality results [35–37]. This model establishes that a determined fraction of diffuse irradiance is directed according to the direction of the solar disk. Models such as that of Hay–Davies [31] describe the irradiance affecting a solar panel by considering its three components, direct, diffuse and reflected irradiance, but take into account the fact that the diffuse component has a preferential direction in which the diffuse radiation is greater. According to Hay [31], the mathematical expression of the model is given by Equation (3), where the first term indicates the direct irradiance I_B, the second term refers to the diffuse irradiance I_D and the third term corresponds to the reflected component, taking into account the visible soil fraction and the albedo, ρ. I_B and I_D are determined by the Collares–Pereira model [38].

$$I = \frac{cos\theta}{cos\theta_z} I_B + \left[\left(\frac{cos\theta}{cos\theta_z} \right) \frac{I_B}{I_{OH}} + \left(1 - \frac{I_B}{I_{OH}} \right) \frac{1 + cos\xi}{2} \right] I_D + \rho \frac{1 - cos\xi}{2} (I_B + I_D) \tag{3}$$

where ξ is the inclination angle of the collector and θ_Z is the solar zenith angle, that is, the angle between the solar vector and the zenith axis.

2.2. *Optimisation of Collector Orientation*

The aim of this study was to establish guidelines for designing facilities with solar trackers on a rotation axis $\vec{e}$. This axis was considered as parallel to the terrain; no restrictions were initially imposed on it. The general results are valid for any disposition.

In this study there were two degrees of freedom for the orientation of a surface, the azimuth χ and inclination β. In the case of single-axis trackers, there would only be the elevation. The orientation of a panel was characterised by a single vector $\vec{n}$, normal to the surface of the panel. The objective was therefore the calculation of $\vec{n}$ such that that the solar capture was the maximum.

Expanding on the treatment of the vectors, the cosines of the angles θ, θ_Z and ξ that appear in the expressions of the different models of the irradiance are expressed as the scalar products of $\vec{s}$, $\vec{n}$ and $\vec{k}$:

$$cos\theta = \vec{s}\cdot\vec{n} \tag{4}$$

$$cos\theta_Z = \vec{s}\cdot\vec{k} \tag{5}$$

$$cos\xi = \vec{k}\cdot\vec{n} \tag{6}$$

Substituting the previous expressions into the Hay–Davies model [31] gives the following:

$$I = \frac{\vec{s}\cdot\vec{n}}{\vec{s}\cdot\vec{k}} I_B + \left[\left(\frac{\vec{s}\cdot\vec{n}}{\vec{s}\cdot\vec{k}}\right)\frac{I_B}{I_{OH}} + \left(1 - \frac{I_B}{I_{OH}}\right)\frac{1+\vec{k}\cdot\vec{n}}{2}\right] I_D + \rho\frac{1-\vec{k}\cdot\vec{n}}{2}(I_B + I_D) \tag{7}$$

To optimise the irradiance $I = I\left(\vec{s}\cdot\vec{n}\ ,\ \vec{k}\cdot\vec{n}\right)$, the Lagrange multiplier method was used with the following restrictions defined: $\vec{e}\cdot\vec{e} = 1$; $\vec{n}\cdot\vec{n} = 1$; $\vec{e}\cdot\vec{n} = 0$, $\vec{e}$ being the ground normal vector.

$$\Phi\left(\vec{n}, \lambda, \mu, \nu\right) = I\left(\vec{s}\cdot\vec{n}\ ,\ \vec{k}\cdot\vec{n}\right) + \lambda\left(1 - \vec{n}\cdot\vec{n}\right) + \mu\left(0 - \vec{e}\cdot\vec{n}\right) + \nu\left(1 - \vec{e}\cdot\vec{e}\right) \tag{8}$$

The differential is described by:

$$d\Phi = \left[\frac{\partial I}{\partial\left(\vec{s}\cdot\vec{n}\right)}\vec{s} + \frac{\partial I}{\partial\left(\vec{k}\cdot\vec{n}\right)}\vec{k} - 2\lambda\vec{n} - \mu\vec{e}\right]\cdot d\vec{n} + \left[1 - \vec{n}\cdot\vec{n}\right]d\lambda + d\mu\left[0 - \vec{e}\cdot\vec{n}\right] + \left[1 - \vec{e}\cdot\vec{e}\right]d\nu \tag{9}$$

by matching the brackets to zero.

$$d\Phi = \left[\frac{\partial I}{\partial\left(\vec{s}\cdot\vec{n}\right)}\vec{s} + \frac{\partial I}{\partial\left(\vec{k}\cdot\vec{n}\right)}\vec{k} - 2\lambda\vec{n} - \mu\vec{e}\right]\cdot d\vec{n} + \left[1 - \vec{n}\cdot\vec{n}\right]d\lambda + d\mu\left[0 - \vec{e}\cdot\vec{n}\right] + \left[1 - \vec{e}\cdot\vec{e}\right]d\nu \tag{10}$$

By naming

$$\vec{u} = \frac{\partial I}{\partial\left(\vec{s}\cdot\vec{n}\right)}\vec{s} + \frac{\partial I}{\partial\left(\vec{k}\cdot\vec{n}\right)}\vec{k} \tag{11}$$

three vectors $\vec{u}$, $\vec{n}$ and $\vec{e}$ appear. These vectors fulfil the relation:

$$\vec{u} - 2\lambda\vec{n} - \mu\vec{e} = 0 \tag{12}$$

So, they are linearly dependent and therefore coplanar.

As $\vec{n}$ is perpendicular to $\vec{e}$, it can be expressed more easily.

$$\vec{n} = \frac{\vec{u} - \left(\vec{u}\cdot\vec{e}\right)\cdot\vec{e}}{\left|\vec{u} - \left(\vec{u}\cdot\vec{e}\right)\cdot\vec{e}\right|} \tag{13}$$

Figure 3 represents the plane formed by the vectors $\vec{u}$, $\vec{n}$ and $\vec{e}$.

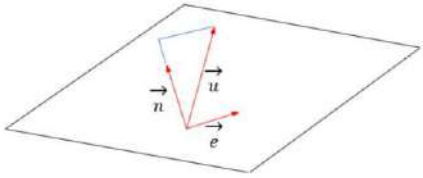

Figure 3. Representation of the plane formed by the vectors $\vec{u}$, $\vec{n}$ and $\vec{e}$.

Replacing the vectors $\vec{e}$ and $\vec{u}$ with their expressions results in the equation that defines the vector $\vec{n}$:

$$\begin{aligned}\vec{n} = &\frac{\frac{\partial I}{\partial\left(\vec{s}\cdot\vec{n}\right)}}{\sqrt{\left(\frac{\partial I}{\partial\left(\vec{s}\cdot\vec{n}\right)}\right)^2+\left(\frac{\partial I}{\partial\left(\vec{k}\cdot\vec{n}\right)}\right)^2+2\left(\frac{\partial I}{\partial\left(\vec{s}\cdot\vec{n}\right)}\right)\left(\frac{\partial I}{\partial\left(\vec{k}\cdot\vec{n}\right)}\right)\vec{s}\cdot\vec{k}-\left(\frac{\partial I}{\partial\left(\vec{s}\cdot\vec{n}\right)}\vec{s}\cdot\vec{e}+\frac{\partial I}{\partial\left(\vec{k}\cdot\vec{n}\right)}\vec{k}\cdot\vec{e}\right)^2}}\vec{s}\\ &+\frac{\frac{\partial I}{\partial\left(\vec{k}\cdot\vec{n}\right)}}{\sqrt{\left(\frac{\partial I}{\partial\left(\vec{s}\cdot\vec{n}\right)}\right)^2+\left(\frac{\partial I}{\partial\left(\vec{k}\cdot\vec{n}\right)}\right)^2+2\left(\frac{\partial I}{\partial\left(\vec{s}\cdot\vec{n}\right)}\right)\left(\frac{\partial I}{\partial\left(\vec{k}\cdot\vec{n}\right)}\right)\vec{s}\cdot\vec{k}-\left(\frac{\partial I}{\partial\left(\vec{s}\cdot\vec{n}\right)}\vec{s}\cdot\vec{e}+\frac{\partial I}{\partial\left(\vec{k}\cdot\vec{n}\right)}\vec{k}\cdot\vec{e}\right)^2}}\vec{k}\\ &-\frac{\frac{\partial I}{\partial\left(\vec{s}\cdot\vec{n}\right)}\vec{s}\cdot\vec{e}+\frac{\partial I}{\partial\left(\vec{k}\cdot\vec{n}\right)}\vec{k}\cdot\vec{e}}{\sqrt{\left(\frac{\partial I}{\partial\left(\vec{s}\cdot\vec{n}\right)}\right)^2+\left(\frac{\partial I}{\partial\left(\vec{k}\cdot\vec{n}\right)}\right)^2+2\left(\frac{\partial I}{\partial\left(\vec{s}\cdot\vec{n}\right)}\right)\left(\frac{\partial I}{\partial\left(\vec{k}\cdot\vec{n}\right)}\right)\vec{s}\cdot\vec{k}-\left(\frac{\partial I}{\partial\left(\vec{s}\cdot\vec{n}\right)}\vec{s}\cdot\vec{e}+\frac{\partial I}{\partial\left(\vec{k}\cdot\vec{n}\right)}\vec{k}\cdot\vec{e}\right)^2}}\vec{e}\end{aligned} \tag{14}$$

This result makes it possible to calculate the optimal direction of the normal vector for any irradiance model in any direction of the rotation axis and for different positions of the sun. By replacing the values of the partial derivatives in Equation (14) with those obtained from Equation (7), we get:

$$\begin{aligned}\frac{\partial I}{\partial\left(\vec{s}\cdot\vec{n}\right)} &= \frac{I_B}{s_z}\left(1+\frac{I_D}{I_{OH}}\right)\\ \frac{\partial I}{\partial\left(\vec{k}\cdot\vec{n}\right)} &= \left(1-\frac{I_B}{I_{OH}}\right)\frac{I_D}{2}-\frac{\rho}{2}\left(I_B+I_D\right)\end{aligned} \tag{15}$$

Utilising Equation (16), the values of $\vec{n}$ can be obtained at any given time for the optimum irradiance incidence.

For example, for the simplest case of a direct irradiance model which only takes into account the first term of Equation (3), and with the rotation axis of the solar panels assumed to be horizontal to the ground, a normal vector like the following results, where the vector $\vec{e}$ is:

$$\begin{aligned}\vec{e} = &\frac{cos\beta\cdot sin\gamma}{\sqrt{sin^2\beta+cos^2\beta cos^2(\gamma-\chi)}}\vec{i}+\frac{cos\beta\cdot cos\gamma}{\sqrt{sin^2\beta+cos^2\beta cos^2(\gamma-\chi)}}\vec{j}\\ &-\frac{sin\beta\cdot cos(\gamma-\chi)}{\sqrt{sin^2\beta+cos^2\beta cos^2(\gamma-\chi)}}\vec{k}\end{aligned} \tag{16}$$

β being the inclination of the terrain, χ the azimuth of the terrain and γ the azimuth of the rotation axis collector.

2.3. Backtracking

In the previous section, the methodology used to determine the orientation of the solar tracker in order to obtain the maximum solar capture was detailed. This section describes the method used to prevent a solar tracker from shading an adjacent tracker. Only two factors needed to be considered for this method: the position of the sun and the orientation of the panels. To study intershading it is convenient to use an auxiliary reference system where the representation plane is perpendicular to the tracker axis. For this purpose, the vector $\vec{q}$ was defined as:

$$\vec{q} = \vec{e} \times \vec{n_T} \tag{17}$$

where $\vec{q}$ is a vector perpendicular to the ground normal vector $\vec{e}$, as well as to the rotation axis vector $\vec{n_T}$. The solar vector $\vec{s}$ and the plane normal vector in the optimal position $\vec{n}$ were named $\vec{s'}$ and $\vec{n'}$ in the reference system composed by $\{\vec{q}, \vec{e}, \vec{n_T}\}$ (Figure 4).

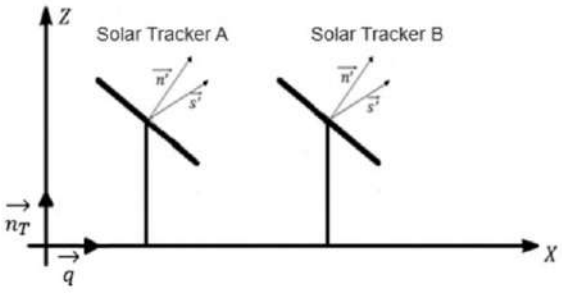

Figure 4. Reference system indicating the solar trackers, normal vector and solar vector.

The procedure used to estimate whether a solar panel B would shade an adjacent panel A was to project the shadow of panel B onto the straight line on which the adjacent panel A lay (Figure 5). Since the sun's rays are parallel to each other, the projection of one point was sufficient. First, a vector was defined from the centre of solar panel B in the direction of the solar rays $\tau\vec{s'}$. Next, the central point of solar panel A was projected onto the centre of panel B, defining $\vec{a}$. The examination of this vector enables the determination of whether shading will occur.

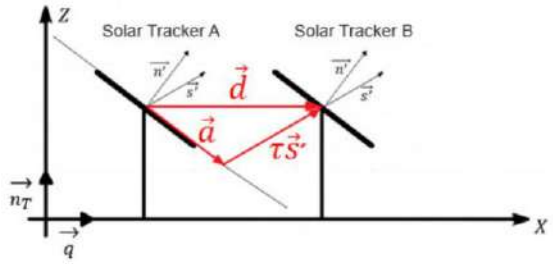

Figure 5. Vectors in the solar trackers reference system.

In order to obtain the vector $\vec{a}$, both terms were multiplied by the vector $\vec{n'}$:

$$\vec{d}\cdot\vec{n'} = 0 + \tau\,\vec{s'}\cdot\vec{n'} \Rightarrow \tau = \frac{n'_x \cdot d}{s'_x \cdot n'_x + s'_z \cdot n'_z} \tag{18}$$

Substituting the value of τ from Equation (19) into Equation (18) results in:

$$\vec{d} = \vec{a} + \frac{n'_x \cdot d}{s'_x \cdot n'_x + s'_z \cdot n'_z}\vec{s'} \tag{19}$$

Vector $\vec{a}$ can be obtained according to the following expression:

$$\vec{a} = \left(d - \frac{n'_x \cdot d}{s'_x \cdot n'_x + s'_z \cdot n'_z} \cdot s'_x\right)\vec{p} - \frac{n'_x \cdot d}{s'_x \cdot n'_x + s'_z \cdot n'_z} \cdot s'_z \cdot \vec{n_T} \tag{20}$$

As mentioned above, the examination of vector $\vec{a}$ enables the determination of whether shading will occur. If the module of the vector is less than the width of the panel, shading will occur.

$$\left|\vec{a}\right| < h \tag{21}$$

To avoid this situation, backtracking was used to look for a new orientation of the panels that prevented shading. The new orientation was intended to involve a minimum deviation from the optimal capture orientation. The new inclination angle α was that which caused the shading of a panel to fall on the edge of the adjacent panel (Figure 6).

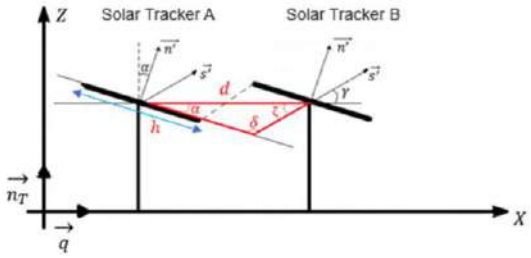

Figure 6. Angle α avoids the shading of solar panels.

This inclination angle α was calculated based on a triangle formed by the line that joins the center of the two panels d, the projection of the centre of the panel on the line of the adjacent $\tau\vec{s'}$ and the distance that corresponds to the module of vector $\vec{a}$ in Figure 5, which in Figure 6 is equivalent to the width of the panels, h.

The angle ζ is the one between the solar vector $\vec{s'}$ and the X axis:

$$\gamma = \arctan\frac{s'_z}{s'_x} \tag{22}$$

The value of the angle δ can already be calculated as:

$$sin\delta = \frac{sin\zeta \cdot d}{a} \tag{23}$$

Therefore, the inclination angle of the solar panel can be calculated as follows:

$$\alpha = \pi - \delta - \zeta \tag{24}$$

The normal vector that leads to the determination of the orientation of the panel in order to avoid shading is:

$$\vec{n'} = sin\alpha\ \vec{p} + cos\alpha\ \vec{n_T} \quad (25)$$

2.4. Software Applications for Analysis

To calculate the irradiance received by each solar panel, a function was implemented in Visual Basic for Applications (VBA) for Excel in which the calculations described above were developed. As seen in Figure 7, the function was based on several input parameters (latitude, Julian day, geometrical values, irradiance model considered) and provided an irradiance value every three minutes. Some restrictions, such as whether it as daytime, the maximum radiation related to the used model and eventual shading with backtracking response were assumed.

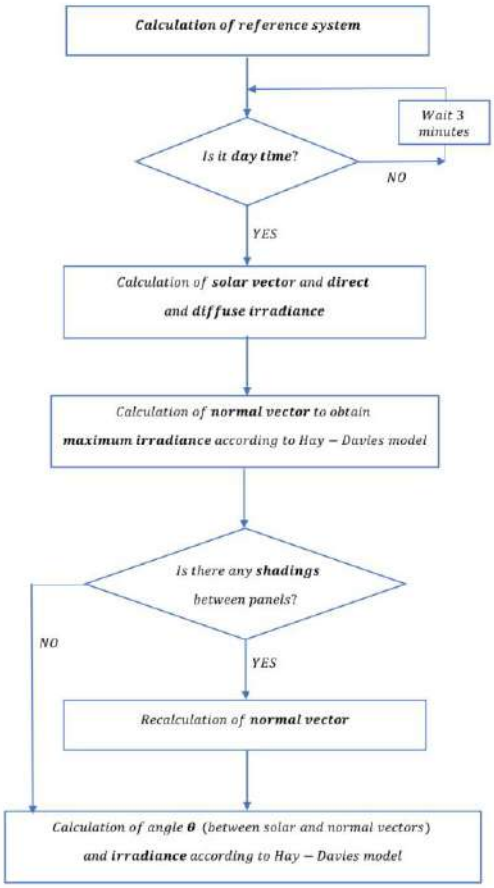

Figure 7. Flux diagram for Visual Basic for Applications (VBA) function.

3. Results and Discussion

The practical results provided the value of the estimated annual radiation using the Hay–Davies model [31] for various land configurations. All the calculations were made for the province of Córdoba, Spain, therefore assuming the same geographical values (latitude = 37.75492° N; longitude = 5.04548° W) and the same climatic values throughout the year, varying only the values of inclination β and azimuth χ for a fixed panel width $h = 3\ m$ and separation between panel lines $d = 6\ m$.

For each inclination β (from 0° to 45°, 1° increment) and terrain azimuth χ (from −60° to 60°, 5° increment), the rotation axis was oriented with a wide range of azimuth γ (from −20° to 20°, 2° increment).

Terrains with negative inclinations were not considered since PV plants are not commonly installed in shaded areas.

For facilities located on terrain with a null azimuth (oriented south), independently of its inclination even if it is null, the optimal orientation of the axis of rotation is southward ($\gamma = 0°$).

For each value of the inclination of the terrain β, it was also observed that the maximum value of irradiance was obtained when the azimuth of the terrain χ was 0°. That is, the optimal situation is when the terrain is oriented south and the axis of rotation is directed in the same direction. If the terrain has another orientation, the value of the optimal angle towards which the axis of rotation should be oriented would move in that same direction. This fact is more evident at higher values of the terrain inclination β, although in no case will the azimuth axis γ be as high as that of the terrain χ.

The results for a case study with a $\beta = 15°$ inclination are presented in Figure 8. Figure 8a shows the variation of radiation with regard to γ when the azimuth of the terrain $\chi = 0°$. However, when the terrain was not oriented to the south, as shown in Figure 8b in which the terrain was turned $\chi = 30°$, the maximum radiation was obtained by orienting the axis with an azimuth γ of 6° towards the south. The losses with regard to the maximum radiation obtained in a terrain are shown in Figure 8c, where it is again verified that, by orienting the axis at 6°, these losses can be minimised. Finally, Figure 8d shows the optimal orientation to direct the axis for the different values of the terrain azimuth χ. In this way it is possible to estimate the orientation that achieves optimal radiation considering the azimuth of the terrain χ.

As already mentioned, for each inclination value the maximum irradiance value was obtained when the terrain had an angle $\chi = 0°$. In addition, as the inclination of the terrain increased, the radiation affecting the panels was greater, as seen in Figure 9. The explanation can be found in the latitude for which the calculations were made and in the fact that the direction of the sun is not perpendicular to the horizontal plane. The inclination of the terrain influenced the radiation, increasing until a value of β of around 21°, where the maximum was reached.

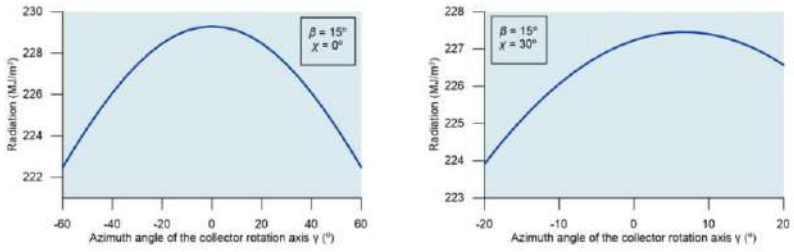

(a) (b)

Figure 8. *Cont.*

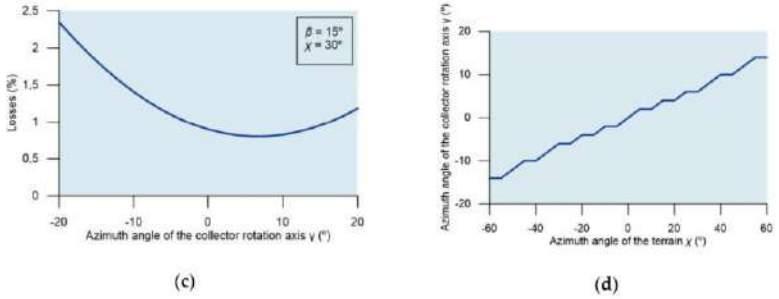

Figure 8. Results for a case study for inclination 15°: (**a**) maximum radiation; (**b**) radiation variation for 30° azimuth; (**c**) maximum radiation loss for 30° azimuth; (**d**) axis azimuth for optimal terrain radiation.

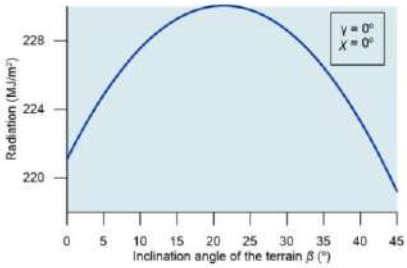

Figure 9. Variation of the maximum radiation affecting the collector with respect to the inclination of the terrain.

The difference observed between the radiation value for a particular axis azimuth and the maximum capture obtained in the optimum direction was greater as the inclination of the terrain increased. Thus, in low-inclination terrains the difference was low and while for steeper inclinations the losses were considerable. Figure 10 shows that, in the specific case of $\beta = 20°$, the losses caused by a bad choice of rotation axis direction can reach values above 7%.

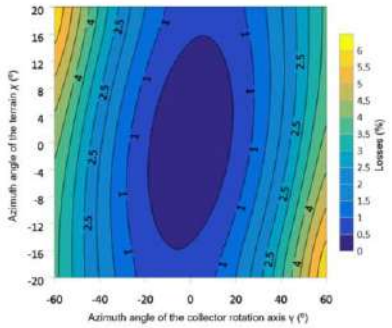

Figure 10. Losses for different axis and terrain azimuth values.

Figure 11 shows the losses for the conditions $\gamma = 0°$ and $\beta = 20°$, considering an azimuth range χ from $-60°$ to $60°$. For terrains that are also oriented towards the south, or close to it, the losses will be zero or very low, but as the azimuth of the terrain increases, the losses become considerable.

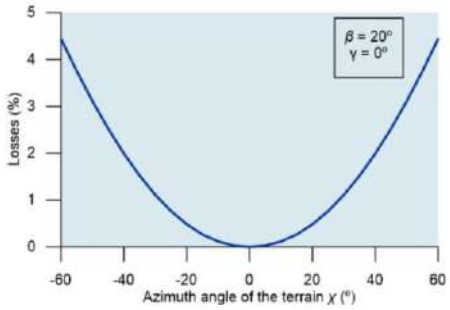

Figure 11. Losses with 0° axis azimuth and 20° inclination.

Thus, it is possible to establish a relationship between the sensitivity of the collector axis azimuth γ and the inclination β and azimuth of the terrain χ. It is worth highlighting the novelty of this result since no references have been found in the literature suggesting this relationship between variables.

Another key factor when configuring the layout of the collectors was the separation between them. This fact had an influence since the greater the panel separation is, the fewer shading effects are produced and the fewer losses due to a decrease in production. On the other hand, it was not possible to separate the rows of collectors as much as desired, since the costs associated with a higher terrain occupation increase rapidly [21]. Figure 12 shows that, depending on this parameter, the irradiance demonstrated asymptotic behaviour. This was because the shadow effects of one collector on another, when separated by a sufficient distance, were no longer perceived, thus resulting in an irradiance value like that of an isolated collector without adjacent collectors.

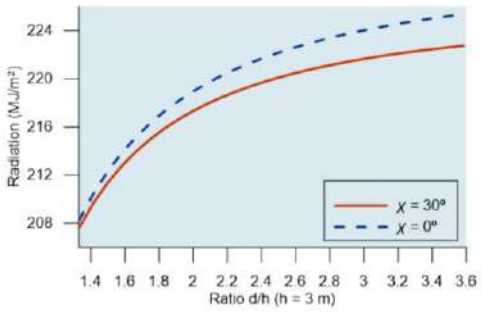

Figure 12. Irradiance by varying the ratio d/h (h = 3 m).

4. Conclusions

In this paper, the solar capture on horizontal one-axis trackers was mathematically modelled, thus establishing the rotation axis orientation for any irradiance model. Backtracking was used to avoid the shading of some panels on adjacent ones, modifying their orientation. The results obtained, combined with those in the literature, amount to an advance in the knowledge on photovoltaic trackers

with axes parallel to the terrain, allowing an optimal design for terrains without the horizontality described in previous works.

A program and a subroutine were implemented in VBA to automatically calculate the radiation affecting a solar tracker for different terrain configurations and for which it was possible to vary the characteristics of the installation, namely the rotation axis orientation and the ratio dimension of the panels h and the separation d between adjacent rows. Simultaneously, the program and subroutine provided the optimal azimuth γ value for the rotation axis to be suitably directed and the loss values for each possible maximum radiation value for each inclination β of the terrain.

The calculations of the amounts of radiation affecting solar panels, assuming fixed width and distance between lines of panels and varying terrain inclinations β and azimuth χ, were made in Córdoba, Spain.

For any given value regarding the terrain inclination β, it was verified that a higher value of radiation was obtained for terrain that was oriented south ($\chi = 0°$). The optimum direction for the rotation axis collector γ should also be southwards.

An important contribution of this research is the relationship established between the azimuth γ of the collector axis and the inclination β and azimuth of the terrain. For terrain that is not south facing, the rotation axis azimuth γ of the solar trackers should be different from zero and varies in the same direction as the land azimuth χ. If the axis of rotation is positioned in a different direction to the optimum, losses in potential energy production arise. These losses vary according to the terrain inclination β. The greater the difference between the optimum azimuth γ and the terrain inclination β, the greater the production losses will be.

Another important conclusion drawn from this research concerns the collector layout on the power plant surface. As the distance d between rows of collectors increases, a greater amount of radiation is generated. Such growth is asymptotic.

Overall, some progress has been achieved towards the objective of deepening knowledge concerning photovoltaic trackers. Consequently, guidelines were proposed for solar capture optimisation in photovoltaic plants. This work opens up further lines of research into the geometric layout optimisation of solar trackers involving more complex models, such as those of Perez [34] and Muneer [33], and real databases.

As a result of the aforementioned conclusions, it is considered that this study can be the basis for further work, such as the study of one-axis solar trackers located on terrains with irregular topographies or of the collector distribution system, considering potential uses of the land.

Author Contributions: Conceptualization, F.J.G.-U., I.M.M.-G. and R.L.-L.; methodology, I.M.M.-G. and L.M.F.-A.; software, J.M.J.-M.; validation, I.M.M.-G. and L.M.F.-A.; formal analysis, L.M.F.-A., I.M.M.-G. and R.L.-L.; bibliographic search, F.J.G.-U. and L.M.F.-A.; data curation, J.M.J.-M. and R.L.-L.; writing—original draft preparation, L.M.F.-A., F.J.G.-U. and I.M.M.-G.; writing—review & editing, F.J.G.-U., I.M.M.-G., R.L.-L. and L.M.F.-A.; supervision, I.M.M.-G., R.L.-L. and L.M.F.-A. All authors have read and agreed to the published version of the manuscript.

Funding: This research received no external funding.

Acknowledgments: This research was partially technically supported by the CLARA Project (European Union's Horizon 2020 research and innovation programme under Grant Agreement No 730482). The authors thank Azul y Verde Energía y Sostenibilidad S.L. for their collaboration in this research. The authors also thank Simon Craig for his contribution to the English edition.

Conflicts of Interest: The authors declare no conflict of interest.

Abbreviations

$\vec{a}$	projection vector of the solar panel being studied for shading
$\vec{d}$	distance between the centers of two adjacent solar collectors
$\vec{e}$	unit vector contained in the collector rotation axis
GCR	ground cover ratio
h	collector width
$\vec{i}, \vec{j}, \vec{k}$	unit vectors associated with a local Cartesian system
I	global solar irradiance on the tilted collector
I_B	direct solar irradiance on the horizontal plane
I_D	diffuse solar irradiance
I_{OH}	extraterrestrial irradiance
$\vec{n}$	normal vector to the surface
$\vec{n'}$	optimal normal vector to the surface
n'_x, n'_y, n'_z	components of optimal normal vector to the surface
$\vec{n_T}$	normal terrain vector
$\vec{p}$	unit vector perpendicular to ground normal vector $\vec{e}$
$\vec{q}$	perpendicular vector to $\vec{n_T}$ and $\vec{e}$
$\vec{s}$	solar vector
s_x, s_y, s_z	components of solar vector
$\vec{s'}$	optimal solar vector
s'_x, ss'_y, s'_z	components of optimal solar vector
$\vec{u}$	irradiance gradient

Greek Letters

α	elevation angle of the collector
β	inclination angle of the terrain
γ	azimuth angle of the collector rotation axis
δ	solar declination
ξ	inclination angle of the collector
θ	angle of incidence of sunbeams on the inclined plane
θ_z	solar zenith angle
λ, μ, υ	Lagrange multipliers
ρ	albedo
τ	scalar multiplying solar vector to accomplish parallelogram rule
φ	latitude
Φ	Lagrange function
χ	azimuth of the terrain
Ω	Earth's rotation speed

References

1. Carballo, J.A.; Bonilla, J.; Roca, L.; Berenguel, M. New low-cost solar tracking system based on open source hardware for educational purposes. *Sol. Energy* **2018**, *174*, 826–836. [CrossRef]
2. United Nations. *The Sustainable Development Goals Report 2019*; United Nations Publications (Department of Economic and Social Affairs): Herndon, VA, USA, 2019.
3. Ribó-Pérez, D.; Van der Weijde, A.H.; Álvarez-Bel, C. Effects of self-generation in imperfectly competitive electricity markets: The case of Spain. *Energy Policy* **2019**, *133*, 110920. [CrossRef]
4. International Renewable Energy Agency. *Renewable Power Generation Costs in 2019*; International Renewable Energy Agency: Abu Dhabi, UAE, 2020; ISBN 978-92-9260-244-4.
5. Kavlak, G.; McNerney, J.; Trancik, J.E. Evaluating the causes of cost reduction in photovoltaic modules. *Energy Policy* **2018**, *123*, 700–710. [CrossRef]

6. Hua, Z.; Ma, C.; Lian, J.; Pang, X.; Yang, W. Optimal capacity allocation of multiple solar trackers and storage capacity for utility-scale photovoltaic plants considering output characteristics and complementary demand. *Appl. Energy* **2019**, *238*, 721–733. [CrossRef]
7. Hafez, A.Z.; Yousef, A.M.; Harag, N.M. Solar tracking systems: Technologies and trackers drive types—A review. *Renew. Sustain. Energy Rev.* **2018**, *91*, 754–782. [CrossRef]
8. Nsengiyumva, W.; Chen, S.G.; Hu, L.; Chen, X. Recent advancements and challenges in Solar Tracking Systems (STS): A review. *Renew. Sustain. Energy Rev.* **2018**, *81*, 250–279. [CrossRef]
9. Koussa, M.; Cheknane, A.; Hadji, S.; Haddadi, M.; Noureddine, S. Measured and modelled improvement in solar energy yield from flat plate photovoltaic systems utilizing different tracking systems and under a range of environmental conditions. *Appl. Energy* **2011**, *88*, 1756–1771. [CrossRef]
10. Bahrami, A.; Okoye, C.O.; Atikol, U. The effect of latitude on the performance of different solar trackers in Europe and Africa. *Appl. Energy* **2016**, *177*, 896–906. [CrossRef]
11. Abdallah, S.; Nijmeh, S. Two axes sun tracking system with PLC control. *Energy Convers. Manag.* **2004**, *45*, 1931–1939. [CrossRef]
12. Braun, J.E.; Mitchell, J.C. Solar geometry for fixed and tracking surfaces. *Sol. Energy* **1983**, *31*, 439–444. [CrossRef]
13. Duffie, J.A.; Beckman, W.A. *Solar Engineering of Thermal Processes*; John Wiley & Sons, Inc.: Hoboken, NJ, USA, 2013; ISBN 9781118671603.
14. Narvarte, L.; Lorenzo, E. Tracking and ground cover ratio. *Prog. Photovolt. Res. Appl.* **2008**, *16*, 703–714. [CrossRef]
15. Parkin, R.E. Solar angles revisited using a general vector approach. *Sol. Energy* **2010**, *84*, 912–916. [CrossRef]
16. Sproul, A.B. Derivation of the solar geometric relationships using vector analysis. *Renew. Energy* **2007**, *32*, 1187–1205. [CrossRef]
17. Fan, X.; Deng, F.; Chen, J. Voltage band analysis for maximum power point tracking of stand-alone PV systems. *Sol. Energy* **2017**, *144*, 221–231. [CrossRef]
18. Satpathy, P.R.; Sharma, R. Diffusion charge compensation strategy for power balancing in capacitor-less photovoltaic modules during partial shading. *Appl. Energy* **2019**, *255*. [CrossRef]
19. Seyedmahmoudian, M.; Horan, B.; Soon, T.K.; Rahmani, R.; Than Oo, A.M.; Mekhilef, S.; Stojcevski, A. State of the art artificial intelligence-based MPPT techniques for mitigating partial shading effects on PV systems—A review. *Renew. Sustain. Energy Rev.* **2016**, *64*, 435–455. [CrossRef]
20. Belhachat, F.; Larbes, C. Modeling, analysis and comparison of solar photovoltaic array configurations under partial shading conditions. *Sol. Energy* **2015**, *120*, 399–418. [CrossRef]
21. Saint-Drenan, Y.M.; Barbier, T. Data-analysis and modelling of the effect of inter-row shading on the power production of photovoltaic plants. *Sol. Energy* **2019**, *184*, 127–147. [CrossRef]
22. Perpiñán, O. Cost of energy and mutual shadows in a two-axis tracking PV system. *Renew. Energy* **2012**, *43*, 331–342. [CrossRef]
23. Deline, C.; Dobos, A.; Janzou, S.; Meydbray, J.; Donovan, M. A simplified model of uniform shading in large photovoltaic arrays. *Sol. Energy* **2013**, *96*, 274–282. [CrossRef]
24. Martínez-Moreno, F.; Muñoz, J.; Lorenzo, E. Experimental model to estimate shading losses on PV arrays. *Sol. Energy Mater. Sol. Cells* **2010**, *94*, 2298–2303. [CrossRef]
25. Panico, D.; Garvison, P.; Wenger, H.; Shugar, D. Backtracking: A novel strategy for tracking PV systems. In Proceedings of the Conference Record of the Twenty-Second IEEE Photovoltaic Specialists Conference, Las Vegas, NV, USA, 7–11 October 1991; Volume 1, pp. 668–673. [CrossRef]
26. Antonanzas, J.; Urraca, R.; Martinez-de-Pison, F.J.; Antonanzas, F. Optimal solar tracking strategy to increase irradiance in the plane of array under cloudy conditions: A study across Europe. *Sol. Energy* **2018**, *163*, 122–130. [CrossRef]
27. Fernández-Ahumada, L.M.; Ramírez-Faz, J.; López-Luque, R.; Varo-Martínez, M.; Moreno-García, I.M.; Casares de la Torre, F. A novel backtracking approach for two-axis solar PV tracking plants. *Renew. Energy* **2020**, *145*, 1214–1221. [CrossRef]
28. Kelly, N.A.; Gibson, T.L. Improved photovoltaic energy output for cloudy conditions with a solar tracking system. *Sol. Energy* **2009**, *83*, 2092–2102. [CrossRef]
29. Quesada, G.; Guillon, L.; Rousse, D.R.; Mehrtash, M.; Dutil, Y.; Paradis, P.-L. Tracking strategy for photovoltaic solar systems in high latitudes. *Energy Convers. Manag.* **2015**, *103*, 147–156. [CrossRef]

30. Fernández-Ahumada, L.M.; Casares, F.J.; Ramírez-Faz, J.; López-Luque, R. Mathematical study of the movement of solar tracking systems based on rational models. *Sol. Energy* **2017**, *150*, 20–29. [CrossRef]
31. Hay, J.E. Calculating solar radiation for inclined surfaces: Practical approaches. *Renew. Energy* **1993**, *3*, 373–380. [CrossRef]
32. Mousazadeh, H.; Keyhani, A.; Javadi, A.; Mobli, H.; Abrinia, K.; Sharifi, A. A review of principle and sun-tracking methods for maximizing solar systems output. *Renew. Sustain. Energy Rev.* **2009**, *13*, 1800–1818. [CrossRef]
33. Muneer, T. Solar radiation model for Europe. *Build. Serv. Eng. Res. Technol.* **1990**, *11*, 153–163. [CrossRef]
34. Perez, R.; Ineichen, P.; Seals, R.; Michalsky, J.; Stewart, R. Modeling daylight availability and irradiance components from direct and global irradiance. *Sol. Energy* **1990**, *44*, 271–289. [CrossRef]
35. Diez-Mediavilla, M.; De Miguel, A.; Bilbao, J. Measurement and comparison of diffuse solar irradiance models on inclined surfaces in Valladolid (Spain). *Energy Convers. Manag.* **2005**, *46*, 2075–2092. [CrossRef]
36. Loutzenhiser, P.G.; Manz, H.; Felsmann, C.; Strachan, P.A.; Frank, T.; Maxwell, G.M. Empirical validation of models to compute solar irradiance on inclined surfaces for building energy simulation. *Sol. Energy* **2007**, *81*, 254–267. [CrossRef]
37. Mubarak, R.; Hofmann, M.; Riechelmann, S.; Seckmeyer, G. Comparison of modelled and measured tilted solar irradiance for photovoltaic applications. *Energies* **2017**, *10*, 1688. [CrossRef]
38. Collares-Pereira, M.; Rabl, A. The average distribution of solar radiation-correlations between diffuse and hemispherical and between daily and hourly insolation values. *Sol. Energy* **1979**. [CrossRef]

Anexo II

Segundo artículo del compendio: “Nuevo sensor omnidireccional basado en software y hardware de código abierto para el seguimiento y retroceso de seguidores solares de doble eje en plantas fotovoltaicas”.

Publicado en la revista Sensors.

Enviado el 1 de enero de 2020, aceptado el 19 de enero de 2021.

Factor de impacto en 2019: 3,275

sensors

MDPI

Article

New Omnidirectional Sensor Based on Open-Source Software and Hardware for Tracking and Backtracking of Dual-Axis Solar Trackers in Photovoltaic Plants

F.J. Gómez-Uceda [1], J. Ramirez-Faz [2], M. Varo-Martinez [3,*] and L.M. Fernández-Ahumada [2]

[1] Department of Mechanics, Campus of Rabanales, University of Cordoba, 14071 Cordoba, Spain; fjgomez@uco.es
[2] Department of Electrical Engineering and Automatics, Campus of Rabanales, University of Cordoba, 14071 Cordoba, Spain; jramirez@uco.es (J.R.-F.); lmfernandez@uco.es (L.M.F.-A.)
[3] Department of Applied Physics, Radiology and Physical Medicine, Campus of Rabanales, University of Cordoba, 14071 Cordoba, Spain
* Correspondence: fa2vamam@uco.es

Abstract: In this work, an omnidirectional sensor that enables identification of the direction of the celestial sphere with maximum solar irradiance is presented. The sensor, based on instantaneous measurements, functions as a position server for dual-axis solar trackers in photovoltaic plants. The proposed device has been developed with free software and hardware, which makes it a pioneering solution because it is open and accessible as well as capable of being improved by the scientific community, thereby contributing to the rapid advancement of technology. In addition, the device includes an algorithm developed ex professo that makes it possible to predetermine the regions of the celestial sphere for which, according to the geometric characteristics of the PV plant, there would be shading between the panels. In this way, solar trackers do not have to locate the Sun's position at all times according to astronomical models, while taking into account factors such as shadows or cloudiness that also affect levels of incident irradiance on solar collectors. Therefore, with this device, it is possible to provide photovoltaic plants with dual-axis solar tracking with a low-cost device that helps to optimise the trajectory of the trackers and, consequently, their radiative capture and energy production.

Keywords: free and open-source hardware (FOSH); sun position sensor; omnidirectional sensor; solar trackers; PV plants; backtracking

Citation: Gómez-Uceda, F.J.; Ramirez-Faz, J.; Varo-Martinez, M.; Fernández-Ahumada, L.M. New Omnidirectional Sensor Based on Open-Source Software and Hardware for Tracking and Backtracking of Dual-Axis Solar Trackers in Photovoltaic Plants. *Sensors* **2021**, *21*, 726. https://doi.org/10.3390/s21030726

Received: 1 January 2021
Accepted: 19 January 2021
Published: 21 January 2021

1. Introduction

The industrial and technological development that society has undergone, as well as the increase in the population worldwide, has led to a growing demand for energy [1,2]. Satisfying this increase in energy demand only by means of traditional methods of energy production based on fossil and nuclear resources entails serious environmental problems that endanger the sustainability of the Earth, such as pollution and climate change [3–5]. In response, the scientific community has highlighted the importance of enhancing the role of renewable energies in the energy models of both developed and developing countries [1,6,7]. In fact, the number of journals and papers related to renewable energies has experienced a remarkable growth [8], which shows the increasing researchers' awareness of the need to contribute to the improvement and the progress of this field of science and its beneficial impact on the challenges of current society.

Among these possible renewable energy sources, solar energy plays a fundamental role [9–11] since, as stated by Kannan and Vakeesan [3], it is an abundant source of energy that, being properly exploited, could be enough to satisfy world energy demand.

Furthermore, it is available all over the planet, its use has no negative impact on the environment and it is a technology that is easily usable at all levels (industrial, domestic, etc.). The technological improvements achieved in recent years have allowed to reduce the production cost of PV energy to values competitive with those of the energy supplied by the grid [12]. As a result, the presence of PV technologies in the energy market has experienced a significant growth [13]. However, in order to continue promoting this expansion, it is necessary to continue researching into new solutions that will maintain their growing development and technological progress [12].

1.1. Literature Review on Solar Tracking

Among the solar energy technologies, photovoltaic (PV) is undergoing a remarkable boom due to its simplicity and low cost, as well as the significantly technological enhancements that it has been experiencing. As a consequence, it is becoming a promising source of electricity generation [14]. However, despite its rapid technological evolution, there is still plenty of room for optimisation in the efficiency of the management of photovoltaic installations, as well as in the configuration of its design, which would lead to a potential increase in its development.

One possible line of technological improvement of PV that has been worked on for decades is solar tracking [9]. It tries to alleviate the negative effects of the high variability of the solar resource, both in time as well as in space, by reorienting the PV panels towards possible directions that increase solar irradiance collection. In order to do so, solar trackers are very useful both in large PV plants connected to the grid and in small domestic installations in which the space available for the installation of the panels is often reduced and, as a consequence, it is necessary to increase the energy generated per square metre of collecting surface [15].

There is a traditional classification of trackers based on the degrees of freedom of the tracking movement according to which they can be categorised into single-axis trackers and dual-axis trackers. The former is characterised by modifying the orientation of the collector plane by turning around a single fixed axis. The latter are characterised by a movement of its plane through the rotation of a system composed of two fixed axes, which allows it to orient itself in any possible direction in the celestial sphere [16]. Although dual-axis trackers are more expensive and require more work to implement and maintain than single-axis trackers, they offer better performance [17–19]. In fact, although some authors affirm that dual-axis monitoring systems have no future due to their complexity and high cost [20,21], Eldin et al. [14] suggest that, at present, this type of technology is widespread throughout the world and that multiple research is being developed to improve both the technology and its efficiency/cost ratio, so that its energy production exceeds and compensates for the costs of the installation and maintenance as well as the energy consumption used in the movement of the trackers.

Another possible classification of solar trackers is the one based on the mechanism that enables monitoring. Thus, on the one hand, there are passive trackers that do not use mechanical devices for movement. To the contrary, in most cases, they are composed of a pair of actuators, filled with expandable gas, which in the case of imbalance, are levelled with equal lighting by means of thermal expansion [22]. In comparison, active solar trackers use motors commonly governed by control signals for movement in search of the position of the Sun, which are very precise devices except on very cloudy days [23].

Finally, depending on the tracking control strategy, a distinction is made between trackers in which the movement, both in azimuth and elevation, is governed by mathematical models (in open loop) and those in which the system feeds back through irradiance sensors (closed loop).

Various literature review works have systematically collected the data obtained by different solar trackers developed by the scientific community, finding that the energy produced by a PV system with tracking is always greater than that of a system without it [9,10], except on spring or summer days with great cloudiness [17,24]. More specifically,

Eldin et al. [14] carried out a study on the convenience of monitoring systems depending on the climatic conditions of the place and verified that the output power of photovoltaic panels with solar monitoring depends on environmental conditions. Thus, while in cold regions with a high incidence of cloudiness, monitoring strategies are profitable for maximising the power of photovoltaic panels, in places with very hot and sunny climates, they are not, due to the negative influence of overheating on performance of photovoltaic panels. Likewise, some authors have analysed the improvements in energy production of PV systems with solar tracking depending on the type of technology used and the latitude of the study site [25–27]. Thus, it has been shown that, in general, the higher the latitude, the better the monitoring efficiency is achieved, reaching improvements of up to 57% [23].

Similarly, with regard to grid-connected PV installations, a recent study [28] has analysed, from a techno-economic-environmental point of view, the use of different solar tracking systems to maximise the photovoltaic power generation in residential solar installations connected to the grid in eight regions of Iran with diverse climates. Based on the study carried out, they found that the dual-axis monitoring system is the most efficient (32% average increase in energy production compared to an installation without monitoring), while the vertical single-axis monitoring system is the most profitable (23% increase in energy production compared to a nonmonitored installation with only 1.6% increase in energy cost). In general terms, the study concludes that the use of the solar tracking system in residential installations connected to the grid significantly reduces the number of panels needed, but this reduction in size is not always profitable due to the high cost of the monitoring units. However, the profitability of the installation increases significantly in all cases when the sale of electricity to the grid is allowed.

As far as the monitoring strategy is concerned, the most frequent in the literature is that based on solar astronomical movement, which aims to minimise the angle of incidence θ between the solar rays and the normal to the capture surface. According to this astronomical tracking strategy, various works [29–34] show prediction models of incident irradiance on the plane of trackers of both single and dual axes, with a degree of accuracy for solar location in the celestial sphere to the order of mrad [35–37]. The models used for astronomical tracking have traditionally been based on spherical trigonometry [31]. However, recently, a new paradigm using vector algebra to define the solar movement and that of the trackers can be found in the literature [38–45]. For this, these models use the solar vector $\vec{s}$, which is a unit vector that is directed to the centre of the solar disk. Its expression in different coordinate systems and the use of the definition of scalar and vector product enable the deduction of the entire system of astronomical relationships that govern the movement of the solar trackers [46].

Furthermore, as previously mentioned, the astronomical tracking strategy seeks the optimisation of the direct component of solar irradiance. Consequently, it is adapted to solar concentrators that are based on the use of this component, but not to flat PV collectors in which the remaining components of irradiance (diffuse and reflected) are also used. Thus, on days when the solar disk is not visible and direct irradiance does not reach the collectors, the efficiency of this monitoring strategy is not satisfactory [23,30] and the capture of the collectors is less than that which would be obtained on a horizontal flat surface. Despite this, it is difficult to find references that determine models for solar tracking on these types of days, so it is necessary to continue developing mathematical equations that also take into account the diffuse and reflected components when trying to maximise radiative collection as part of solar tracking strategy.

On the other hand, the energy reduction caused by shading is particularly significant for PV installations. In addition, the shaded cells become overheated, which may lead to a fast degradation of the modules. Backtracking is applied to prevent the inter-shading of collectors. This technique consists of shifting the collectors to positions where shadows no longer appear [26,32,47]. Combining these two requirements (optimising global irradiance and performing backtracking) leads to a differentiation within the dedicated and specific tracking strategy for PV plants, studied further in this article.

In this line of work, a novel solar tracking strategy with back-tracking has been proposed to optimise the capture of solar irradiance at all times while avoiding inter-shading between collectors in PV plants with dual-axis tracking [39–41]. In this study, based on empirical models for the characterisation of the hemispheric distribution of irradiance, the authors quantify the increases in solar incidence on collectors at a higher value than 2%. In order to implement this strategy in existing facilities, the device presented in this article is developed and built.

Likewise, other authors [17,48–50] have implemented tracking systems with sensors that follow the position of the Sun with great precision and that have the advantages of easy implementation, simple design, low cost and a high level of adaptability. However, it is necessary to continue advancing in the search for tracking strategies that enable constant identification of the direction of the celestial sphere in which solar irradiance is maximum in a simple way regarding the hardware and software necessary for its implementation and that does not imply an increase in the cost of the technology, either in implementation or maintenance.

1.2. Literature Review on Free and Open-Source Hardware and Software Applied to PV Energy

Despite the great progress that new technologies have experienced in recent decades, the energy supply network based on traditional technologies has not evolved at the same rates [5]. However, this is different in the case of renewable energies. In that sense, it is increasingly common to find in the literature proposals based on free hardware in the field of photovoltaic solar energy, in general, and in solar tracking, in particular. Thus, for example, the use of microcontrollers (many based on free hardware) in the implementation of various photovoltaic tracking strategies presents an important competitive advantage at an economic level compared to control based on traditional PLCs [51]. In general terms, with the use of technologies based on free hardware in the field of solar PV energy, not only are lower costs sought, but it is also intended that the results and yields obtained are similar to or better than those achieved by commercial solutions [52]. In this sense, as it is a free hardware system, it can be shared among the scientific community and can be edited and improved by different experts [53]. Another advantage is the fact that the application of the devices shows a wide range of possibilities both at the level of capture (irradiance, temperature, and humidity) and control of the complex processes in which it works [54]. In addition, the possibility of safely, quickly and easily storing the huge amount of data generated by any photovoltaic installation is an important milestone in working with free hardware devices [55].

Among some of the devices found in the literature is the one by Gutierrez et al. [15] that presents a single-axis solar tracker for the integration of buildings controlled with an open-loop control strategy implemented through Arduino and IoT. This makes it a low-cost device with a flexible implementation and applicable anywhere in the world. A new electronic sensor based on free hardware has also been developed, validated and patented to measure radiation and global radiation on the horizontal surface [56]. The device is characterised by high precision and the technologies used in its implementation (Arduino and IoT) make it a low-cost device with a high level of connectivity and ubiquity, which is why it is easily applicable to the monitoring and control of any PV plant and, especially, to "smart-grid" solutions. Paredes-Parra et al. [57] have also developed a low-cost and open-source system, based on IoT and LoRa, which allows remote monitoring and real-time operation of a PV plant and, therefore, facilitating maintenance and supervision tasks. Similarly, Pereira et al. [58] have developed a new multi-user remote data acquisition and transmission system, based on Raspberry Pi and IoT technology, to monitor a photovoltaic plant in real time. Therefore, it can be affirmed that the relationship established in the different levels of aggregation of solar energy (generation, smart grids and integration) is a field in which the use of the aforementioned technologies finds an interesting space due to the versatility shown [59,60].

In accordance with all the above and combining the two lines of work presented, this paper describes a sensor that uses an onmidirectional solar tracker, based on Free and open-source hardware (FOSH), which acts as a server of position for dual-axis PV trackers, identifying at each instant in time, the optimal orientation of the PV panels from instantaneous irradiance measurements. With this, the solar trackers do not have to search for the position of the sun using algorithms based on solar geometry while taking into account other conditions (cloudiness, shading between panels, etc.) that also influence the irradiance received by the capturing surfaces. In this way, it is possible to provide PV plants with dual-axis solar tracking with a low-cost device that helps to optimise the trajectory of its trackers and, consequently, its radiative capture and energy production.

Following this introduction, the remainder of the article is organised as follows: in the next section, Section 2, the proposed design and the algorithms implemented in the device are outlined; Section 3 presents how the system was tested for a PV plant in Peñarroya (Spain) and discusses the results. In Section 4, conclusions are drawn based on the work developed.

2. Proposed Design

To achieve the objective described above, the device presented makes a scan of the celestial sphere, during which the incident irradiance measurement is carried out in order to determine the orientation for which this magnitude is maximum. However, as a novelty, the device incorporates a dichotomous algorithm, designed by the authors [39,40] that, prior to the scanning of the celestial sphere, identifies those orientations of the solar trackers for which there would be inter-shading between the collectors. With this, the proposed device restricts the search field for the orientation of maximum irradiance to the set of spatial directions in which there is no inter-shading, which in practice implies a backtracking strategy. Once the direction of maximum irradiance has been identified, the azimuth (γ) and elevation (α) angles corresponding to it, stored in the device that acts as a position server, are made available to the solar trackers of the PV installation for their orientation towards the position of maximum capture.

The technological solution presented consists of a pan-tilt type orientation mechanism that allows the positioning of an irradiance sensor in any direction of the celestial sphere, characterised by its azimuth (γ) and its elevation (α), as well as an irradiance measurement and control system in real time. The mechanism is controlled by a microprocessor that is also in charge of carrying out the irradiance readings and their transmission to the solar servers. For its operation, the necessary algorithms have been developed and implemented to adjust the movements of the solar trackers so that optimal energy production is achieved. Likewise, the complete architecture of the device has been developed, based on Free and Open-Source hardware (FOSH) and a simple control system with functionalities associated with IoT technologies. All of this makes the device an economically competitive tilt and azimuth server, capable of integrating into dual-axis photovoltaic installations and favouring the optimisation of its energy production. This previous dichotomous algorithm for the detection of inter-shading as well as the electronic and mechanical design of the device is described below.

2.1. Algorithm for the Detection of Inter-Shading between Collectors

As mentioned above, the device includes a simple and programmable algorithm in 8-bit AVR RISC microprocessors that, taking into account the characteristics of the PV installation, enables one to know whether a certain orientation (γ, α) of the collectors would imply the partial inter-shading between them for a certain Julian day (d_j) and a specific solar hour (t) prior to the scanning of the celestial sphere. This algorithm is supported by a novel tracking strategy developed by the authors and the one that is based on Minkowski algebra [39,40].

This procedure can be understood as a Boolean function dependent on (γ, α, d_j, t) in which the result "TRUE" implies the existence of inter-shading and "FALSE," the absence. As auxiliary information, this function requires:

1. The width (a) and height (b) of the solar collectors.
2. The set of Cartesian coordinates (x, y, z) of the base of each solar tracker, using as a reference system a local coordinate system in which the Ox axis goes to the West, the Oy to the South and the Oz to the point Zenith. This information is structured by three arrays $x[i], y[i], z[i]$ in which i is the index assigned to each solar tracker (Figure 1), so that $1 < i < N$ is verified, where N is the number of trackers in the installation.
3. The solar vector or unit vector that points to the solar disk at each instant of time that, in the reference system considered, is given by the Equation (1):

$$\begin{aligned} &\vec{s} = s_x\vec{\imath} + s_y\vec{\jmath} + s_z\vec{k} = \\ &= sin\,\Omega\,t\ \ cos\,\delta\,\vec{\imath} + \\ &+(cos\,\Omega\,t\,cos\,\delta\,sin\,\varphi - sin\,\delta\,cos\,\varphi)\vec{\jmath} + \\ &+(cos\,\Omega\,t\,cos\,\delta\,cos\,\varphi + sin\,\delta\,sin\,\varphi)\vec{k}, \end{aligned} \tag{1}$$

where φ is the latitude, Ωt is the hourly angle, defined as the product of the Earth rotation speed ($\Omega = 2\pi/24\,rad/h$) and the time elapsed since solar noon, and δ is the solar declination given by Equation (2), being Γ and auxiliary angle dependent on the Julian day according to Equation (3)

$$\begin{aligned} &\delta(rad) = [0.006918 - 0.399912\,cos(\Gamma) + \\ &+0.070257 sin(\Gamma) - 0.006758\,cos(2\Gamma) + \\ &+0.000907 sin(2\Gamma) - 0.002697\,cos(3\Gamma) + \\ &+0.00148 sin(3\Gamma)], \end{aligned} \tag{2}$$

$$\Gamma(rad) = \frac{2\pi(d_j - 1)}{365} \tag{3}$$

4. The unit vector $\vec{n}$, which indicates the direction towards which the solar trackers are oriented, being perpendicular to the collectors, and which is given by the Equation (4).

$$\vec{n} = \cos\alpha \cdot \sin\gamma\vec{\imath} + cos\,\alpha \cdot \cos\gamma\,\vec{\jmath} + \sin\alpha\,\vec{k}, \tag{4}$$

5. The unit vectors $\vec{u}$ y $\vec{v}$ included in the collector plane, where $\vec{u}$ is horizontal (Equation (5)) and $\vec{v}$ (Equation (6)) perpendicular to $\vec{u}$.

$$\vec{u} = -cos\,\gamma\,\vec{\imath} + \sin\gamma\,\vec{\jmath}, \tag{5}$$

$$\vec{v} = sin\,\alpha \cdot cos\,\gamma\vec{\imath} - sin\,\alpha \cdot cos\,\gamma\,\vec{\jmath} + cos\,\alpha\,\vec{k}. \tag{6}$$

Figure 2 shows the flow chart of the designed and implemented procedure.

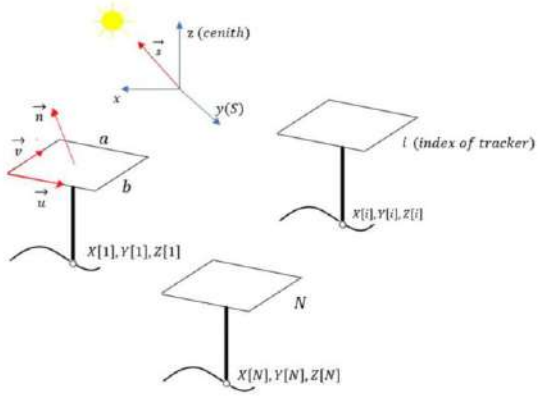

Figure 1. Geometric elements necessary to determine the existence of inter-shading according to the algorithm of Fernandez-Ahumada et al. [39,40].

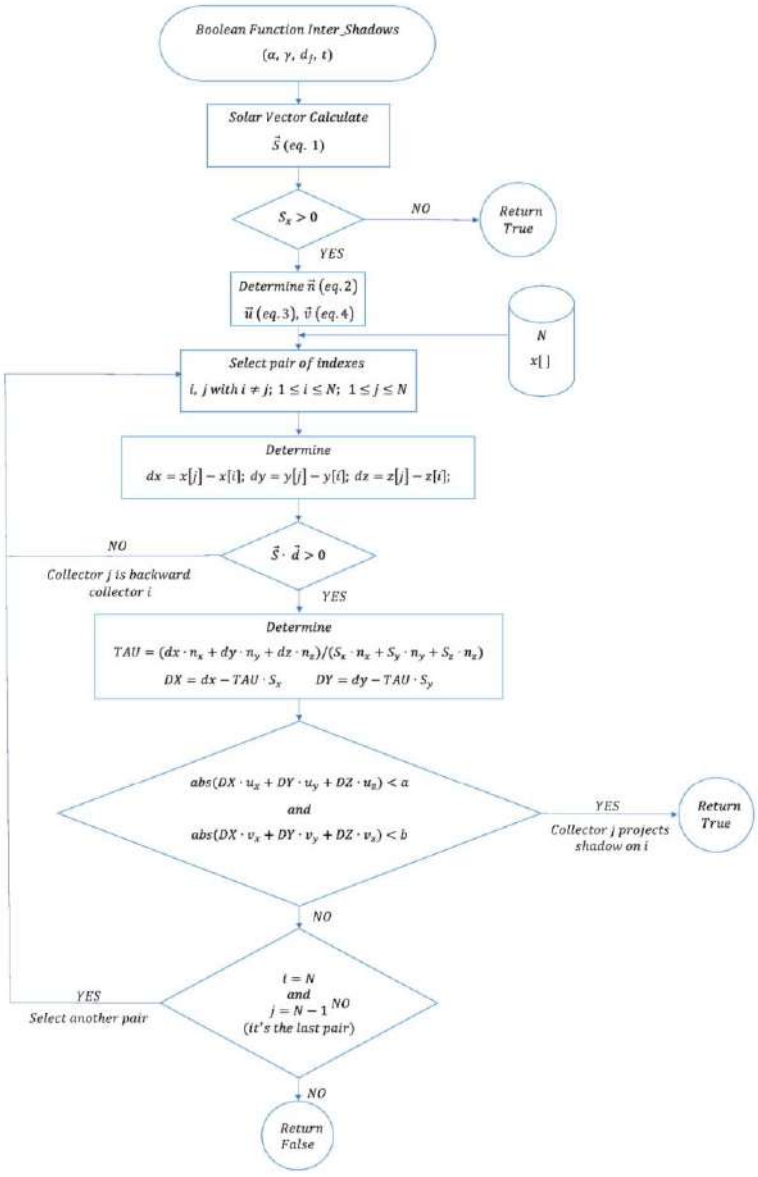

Figure 2. Flow chart of the designed procedure.

2.2. Design of the Proposed Technological Solution

The mechanical design of the proposed device has been resolved by means of a flat surface with two degrees of freedom (Figure 3). The manufacture has been carried out by means of additive printing on acrylonitrile butadiene styrene (ABS) filament, a thermoplastic polymer with good properties with regard to distortion and softening temperatures, 96 and 93 °C, respectively. The whole set remains inside a transparent methacrylate dome.

Figure 3. (a) Design of the system, (b) electronical components, and (c) photography of the prototype.

Figure 4 schematically shows the concept of the electronic design of the system in which four blocks are distinguished: sensors, processing, actuators and communications.

- Sensors: On the one hand, the system includes a sensor system whose purpose is to know the solar time corresponding to orientations that are not allowed because they cause inter-shading between the collectors. For this, among the different options to obtain the time (internal clock of the microcontroller, time server or external RTC module), in this prototype, a DS1307 real-time clock has been chosen, with autonomous power supply by means of a CR2025 battery. Likewise, for the irradiance measurement, a calibrated photovoltaic cell of the Fadisol C-0121 type has

been used that provides a linear current output with respect to irradiance, comprised between 36 mA for 125 W/m² and 288 mA for 1000 W/m². The measurement of the intensity of the electric current provided by these short-circuited photovoltaic cells is measured by means of an INA219 module, consisting of a shunt equipped with a 12-bit analog-digital converter and I2C output. In this way, adjusting the gain in the module configuration, an accuracy of 0.1 mA and a maximum intensity of 400 mA are obtained. Finally, an initialisation of the azimuth and elevation position has been provided, using two mechanical micro-switches that indicate the zero relative position to the microcontroller.

- Processing: In the philosophy of this work, several alternatives for processing have been evaluated, opting for a TTGO ESP32 Lora development board. The ESP32 microcontroller integrates analog and digital inputs and outputs, as well as various communication interfaces, both wireless (Wi-Fi and Bluetooth Low Energy) and wired (I2C, SPI, UART). The selected board also has a LoRa communication module, model SEMTECH SX1276 that enables communication at a frequency of 868 MHz.
- Drive: Two 28BYJ-48 stepper motors, powered at 5 V, with 4096 steps per revolution that provide a maximum precision of 0.001534 radians, have been used to drive the two axes of movement of the omnidirectional server presented. The management of the stepper motors requires a controller, for which two units of the type LM298 have been used.
- Communications: Finally, it has been considered that the communications between the position server and the solar trackers require a range according to the typical dimensions of photovoltaic installations. The receiving devices of the orientation command can be arranged in a radius of up to 15 km around the server [61], which is achieved with direct vision between antennas, in optimal conditions, while in unfavourable conditions, such as suburban areas, 3 km are reached [62].

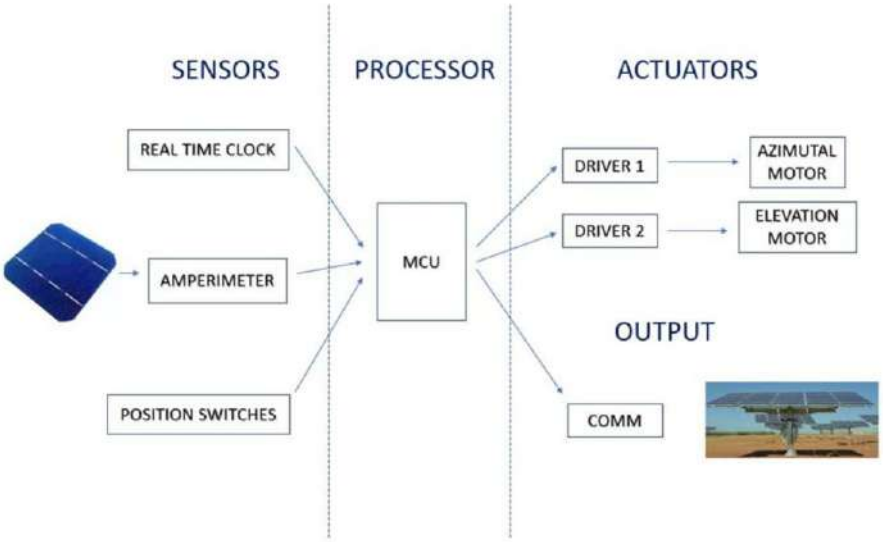

Figure 4. Scheme of principle of the proposed system.

3. Results

This section shows the results obtained when applying this device to the "Peñarroya I" PV plant, situated at a location of 38.299224° N latitude and −5.303114° longitude. The plant consists of 29 dual-axis solar trackers whose collectors measure 12 m wide (*a*) by 5 m high (*b*). Figure 5 shows its distribution in plan as well as the index assigned to each one and the reference system used to study the system. Table 1 shows the coordinates of the base of each collector.

Figure 5. Dual-axis trackers plant Peñarroya I.

Table 1. Coordinates (m) considered for each tracker.

Tracker	x (m)	y (m)	z (m)
1	18.50	22.70	0.00
2	22.29	40.70	0.00
3	26.08	58.71	0.00
4	29.88	76.71	0.00
5	33.67	94.72	0.00
6	37.46	112.72	0.00
7	41.50	17.86	0.00
8	45.29	35.86	0.00
9	49.08	53.87	0.00
10	52.87	71.87	0.00
11	56.66	89.88	0.00
12	60.46	107.88	0.00
13	64.49	13.01	0.00
14	68.28	31.02	0.00
15	72.08	49.02	0.00
16	75.87	67.03	0.00
17	79.66	85.03	0.00
18	83.45	103.04	0.00
19	87.49	8.17	0.00
20	91.28	26.17	0.00
21	95.07	44.18	0.00
22	98.86	62.18	0.00
23	102.66	80.19	0.00

24	106.45	98.19	0.00
25	114.27	21.33	0.00
26	118.07	39.34	0.00
27	121.86	57.34	0.00
28	125.65	75.35	0.00
29	129.44	93.35	0.00

Figure 6 shows the graphic representation of the data obtained by the proposed omnidirectional sensor at different times of the year in Lambert projection hemispheric diagram mode [63]. These figures show the existence of two regions. Thus, the grey region represents the directions of the celestial sphere in which no measurements are taken since it corresponds to positions for which the algorithm prior to tracking indicates inter-shading of collectors. On the other hand, the blue region corresponds to the orientations of the solar servers for which there is no inter-shading and in which, consequently, irradiance (W/m²) measurements are made, which are represented by the corresponding iso-level curves (grey lines).

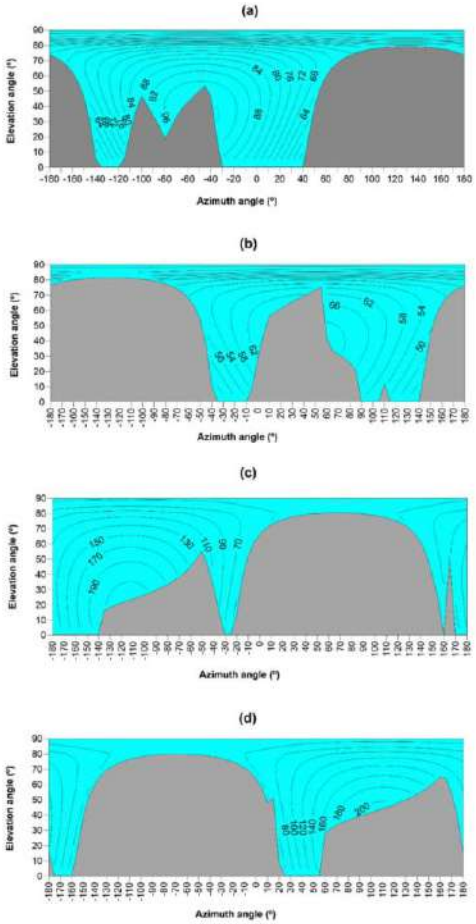

Figure 6. Simulation of the irradiance (W/m²) values registered by the proposed device and the fragmentation of the celestial sphere at different moments of time: (**a**) 21 December at 8:24 a.m. in True Solar Time, (**b**) 21 December at 15:24 p.m. in True Solar Time, (**c**) 21 June at 7:30 a.m. in True Solar Time, and (**d**) 21 June at 15:48 p.m. in True Solar Time.

The information shown on each chart is obtained by the sensor during every scanning cycle along the celestial sphere. There is evidence that this is the most complete traceability criterion available in the literature [26,47,64,65]. In general, these methods are limited to the evaluation of installations on flat surfaces, normally horizontal, where only the potential shadows produced by the adjacent collectors are considered. These methods are also limited by the type of tracking they have been developed for. Even for certain types

of tracking, such as the tracking of a vertical axis, they have not been computerized due to the lack of a published algorithm [66]. The lack of open-source devices to solve optimal tracking, including backtracking, and of generic algorithms is also evident upon consulting commercial devices to manage backtracking. Although some manufacturers implement algorithms based on artificial intelligence [67,68] or on customized systems [69], authors have not found the theoretical basis of these published.

4. Conclusions

The present work shows the construction and design of a device capable of determining the incident solar irradiance on the collector planes of a PV plant with dual-axis trackers depending on their orientation (azimuth and elevation). From this irradiance, obtained by means of instantaneous measurements carried out while tracking the celestial sphere, the device is capable of determining the orientation of the solar trackers for which the incident irradiance on the collectors would be maximum, which allows optimising their energy capture and, consequently, the energy production of the PV plant.

The device described has been developed as Free and open-source hardware (FOSH), which, together with its publication in Open Access, makes it possible for the scientific and/or technological community to access all the details and therefore be able to analyse, modify or improve its design. Thus, it is presented as a pioneering technology in the sector as it is a solution that is operational but simultaneously open to improvement by the scientific community in the framework of collaborative scientific-technical projects, assuming a revolution in the progress of science and technology.

Furthermore, as a novelty, in this device an ex professo algorithm has been implemented to discriminate at all times those celestial orientations that would imply inter-shading between the collectors of the PV plant. To do this, the device integrates the implementation of tracking and backtracking methodologies characterised and simulated by the authors [39,40] (Fernández-Ahumada et al., 2020b, 2020a) in different photovoltaic plants under irradiance conditions described by empirical models. In this way, the solar trackers do not have to calculate the solar position using astronomical algorithms while taking into account other factors that also affect the incident solar irradiance, such as cloud cover, inter-shading between collectors, etc.

According to the aforementioned, the authors consider that the implementation of this device in photovoltaic plants will make it possible to improve the production of the PV plants while managers will be able to have real information both in terms of collectors and in other alternatives.

Author Contributions: Conceptualization, J.R.-F. and L.M.F.-A.; methodology, M.V.-M.; software, F.J.G.-U. and L.M.F.-A.; validation, F.J.G.-U., J.R.-F. and M.V.-M.; formal analysis, F.J.G.-U., L.M.F.-A. and M.V.M.; investigation, F.J.G.-U. and J.R.-F.; resources, F.J.G.-U. and J.R.-F.; data curation, F.J.G.-U. and M.V.-M.; writing—original draft preparation, F.J.G.-U., L.M.F.-A. and M.V.-M.; writing—review and editing, L.M.F.-A. and M.V.-M.; visualization, J.R.-F.; supervision, J.R.-F. and L.M.F.-A.; project administration, J.R.-F. and L.M.F.-A.; funding acquisition, M.V.-M. All authors have read and agreed to the published version of the manuscript.

Funding: This research is partially supported by the CLARA Project, which has received funding from the European Union's Horizon 2020 research and innovation programme under Grant Agreement No 730482.

Institutional Review Board Statement: Not applicable.

Informed Consent Statement: Not applicable.

Data Availability Statement: Data sharing not applicable.

Acknowledgments: The authors thank Azul y Verde Energía y Sostenibilidad S.L. for their collaboration in this research.

Conflicts of Interest: The authors declare no conflict of interest.

Glossary

a	solar collector width
b	solar collector height
d_j	Julian day
i	index assigned to each solar tracker
j	secondary index assigned to each solar tracker ($i \neq j$)
N	number of solar trackers in the installation
$\vec{i}, \vec{j}, \vec{k}$	unit vectors associated to a local Cartesian system
$\vec{s}$	solar vector
s_x, s_y, s_z	components of solar vector
$\vec{n}$	unit vector perpendicular to the collector surface that indicates the direction towards the tracker is oriented
$\vec{u}$	unit horizontal vector included in the collector plane
$\vec{v}$	unit vector included in the collector plane and perpendicular to $\vec{u}$
t	specific solar hour
x, y, z	Cartesian coordinates of the base of each solar tracker
$x[i], y[i], z[i]$	arrays containing information about coordinates of each solar tracker

Greek Letters

α	elevation angle of the collector
γ	azimuth angle of the collector rotation axis
φ	latitude
Ω	Earth's rotation speed
δ	solar declination
θ	angle of incidence of sunbeams on the inclined plane
Γ	auxiliary angular magnitude dependent on the Julian day

References

1. Carballo, J.A.; Bonilla, J.; Roca, L.; Berenguel, M. New low-cost solar tracking system based on open source hardware for educational purposes. *Sol. Energy* **2018**, *174*, 826–836.
2. Panwar, N.L.; Kaushik, S.C.; Kothari, S. Role of renewable energy sources in environmental protection: A review. *Renew. Sustain. Energy Rev.* **2011**, *15*, 1513–1524.
3. Kannan, N.; Vakeesan, D. Solar energy for future world—A review. *Renew. Sustain. Energy Rev.* **2016**, *62*, 1092–1105.
4. Obara, S.; Matsumura, K.; Aizawa, S.; Kobayashi, H.; Hamada, Y.; Suda, T. Development of a solar tracking system of a nonelectric power source by using a metal hydride actuator. *Sol. Energy* **2017**, *158*, 1016–1025.
5. Caballero, V.; Vernet, D.; Zaballos, A. A Heuristic to Create Prosumer Community Groups in the Social Internet of Energy. *Sensors* **2020**, *20*, 3704.
6. De Castro, C.; Mediavilla, M.; Miguel, L.J.; Frechoso, F. Global solar electric potential: A review of their technical and sustainable limits. *Renew. Sustain. Energy Rev.* **2013**, *28*, 824–835.
7. Jacobson, M.Z.; Delucchi, M.A. Providing all global energy with wind, water, and solar power, Part I: Technologies, energy resources, quantities and areas of infrastructure, and materials. *Energy Policy* **2011**, *39*, 1154–1169.
8. Novas, N.; Alcayde, A.; Robalo, L.; Manzano-Agugliaro, F.; Montoya, F.G. Energies and Its Worldwide Research. *Energies* **2020**, *13*, 6700.
9. Nsengiyumva, W.; Chen, S.G.; Hu, L.; Chen, X. Recent advancements and challenges in Solar Tracking Systems (STS): A review. *Renew. Sustain. Energy Rev.* **2018**, *81*, 250–279.
10. Sumathi, V.; Jayapragash, R.; Bakshi, A.; Kumar Akella, P. Solar tracking methods to maximize PV system output—A review of the methods adopted in recent decade. *Renew. Sustain. Energy Rev.* **2017**, *74*, 130–138.
11. Casares, F.J.; Lopez-Luque, R.; Posadillo, R.; Varo-Martinez, M. Mathematical approach to the characterization of daily energy balance in autonomous photovoltaic solar systems. *Energy* **2014**, *72*, 393–404.
12. D'Adamo, I.; Gastaldi, M.; Morone, P. The post COVID-19 green recovery in practice: Assessing the profitability of a policy proposal on residential photovoltaic plants. *Energy Policy* **2020**, *147*.
13. IRENA. *Renewable Capacity Statistics 2020*; IRENA: Abu Dhabi, UAE, 2020.
14. Eldin, S.S.A.; Abd-Elhady, M.S.; Kandil, H.A. Feasibility of solar tracking systems for PV panels in hot and cold regions. *Renew. Energy* **2016**, *85*, 228–233.

15. Gutierrez, S.; Rodrigo, P.M.; Alvarez, J.; Acero, A.; Montoya, A. Development and Testing of a Single-Axis Photovoltaic Sun Tracker through the Internet of Things. *Energies* **2020**, *13*, 2547.
16. Lee, C.-Y.; Chou, P.-C.; Chiang, C.-M.; Lin, C.-F. Sun Tracking Systems: A Review. *Sensors* 2009, *9*, 3875–3890.
17. Koussa, M.; Cheknane, A.; Hadji, S.; Haddadi, M.; Noureddine, S. Measured and modelled improvement in solar energy yield from flat plate photovoltaic systems utilizing different tracking systems and under a range of environmental conditions. *Appl. Energy* **2011**, *88*, 1756–1771.
18. Maatallah, T.; El Alimi, S.; Nassrallah, S. Ben Performance modeling and investigation of fixed, single and dual-axis tracking photovoltaic panel in Monastir city, Tunisia. *Renew. Sustain. Energy Rev.* **2011**, *15*, 4053–4066.
19. Seme, S.; Štumberger, G.; Voršič, J. Maximum efficiency trajectories of a two-axis sun tracking system determined considering tracking system consumption. *IEEE Trans. Power Electron.* **2011**, *26*, 1280–1290.
20. Huang, B.J.; Ding, W.L.; Huang, Y.C. Long-term field test of solar PV power generation using one-axis 3-position sun tracker. *Sol. Energy* **2011**, *85*, 1935–1944.
21. Ismail, M.S.; Moghavvemi, M.; Mahlia, T.M.I. Design of an optimized photovoltaic and microturbine hybrid power system for a remote small community: Case study of Palestine. *Energy Convers. Manag.* **2013**, *75*, 271–281.
22. Narendrasinh Parmar, A.J.; Parmar, A.N.; Gautam, V.S. Passive Solar Tracking System. *Int. J. Emerg. Technol. Adv. Eng.* **2008**, *5*, 138–142.
23. Mousazadeh, H.; Keyhani, A.; Javadi, A.; Mobli, H.; Abrinia, K.; Sharifi, A. A review of principle and sun-tracking methods for maximizing solar systems output. *Renew. Sustain. Energy Rev.* **2009**, *13*, 1800–1818.
24. Quesada, G.; Guillon, L.; Rousse, D.R.; Mehrtash, M.; Dutil, Y.; Paradis, P.-L. Tracking strategy for photovoltaic solar systems in high latitudes. *Energy Convers. Manag.* **2015**, *103*, 147–156.
25. Huld, T.; Cebecauer, T.; Súri, M.; Dunlop, E.D. Analysis of one-axis tracking strategies for PV systems in Europe. *Prog. Photovolt. Res. Appl.* **2010**, *18*, 183–194.
26. Lorenzo, E.; Pérez, M.; Ezpeleta, A.; Acedo, J. Design of tracking photovoltaic systems with a single vertical axis. *Prog. Photovolt. Res. Appl.* **2002**, *10*, 533–543.
27. Perpiñan, O.; Lorenzo, E.; Castro, M.A.; Eyras, R. Energy payback time of grid connected PV systems: Comparison between tracking and fixed systems. *Prog. Photovolt. Res. Appl.* **2009**, *17*, 137–147.
28. Vaziri Rad, M.A.; Toopshekan, A.; Rahdan, P.; Kasaeian, A.; Mahian, O. A comprehensive study of techno-economic and environmental features of different solar tracking systems for residential photovoltaic installations. *Renew. Sustain. Energy Rev.* **2020**, *129*, 109923.
29. Braun, J.E.; Mitchell, J.C. Solar geometry for fixed and tracking surfaces. *Sol. Energy* **1983**, *31*, 439–444.
30. Duffie, J.A.; Beckman, W.A. *Solar Engineering of Thermal Processes*, 4th ed.; John Wiley and Sons: Hoboken, NJ, USA, 2013; ISBN 9780470873663.
31. Meinel, A.B.; Meinel, M.P. *Applied Solar Energy*; Addison-Wesley Pub. Co.: Boston, MA, USA, 1979.
32. Narvarte, L.; Lorenzo, E. Tracking and ground cover ratio. *Prog. Photovolt. Res. Appl.* **2008**, *16*, 703–714.
33. Neville, R.C. Solar energy collector orientation and tracking mode. *Sol. Energy* **1978**, *20*, 7–11.
34. Riley, D.; Hansen, C. Sun-Relative Pointing for Dual-Axis Solar Trackers Employing Azimuth and Elevation Rotations. *J. Sol. Energy Eng.* **2015**, doi:10.1115/1.4029379.
35. Blanco-Muriel, M.; Alarcón-Padilla, D.C.; López-Moratalla, T.; Lara-Coira, M. Computing the solar vector. *Sol. Energy* **2001**, *70*, 431–441.
36. Grena, R. An algorithm for the computation of the solar position. *Sol. Energy* **2008**, *82*, 462–470.
37. Reda, I.; Andreas, A. Solar position algorithm for solar radiation applications. *Sol. Energy* **2004**, *76*, 577–589.
38. Chong, K.K.; Wong, C.W. General formula for on-axis sun-tracking system and its application in improving tracking accuracy of solar collector. *Sol. Energy* **2009**, *83*, 298–305.
39. Fernández-Ahumada, L.M.; Ramírez-Faz, J.; López-Luque, R.; Varo-Martínez, M.; Moreno-García, I.M.; Casares de la Torre, F. Influence of the design variables of photovoltaic plants with two-axis solar tracking on the optimization of the tracking and backtracking trajectory. *Sol. Energy* **2020**, *208*, 89–100.
40. Fernández-Ahumada, L.M.; Ramírez-Faz, J.; López-Luque, R.; Varo-Martínez, M.; Moreno-García, I.M.; Casares de la Torre, F. A novel backtracking approach for two-axis solar PV tracking plants. *Renew. Energy* **2020**, *145*, 1214–1221.
41. Fernández-Ahumada, L.M.; Casares, F.J.; Ramírez-Faz, J.; López-Luque, R. Mathematical study of the movement of solar tracking systems based on rational models. *Sol. Energy* **2017**, *150*, 20–29.
42. Jolly, P.G. Derivation of solar angles using vector algebra. *Sol. Energy* **1986**, *37*, 429–430.
43. Parkin, R.E. Solar angles revisited using a general vector approach. *Sol. Energy* **2010**, *84*, 912–916.
44. Rapp-Arrarás, Í.; Domingo-Santos, J.M. Algorithm for the calculation of the horizontal coordinates of the Sun via spatial rotation matrices. *Renew. Energy* **2009**, *34*, 876–882.
45. Sproul, A.B. Derivation of the solar geometric relationships using vector analysis. *Renew. Energy* **2007**, *32*, 1187–1205.
46. Torres-Roldán, M.; López-Luque, R.; Varo-Martínez, M. Design of an innovative and simplified polar heliostat for integration in buildings and urban environments. *Sol. Energy* **2015**, *119*, 159–168.
47. Lorenzo, E.; Narvarte, L.; Muñoz, J. Tracking and back-tracking. *Prog. Photovolt. Res. Appl.* **2011**, *19*, 747–753.
48. Kelly, N.A.; Gibson, T.L. Improved photovoltaic energy output for cloudy conditions with a solar tracking system. *Sol. Energy* **2009**, *83*, 2092–2102.

49. Salgado-Conrado, L. A review on sun position sensors used in solar applications. *Renew. Sustain. Energy Rev.* **2018**, *82*, 2128–2146.
50. Yao, Y.; Hu, Y.; Gao, S.; Yang, G.; Du, J. A multipurpose dual-axis solar tracker with two tracking strategies. *Renew. Energy* **2014**, *72*, 88–98.
51. Singh, R.; Kumar, S.; Gehlot, A.; Pachauri, R. An imperative role of sun trackers in photovoltaic technology: A review. *Renew. Sustain. Energy Rev.* **2018**, *82*, 3263–3278.
52. Fuentes, M.; Vivar, M.; Burgos, J.M.; Aguilera, J.; Vacas, J.A. Design of an accurate, low-cost autonomous data logger for PV system monitoring using Arduino™ that complies with IEC standards. *Sol. Energy Mater. Sol. Cells* **2014**, *130*, 529–543.
53. Pearce, J.M. *Open-Source Lab*; Elsevier: Amsterdam, The Netherlands, 2014; ISBN 9780124104624.
54. García-Valverde, R.; Chaouki-Almagro, S.; Corazza, M.; Espinosa, N.; Hösel, M.; Søndergaard, R.R.; Jørgensen, M.; Villarejo, J.A.; Krebs, F.C. Portable and wireless IV-curve tracer for >5 kV organic photovoltaic modules. *Sol. Energy Mater. Sol. Cells* **2016**, *151*, 60–65.
55. Gad, H.E.; Gad, H.E. Development of a new temperature data acquisition system for solar energy applications. *Renew. Energy* **2015**, *74*, 337–343.
56. Rus-Casas, C.; Hontoria, L.; Fernández-Carrasco, J.I.; Jiménez-Castillo, G.; Muñoz-Rodríguez, F. Development of a utility model for the measurement of global radiation in photovoltaic applications in the internet of things (IoT). *Electronics* **2019**, *8*, 304.
57. Paredes-Parra, J.M.; García-Sánchez, A.J.; Mateo-Aroca, A.; Molina-García, Á. An alternative internet-of-things solution based on LOra for PV power plants: Data monitoring and management. *Energies* **2019**, *12*, 881.
58. Pereira, R.I.S.; Dupont, I.M.; Carvalho, P.C.M.; Jucá, S.C.S. IoT embedded linux system based on Raspberry Pi applied to real-time cloud monitoring of a decentralized photovoltaic plant. *Meas. J. Int. Meas. Confed.* **2018**, *114*, 286–297.
59. Batista, N.C.; Melício, R.; Mendes, V.M.F. Layered Smart Grid architecture approach and field tests by ZigBee technology. *Energy Convers. Manag.* **2014**, *88*, 49–59.
60. Coelho, V.N.; Weiss Cohen, M.; Coelho, I.M.; Liu, N.; Guimarães, F.G. Multi-agent systems applied for energy systems integration: State-of-the-art applications and trends in microgrids. *Appl. Energy* **2017**, *187*, 820–832.
61. Sinha, R.S.; Wei, Y.; Hwang, S.H. A survey on LPWA technology: LoRa and NB-IoT. *ICT Express* **2017**, *3*, 14–21.
62. Augustin, A.; Yi, J.; Clausen, T.; Townsley, W.M. A study of Lora: Long range & low power networks for the internet of things. *Sensors* **2016**, *16*, 1466.
63. Ramírez-Faz, J.; López-Luque, R. Development of a methodology for quantifying insolation variables in windows and building openings. *Renew. Energy* **2012**, *37*, 426–433.
64. Panico, D.; Garvison, P.; Wenger, H.; Shugar, D. Backtracking: A novel strategy for tracking PV systems. In Proceedings of the The Conference Record of the Twenty-Second IEEE Photovoltaic Specialists Conference, Las Vegas, NV, USA, 7–11 October 1991; pp. 668–673.
65. Schneider, D. Control Algorithms for Large-scale Single-axis Photovoltaic Trackers. *Acta Polytech.* **2012**, *52*, 86–92.
66. PVsyst SA PVsyst. Photovoltaic Software. Available online: https://www.pvsyst.com/help/near_shadings_backtracking.htm (accessed on 14 January 2021).
67. Array Tecnhologies Backtracking and Diffuse Light Strategies with SmarTrack from Array Technologies. Available online: https://arraytechinc.com/smartrack-backtracking/ (accessed on 14 January 2021).
68. Nextracker TM TrueCapture Smart Control System in Action—Nextracker. Available online: https://www.nextracker.com/2019/05/truecapture-smart-control-system-in-action/ (accessed on 14 January 2021).
69. STI Norland Dual-Row Single-Axis Tracker-STI H250. Available online: https://www.stinorland.com/sites/default/files/sti-h250-dual_row-data_sheet.pdf (accessed on 14 January 2021).

Anexo III

Tercer artículo del compendio: “Estudio de la dependencia de la radiación solar con respecto a las variables de diseño en instalaciones solares fotovoltaicas con seguimiento óptimo de doble eje”.

Publicado en la revista Applied Sciences.

Enviado el 18 de marzo de 2021, aceptado el 23 de abril de 2021.

Factor de impacto en 2019: 2,474.

applied sciences

MDPI

Article

Study of the Dependence of Solar Radiation Regarding Design Variables in Photovoltaic Solar Installations with Optimal Dual-Axis Tracking

Francisco Javier Gómez-Uceda [1], Isabel Maria Moreno-Garcia [2,*], Álvaro Perez-Castañeda [3] and Luis Manuel Fernández-Ahumada [4]

1 Department of Mechanics Engineering, Universidad de Córdoba, 14071 Cordoba, Spain; fjgomez@uco.es
2 Department of Electronic and Computer Engineering, Universidad de Córdoba, 14071 Cordoba, Spain
3 Physics for Renewable Energies Research Group, Universidad de Córdoba, 14071 Cordoba, Spain; perezcastanedaalvaro@gmail.com
4 Department of Electrical Engineering and Automatics, Universidad de Córdoba, 14071 Cordoba, Spain; lmfernandez@uco.es
* Correspondence: isabel.moreno@uco.es; Tel.: +34-9572-12533

Abstract: Solar tracking is an efficient strategy to increase the radiative capture of photovoltaic collectors. Within the multiple efforts made in recent decades to improve the production of these facilities, various works have studied solutions to optimize the number of rotation axes (single or dual rotation axes), the degree of collector coverage, the distances between trackers, the geometric arrangement of trackers or the minimization of shading between collectors. However, although in this type of installation it is common to find collectors with geometric shapes other than rectangles, no studies on the influence of the shape of the collectors on the radiative incidence are found in the literature. In this connection, the present work systematically addresses the study of incident solar radiation in photovoltaic installations with dual-axis trackers with collectors of different geometric shapes. By means of the exhaustive study, the conclusion is drawn that, for dual-axis photovoltaic installations with an optimal tracking strategy, the main variables that influence the annual radiative incidence are the spacing between collectors, the coverage ratio (GCR), and the collector surface, while the type of arrangement of collectors and the shape of these do not show predictive values.

Keywords: photovoltaics; dual-axis solar trackers; shading in PV plants; solar tracking; backtracking

Citation: Gómez-Uceda, F.J.; Moreno-Garcia, I.M.; Perez-Castañeda, Á.; Fernández-Ahumada, L.M. Study of the Dependence of Solar Radiation Regarding Design Variables in Photovoltaic Solar Installations with Optimal Dual-Axis Tracking. *Appl. Sci.* **2021**, *11*, 3917. https://doi.org/10.3390/app11093917

Academic Editors: Giovanni Petrone and Richard Yong Qing Fu

Received: 18 March 2021
Accepted: 23 April 2021
Published: 26 April 2021

1. Introduction

There is no doubt about the important role that energy plays in our societies. Its implications go beyond mere technical aspects. Social structuring, economic development, and the environment, among others, are aspects that make up the complex implication of energy in the global agenda [1]. In this context, renewable energies have been experiencing sustained growth in recent years. Thus, the International Energy Agency (IEA) foresees a record increase of 218 GW in the year 2021 in the net capacity of renewable electricity installed in the world, in an average scenario, that could reach up to 266 GW, in an accelerated scenario [2]. In fact, during the first quarter of 2020, renewable energies were the only source of electricity whose demand increased despite the 2.5% decrease in global electricity demand caused by the blockades implemented by different governments to curb the spread of COVID-19 [3].

Within the field of renewables, solar energy, in general, and photovoltaic (PV), in particular, are candidates to satisfy a large part of the global energy demand in the coming years due to their abundance and competitiveness [4]. In fact, in the IEA predictions for the year 2021, solar PV accounts for 54% of the growth in the world's installed net renewable electricity capacity [2]. The remarkable progress that the technology associated with the

implementation of photovoltaic energy has been experiencing has not only driven its boom in recent years [5,6] but this growth is expected to accelerate during the 2023–25 period [2].

One of the fundamental factors in the energy production of PV plants is the incident solar irradiance on the collectors. Among the various strategies that exist to increase this irradiance in solar collectors and, therefore, energy production in PV plants, is solar tracking, which is a technological niche in which there are still possible improvements that can contribute to such an increase [5]. This strategy is in contrast with fixed panel structures that have a constant orientation towards the sun depending on the latitude of the place where the PV installation is located. Thus, in the case of solar trackers, the PV modules move while looking for an orientation that generates more energy, either by capturing solar energy for as long as possible [7] or by capturing maximum solar irradiance [8,9].

The most common classification of trackers is established based on the number of axes used to move the modules. Thus, we speak of tracking systems on one axis (movement in azimuth or elevation) or on two axes (movement in azimuth and elevation). Improving the technology of solar tracking systems is an important objective considering the high demand of energy resources, being the research niche for many authors. For example, in [7], different tracker motion control systems are studied with regard to their economic evaluation. In [8], the different solar trackers are studied in depth, performing a comparison between them in terms of efficiency, performance, advantages, and disadvantages, while other studies perform an in-depth review of the related literature to define the advantages of the applicability of solar tracking [10,11].

In the scientific literature, there are studies that question the use of trackers with one or two axes versus fixed systems or one axis versus two. Specifically, various studies are being developed that question the various possibilities that arise in terms of efficiency, cost, location, production, etc., which is a real scientific challenge. For example, in [12–14], authors analyze the effect of different solar trackers strategies considering the location. Other authors provide profits of the tracking photovoltaic systems in comparison with fixed photovoltaic systems [15,16]. An interesting result is the one presented in [17], where a method for optimal storage capacity was calculated under the power-curtailment and storage/discharge requirements. Hence, although solar tracking systems have a higher cost than fixed systems, their maintenance is more complex and their exposure to environmental conditions is greater [18]; the performance of dual-axis trackers are greater than those of fixed systems [19,20] and single-axis trackers [21–23]. Bahrami states in [21] that a dual-axis tracking system would result in greater irradiance than a single-axis due to its ability to minimize losses associated with cosine effect. Authors in [22] highlight their conclusion that using the two-axis sun tracker system enables the PV panel to collect and produce higher amounts of electrical energy than using single-axis and fixed structures; their study considered five configurations of sun tracking systems and two traditional fixed panels. The results presented in [23] show that the optimal trajectories for the tilt and azimuth angle depend on the available solar radiation, solar cell efficiency, tracking system consumption, and the optimization bounds. Therefore, based on these studies, it can be affirmed that the choice of the type of strategy depends on several factors, it being necessary to delve into the technological and economic components to reach useful conclusions [5].

Regarding the tracking mechanism, different driver methods can be distinguished to achieve the objectives of the collector movement [8]. Among them, the sensor driver systems stand out, whose operation is based on the variation of light received by optical sensors that cause the movement of the collectors looking for the position of the sun. Additionally, there are microprocessor driver systems that incorporate small processors with movement strategies programmed through mathematical models to locate the position of the sun. Within these in the bibliography are the open-loop driver systems that modify the movement of the actuators of the modules from mathematical equations that fix the position of the sun from the day and the hour. In contrast, closed-loop driver systems modify the movement of the actuators based on the information provided by position

sensors, recalculating the position of the sun. Finally, intelligent driver systems incorporate artificial intelligence techniques to control the movement of collectors [24].

Another of the determining factors in the performance of a PV plant is the shading of its modules, since these shadows not only imply a lower incident irradiance [25] but also give rise to the appearance of hot spots that bring with them overheating and losses in energy production [26]. In this regard, the behavior of PV modules when they are partially shaded has been widely debated. Several simulation models have been used to find a configuration less susceptible to shadow problems of solar cells [27–30]. Specifically, Díaz-Dorado et al. [31] have analyzed the effect of shading in a PV tracker with partially shaded astronomical tracking based on the exact arrangement of shaded cells and modules. Other authors have analyzed the energy cost in the production of PV plants as a function of the connections between the cells and the modules [32] of the ground cover ratio (GCR) of the plant that depends on the variables of their design [33] or of the tracking strategy [26,34].

One possible solution to alleviate the effect of shadows in PV plants with solar tracking is back tracking [35], which consists of modifying the orientation of the collecting surfaces in shading situations between panels in order to eliminate such shadows. Another possible solution is to modify the geometry of the collecting surfaces. Thus, although most of the PV panels found in PV plants connected to grids are rectangular, there are already some installations with dual-axis solar tracking where the collectors have other geometric shapes, such as those developed by the Deger Ibérica company in Tarragona (Spain), Ontario (Canada), or Estonia, with 15.6 kWp, 24 MWp, and 100 kWp installed, respectively [36]. However, no previous works have been found in the literature aimed at characterizing the geometric shape of the collectors or their degree of modularity in terms of optimizing the performance of a photovoltaic installation in the event of the possible incidence of shading.

In this context, in the present work, the annual radiative uptake has been quantified in a wide set of PV installations with dual-axis monitoring with different geometries in which the shape of the collectors and the design parameters have been systematically varied. For each case, it has been assumed that the collectors follow the optimal solar tracking strategy proposed by Fernández-Ahumada et al. [37,38]. Unlike traditional solar tracking methods that search for the position of the sun at each moment using astronomical models [39–41], according to this strategy, the collecting planes are oriented at each instant of time towards the direction of space in which the irradiance is maximum, except during the moments when such orientation implies the shading of one collector over another. When this occurs, normally at the beginning and end of the day, the collectors are oriented in the direction in which, without causing shading, the incident irradiance on the collectors is maximum. In this way, the production of each installation, which is considered proportional to annual solar radiation, is calculated under the hypothesis that each installation will follow an optimal tracking strategy adapted to its own geometry. Therefore, this study aims to advance the characterization of the electrical behavior of shaded solar trackers, which is an issue where the scientific community has made a considerable effort, simulating tracking strategies for an improvement in photovoltaic production [12,14,42].

To achieve this objective, after this introduction in which the scientific advances made by the scientific community in the field of solar tracking in PV plants are presented, the following section describes the methodology followed in this study to simulate annual solar radiation incident on collectors with a dual-axis tracking strategy that optimizes radiative uptake while avoiding shading between collectors. Similarly, the methodology established for the study of the influence of the design parameters of a PV plant on this annual solar irradiance is explained. Based on this, Section 3 presents the results when applying the methodology described to an existing PV plant ("El Molino", Córdoba, Spain) with its design parameters systematically modified. Similarly, an adjustment model is proposed that represents in a simplified manner the dependence of the annual solar irradiance with respect to the design variables studied, and these dependencies are quantified. Finally, in Section 4, the main conclusions of the present study are presented.

2. Methodology

2.1. Vector Treatment of the Solar Position and the Estimation of the Solar Irradiance in the Celestial Sphere

In accordance with the above, this work presents a study of the influence of design variables on the performance of a PV plant with dual-axis tracking and optimal tracking strategy. This tracking strategy, which is described in the following section, will determine the orientation of the solar collectors at all times, which allows for optimizing radiative capture while avoiding shadows between collectors. In the present work, to determine at each instant of time the orientation of these collectors, as well as the position of the Sun in the celestial sphere, vector notation is used.

Figure 1 shows the coordinate system used, with the Ox axis oriented towards the west, the Oy axis towards the south, and the Oz axis towards the zenith. In this equation, $\vec{i}$, $\vec{j}$, and $\vec{k}$ are the unit vectors on the axes Ox, Oy, and Oz, respectively; the unit vector that points towards the Sun, called the solar vector, $\vec{s}$, will be expressed by Equation (1), in which φ is the latitude of the place, δ the declination, and t the solar hour.

$$\vec{s} = s_x\vec{i} + s_y\vec{j} + s_z\vec{k} = \sin\Omega t\cos\delta\,\vec{i} + (\cos\Omega t\cos\delta\sin\varphi - \sin\delta\cos\varphi)\,\vec{j} + (\cos\Omega t\cos\delta\cos\varphi + \sin\delta\sin\varphi)\,\vec{k} \quad (1)$$

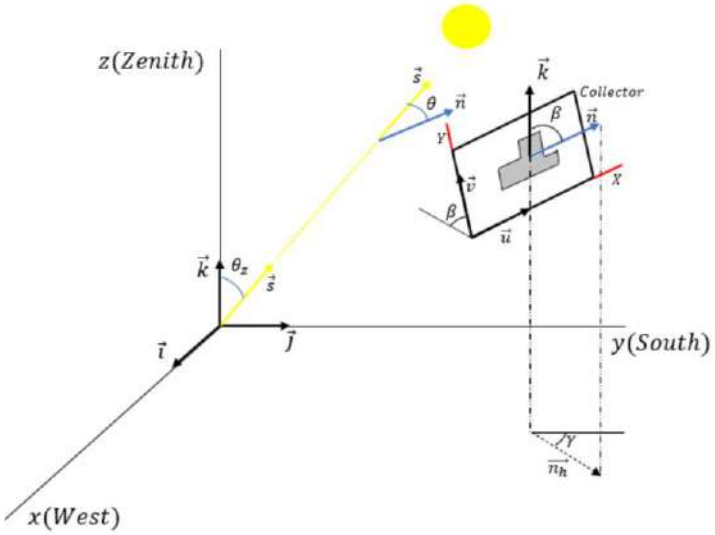

Figure 1. Astronomical and geometric magnitudes considered.

Equation (2) shows the mathematical expression proposed by Spencer (1971) for calculating the declination, δ, as a function of the daily angle, Γ, which in turn depends on the Julian day, d_n, according to Equation (3).

$$\delta(rad) = 0.006918 - 0.399912\cos(\Gamma) + 0.070257\sin(\Gamma) - 0.006758\cos(2\Gamma) + 0.000907\sin(2\Gamma) - 0.002697\cos(3\Gamma) + 0.00148\sin(3\Gamma) \quad (2)$$

$$\Gamma(rad) = \frac{2\pi(d_n - 1)}{365} \quad (3)$$

The orientation of the collector plane at each instant of time can be represented by the unit vector perpendicular to it, $\vec{n}$, or by the pair of unit vectors, $\vec{u}$ and $\vec{v}$, contained

in the collector plane, of which $\vec{u}$ is horizontal and $\vec{v}$ is parallel to the maximum slope direction of the collector plane (Figure 1). Thus, γ and β being the angles representing the azimuth and inclination of the collectors, respectively, the vectors $\vec{n}$, $\vec{u}$, and $\vec{v}$ will be given by Equations (4)–(6), respectively.

$$\vec{n} = \sin\beta \sin\gamma \vec{i} + \sin\beta\cos\gamma \vec{j} + \cos\beta \vec{k} \quad (4)$$

$$\vec{u} = -\cos\gamma \vec{i} + \sin\gamma \vec{j} \quad (5)$$

$$\vec{v} = -\cos\beta \sin\gamma \vec{i} - \cos\beta\cos\gamma \vec{j} + \sin\beta \vec{k} \quad (6)$$

For the characterization of the incident solar irradiance on the collector planes, the model of Perez et al. [43] has been used. According to this model, the global solar irradiance, I, on an inclined plane at an angle β is the sum of the direct, diffuse, and reflected irradiance on an inclined plane, which, in turn, depends on the direct irradiance, I_B, and diffuse, I_D, on a horizontal surface, according to Equation (7), where θ is the angle between the normal vector and the collector plane $\left(\vec{n}\right)$ and the solar vector $\left(\vec{s}\right)$, θ_z is the zenith angle, ρ is the albedo of the surface of incidence of the irradiance before being reflected towards the collector, a and b are parameters given by Equations (8) and (9), and F_1 and F_2 are the weighting factors for the decomposition of the inclined diffuse radiation, the second addition, in the three subcomponents considered by the authors: isotropic diffuse, circumsolar diffuse, and diffuse from the horizon (Perez et al., 1990).

$$I = \frac{\cos\theta}{\cos\theta_z} I_B + \left[(1-F_1)\frac{1+\cos\beta}{2} + F_1\frac{a}{b} + F_2\sin\beta\right] I_D + \rho\frac{1-\cos\beta}{2}(I_B + I_D) \quad (7)$$

$$a = \max(\cos\theta,\ 0) \quad (8)$$

$$b = \max(\cos 85^\circ, \cos\theta_z) \quad (9)$$

Substituting the vector expressions (10)–(12) in Equation (7), we obtain Equation (13), in which the dependence of I on $\vec{n}$ is made explicit,

$$\cos\beta = \vec{k}\cdot\vec{n} \quad (10)$$

$$\cos\theta = \vec{s}\cdot\vec{n} \quad (11)$$

$$\cos\theta_z = \vec{s}\cdot\vec{k} \quad (12)$$

$$I = \frac{\vec{s}\cdot\vec{n}}{\vec{s}\cdot\vec{k}} I_B + \left[(1-F_1)\frac{1+\vec{k}\cdot\vec{n}}{2} + F_1\frac{\vec{s}\cdot\vec{n}}{b} + F_2\sqrt{1-\left(\vec{k}\cdot\vec{n}\right)^2}\right] I_D + \rho\frac{1-\vec{k}\cdot\vec{n}}{2}(I_B + I_D) \quad (13)$$

The production of a PV plant will be greater to the extent that the incident irradiance on its collectors is greater. In this regard, Fernández-Ahumada et al. [37] showed that the incident irradiance on the collectors is maximum when they are oriented in such a way that their normal vector verifies Equation (14). In accordance with this result, the authors propose a new tracking strategy for PV plants with dual-axis trackers in which they are oriented according to Equation (14), and consequently, radio capture and energy production are optimized.

$$\vec{n} = \frac{\frac{\partial I}{\partial\left(\vec{s}\cdot\vec{n}\right)}\vec{s} + \frac{\partial I}{\partial\left(\vec{k}\cdot\vec{n}\right)}\vec{k}}{\sqrt{\left(\frac{\partial I}{\partial\left(\vec{s}\cdot\vec{n}\right)}\right)^2 + \left(\frac{\partial I}{\partial\left(\vec{k}\cdot\vec{n}\right)}\right)^2 + 2\left(\frac{\partial I}{\partial\left(\vec{s}\cdot\vec{n}\right)}\right)\left(\frac{\partial I}{\partial\left(\vec{k}\cdot\vec{n}\right)}\right)\vec{s}\cdot\vec{k}}} \quad (14)$$

Therefore, when applying this tracking strategy to the model of Perez et al. (1990), the partial derivatives given by expressions (15) and (16) are obtained. Substituting these results in Equation (14), Equation (17) is obtained, which represents the direction of the normal vector to the collecting planes corresponding to the optimal tracking strategy proposed by Fernández-Ahumada et al. [37] for PV plants with dual-axis tracking.

$$\vec{n} = \frac{\frac{\partial I}{\partial\left(\vec{s}\cdot\vec{n}\right)}\vec{s} + \frac{\partial I}{\partial\left(\vec{k}\cdot\vec{n}\right)}\vec{k}}{\sqrt{\left(\frac{\partial I}{\partial\left(\vec{s}\cdot\vec{n}\right)}\right)^2 + \left(\frac{\partial I}{\partial\left(\vec{k}\cdot\vec{n}\right)}\right)^2 + 2\left(\frac{\partial I}{\partial\left(\vec{s}\cdot\vec{n}\right)}\right)\left(\frac{\partial I}{\partial\left(\vec{k}\cdot\vec{n}\right)}\right)\vec{s}\cdot\vec{k}}} \quad (15)$$

$$\frac{\partial I}{\partial\left(\vec{k}\cdot\vec{n}\right)} = \left(\frac{(1-F_1)}{2} - F_2\frac{\vec{k}\cdot\vec{n}}{\sqrt{1-\left(\vec{k}\cdot\vec{n}\right)^2}}\right)I_D - \rho\frac{(I_B+I_D)}{2} \quad (16)$$

$$\vec{n}_j = \frac{\left(\frac{I_B}{\vec{s}\cdot\vec{k}}+F_1\frac{I_D}{b}\right)\vec{s} + \left(\frac{(1-F_1)\,I_D}{2} - F_2\frac{\vec{k}\cdot\vec{n}}{\sqrt{1-\left(\vec{k}\cdot\vec{n}\right)^2}}I_D - \rho\frac{(I_B+I_D)}{2}\right)\vec{k}}{\sqrt{\left(\frac{I_B}{\vec{s}\cdot\vec{k}}+F_1\frac{I_D}{b}\right)^2 + \left(\frac{(1-F_1)\,I_D}{2} - F_2\frac{\vec{k}\cdot\vec{n}}{\sqrt{1-\left(\vec{k}\cdot\vec{n}\right)^2}}I_D - \rho\frac{(I_B+I_D)}{2}\right)^2 + 2\left(\frac{I_B}{\vec{s}\cdot\vec{k}}+F_1\frac{I_D}{b}\right)\left(\frac{(1-F_1)\,I_D}{2} - F_2\frac{\vec{k}\cdot\vec{n}}{\sqrt{1-\left(\vec{k}\cdot\vec{n}\right)^2}}I_D - \rho\frac{(I_B+I_D)}{2}\right)\vec{s}\cdot\vec{k}}} \quad (17)$$

Given the difficulty of solving the variable $\vec{n}$ in Equation (17), an iterative method based on the series convergence of vectors $\left\{\vec{n}_0\left(=\vec{s}\right), \vec{n}_1, \vec{n}_2, \ldots, \vec{n}_j\right\}$ is proposed, in which each vector $\vec{n}_j$ is obtained as a function of $\vec{n}_{j-1}$ according to Equation (18), and consequently, $\vec{n}$ will be given by Equation (19). Given the nature of the problem, in this work, it has been considered that $j = 25$ is a sufficiently high value since the correct convergence of this value has been verified for all the practical cases studied.

$$\vec{n}_j = \frac{\left(\frac{I_B}{\vec{s}\cdot\vec{k}}+F_1\frac{I_D}{b}\right)\vec{s} + \left(\frac{(1-F_1)\,I_D}{2} - F_2\frac{\vec{k}\cdot\vec{n}_{j-1}}{\sqrt{1-\left(\vec{k}\cdot\vec{n}_{j-1}\right)^2}}I_D - \rho\frac{(I_B+I_D)}{2}\right)\vec{k}}{\sqrt{\left(\frac{I_B}{\vec{s}\cdot\vec{k}}+F_1\frac{I_D}{b}\right)^2 + \left(\frac{(1-F_1)\,I_D}{2} - F_2\frac{\vec{k}\cdot\vec{n}}{\sqrt{1-\left(\vec{k}\cdot\vec{n}\right)^2}}I_D - \rho\frac{(I_B+I_D)}{2}\right)^2 + 2\left(\frac{I_B}{\vec{s}\cdot\vec{k}}+F_1\frac{I_D}{b}\right)\left(\frac{(1-F_1)\,I_D}{2} - F_2\frac{\vec{k}\cdot\vec{n}}{\sqrt{1-\left(\vec{k}\cdot\vec{n}\right)^2}}I_D - \rho\frac{(I_B+I_D)}{2}\right)\vec{s}\cdot\vec{k}}} \quad (18)$$

$$\vec{n} = \lim_{j\to\infty}\vec{n}_j \quad (19)$$

2.2. Method to Avoid Inter-Shading of Collectors

According to the studies found in the bibliographic review, the shading of solar panels negatively affects their energy production. Therefore, to optimize the performance of a PV plant with dual-axis solar trackers, as those discussed in this study, it is necessary to accompany an adequate tracking strategy with a procedure that prevents the collectors from shading each other.

In this regard, Fernández-Ahumada et al. [38] presented a dichotomous criterion to quickly determine whether or not there is inter-shading between collectors. The method is based on the fact that, in an installation with collectors of the same geometric shape oriented towards the same direction of the celestial sphere (characterized by its normal vector, $\vec{n}$), the shadow cast by a collector Π_i on the plane ψ that contains the reference collector Π_0 is a polygon Π'_i with the same shape as the contour of the collector (Figure 2).

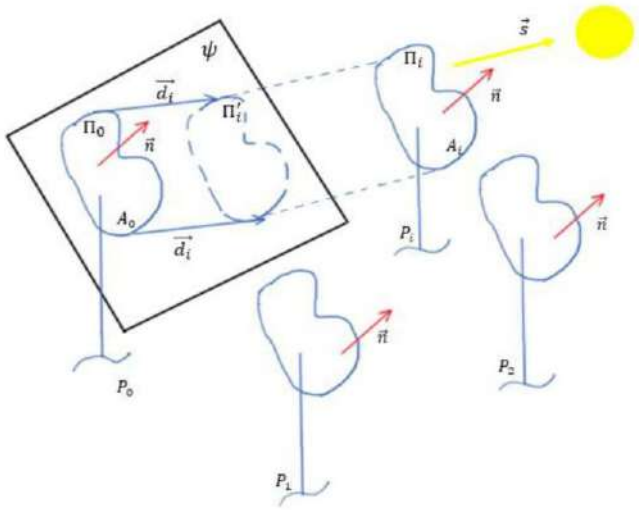

Figure 2. Astronomical and geometric magnitudes considered.

Hence, vector $\vec{d}_i$ is the geometric displacement vector from polygon Π_0 to Π'_i. This vector, as shown by the authors, is obtained through the Equation (20), although it must be considered that, for the collector Π_i to be able to shade the collector Π_0, the conditions expressed in Equations (21)–(23) must be fulfilled.

$$\vec{d_i} = \vec{P_o P_i} - \frac{\vec{P_o P_i} \cdot \vec{n}}{\vec{s} \cdot \vec{n}} \vec{s} \tag{20}$$

$$\vec{s} \cdot \vec{k} > 0 \tag{21}$$

$$\vec{s} \cdot \vec{n} > 0 \tag{22}$$

$$\vec{P_0 P_i} \cdot \vec{n} > 0 \tag{23}$$

From expression (20), given that $\vec{d}_i$ is a vector included in the collector plane ψ, Equations (24) and (25) allow for determination of the components of this vector in the OXY reference system contained in the plane ψ and defined by the vectors $\vec{u}$ y $\vec{v}$.

$$d_{Xi} = \vec{d}_i \cdot \vec{u} \tag{24}$$

$$d_{Yi} = \vec{d}_i \cdot \vec{v} \tag{25}$$

Knowing $\vec{d}_i$ and its components d_{Xi} and d_{Yi}, the dichotomous criterion proposed by Fernández-Ahumada et al. [38], based on Minkowski's algebra [44–46] and whose validity is demonstrated in Appendix A, it is established that there will be an intersection of the polygons Π_0 and Π'_i. Therefore, mutual shading between the panels Π_0 y Π_i, if, when representing vector $\vec{d}_i$ from the origin of coordinates, the end of the vector is included within the plane curve Σ, which is obtained as the envelope of the family of all polygons that can be drawn on the plane ψ by translating the polygon Π_0 with the condition that its perimeter is in contact with the coordinate origin of the reference system contained in ψ (Figure 3).

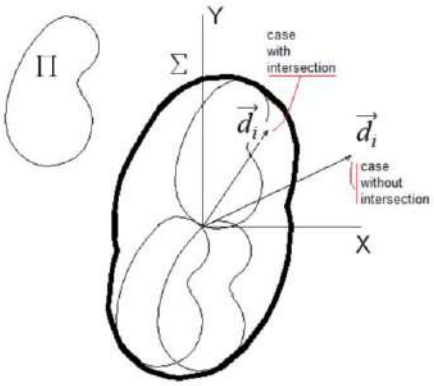

Figure 3. Determination of Σ, auxiliary curve of the intersection criterion and existence of shadow between panels.

It is important to note that, since photovoltaic collectors are built by annexing rectangular photovoltaic modules, the resulting geometric shape for the collector is, in general, a closed polygon in which all sides of the perimeter are contained in two directions perpendicular to each other, as shown by the orange line in Figure 4. This fact leads to the determination of the envelope Σ being simplified and able to be performed analytically. Furthermore, this envelope (blue trace in Figure 4) will also be a closed polygon with the sides parallel and perpendicular to the directions of the perimeter of the collectors (Figure 4). Therefore, the envelope is mathematically described by the coordinates $X_{env}(k)$ and $Y_{env}(k)$ of each vertex k of the polygon ($1 < k < N_{env}$, N_{env} being the total number of vertices of Σ). In Appendix B, the analytical obtaining of the enclosure for photovoltaic collectors is detailed in a generic way.

According to Figure 4, the end of vector $\vec{d}_i$ would be located inside the envelope Σ and, therefore, there would be shading between the panels Π_0 y Π_i if there is some vertex k for which the mathematical condition given by Equation (26) is fulfilled.

$$\begin{gathered}[sign(d_{Xi}) = sign\ (X_{env}(k))]\ and [sign(d_{Yi}) = sign\ (Y_{env}(k))] and \\ [|d_{Xi}| < |X_{env}(k)|]\ and\ [|d_{Yi}| < |Y_{env}(k)|]\end{gathered} \tag{26}$$

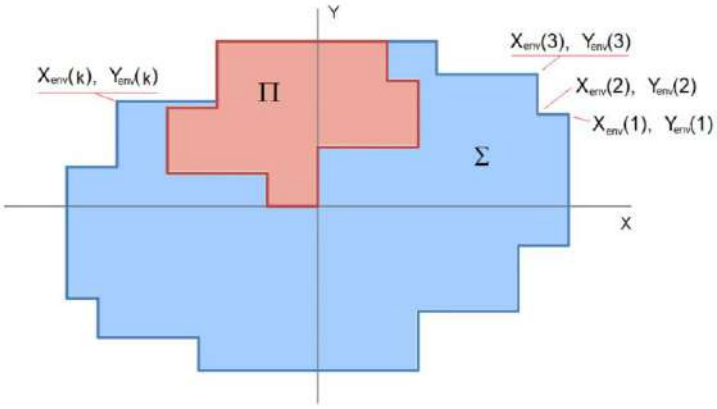

Figure 4. Form. Generic shape of a solar collector (orange) and its envelope Σ (blue).

In accordance with the above, Figure 5 shows, by means of a flow diagram, the inter-shading $\left(\vec{n}\right)$ function, especially designed to implement the method described in this section to determine the existence of shadow between modules in PV installations with dual-axis tracking and regular distribution of collectors. This Boolean function depends on the vector $\vec{n}$, Equation (19), returning a value "true" if $\vec{n}$ implies inter-shading and "false" otherwise. As can be seen in Figure 5, only possible shading is studied in the reference collector, considered representative of the set, which is totally surrounded by N_t trackers.

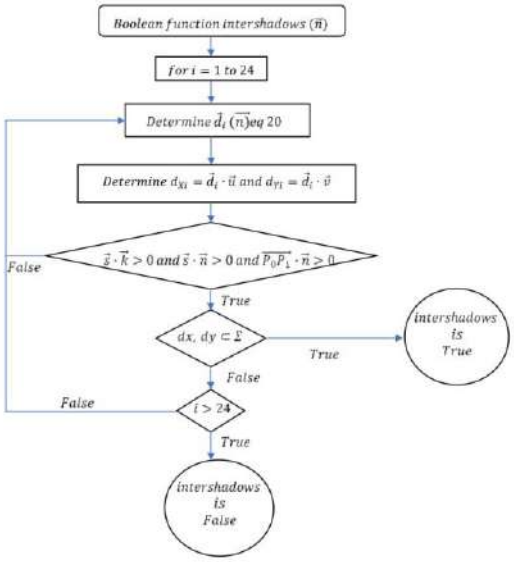

Figure 5. Flow diagram of the inter-shading function $\vec{n}$

In this way, in the case that the value of $\vec{n}$, obtained from Equation (19), does not imply shadows between collectors, $intershadows\left(\vec{n}\right) = False$, the optimal tracking strategy will propose the orientation of the collectors according to the address of $\vec{n}$. On the contrary, if the value of $\vec{n}$, obtained from Equation (19), implies shadows between collectors, $intershadows\left(\vec{n}\right) = True$, the orientation that does not imply shadows and that maximizes the incident irradiance must be sought. In that case, back tracking is used following the process indicated in Figure 6.

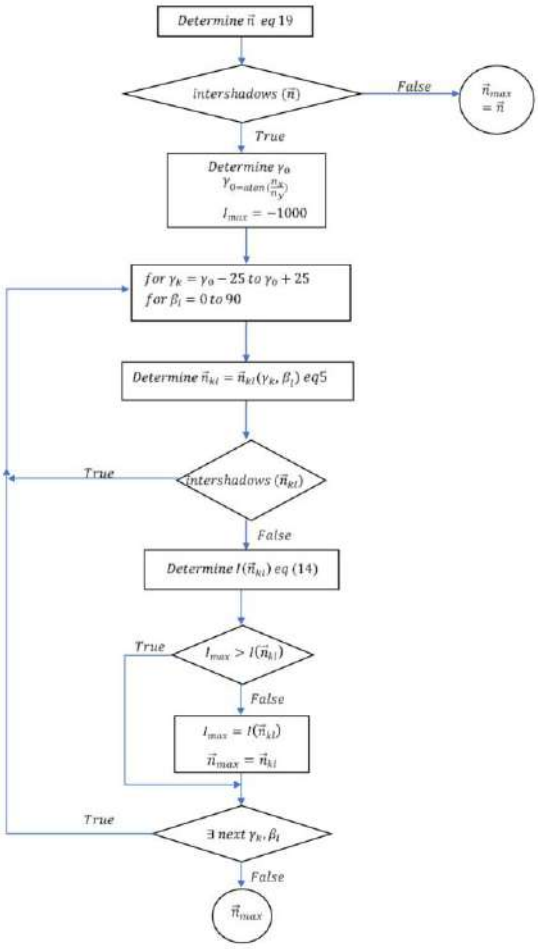

Figure 6. Flow diagram to determine the orientation $\vec{n}$ of maximum irradiance uptake without any inter-shading between collectors.

2.3. Calculation Scheme of Intercepted Solar Radiation

With the methodology described for solar tracking, the incident solar irradiance on solar collectors has been simulated for the 12 representative days, according to Klein [47]. From this irradiance, the incident radiation on the collectors on each representative day m has been calculated using Equation (27), where the integral has been approximated by discretizing the sum in time intervals of three minutes.

$$H_m = \int_{t_{sunrise,m}}^{t_{sunset,m}} \left[\frac{\vec{s}\cdot\vec{n}}{\vec{s}\cdot\vec{k}} I_B + \left[(1-F_1)\frac{1+\vec{k}\cdot\vec{n}}{2} + F_1\frac{\vec{s}\cdot\vec{n}}{b} + F_2\sqrt{1-\left(\vec{k}\cdot\vec{n}\right)^2} \right] I_D + \rho\frac{1-\vec{k}\cdot\vec{n}}{2}(I_B+I_D) \right] dt \quad (27)$$

Once the daily radiation has been calculated for the representative days proposed by Klein [47] for each of the 12 months of the year (m = 1,2, ... , 12), the annual global radiation (H_{year}) is calculated according to Equation (28), where N_m is the number of days in the month m.

$$H_{year} = \sum_{m=1}^{12} N_m \cdot H_m \quad (28)$$

2.4. Cases Analyzed

In this work, the effect of the shape of the collectors on the capture of annual radiation in a PV plant with dual-axis tracking has been studied. To generate the study scenarios, the design of "El Molino", a photovoltaic installation located in Córdoba (latitude = 37.75492° N; longitude = 5.04548° W) was used as a starting point. It is an installation with dual-axis trackers (with azimuth and elevation movement) and rectangular collectors 8 m wide and 5 m high. Each collector is made up of 25 photovoltaic modules 1m high and 1.6m wide (Figure 7a). The trackers are arranged in a regular grid on horizontal ground, initially separated by a distance D_{EW} = 20 m in the EW direction and D_{NS} = 14 m in the NS direction (Figure 7b).

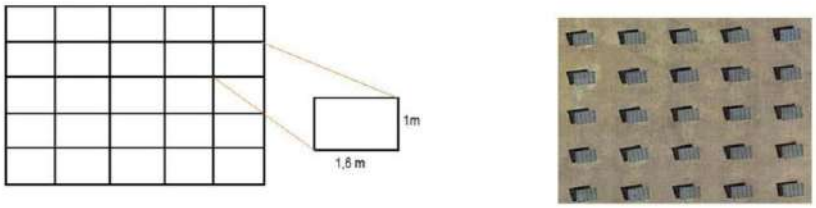

Figure 7. Design characteristics of the "El Molino" facility: (**a**) Constitution of the collectors; (**b**) Arrangement of collectors.

Case studies arise by introducing different variations in the original design and crossing all possible sources of variation. Specifically, the variations introduced consist of:

- *Modification of the collector shape.* The possibility of introducing cuts at the vertices has been considered to study the collectors with the shape indicated in Figure 8. Letting (X_{ul}, Y_{ul}), (X_{ur}, Y_{ur}), (X_{dl}, Y_{dl}), and (X_{dr}, Y_{dr}) be the coordinates of the vertices corresponding to the cuts made in the upper left, upper right, lower left, and lower right corners, the possible values considered (in metres) for each of these pairs were (0,0), (1,1.6), (1,3.2), (2,1.6), and (2,3.2). The crossing of all the possibilities generated $N_G = 5^4 = 625$ different forms of collector.
- *Modification of the inter-distances.* Letting D_{NS} be the distance in the NS direction between rows of collectors and D_{EW} the distance in the EW direction between columns of collectors, the possibilities D_{NS} = 10 m, 12.5 m, 15 m, 17.5 m, and 20 m and

D_{EW} = 10 m, 15 m, 20 m, and 25 m were studied. The crossing of these possibilities gave rise to N_D = 20 designs of different distances.

- *Modification of the spatial distribution of the solar trackers.* For each pair of distances (D_{NS}, D_{EW}), N_S = 2, possible spatial distributions of the solar trackers in the plant were studied, both the regular grid arrangement oriented to the south (Figure 9a) and staggered (Figure 9b). In both configurations, it was considered that the reference collector in the study (i = 0) was surrounded by 24 collectors.

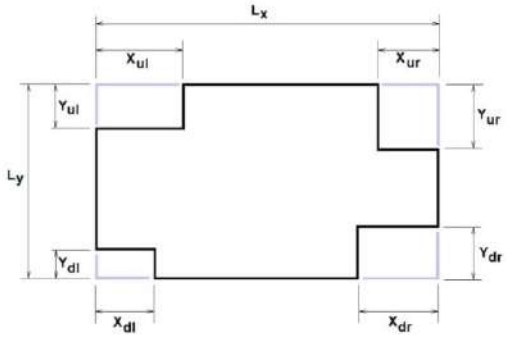

Figure 8. Generic way of describing the clipped vertex collector.

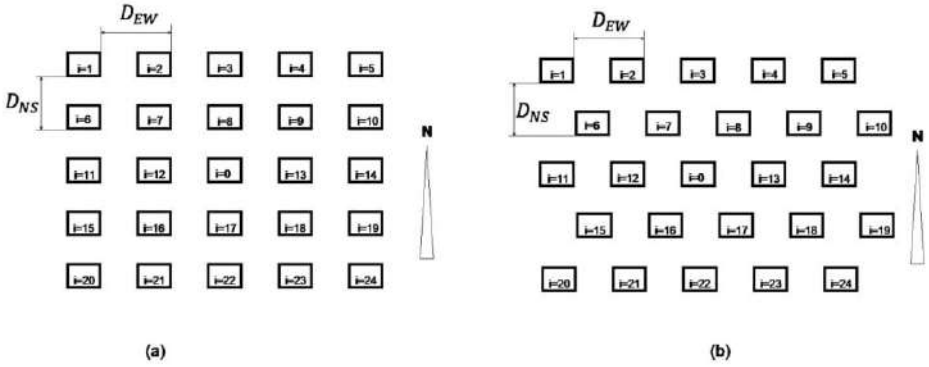

Figure 9. Considered spatial arrangements and location of the reference collector in the study (i = 0): (**a**) regular grid; (**b**) staggered.

The crossing of all the possibilities generated $N_T = N_G \cdot N_D \cdot N_S$ = 25,000 different combinations of geometric designs for the PV plant "El Molino" with dual-axis tracking and its collectors. For each of these designs, the annual incident radiation on the collectors was obtained by the method set forth, Equation (28), considering the 12 characteristic days proposed by Klein [47], and the monthly mean radiation values [48] set forth in Table 1.

Table 1. Data considered for the estimation of the annual solar irradiance in "El Molino" PV Plant (Cordoba, Spain): horizontal daily radiation, H [48] and representative day proposed by [47] each month of the year.

Month	H (J/m^2)	Representative Day
January	7,401,000	17
February	11,097,000	47
March	14,158,000	75
April	17,307,000	105
May	19,017,000	135
June	24,263,000	162
July	25,719,000	198
August	23,411,000	228
September	17,983,000	258
October	11,895,000	288
November	8,228,000	318
December	6,237,000	344

3. Results

This section describes the incident radiation values on collectors and the results of the study of the influence of the design variables on the solar incidence on the PV plant designs considered. The synoptic values obtained for the annual incident radiation in collectors are summarized in Table 2. Figure 10 shows the distribution of values obtained depending on the membership intervals.

Table 2. Descriptive parameters of the set of values of H_{year} (kWh/m^2).

Number of Cases	25,000
Average	2172.0
Minimum	2040.2
Maximum	2233.8
Median	2189.6

In the set of values obtained, it is observed that certain forms of the collector offer the same value. These are the cases in which the set of cuts A, B, C and D of Figure 11a are permuted as shown in Figure 11b–d,f–i. A detailed analysis of the procedure followed makes it possible to verify that the shape of the solar collector does not influence directly but rather through its envelope. As a consequence, the collector shapes of the first column (11 (a), 11 (b), 11 (c), 11 (d)) give rise to identical annual radiation results since they all give rise to the same envelope Σ (represented in Figure 11e). On the other hand, the coincidence of radiation outcomes in the results between the collector shapes of the first (Figure 11a–d) and the second column (Figure 11f–i) should be understood as a consequence of the symmetry with respect to the NS axis of the studied configurations and of the symmetry with respect to this plane in the positions of the sun between the hours of the morning and afternoon.

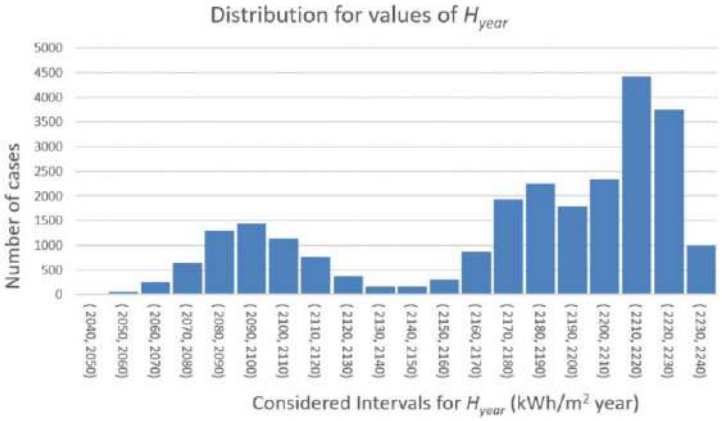

Figure 10. Distribution of annual solar radiation values (H) according to membership intervals.

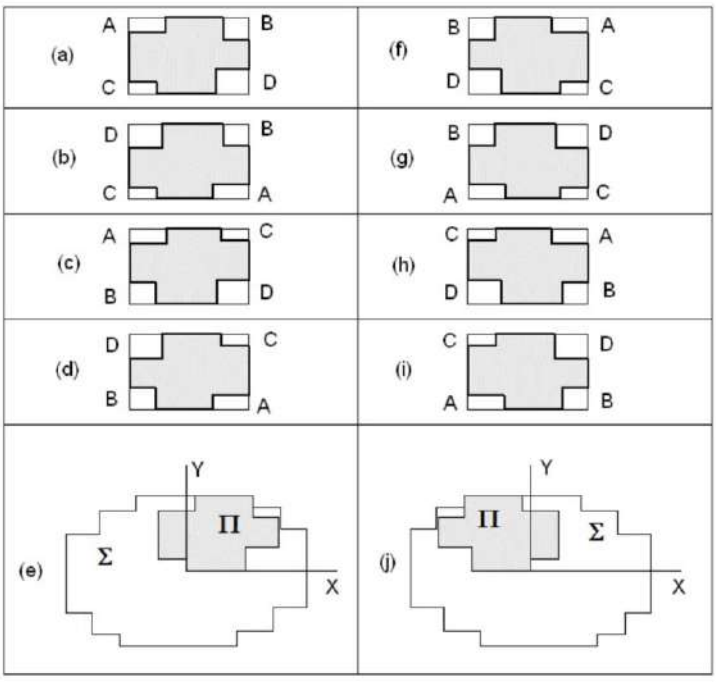

Figure 11. Set of collector shapes that generate identical annual incident radiation results. The forms (**a**–**d**) generate the same envelope Σ (**e**) and the set of symmetric figures with respect to a vertical axis (**f**–**i**) generate a symmetric envelope Σ′ of Σ (**j**).

The dependence of the values obtained with respect to the considered design variables was studied using an approximation and simplified model, in which the calculated annual radiation was expressed as a function of the following explanatory variables:

- Collector surface $S_{col}\,(m^2)$.
- Distance between trackers in east–west direction, $D_{EW}\ (m)$
- Distance between trackers in north–south direction, $D_{NS}\ (m)$
- Discriminatory variable of the type of configuration T (T = 1 for staggered configurations and T = 0 for regular grids).

In this sense, it is worth highlighting that the model described and used (for each of the 25,000 cases) can be considered a mathematical function of the variables proposed. However, the complexity of the model and the need to aggregate results on the different representative days made it difficult to know the weight or influence of each variable on the final results. Thus, to overcome this difficulty, this paper proposes to replace this complex function with a mathematical function of simple expression reproducing the result of the complex model with the least possible error. The reader should assume that this is not a statistical problem but rather a problem of adjustment or approximation of a simple expression function to a complex function, so that statistical methods are not applicable. To address the fit, the set of simple variables was extended with composite variables obtained as products and ratios of simple variables. The proposed function (29) was selected from the set of fits to linear functions of composite variables. It lacks a clear physical meaning, but it allows for reproduction of the results of the model with an average relative error equal to 2.561 kWh/m^{2}year; therefore, it is considered suitable for the study of the relative weight of the variables.

Equation (29) shows the mathematical expression of this model for which the parameters a, b, c, d, e, f, g, h, l, r, and w have been obtained by the least squares method (Table 3), with an adjustment coefficient $R^2 = 0.993$. Table 4 shows the synoptic values of the estimation errors of the model ε and ε_{rel}, given by Equations (30) and (31), where H_{year}^{est} is the annual solar irradiance on the solar collectors estimated according to Equation (28) and H_{year}^{adj} is the one approximated by the model (29). The low value obtained for the mean square error means that the equation can be considered valid for the study of dependence of the annual solar irradiance with respect to the variables S_{col}, D_{EW}, D_{NS}, and T.

$$H_{year}^{adj} = a + b\,S_{col} + c\,D_{EW} + \frac{d}{D_{EW}} + eD_{NS} + f\,{D_{NS}}^2 + g\,\frac{D_{EW}}{D_{NS}} + h\left(\frac{D_{EW}}{D_{NS}}\right)^2 + l\,\frac{S_{col}}{D_{NS}\,D_{EW}} + r\,\frac{D_{NS}\,D_{EW}}{S_{col}} + w\,T \quad (29)$$

$$\varepsilon = \left|H_{year}^{est} - H_{year}^{adj}\right| \quad (30)$$

$$\varepsilon_{rel} = \frac{\left|H_{year}^{est} - H_{year}^{adj}\right|}{H_{year}^{est}} \quad (31)$$

Table 3. Values obtained for the model of Equation (29).

Parameter	Units	Value
a	kWh/m^2 year	2656.366
b	kWh/m^4 year	−0.960
c	kWh/m^3 year	6.921
d	kWh/m year	−25.783
e	kWh/m^{3}year	−756.012

Table 3. *Cont.*

Parameter	Units	Value
f	kWh/m^4 year	0.512
g	kWh/m^2 year	−167.750
h	kWh/m^2 year	19.071
l	kWh/m^2 year	−364.603
r	kWh/m^2 year	−1.365
w	kWh/m^2 year	−1.661

Table 4. Synoptics of the errors ε Equation (30) and ε_{rel} Equation (31) obtained for the model given by Equation (29).

	ε (kWh/m^2 year)	ε_{rel} (Dimensionless)
Number of cases	25,000	25,000
Average	3.302	1.53×10^{-3}
Minimum	4.67×10^{-4}	2.099×10^{-7}
Maximum	35.913	1.66×10^{-2}
Median	2.561	1.15×10^{-3}

It is important to note that the model adjusted in Equation (30) does not consider the geometric shape of the collectors itself since, given that the mean error, $\bar{\varepsilon}$, of the proposed model is 3.3 kWh/m^{2}year (Table 4), the geometric shape would not have an explanatory capacity superior to this $\bar{\varepsilon}$. This reasoning allowed us to conclude the little influence of the shape of the collectors in facilities that follow the tracking/ back-tracking policy considered in this work.

For a better interpretation of the adjusted Equation (29), we can consider it as the addition of four terms separated by parentheses in Equation (32).

$$H_y^{adj} = a + \{b\, S_{col}\} + \left\{ c\, D_{EW} + \frac{d}{D_{EW}} + e D_{NS} + f\, {D_{NS}}^2 + g\, \frac{D_{EW}}{D_{NS}} + h \left(\frac{D_{EW}}{D_{NS}} \right)^2 \right\} + \left\{ l\, \frac{S_{col}}{D_{NS}\, D_{EW}} + r\, \frac{D_{NS}\, D_{EW}}{S_{col}} \right\} + \{wT\} \quad (32)$$

The first term only depends on the collector surface S_{col}. Given that $b < 0$, it was found that, as the collectors were larger, the lower the annual incident radiation. This effect was due to the greater possibility of inter-shading as the collectors had more surface area. With the cases studied, the variation interval of the final result due exclusively to this term was 24 kWh/m^2 year.

The second term marks the importance of the geometric design of the plant given by D_{EW} and D_{NS}, regardless of whether it is a staggered or grid configuration. In the group of cases studied, the variation interval was 116 kWh/m^2 year.

The third term is interpreted as a function of the ground cover ratio (GCR) parameter defined by Equation (33).

$$GCR = \frac{S_{col}}{D_{NS}\, D_{EW}} \quad (33)$$

According to this definition, the third term considered in the model given by Equation (29) can be rewritten obtaining the expression (34). Thus, this term showed

that the variation in this term was 104 kWh/m^2 year for the GCR values considered in the set of cases studied.

$$\left\{ l \frac{S_{col}}{D_{NS}\, D_{EW}} + m \frac{D_{NS}\, D_{EW}}{S_{col}} \right\} = \left\{ l\, GCR + \frac{m}{GCR} \right\} \quad (34)$$

Finally, given that the parameter w was negative, the term $\{wT\}$ implied a small difference of 1.6 kWh/m^2 year to the detriment of the installations that were arranged in a staggered pattern compared to those with a regular grid.

4. Conclusions

This work presents a novel methodology for the productive study of PV solar collectors mounted on dual-axis trackers. The study, applied to multiple cases, generated as variations with respect to the design adopted in an existing PV Plant ("El Molino", located in Córdoba) allows for identification of the design variables that fundamentally influence the annual incident irradiation on the solar collectors and, therefore, on the energy production of the PV plant. Specifically, by systematically varying the geometry of the collectors, the distance between them, and their spatial distribution, 25,000 case studies were simulated. For all of them, the annual incident solar radiation on the solar collectors was calculated, using for this the irradiance estimation model of Perez [43] and assuming that they were governed by a tracking strategy that optimized radiative capture while avoiding inter-shading between collectors [37,38]. Although a comprehensive methodology was used to study the case, it was difficult with the data set to understand the influence of each variable on the final result. Therefore, a simple function was fitted, which accurately reproduced the result of the complex model $\varepsilon\_rel = 0.00115$. From the irradiance data obtained for the different PV plant designs, a simple mathematical model has been obtained, Equation (29) with a high level of adjustment $(R^2 = 0.993)$ that represents the dependence of the annual solar irradiance on the PV plant with respect to design variables such as collector surface, S_{col}, NS and EW distances between collectors D_{NS} and D_{EW}, and spatial distribution of the collectors: regular or staggered grid. Thus, the proposed model has made it possible to identify that the main variables that influence the annual incidence of irradiance are, in order of greatest influence, the geometric design of the plant as a function of the distances between its collectors, $(D_{NS},\ D_{EW})$, the GCR of the installation and the surface of its collectors (S_{col}), which can lead to variations in the electrical production of the PV plant of up to 116 kWh/m^{2}year, 104 kWh/m^{2}year, and 24 kWh/m^{2}year. However, for practical purposes, with regard to the spatial distribution of the collectors, it is not appropriate to assume a better behaviour of the regular grid arrangement with respect to the staggered shape since the margin of 1.6 kWh/m^{2}year for this variable falls within the uncertainty margin of the radiation prediction models. Similarly, the geometric shape of the collectors does not exert a significant influence on the irradiance received since it gives rise to variations of 3.3026 kWh/m^{2}year, which, therefore, are lower than the uncertainty margin of the estimation model itself. Future works will study the influence of the shape in confluence with the orientation of the terrain.

Author Contributions: Conceptualization, F.J.G.-U., I.M.M.-G., and L.M.F.-A.; methodology, I.M.M.-G. and L.M.F.-A.; software, Á.P.-C.; validation, I.M.M.-G. and L.M.F.-A.; formal analysis, L.M.F.-A., I.M.M.-G., and F.J.G.-U.; bibliographic search, F.J.G.-U. and L.M.F.-A.; data curation, Á.P.-C.; writing—original draft preparation, L.M.F.-A., F.J.G.-U., and I.M.M.-G.; writing—review and editing, F.J.G.-U., I.M.M.-G., and L.M.F.-A.; supervision, I.M.M.-G. and L.M.F.-A. All authors have read and agreed to the published version of the manuscript.

Funding: This research is partially supported by the CLARA Project, which has received funding from the European Union's Horizon 2020 research and innovation programme under Grant Agreement No 730482.

Acknowledgments: Authors appreciate the support of Professor Rafael López-Luque.

Conflicts of Interest: The authors declare no conflict of interest.

Abbreviations

A_0	reference collector surface
A_i	generic collector surface
D_{EW}	distance between trackers in east–west direction
$\vec{d}_i$	geometric displacement vector from polygon Π_0 to Π'_i
d_n	Julian day
D_{NS}	distance between trackers in north–south direction
d_{Xi}	X component of $\vec{d}_i$
d_{Yi}	Y component of $\vec{d}_i$
F_1, F_2	weighting factors for the decomposition of the inclined diffuse radiation
GCR	ground cover ratio
H_m	incident radiation on the collectors on each representative day of a month according to Klein
H_{year}	annual global radiation
H_{year}^{est}	annual solar irradiance on the solar collectors estimated according to Equation (28)
H_{year}^{adj}	annual solar irradiance on the solar collectors estimated according to Equation (29)
$\vec{i}$, $\vec{j}$, $\vec{k}$	unit vectors associated to a local Cartesian system
I	global solar irradiance on the tilted collector
I_B	direct solar irradiance on horizontal plane
I_D	diffuse solar irradiance
L_x	horizontal longitude of the collector before cuts
L_y	vertical longitude of the collector before cuts
$\vec{n}$	normal vector to the surface
N_D	different design of the inter-distances between collectors
N_G	different forms of collector shape
N_m	number of days in the month m
N_S	possible spatial distributions of the solar trackers in the plant
N_T	different combinations of geometric designs result of crossing $N_G \cdot N_D \cdot N_S$
P_0	position of the reference collector
P_i	position of a generic collector
$\vec{s}$	solar vector
S_{col}	collector surface
s_x, s_y, s_z	components of solar vector
T	discriminatory variable of the type of configuration
X_{dl}	x-coordinate of the vertex corresponding to the cut made in the lower left corner
X_{dr}	x-coordinate of the vertex corresponding to the cut made in the lower right corner
X_{env}	array with the x-coordinates of the collector shape
X_{ul}	x-coordinate of the vertex corresponding to the cut made in the upper left corner
X_{ur}	x-coordinate of the vertex corresponding to the cut made in the upper right corner
Y_{dl}	y-coordinate of the vertex corresponding to the cut made in the lower left corner
Y_{dr}	y-coordinate of the vertex corresponding to the cut made in the lower right corner
Y_{env}	array with the y-coordinates of the collector shape
Y_{ul}	y-coordinate of the vertex corresponding to the cut made in the upper left corner
Y_{ur}	y-coordinate of the vertex corresponding to the cut made in the upper right corner
$\vec{u}$	horizontal vector to the maximum slop direction of the collector plane
v	parallel vector to the maximum slop direction of the collector plane

Greek Letters

β	inclination angle of the terrain
γ	azimuth angle of the collector rotation axis
δ	solar declination
ε	estimation error of the proposed model
ε_{rel}	relative error of the proposed model
θ	angle of incidence of sunbeams on the inclined plane
θ_z	solar zenith angle
ρ	albedo

φ	latitude
Ω	Earth's rotation speed
Γ	daily angle
Π_0	reference polygon collector
Π_i	generic polygon collector
Π'_i	projection of generic polygon collector over ψ
ψ	plane that contains the reference collector Π_0

Appendix A. Demonstration of the Dicotomic Criterion for Determining the Intershading between Solar Collectors

To determine if there is inter-shading between collectors, in this work, a dichotomous criterion is used, based on Minkowski's algebra [44–46], according to which there is inter-shading between two collectors Π_0 y Π_i if and only if the displacement vector $\vec{d}_i$ from collector Π_0 to Π'_i, which is the projection of collector Π_i on the plane ψ that contains Π_0 and can be considered a translation of Π_0, is included within the plane curve Σ, which is obtained as the envelope of the family of all polygons that can be drawn in the plane ψ when translating the polygon Π_0, with the condition that its perimeter is in contact with the origin of the reference system contained in ψ.

Thus, this appendix demonstrates this dichotomous criterion for two generic surfaces Π and its translation Π_T.

"A polygon Π and its translation Π_T intersect if and only if the translation vector $\vec{OP}$ of Π_T with respect to Π is included in the envelope Σ".

The demonstration has two steps:

- Step 1: If $\vec{OP}$ is included in Σ, Π and Π_T intersect.

Since $\vec{OP}$ is included in Σ (Figure A1a), there will be at least one polygon Π that, passing through the origin of coordinates O, encloses point P (Figure A1b). If this polygon is translated following $\vec{OP}$, it is evident that point O is translated to P (Figure A1c). Since this point P, the boundary of Π_T, is interior to Π, there will be an intersection between Π and Π_T.

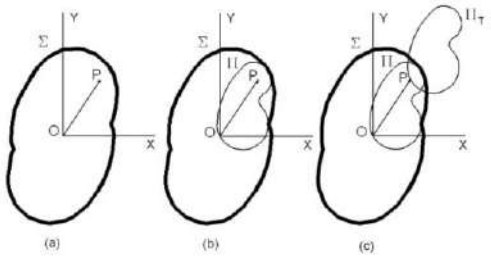

Figure A1. Demonstration sequence: If $\vec{OP}$ is included in Σ, Π and Π_T intersect.

- Step 2: If Π and Π_T intersect, $\vec{OP}$ is included in Σ.

If Π and Π_T intersect, there will exist, at least. a point P, of the perimeter of Π_T that is included in Π. By calling O the origin of P, it is possible to define the vector $\vec{OP}$ (Figure A2a). If the system of coordinate axes passing through O is considered and the envelope Σ is drawn, it is evident that the point P is included in Σ (Figure A2b).

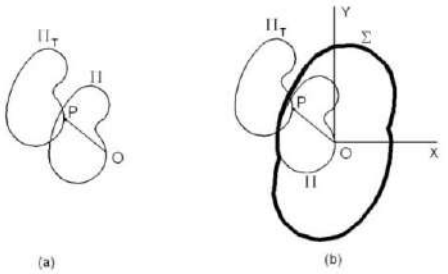

Figure A2. Demonstration sequence: If Π and Π_T intersect, $\vec{OP}$ is included in Σ.

Appendix B. Obtaining the Generic Form σ for Collectors with Cuts

In this appendix, the procedure for obtaining the flat curve Σ associated with a collecting surface Π with a generic shape is explained in detail so that it is valid for all the collector shapes considered in this work.

Letting a plane ψ and a reference system OXY be in this plane, we considered a polygon Π contained in ψ with the shape of a rectangle with sides L_X and L_Y with the vertices trimmed, the coordinates of these vertices being: (X_{ul}, Y_{ul}), (X_{ur}, Y_{ur}), (X_{dl}, Y_{dl}), and (X_{dr}, Y_{dr}) (Figure A3).

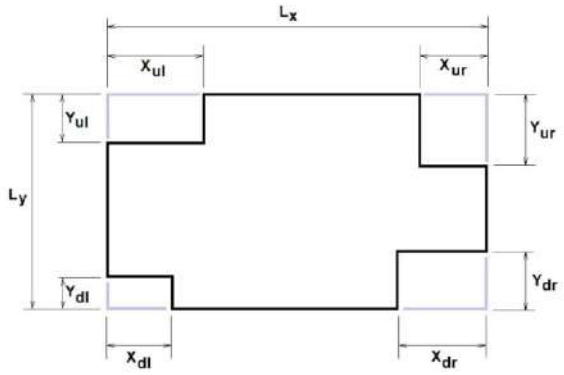

Figure A3. Representation of the generic collector surface Π based on a rectangle with sides L_X and L_Y with the vertices cut off.

The analysis of all the translations allows us to obtain the coordinates of the perimeter of Σ. In general, Σ is a polygon with 28 vertices that depend on the dimensions reflected in Figure A3 according to expression (A1).

$$\Sigma = \Sigma(L_x, L_y, X_{ul}, Y_{ul}, X_{ur}, Y_{ur}, X_{dl}, Y_{dl}, X_{dr}, Y_{dr}) \quad \text{(A1)}$$

In this way, these coordinates can be structured in two arrays of 28 elements Xenv (28) and Yenv (28). Next, the VBA programming code that allows obtaining each of these coordinates is shown.

```
Xenv(1) = Lx − Xur − Xdl: Yenv(1) = Ly
If Yur<Ydl Then
Xenv(2) = Xenv(1): Yenv(2) = Yenv(1) − Yur
Xenv(3) = Xenv(1) + Xur: Yenv(3) = Yenv(1) − Yur
```

```
Else
Xenv(2) = Xenv(1): Yenv(2) = Yenv(1) − Ydl
Xenv(3) = Xenv(1) + Xdl: Yenv(3) = Yenv(1) − Ydl
End If

Xenv(7) = Lx: Yenv(7) = Ly − Yur − Ydl
If Xur<Xdl Then
Xenv(6) = Xenv(7) − Xur: Yenv(6) = Yenv(7)
Xenv(5) = Xenv(7) − Xur: Yenv(5) = Yenv(7) + Yur
Else
Xenv(6) = Xenv(7) − Xdl: Yenv(6) = Yenv(7)
Xenv(5) = Xenv(7) − Xdl: Yenv(5) = Yenv(7) + Ydl
End If
Xenv(4) = Xenv(3): Yenv(4) = Yenv(5)

Xenv(11) = Lx: Yenv(11) = -Ly + Ydr + Yul
If Xdr<Xul Then
Xenv(11) = Xenv(11) − Xdr: Yenv(11) = Yenv(11)
Xenv(10) = Xenv(11) − Xdr: Yenv(10) = Yenv(11) − Ydr
Else
Xenv(11) = Xenv(11) − Xul: Yenv(11) = Yenv(11)
Xenv(10) = Xenv(11) − Xul: Yenv(10) = Yenv(11) − Yul
End If
Xenv(11) = Xenv(12): Yenv(11) = Yenv(10)

Xenv(14) = Lx − Xdr − Xul: Yenv(14) = -Ly
If Ydr<Yul Then
Xenv(13) = Xenv(14): Yenv(13) = Yenv(14) + Ydr
Xenv(12) = Xenv(14) + Xdr: Yenv(12) = Yenv(14) + Ydr
Else
Xenv(13) = Xenv(14): Yenv(13) = Yenv(14) + Yul
Xenv(12) = Xenv(14) + Xul: Yenv(12) = Yenv(14) + Yul
End If

For i = 15 To 211
Xenv(i) = -Xenv(i − 14)
Yenv(i) = -Yenv(i − 14)
Next i
```

However, when there is some kind of symmetry or when any of the dimensions of the cutouts is null, some coordinates contained in the Xenv () and Yenv () arrays will be repeated. In these cases, the number of vertices of Σ will be less than 28. After eliminating the possible repeated points, it is mathematically verified that there are four combinations or symmetries that generate the same polygon Σ Equation (A2).

$$\begin{gathered}\Sigma\left(L_x, L_y, X_{ul}, Y_{ul}, X_{ur}, Y_{ur}, X_{dl}, Y_{dl}, X_{dr}, Y_{dr}\right) = \\ \Sigma\left(L_x, L_y, X_{dr}, Y_{dr}, X_{ur}, Y_{ur}, X_{dl}, Y_{dl}, X_{ul}, Y_{ul}\right) = \\ \Sigma\left(L_x, L_y, X_{ul}, Y_{ul}, X_{dl}, Y_{dl}, X_{ur}, Y_{ur}, X_{dr}, Y_{dr}\right) = \\ \Sigma\left(L_x, L_y, X_{dr}, Y_{dr}, X_{ur}, Y_{ur}, X_{dl}, Y_{dl}, X_{ul}, Y_{ul}\right)\end{gathered} \tag{A2}$$

In this way, it is possible to obtain the envelope Σ to the family of polygons Π on which the dichotomous criterion of inter-shading between collectors will be based.

References

1. López, I.; Arriaga, A.; Pardo, M. La dimensión social del concepto de desarrollo sostenible: ¿La eterna Olvidada? *Rev. Span. Sociol.* **2018**, *27*. [CrossRef]
2. International Energy Agency (IEA). *Renewables 2020*; IEA: Paris, France, 2020.
3. Andre, T.; Guerra, F. *Renewables Global Status Report*; REN21: Paris, France, 2020; ISBN 978-3-948393-00-7.
4. Kannan, N.; Vakeesan, D. Solar energy for future world: A review. *Renew. Sustain. Energy Rev.* **2016**, *62*, 1092–1105. [CrossRef]
5. Eldin, S.A.S.A.S.; Abd-Elhady, M.S.S.; Kandil, H.A.A. Feasibility of solar tracking systems for PV panels in hot and cold regions. *Renew. Energy* **2016**, *85*, 228–233. [CrossRef]
6. Salas, V.; Olias, E. Overview of the photovoltaic technology status and perspective in Spain. *Renew. Sustain. Energy Rev.* **2009**, *13*, 1049–1057. [CrossRef]
7. Singh, R.; Kumar, S.; Gehlot, A.; Pachauri, R. An imperative role of sun trackers in photovoltaic technology: A review. *Renew. Sustain. Energy Rev.* **2018**, *82*, 3263–3278. [CrossRef]
8. AL-Rousan, N.; Isa, N.A.M.; Desa, M.K.M. Advances in solar photovoltaic tracking systems: A review. *Renew. Sustain. Energy Rev.* **2018**, *82*, 2548–2569. [CrossRef]
9. Frydrychowicz-Jastrzębska, G.; Bugała, A. Modeling the Distribution of Solar Radiation on a Two-Axis Tracking Plane for Photovoltaic Conversion. *Energies* **2015**, *8*, 1025–1041. [CrossRef]
10. Hafez, A.Z.; Yousef, A.M.; Harag, N.M. Solar tracking systems: Technologies and trackers drive types—A review. *Renew. Sustain. Energy Rev.* **2018**, *91*, 754–782. [CrossRef]
11. Lee, C.-Y.; Chou, P.-C.; Chiang, C.-M.; Lin, C.-F. Sun Tracking Systems: A Review. *Sensors* **2009**, *9*, 3875–3890. [CrossRef]
12. Antonanzas, J.; Urraca, R.; Martinez-de-Pison, F.J.; Antonanzas, F. Optimal solar tracking strategy to increase irradiance in the plane of array under cloudy conditions: A study across Europe. *Sol. Energy* **2018**, *163*, 122–130. [CrossRef]
13. Bahrami, A.; Okoye, C.O. The performance and ranking pattern of PV systems incorporated with solar trackers in the northern hemisphere. *Renew. Sustain. Energy Rev.* **2018**, *97*, 138–151. [CrossRef]
14. Quesada, G.; Guillon, L.; Rousse, D.R.; Mehrtash, M.; Dutil, Y.; Paradis, P.-L. Tracking strategy for photovoltaic solar systems in high latitudes. *Energy Convers. Manag.* **2015**, *103*, 147–156. [CrossRef]
15. Hammad, B.; Al-Sardeah, A.; Al-Abed, M.; Nijmeh, S.; Al-Ghandoor, A. Performance and economic comparison of fixed and tracking photovoltaic systems in Jordan. *Renew. Sustain. Energy Rev.* **2017**, *80*, 827–839. [CrossRef]
16. Talavera, D.L.; Muñoz-Cerón, E.; Ferrer-Rodríguez, J.P.; Pérez-Higueras, P.J. Assessment of cost-competitiveness and profitability of fixed and tracking photovoltaic systems: The case of five specific sites. *Renew. Energy* **2019**, *134*, 902–913. [CrossRef]
17. Hua, Z.; Ma, C.; Lian, J.; Pang, X.; Yang, W. Optimal capacity allocation of multiple solar trackers and storage capacity for utility-scale photovoltaic plants considering output characteristics and complementary demand. *Appl. Energy* **2019**, *238*, 721–733. [CrossRef]
18. Ali Jallal, M.; Chabaa, S.; Zeroual, A. A novel deep neural network based on randomly occurring distributed delayed PSO algorithm for monitoring the energy produced by four dual-axis solar trackers. *Renew. Energy* **2020**, *149*, 1182–1196. [CrossRef]
19. Eke, R.; Senturk, A. Performance comparison of a double-axis sun tracking versus fixed PV system. *Sol. Energy* **2012**, *86*, 2665–2672. [CrossRef]
20. Şenpinar, A.; Cebeci, M. Evaluation of power output for fixed and two-axis tracking PVarrays. *Appl. Energy* **2012**, *92*, 677–685. [CrossRef]
21. Bahrami, A.; Okoye, C.O.; Atikol, U. The effect of latitude on the performance of different solar trackers in Europe and Africa. *Appl. Energy* **2016**, *177*, 896–906. [CrossRef]
22. Koussa, M.; Cheknane, A.; Hadji, S.; Haddadi, M.; Noureddine, S. Measured and modelled improvement in solar energy yield from flat plate photovoltaic systems utilizing different tracking systems and under a range of environmental conditions. *Appl. Energy* **2011**, *88*, 1756–1771. [CrossRef]
23. Seme, S.; Štumberger, G.; Voršič, J. Maximum efficiency trajectories of a two-axis sun tracking system determined considering tracking system consumption. *IEEE Trans. Power Electron.* **2011**, *26*, 1280–1290. [CrossRef]
24. Gómez-Uceda, F.J.; Ramírez-Faz, J.; Varo-Martínez, M.; Fernández-Ahumada, L.M. New Omnidirectional Sensor Based on Open-Source Software and Hardware for Tracking and Backtracking of Dual-Axis Solar Trackers in Photovoltaic Plants. *Sensors* **2021**, *21*, 726. [CrossRef]
25. Fernández-Ahumada, L.M.; Ramírez-Faz, J.; López-Luque, R.; Varo-Martínez, M.; Moreno-García, I.M.; Casares de la Torre, F. Influence of the design variables of photovoltaic plants with two-axis solar tracking on the optimization of the tracking and backtracking trajectory. *Sol. Energy* **2020**, *208*, 89–100. [CrossRef]
26. Lorenzo, E.; Pérez, M.; Ezpeleta, A.; Acedo, J. Design of tracking photovoltaic systems with a single vertical axis. *Prog. Photovolt. Res. Appl.* **2002**, *10*, 533–543. [CrossRef]
27. Karatepe, E.; Boztepe, M.; Çolak, M. Development of a suitable model for characterizing photovoltaic arrays with shaded solar cells. *Sol. Energy* **2007**, *81*, 977–992. [CrossRef]
28. Kaushika, N.D.; Gautam, N.K. Energy yield simulations of interconnected solar PV arrays. *IEEE Trans. Energy Convers.* **2003**, *18*, 127–134. [CrossRef]
29. Woyte, A.; Nijs, J.; Belmans, R. Partial shadowing of photovoltaic arrays with different system configurations: Literature review and field test results. *Sol. Energy* **2003**, *74*, 217–233. [CrossRef]

30. Trzmiel, G.; Gluchy, D.; Kurz, D. The impact of shading on the exploitation of photovoltaic installations. *Renew. Energy* **2020**, *153*, 480–498. [CrossRef]
31. Diaz-Dorado, E.; Suárez-García, A.; Carrillo, C.J.; Cidrás, J. Optimal distribution for photovoltaic solar trackers to minimize power losses caused by shadows. *Renew. Energy* **2011**, *36*, 1826–1835. [CrossRef]
32. Martínez-Moreno, F.; Muñoz, J.; Lorenzo, E. Experimental model to estimate shading losses on PV arrays. *Sol. Energy Mater. Sol. Cells* **2010**, *94*, 2298–2303. [CrossRef]
33. Perpiñán, O. Cost of energy and mutual shadows in a two-axis tracking PV system. *Renew. Energy* **2012**, *43*, 331–342. [CrossRef]
34. Narvarte, L.; Lorenzo, E. Tracking and ground cover ratio. *Prog. Photovolt. Res. Appl.* **2008**, *16*, 703–714. [CrossRef]
35. Panico, D.; Garvison, P.; Wenger, H.; Shugar, D. Backtracking: A novel strategy for tracking PV systems. In Proceedings of the Conference Record of the Twenty-Second IEEE Photovoltaic Specialists Conference 1991, Las Vegas, NV, USA, 7–11 October 1991; pp. 668–673.
36. DEGERiberica. Referencias. Available online: https://degeriberica.com/referencias/ (accessed on 20 January 2021).
37. Fernández-Ahumada, L.M.; Casares, F.J.; Ramírez-Faz, J.; López-Luque, R. Mathematical study of the movement of solar tracking systems based on rational models. *Sol. Energy* **2017**, *150*, 20–29. [CrossRef]
38. Fernández-Ahumada, L.M.; Ramírez-Faz, J.; López-Luque, R.; Varo-Martínez, M.; Moreno-García, I.M.; Casares de la Torre, F. A novel backtracking approach for two-axis solar PV tracking plants. *Renew. Energy* **2020**, *145*, 1214–1221. [CrossRef]
39. Braun, J.E.; Mitchell, J.C. Solar geometry for fixed and tracking surfaces. *Sol. Energy* **1983**, *31*, 439–444. [CrossRef]
40. Reda, I.; Andreas, A. Solar position algorithm for solar radiation applications. *Sol. Energy* **2004**, *76*, 577–589. [CrossRef]
41. Riley, D.; Hansen, C. Sun-Relative Pointing for Dual-Axis Solar Trackers Employing Azimuth and Elevation Rotations. *J. Sol. Energy Eng.* **2015**, *137*, 031008. [CrossRef]
42. Kelly, N.A.; Gibson, T.L. Improved photovoltaic energy output for cloudy conditions with a solar tracking system. *Sol. Energy* **2009**, *83*, 2092–2102. [CrossRef]
43. Perez, R.; Ineichen, P.; Seals, R.; Michalsky, J.; Stewart, R. Modeling daylight availability and irradiance components from direct and global irradiance. *Sol. Energy* **1990**, *44*, 271–289. [CrossRef]
44. Avnaim, F.; Boissonnat, J.-D. Polygon placement under translation and rotation. *RAIRO Theor. Inform. Appl.* **1989**, *23*, 5–28. [CrossRef]
45. Chazelle, B. The polygon containment problem. *Adv. Comput. Res.* **1983**, *1*, 1–33.
46. Lozano-Pérez, T. Spatial Planning: A Configuration Space Approach. *IEEE Trans. Comput.* **1983**. [CrossRef]
47. Klein, S.A. Calculation of monthly average insolation on tilted surfaces. *Sol. Energy* **1977**, *19*, 325–329. [CrossRef]
48. Posadillo, R.; López Luque, R. A sizing method for stand-alone PV installations with variable demand. *Renew. Energy* **2008**, *33*, 1049–1055. [CrossRef]